AN INVESTIGATION OF THE HEAT TRANSFER IN AN ELECTRICALLY HEATED TUBULAR WIRE STRAND FURNACE.

By

James N. Massey

A Thesis submitted for the degree of

Doctor of Philosophy

At The University of Salford.

Department of Aeronautical and Mechanical Engineering

University of Salford.

April 1993.

CONTENTS. Page

Page

Page

Page

Page

Page

Page

Page

Page

Page

LIST OF TABLES.

Page

Chapter 5.

Chapter 7.

Chapter 8.

Page

Chapter 9.

Appendix B.

Appendix C.

Page

Page

LIST OF FIGURES.

Page

Chapter 1.

Chapter 2.

Chapter 3.

Page

Chapter 4.

Chapter 5.

Page

Chapter 6.

Page

Chapter 7.

Page

Page

Chapter 9.

Page

Page

ACKNOWLEDGEMENTS.

I would like to express my gratitude to all those without whom this project would not have been possible. Special thanks go to my supervisor Dr Ken Flower for his continued help and support, both moral and academic, John Thorpe for his excellent technical assistance, and to all the workshop and technical staff in the Department of Aeronautical and Mechanical Engineering.

I would also like to thank Mr G. Ward, and the staff of Meltech Furnaces Ltd, for their financial and technical support, and The Science and Engineering Research Council, for providing the financial means to complete the project. Thanks are also due to Critchley, Sharp and Tetlow, The Yorkshire Electricity Board and the Electricity Research Centre for the use of their facilities and equipment

Finally, many thanks to my parents and friends for their time and support, which was invaluable to me at all stages of the project.

ABSTRACT.

This thesis investigates the heat transfer involved in the heating of wire in an Electrically-Heated Tubular Strand Annealing Furnace. The fundamental concepts of the furnace are explained, followed by the rationale behind the basic design of the furnace.

This is followed by an experimental investigation of a furnace which is actually used in production at a local wire factory. The overall efficiency of this furnace in heating wire is found to be 69%, as compared with the manufacturer's estimate of 78%. As a consequence of this work, a prototype furnace rig has been designed and set up in the Thermodynamics laboratory, where tests have been carried out on the heating of 2,3 and 4 mm diameter, Austenitic stainless steel, over a temperature range of 20-1000°C. The results from these experiments are then presented, and the prototype furnace is found to be able to anneal Stainless Steel wire at a maximum rate of 5.4 Kg per hour, with an overall efficiency of 60%

The results of the experiments have been analyzed and are subsequently discussed, and the wire temperature profiles corrected for thermocouple installation error. A model is developed to predict the heating of wire due to radiant heat transfer in the prototype furnace. This model is used to predict the temperature profiles of 2,3 and 4 mm diameter, Austenitic Stainless Steel wire being heated in the furnace, with the three heater zones at a set temperature of 1000°C. The results from these simulations suggest that over all the tests presented, the heat transferred to the wire by radiation provides approximately 65% of the energy which is required to heat the wire at the experimentally determined rate.

A second prediction model is then developed which considers the heat transfer to the wire from the process tube by convection, in addition to radiation. The wire temperature profiles predicted using this model are determined to be within approximately 5% of the experimental results. A more complex model is discussed and has been developed, leading to the final model of a multi-tube furnace, and this is used to predict the wire temperature profiles for the multi-tube furnace on which the experimental work was carried out. These are found to be within approximately 10% of the experimental results. This model is then developed into a design tool, for use by the manufacturers to predict the performance of a given furnace design.

CHAPTER 1 INTRODUCTION.

1.1 OBJECTIVE.

The main objective of this project was to investigate the radiant heating in a relatively recently developed wire and strip furnace, manufactured by Meltech Furnaces Ltd (Blackburn). Although the furnace was already being successfully used by many of Meltech's customers, the specific performance parameters of the basic concept of the furnace design were not known. Whilst it was obviously possible to produce a competitive furnace without knowledge of these parameters, there were distinct advantages in ascertaining them.

In the short term, a full knowledge of the physical mechanisms occurring in the furnace could result in the manufacturer being able to design a furnace to a given production specification for a prospective customer. Prior to this project, there was minimal data available for designers to use in producing a furnace with given throughput and process temperatures. Hence much 'guesswork' was required, followed by adjustments after delivery. Therefore, once all the data is available, it will be possible to produce a furnace design, and a quote, more quickly and more accurately.

There is also a long term advantage in possessing this data. At the outset of this project the Meltech furnace was very competitive in terms of capital cost, running costs and quality of product. In order to maintain this position, it was essential to try to progressively improve the product both in terms of operational efficiency, and quality of output.

1.1 BACKGROUND.

This section deals with the question of 'what exactly was the need for such a furnace ?', and how a tubular furnace fulfils such a need. The majority of wire manufactured these days is by cold rolling metal rods. This involves a metal rod undergoing a number of cold rolling operations in order to reduce its diameter to the given size. The action of cold rolling the rod gives rise to the wire being work-hardened by the time it attains its required diameter. When a metal is deformed, stress dislocations are produced in its structure. These dislocations interact with each other, making further deformation of the metal more difficult. This phenomena is known as work-hardening, which is a common and useful means of strengthening metals. However there are two major disadvantages attributed to the metal structure produced in this way;

- The work hardening of a metal is not easily controllable. Certain parts of the metal may be approaching fracture stress, producing localised weaknesses.

- Metals used under high temperatures will become annealed, thus losing their required properties.

A common means of reducing these dislocations, thus rendering the wire more workable, is to anneal the wire. The process of annealing involves heating the wire to the recrystallisation temperature of its metal, which is generally 30 to 40 percent of its melting point.

The wire is then held or 'soaked' at that temperature for a length of time before cooling. The length of the required soak period depends on the type of wire, its initial condition, and the desired properties of the end product. A good starting point for any further heat treatment of a wire is a fully annealed structure.

A common means of annealing wire is to heat coils of wire in what is known as a batch furnace. A batch furnace is essentially a large oven, containing a specified ratio of gases known as a 'furnace atmosphere'. This atmosphere is induced in the furnace in order prevent oxidation of the wire. This atmosphere may consist of either combustion gases or specified mixtures of gases such as Hydrogen, Nitrogen, Argon, air etc. When a batch of wire coils is placed in the batch furnace, it is heated to the required annealing temperature and held at that temperature for the required soak time. There are however inherent disadvantages with this method ;

- Most of the energy supplied to the furnace is wasted in the form of heat lost in heating the whole mass of the furnace and the furnace atmosphere each time a batch is replaced.

- It is very difficult to ascertain the extent of heat treatment attained in all parts of a batch, as there is no guarantee that the required temperature had been attained throughout the batch.

- Time is wasted whilst the furnace is purged, and the required atmosphere maintained.

A process which would overcome these disadvantages is the continuous heat treatment of wire. This involves passing the wire at a constant rate, either in the form of coils, or in strands, through a furnace with a controllable temperature along its length. Such a temperature profile is attained by using a number of individually controlled heated sections, or 'zones' along the length of the furnace.

In the case of a strand furnace, the loss of heat and furnace atmosphere is minimised by passing the strands through heated process tubes inside the furnace. The furnace being investigated is an example of a 'tubular' furnace, which uses electrically heated and controlled zones, leading to the following advantages over an equivalent furnace with gas powered heaters;

- Electrically heated furnaces use less energy ,both whilst the furnace is heating up and when running.

- Electricity is more conducive to a better working environment around the furnace than gas. This is because less fumes are produced and less hazardous materials are being used.

- The size of an electrically heated furnace is smaller than an equivalent gas heated furnace.

The next section deals with the concept of the basic design of the Meltech continuous strand furnace.

1.3 INTRODUCTION TO THE 'MELTECH' FURNACE.

A schematic diagram of the basic design of the Meltech furnace is shown in figures (1-1) and (1-2). The central components of this design are the process tubes, whose number vary according to the desired production capacity of a specific furnace. Each strand of wire is pulled through the furnace at a constant rate by mandrels at the output end of the furnace. The atmosphere inside the process tubes is that of a reducing gas, which flows down the tube at such a rate that the volume of gas in the tube is replaced approximately three times per minute. The direction of gas flow may either be co-flow (ie from the cold end to the hot end of the furnace, with the wire flow), or counter-flow. The most commonly used tube material is presently the Inconel range of Nickel-Chromium-iron alloys, which have excellent physical and thermal properties at elevated temperatures.

Each process tube rests on a rail, which is made of Nitrasil, a type of Silicon Nitride, which is rigid at high temperatures, to prevent it from sagging under its own weight. A typical heating zone is made up of top and bottom heaters, with a bridge, shaped from ceramic fibre block, at each end to support the rails. The heaters are in the form of rectangular ceramic fibre blocks, with embedded Kanthal APM elements. The two sides of a zone are made up of rigidized ceramic fibre blocks, which help to support the top heater.

Each heater is supplied via either a solid state relay, or a thyristor stack, the operation of which is determined by a three part (Proportional-Integral-Differential) temperature controller.

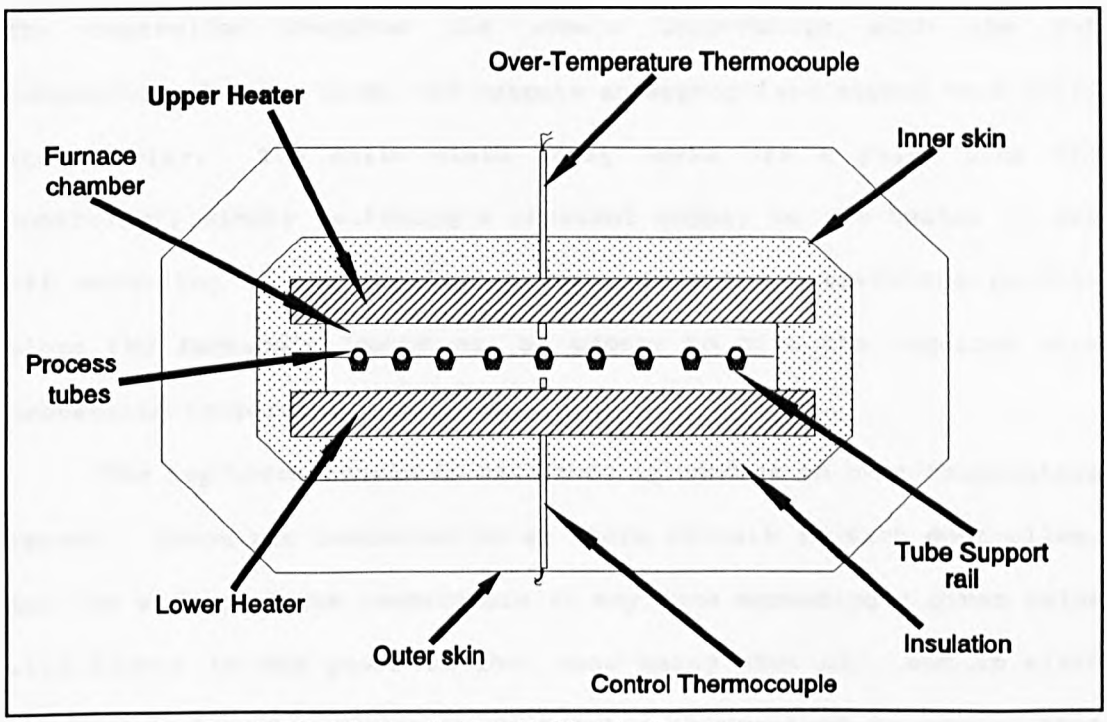

Figure 1-1. Frontal view of the Meltech furnace.

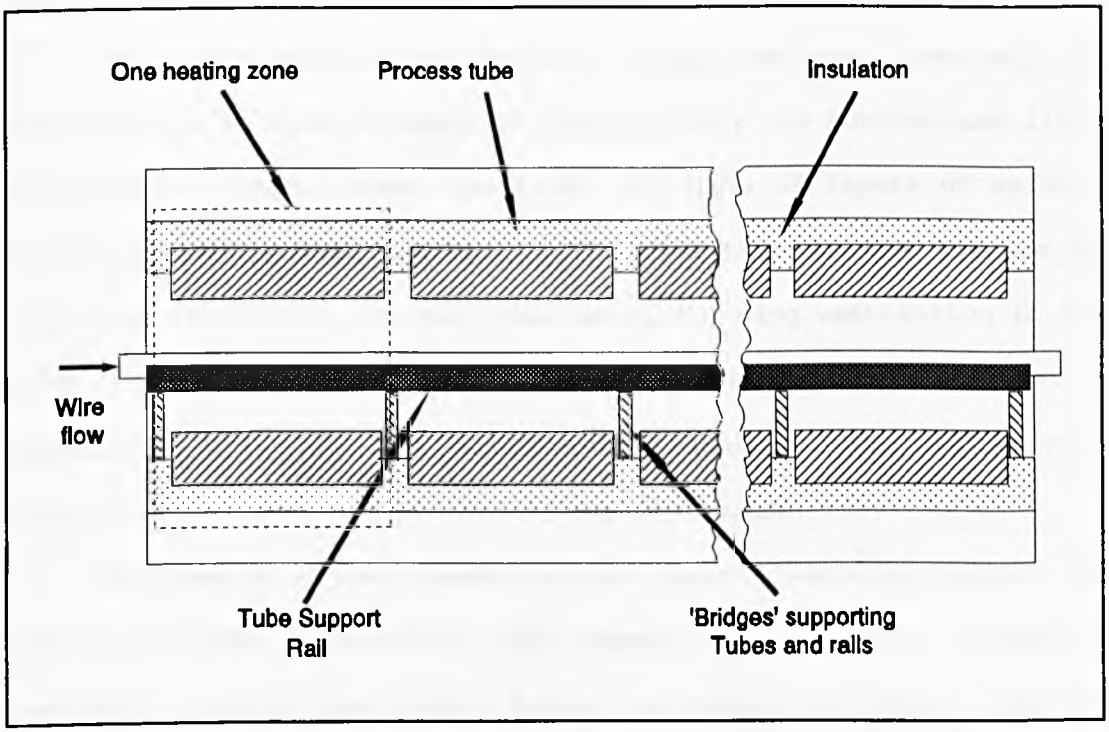

Figure 1-2. Side view of the Meltech furnace.

The zone's temperature is sensed by the control thermocouple, which is situated just below the tubes, in the centre of the zone.

The controller compares the zone's temperature with the set temperature for the zone, and outputs an appropriate signal to a solid state relay. The solid state relay works off a pulse from the controller, simply switching a constant supply to the heater on and off according to the required power. Thus the temperature profile along the furnace's length can be preset to give the required wire processing temperature profiles.

The top thermocouple in each zone is used as an over-temperature sensor. These are connected to an alarm circuit in each controller, and the effect of the temperature in any zone exceeding a given value will result in the power to that zone being shut off, and an alarm sounding. The over-temperature sensing is required to ensure that there is no melt-down of tubes or wire in the event of a fault.

The space between the furnace chamber and the inner skin is insulated to an average depth of approximately one hundred and fifty millimetres. This thermal insulation consists of layers of ceramic fibre blanket packed together. The inner-skin of the furnace is supported inside a perforated outer-skin, allowing ventilation in the space between them. This enables the outer-skin to remain at a temperature of only a few degrees above ambient, even with a core temperature of over a thousand degrees centigrade.

The use of modern insulating and support materials gives the overall furnace a relatively low thermal mass and very effective insulation when compared with a larger gas fired alternative. The low thermal mass of the furnace means that it requires less energy to attain its operating temperature, which leads to shorter start-up periods. The effective insulation of the furnace chamber provokes very efficient running of the furnace.

CHAPTER 2. INTRODUCTION TO THE BASIC THEORY REQUIRED FOR CALCULATING HEAT TRANSFERS IN THE FURNACE.

2.1 INTRODUCTION.

This section gives a brief outline of the theory involved in a simple analysis of the heat transfer in the tube furnace. The chapter then goes on to explain how this theory can be applied to the furnace. The main route of energy transfer in the furnace is in the form of heat transfer from the heaters to the wires, via the process tubes. All the heat transfers take place in a furnace atmosphere; Hydrogen or Nitrogen inside the tubes, and air in the furnace chamber. Therefore there are three modes by which heat is considered to be transferred from the heater panels to the tubes, and from the tubes to the wire. These three modes of heat transfer are conduction, convection and radiation, and these are well explained in Holman [1].

In order for the initial analysis to be made as simple as possible, it was assumed at this point that the only mode of heat transfer taking place in the furnace was radiation (ie between the heaters and tubes, and the tubes and wires). This assumption was based on the fact that when large temperature differences are being considered, conduction and convection are negligible compared to radiation. This is because radiation is based on the difference in the fourth powers of the temperatures involved, whilst the other two are based simply on the difference in the temperatures involved.

2.2 APPLYING RADIATION HEAT TRANSFER THEORY TO THE FURNACE.

This section describes the way that the theory of radiation heat transfer can be applied to a tubular furnace of the configuration identified in chapter 1. Holman [2] gives a detailed account of the various aspects of radiant heat transfer. In order to calculate the radiant transfer in the furnace, it was necessary to consider the heat transfer from the heaters to the tubes, and from the tubes to the wires. To permit the theoretical analysis of this heat transfer the following assumptions were made,

- Each heater had a constant temperature across its area at any given time (ie it was isothermal).

- The tube was circumferentially isothermal at any given point along its length.

- All the tubes were of the same dimensions and material, thus they had the same thermal properties.

- The wire which passed through all the tubes was of the same diameter and material.

- The temperature of the outside of a tube's wall was the same as that of the inside of the wall at any given point on the tube.

- Conduction of heat along the tube walls and along the wires was negligible.

- The effects of the tube support rails and bridges could be neglected.

A general arrangement of process tubes and heaters is shown in figure (2-1) below.

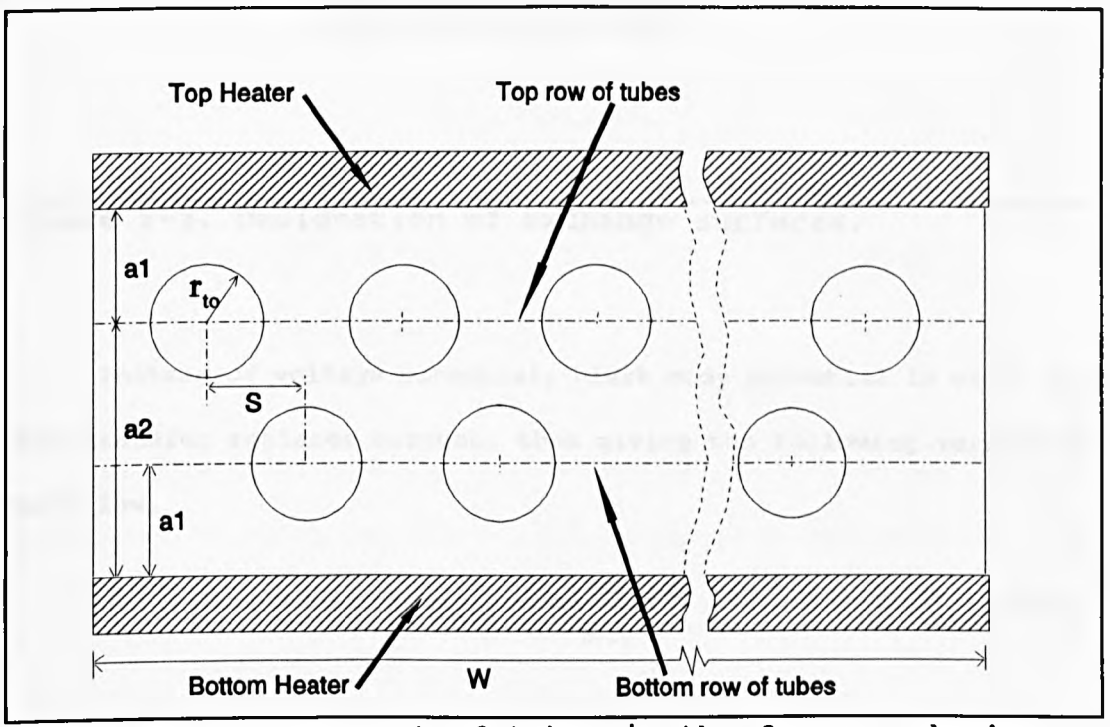

Figure 2-1 Arrangement of tubes in the furnace chamber.

The designation of the exchange surfaces for radiant heat transfer from the heaters to a single tube and wire is illustrated in figure (2-2). Holman [2] describes a method of determining radiative heat transfer between more than two surfaces, known as the network theory. This method splits the problem into a series of thermal resistances, which are analogous to electrical resistance, as illustrated in figure (2-3(i)).

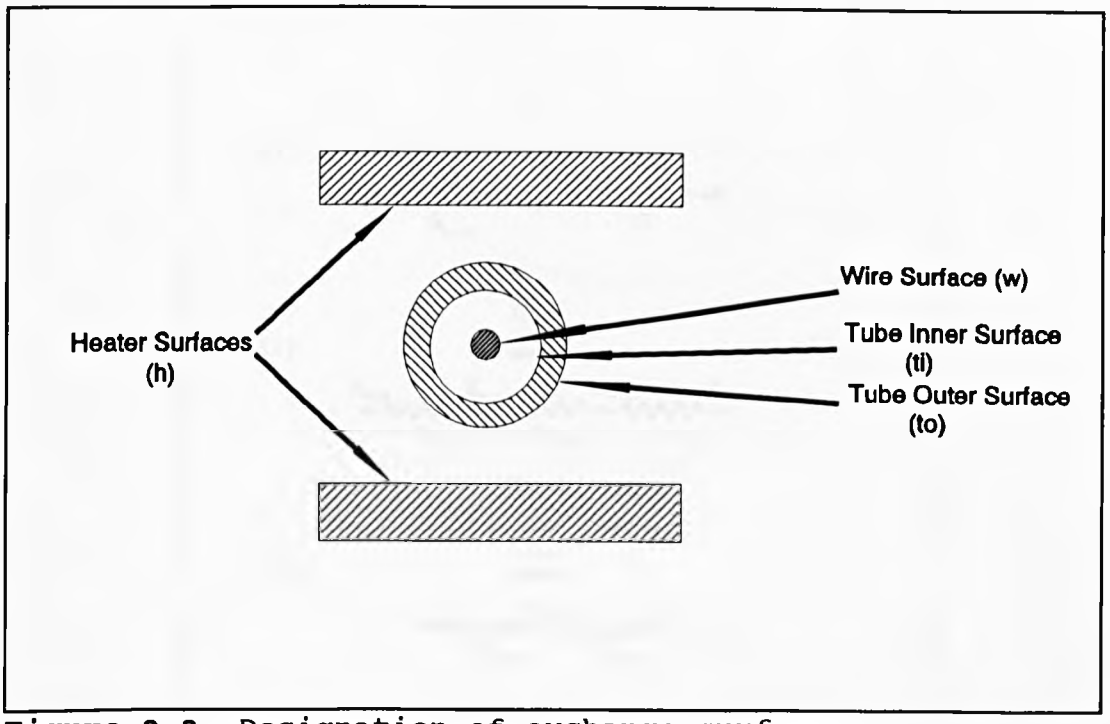

Figure 2-2. Designation of exchange surfaces.

Instead of voltage potential, black body potential is used, and heat transfer replaces current, thus giving the following version of Ohm's law,

$$q_{h-to}=\frac{E_{b,h}-E_{b,to}}{R_{h-to}} \qquad \textbf{(2-1)}$$

If the outside of the tube is considered not to exchange heat with the other tubes, or the side walls of the furnace, then the only heat transfer is between it and the area of heaters which it can see.

Similarly, as the wire is enclosed by the tube, it only exchanges heat with the inner surface of the tube. Therefore all the heat absorbed by the outer surface of the tube is then transferred to the inner surface, and then to the wire.

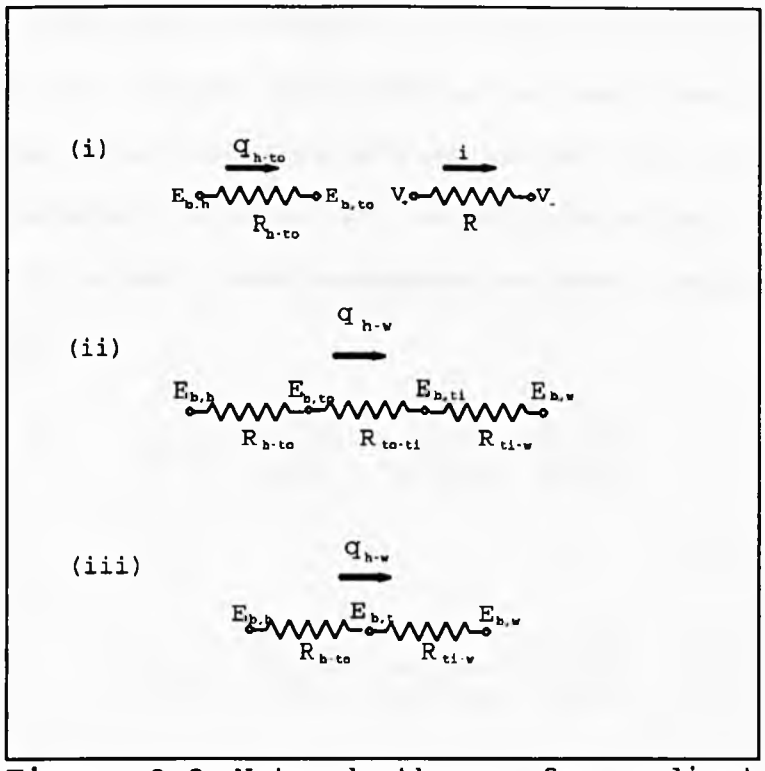

Figure 2-3 Network theory for radiant heat transfer.

Hence a network of thermal resistances can be produced, as shown in figure (2-3(ii)). As the assumption has been made that the inner surface of the tube is at the same temperature as the outer surface, the following simplifications can be made,

$$E_{b,to}=E_{b,ti}=E_{b,t} \qquad \textbf{(2-2)}$$

And therefore,

$$R_{to\text{-}ti}=0 \qquad \textbf{(2-3)}$$

Thus the network is simplified to that shown in figure (2-3(iii)).

Each of the network elements in figure (2-3(iii)) is made up of three parts; two 'surface' resistances and a 'space' resistance. A surface resistance joins a surface and its radiosity potential, and the space resistance joins the two radiosity potentials. Therefore the two network elements have resistances as shown by equations (2-4) and (2-5) below.

$$R_{h-to}=\frac{(1-\epsilon_h)}{\epsilon_h \cdot A_h}+\frac{1}{A_h \cdot F_{h-to}}+\frac{(1-\epsilon_t)}{\epsilon_t \cdot A_{to}} \qquad \textbf{(2-4)}$$

$$R_{ti-w}=\frac{(1-\epsilon_t)}{\epsilon_t \cdot A_{ti}}+\frac{1}{A_{ti} \cdot F_{ti-w}}+\frac{(1-\epsilon_w)}{\epsilon_w \cdot A_w} \qquad \textbf{(2-5)}$$

The total resistance between the heater surface and surface of the wire is the summation of the two resistances above, as in equation (2-6).

$$R_{h-w}=R_{h-to}+R_{ti-w} \qquad \textbf{(2-6)}$$

Thus the radiant heat transfer from surface one to surface three is given by,

$$Q_{h-w}=\frac{E_{b,h}-E_{b,w}}{R_{h-w}} \qquad \textbf{(2-7)}$$

Where $E_{b,h}$ and $E_{b,w}$ are the black body potentials of the heaters and the wire respectively, and are found from the Stefan-Boltzmann equation, as in equation (2-8) overleaf.

$$E_{b,h}=\sigma \cdot T_h^4$$
$$E_{b,w}=\sigma \cdot T_w^4 \qquad (2\text{-}8)$$

Where $\sigma=5.669 \times 10^{-8}$ $(W/M^2.K^4)$ and T_h and T_w are the absolute temperatures of the heaters and the wire respectively.

The thermal resistance is dependent on both the thermal properties of the surfaces, and the geometrical configuration of the surfaces. The thermal properties involved are the emissivities of the surfaces, ϵ_h, ϵ_t and ϵ_w. The emissivities are dependent on many factors, such as wavelength of incident radiation, direction of radiation, condition of surface and surface temperature. For the purposes of this analysis, total hemispherical emissivity is considered for a given surface condition. The Total Hemispherical Emissivity is only dependent on surface temperature. Therefore the emissivities of the surfaces are given as a function of their temperature ,

$$\epsilon_h=\epsilon_h(T_h)$$
$$\epsilon_t=\epsilon_t(T_t) \qquad (2\text{-}9)$$
$$\epsilon_w=\epsilon_w(T_w)$$

A number of functions for the emissivity of various materials with various surface conditions are given in appendix C.

The following geometric factors are also required in order to calculate the thermal resistances $R_{h\text{-}to}$ and $R_{ti\text{-}w}$.

A_h : The exchange area on the heaters' surface.

A_{to}: The exchange area on the outer surface of the tube.

A_{ti}: The exchange area on the inner surface of the tube.

A_w : The exchange area on the surface of the wire.

$F_{h\text{-}to}$: The proportion of the radiant energy leaving area A_h which is incident on area A_{to}.

$F_{ti\text{-}w}$: The proportion of the radiant energy leaving area A_{ti} which is incident on area A_w.

Initially the exchange areas of the surfaces were considered. An exchange area is defined as the area on a surface which exchanges heat by radiation with the exchange area on another surface. The exchange areas for two surfaces exchanging heat with each other by radiation may be defined as all parts of each surface which view directly any part of the other surface. As the surfaces are not isothermal along the length of the furnace, it is necessary to consider exchange between areas of differential length dx, as in figure (2-4).

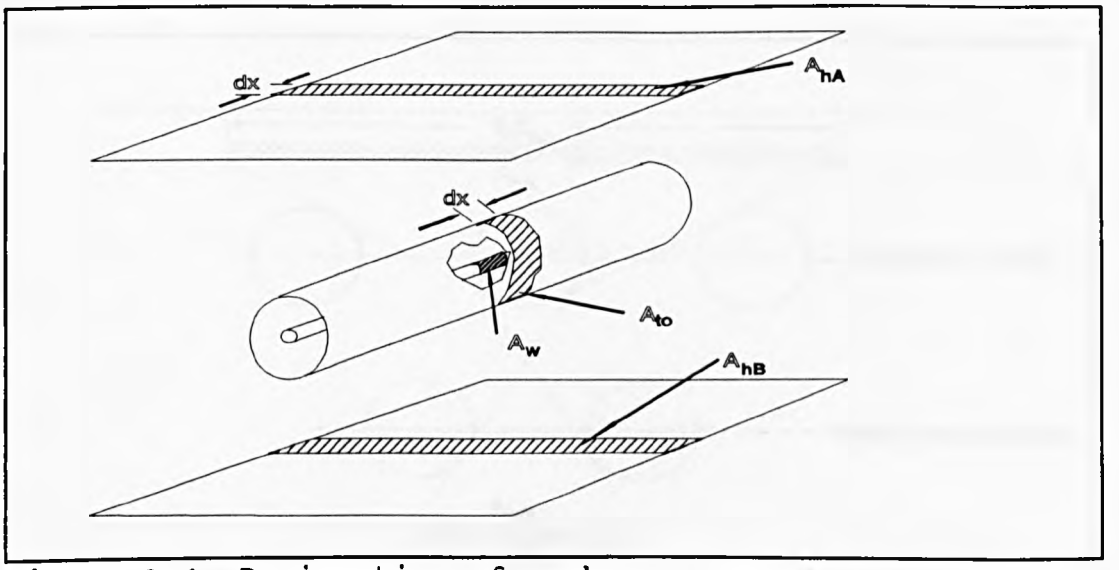

Figure 2-4. Designation of exchange areas.

The required areas on the wire and on the inside of the tube are respectively,

$$A_w = \Pi \cdot D_w \cdot dx$$
$$A_{ti} = \Pi \cdot D_{ti} \cdot dx \qquad \textbf{(2-10)}$$

The exchange area on the outside of the tube does not extend all around the circumference of the tube, as some of the tube does not actually see either the top heater, or the bottom heater. However, this is taken into account by the view factor, so the exchange area can be written,

$$A_{to} = \Pi \cdot D_{to} \cdot dx \qquad \textbf{(2-11)}$$

The determination of the exchange area of the surface of the two heater panels is less straight-forward. If the configuration of tubes shown in figure (2-1) is considered, it is evident that a given tube on either row has its view of the heaters obstructed by adjacent tubes. The areas of each panel which view a given tube (surface to) on the top row are shown in figure (2-5).

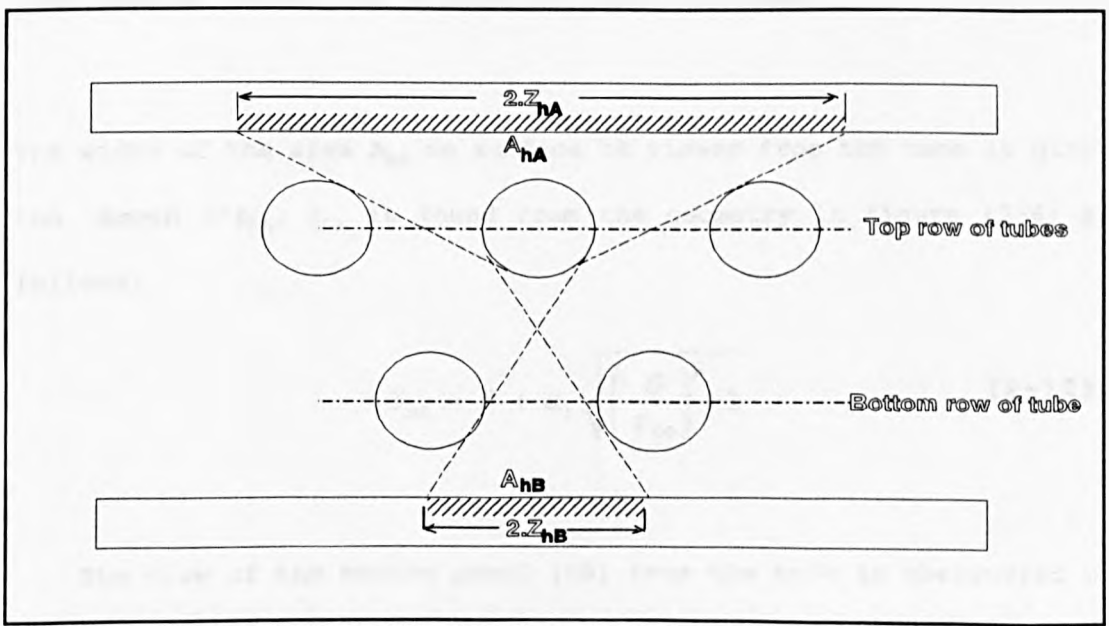

Figure 2-5 Areas on the heater panels which view a tube on the top row.

The top panel is labelled surface hA, and the bottom panel is labelled surface hB for the purpose of this analysis. The view of the top heater panel from a tube on the top row is obstructed by the two adjacent tubes in that row, as depicted in figure (2-6) below.

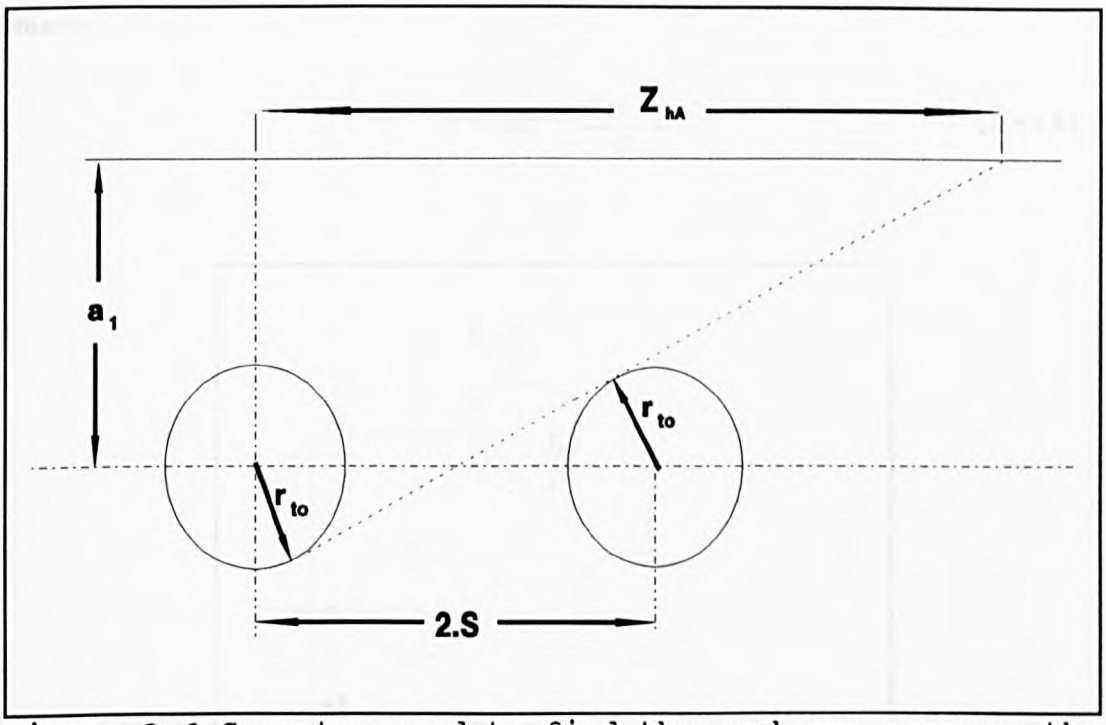

Figure 2-6 Geometry used to find the exchange area on the top heater panel to a tube on the top row.

The width of the area A_{hA} on surface hA viewed from the tube is given the length $2*Z_{hA}$. Z_{hA} is found from the geometry in figure (2-6) as follows;

$$Z_{hA} = S + a_1 \cdot \sqrt{\left(\frac{S}{r_{to}}\right)^2 - 1} \qquad \textbf{(2-12)}$$

The view of the bottom panel (hB) from the tube is obstructed on either side by tubes on the bottom row. The length of the area A_{hB} on surface hB viewed from the tube is given the length $2*Z_{hB}$.

The value of Z_{hB} is calculated from the dimensions and geometry shown in figure (2-7), as follows,

$$Z_{hB} = S + a_1 \cdot \tan\alpha - \frac{r_{to}}{\sin\alpha} \qquad \textbf{(2-13)}$$

Where,

$$\alpha = \tan^{-1} \cdot \frac{a_2 - a_1}{S} \qquad \textbf{(2-14)}$$

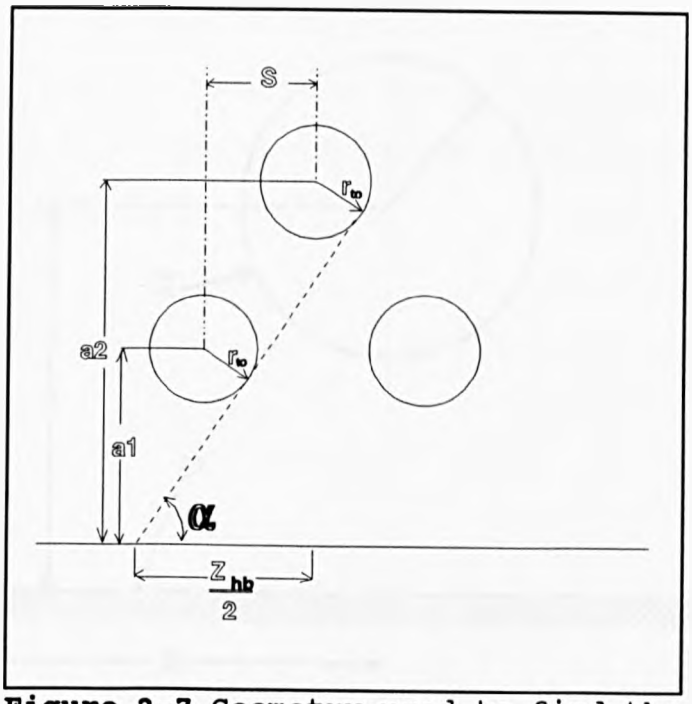

Figure 2-7 Geometry used to find the exchange area on the bottom heater panel.

Therefore the total length of the heater panels which are viewed from a tube on the top row is,

$$Z_h = 2 \cdot (Z_{hA} + Z_{hB}) \qquad \textbf{(2-15)}$$

Due to the symmetry of the geometry, it can be assumed that this exchange area of the heater applies to all tubes on the top and bottom rows of the chamber.

The next task was to determine the view factor from the exchange area on the heater panels to the tubes. The geometry in figure (2-8) is that of a flat rectangle of finite width '2b' and finite length, a distance 'a' from the axis of a parallel cylinder of radius 'r' and of finite length.

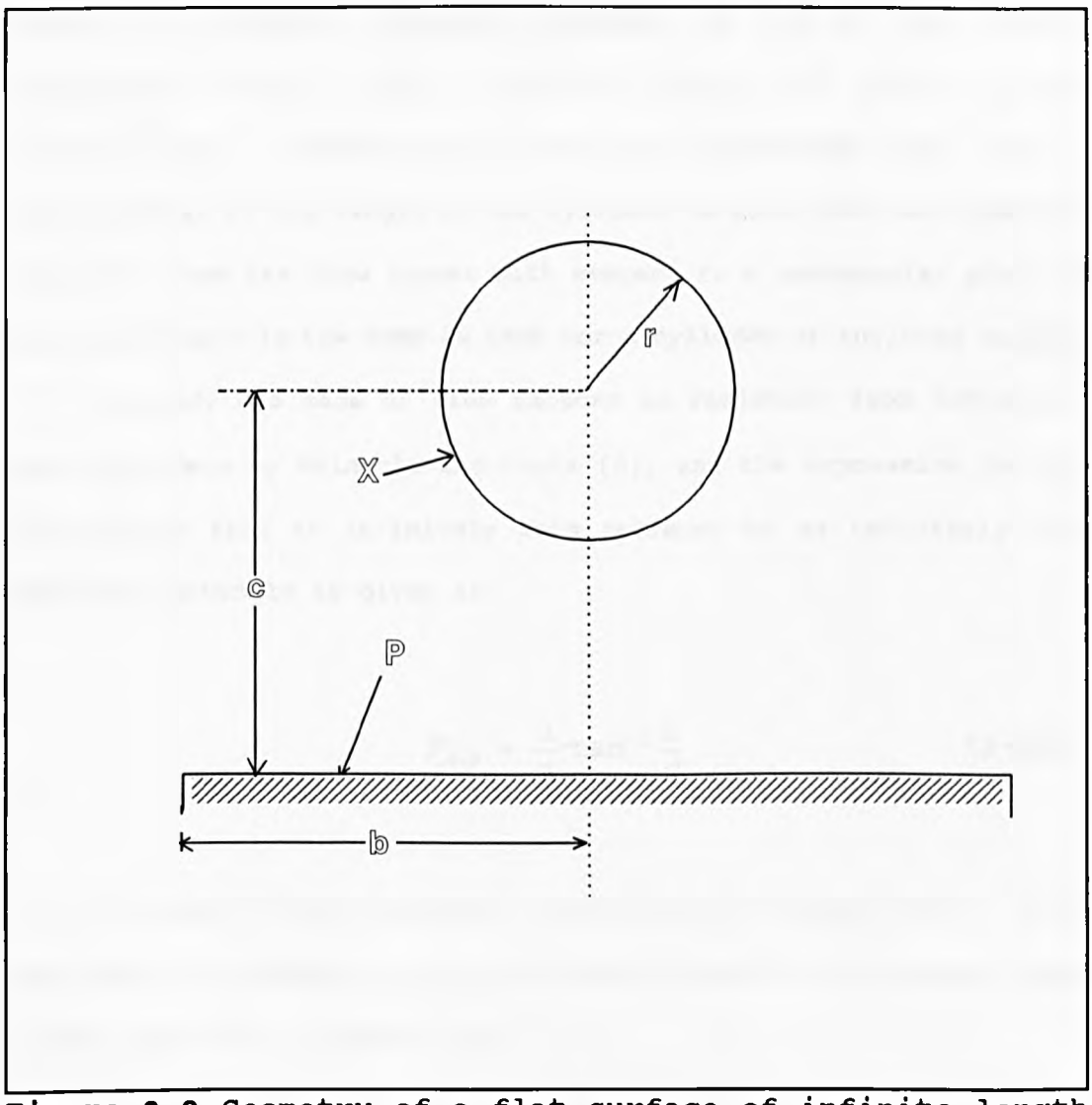

Figure 2-8 Geometry of a flat surface of infinite length radiating to a cylinder of infinite length.

Leuenberger and Person [3] present a number of radiation view factors for cylindrical assemblies. The view factor from a differential area on one surface to a differential area on another surface is found using the laws of geometrical optics.

This is then integrated over the whole area of both the required surfaces, to give the view factor from one finite surface to another, resulting in a complex algebraic expression. The view factor for the configuration shown in figure (2-8) is considered by Wiebelt and Ruo [4], who present values for the view factor F_{p-x} from a rectangular plane to a parallel cylinder, obtained by use of the Contour Integration method, using a digital computer to carry out the numerical work. Observation of the results presented gives rise to the fact that if the length of the cylinder is more than ten times its diameter, then its view factor with respect to a rectangular plane of the same length is the same as that for a cylinder of infinite length.

A study was made of view factors in radiation from infinitely long cylinders by Feingold and Gupta [5], and the expression for the view factor from an infinitely long cylinder to an infinitely long parallel rectangle is given as,

$$F_{x-p} = \frac{1}{\pi} \cdot \tan^{-1} \frac{b}{c} \qquad \textbf{(2-16)}$$

In terms of the dimensions illustrated in figure (2-8). Using the theory of reciprocity, the view factor from the rectangular plane to the cylinder is found to be,

$$F_{p-x} = \frac{r}{b} \cdot \tan^{-1} \frac{b}{c} \qquad \textbf{(2-17)}$$

In the case of the top heater panel (A), $b=Z_{hA}$ and $c=a_1$. Therefore the configuration factor F_{hA-to} is given by,

$$F_{hA-to} = \frac{r_{to}}{Z_{hA}} \cdot \tan^{-1} \frac{Z_{hA}}{a_1} \qquad \textbf{(2-18)}$$

In the case of the bottom heater panel (B), $b=Z_{hB}$ and $c=a_2$. Therefore the configuration factor $F_{hB\text{-}to}$ is given by,

$$F_{hB\text{-}to}=\frac{r_{to}}{Z_{hB}}\cdot\tan^{-1}\frac{Z_{hB}}{a_2} \qquad \textbf{(2-19)}$$

If q represents the heat flux over both heater areas, then the total heat from the exchange area on the top heater (A) is given by,

$$Q_A = 2\cdot q\cdot Z_{hA}\cdot dx \qquad \textbf{(2-20)}$$

Thus the heat reaching the tube area A_{to} from the heater area A_{hA} is given by,

$$Q_{hA\text{-}to}= 2\cdot F_{hA\text{-}to}\cdot q\cdot Z_{hA}\cdot dx \qquad \textbf{(2-21)}$$

Similarly the total heat from the bottom heater (B) is given by,

$$Q_B = 2\cdot q\cdot Z_{hB}\cdot dx \qquad \textbf{(2-22)}$$

Thus the heat reaching the tube area A_{to} from heater area A_{hB} is given by,

$$Q_{hB\text{-}to}= 2\cdot F_{hB\text{-}to}\cdot q\cdot Z_{hB}\cdot dx \qquad \textbf{(2-23)}$$

Therefore the total heat leaving the two areas is given by,

$$Q = Q_A+Q_B= 2\cdot(Z_{hA}+Z_{hB})\cdot q\cdot dx \qquad \textbf{(2-24)}$$

And the total heat incident on the tube area A_{to} from the heaters can be deduced from an energy balance and is given by,

$$Q_{h\text{-}to}=Q_{hA\text{-}to}+Q_{hB\text{-}to}= 2\cdot(F_{hA\text{-}to}\cdot Z_{hA}+F_{hB\text{-}to}\cdot Z_{hB})\cdot q\cdot dx \qquad (2\text{-}25)$$

Thus the proportion of the total heat leaving the heaters which is incident on the tube is given by,

$$F_{h\text{-}to}=\frac{Q_{h\text{-}to}}{Q} \qquad (2\text{-}26)$$

$$F_{h\text{-}to}=\frac{F_{hA\text{-}to}\cdot Z_{hA}+F_{hB\text{-}to}\cdot Z_{hB}}{Z_{hA}+Z_{hB}} \qquad (2\text{-}27)$$

And the exchange area on the heaters is given by,

$$A_h=A_{hA}+A_{hB}= 2\cdot(Z_{hA}+Z_{hB})\cdot dx \qquad (2\text{-}28)$$

Due to the symmetry of the arrangement the view factors and exchange areas for all the tubes are equal to those given above. (NB. It is assumed that the effects of the side walls are negligible.)

The view factor between the inside of the tube and the wire is analogous to that of two concentric, parallel cylinders of infinite length. As the wire is fully enclosed inside the tube, the view factor from the wire to the inner surface of the tube, $F_{w\text{-}ti}$ is 1. Using the theory of reciprocity, the view factor from the tube to the wire is found as follows,

$$F_{ti\text{-}w} = \frac{A_w}{A_{ti}}\cdot F_{w\text{-}ti} = \frac{D_w}{D_{ti}} \qquad (2\text{-}29)$$

This completes the determination of all the variables required to find the thermal resistance R_{h-w}, and hence the radiant heat transferred.

2.3 THEORY OF THE HEAT ABSORBED BY THE WIRE.

When an enclosure contains a body of mass M (Kg) and is given energy E (Joules), the temperature T (K) of that mass will increase by dT, which is given by,

$$dT = \frac{E}{M \cdot C(T)} \qquad \textbf{(2-30)}$$

Where C(T) is the specific heat of the material (Joules/Kg.K) and is a function of the temperature of the material. A number of C(T) functions are shown in Appendix C. If equation (2-30) is differentiated with respect to time t, then the following expression will result,

$$dT = \frac{Q}{\dot{M} \cdot C(T)} \qquad \textbf{(2-31)}$$

Where Q is the rate of heat transfer to the body (Watts) and $\dot{M}$ is the mass flow rate of material (Kg/sec).

2.4 A SIMPLE MODEL FOR THE HEAT TRANSFER.

Equation (2-31) can be used to give the temperature rise of a differential length dx of wire passing through the furnace. Thus if an element of wire is considered of length dx, and cross-sectional area of A_{dx}, then the mass of this element is,

$$M_{dx}=\rho \cdot A_{dx} \cdot dx \qquad (2\text{-}32)$$

Where ρ is the density of the wire material. The mass flow rate of wire through the given enclosure of length dx is therefore given by,

$$\dot{M}=\rho \cdot A_{dx} \cdot V \qquad (2\text{-}33)$$

Where V is the wire speed in metres per second.

Therefore if the heat transfer rate to the element of length dx is given by Q, then the rise in the temperature of the element is given by,

$$dT=\frac{Q}{\rho \cdot A_{dx} \cdot V \cdot C} \qquad (2\text{-}34)$$

Rewriting equation (2-34) in terms of the variables used in the radiant heat analysis gives,

$$dT_w=\frac{4 \cdot Q_{h\text{-}w}}{\rho_w \cdot \pi \cdot D_w^2 \cdot C(T_w)} \qquad (2\text{-}35)$$

Where $Q_{h\text{-}w}$ is the radiant heat transferred from the heaters at a given point along the wire.

In order to produce a temperature profile of the wire along the isothermal heating zone due to the radiant heat transfer from the heaters, an iterative procedure is required.

As the initial temperature of the wire at the start of an element dx is known, the radiant heat transfer to the wire can then be found using equation (2-7). The radiant heat transfer (Q_{h-w}), the mass flow rate and the specific heat of the wire are then substituted into equation (2-35) in order to find the temperature rise of the wire, dT_w along the length dx of the elemental wire area. This temperature rise is then added to the initial temperature to become the initial temperature for the next iteration.

In some cases the radiant heat transfer to the wire resulting from the temperature difference between the wire and heaters was in excess of the maximum rating of the heater panels used. In such an event the temperature rise dT_w was calculated from the heater's maximum power rating. The total length of the heaters required was determined by the number of iterations which were required for the wire to reach its required process temperature and to undergo the required 'soak' time at this temperature. A summation of the iterated heat transfers was then carried out to obtain the total heat transferred to the wire as it passed through the furnace. This value was then multiplied by the number of wires which were being processed to provide the total heat transferred from the heaters. This method presented a model of the heating process of the wire. However a considerable number of calculations are necessary to obtain reasonable results. This is because the required properties of the tube are temperature dependent, thus requiring the temperature of the tube to be calculated which involves another iterative process.

However initial calculations were carried out using constant thermophysical properties for the tube.

The final point to consider here is that the radiative transfer was only considered in two dimensions (ie only from an element on the tube to the adjacent element on the wire) as illustrated in figure (2-9(i)). A more comprehensive model would have considered the heat transfer from the whole of the tube to a single element on the wire as in figure (2-9(ii)).

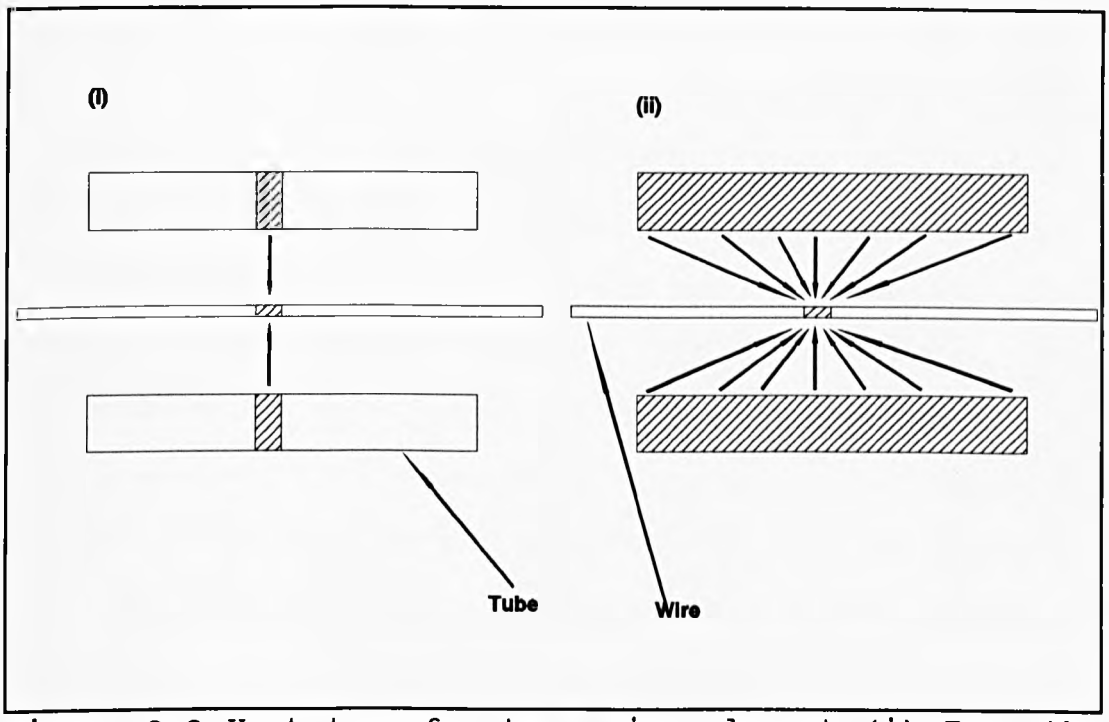

Figure 2-8 Heat transfer to a wire element (i) From the adjacent tube element,(ii) From the whole of the tube surface.

Because the tube is not isothermal, many isothermal surface elements need to be considered, thus requiring a large number of numerical calculations to determine the heat transfer from the whole tube to a single element on the wire.

Although the surface of the tube is not isothermal, the total heat transfer from the tube element to the wire element as in figure (2-8(i)) may be considered to be approximately equal to the total heat transfer from that tube element to all the elements on the wire when heat is being transferred from the whole area on the tube surface to the whole area on the wire surface. Therefore the heat transfer from an elemental area on the tube to the adjacent wire element can be considered to be approximately equal to that from the whole area on the tube surface to the wire element.

CHAPTER 3. EXPERIMENTAL WORK CARRIED OUT 'ON SITE' AT CRITCHLEY SHARP AND TETLOWS.

3.1 INTRODUCTION.

In order to verify any theoretical model produced, it was essential to acquire some data on a furnace to which the model was to be applied. The data required was the parameters of the furnace which effect the performance of the furnace. The data was collected from a nineteen-tube, twelve-zone Meltech furnace, which was in operation at Critchley, Sharp and Tetlow.

The furnace was used to anneal austenitic stainless steel wire of a variety of compositions and diameters, using a furnace atmosphere of pure hydrogen flowing at approximately two tube volumes per minute in the opposite direction to the wire. The hydrogen from the tubes ignited harmlessly as it passed out of the end of the tubes. The basic dimensions of the furnace are given in figures (3-1) and (3-2).

The twelve zones were each heated by a pair of electric heaters, each pair with a total power rating of 6.4 Kilowatts, giving the furnace a total power rating of 76.8 Kilowatts.

There were two types of experiment which were carried out on the furnace in order to establish the various factors of its operation. The first of these was a start-up test which involved measuring various parameters of the furnace whilst it heated up to its required operating temperature.

The other test carried out was the running test,which was to determine the parameters of the furnace whilst it was processing wire.

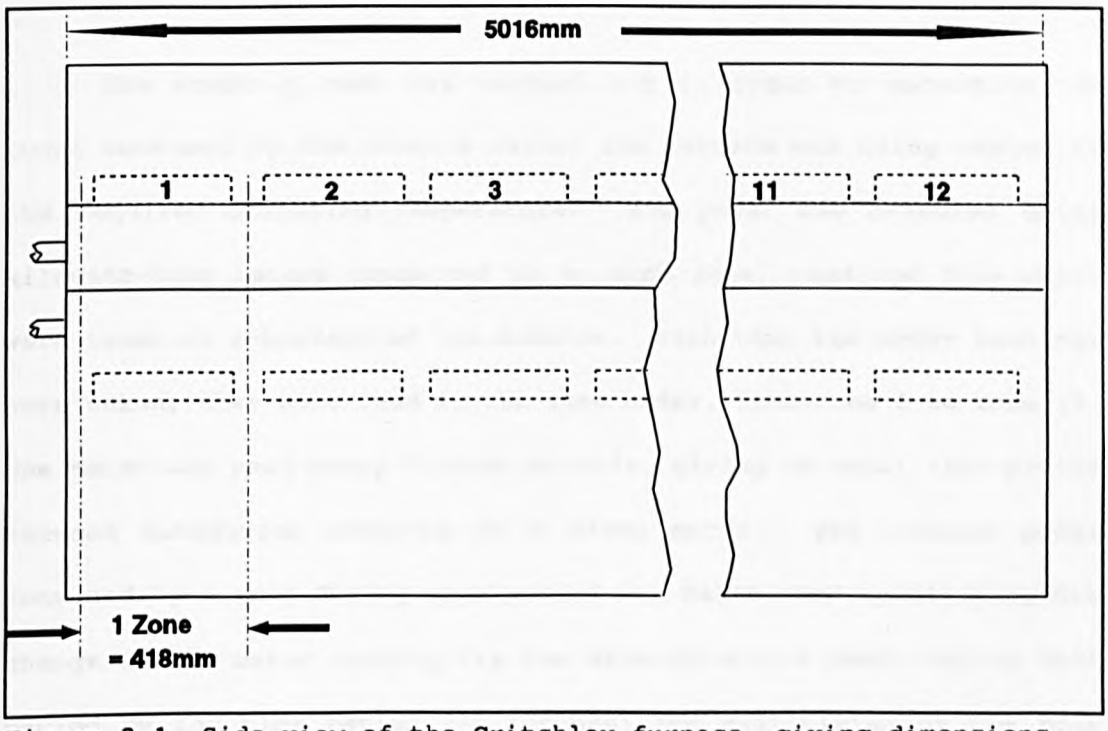

Figure 3-1. Side view of the Critchley furnace, giving dimensions.

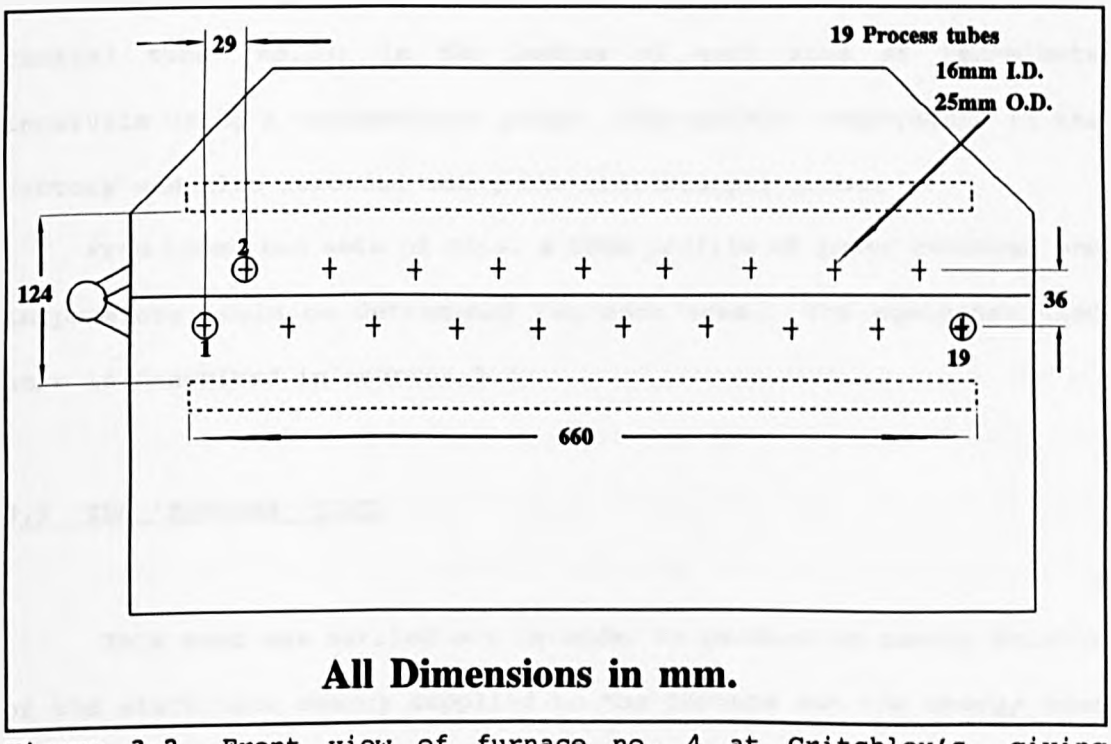

Figure 3-2. Front view of furnace no. 4 at Critchley's, giving dimensions.

3.2 THE 'START-UP' TEST.

The start-up test was carried out in order to determine the power consumed by the heaters whilst the furnace was being heated to its required operating temperature. The power was measured using kilowatt-hour meters connected up to each zone, readings from which were taken at intervals of ten minutes. Each time the meter readings were taken, they were read in the same order, from zone 1 to zone 12. One meter was read every fifteen seconds, giving an equal time period between subsequent readings of a given meter. The average power consumed by a zone during each period was calculated by dividing the change in its meter reading (ie the kilowatt-hours used) during that period by the time period (in seconds) and multiplying by one hour (3600 seconds).

In addition to this, temperature readings were taken in the central tube (no.10) in the centre of each zone at ten-minute intervals using a thermocouple probe. The ambient temperature in the factory was also recorded using the thermocouple probe.

From these two sets of data, a time profile of power consumed and temperature could be determined for each zone. The equipment used here is described in section 3.4 .

3.3 THE 'RUNNING' TEST.

This test was carried out in order to produce an energy balance of the electrical energy supplied to the furnace and the energy used to heat the wire. Data from this test was also used in a simple analysis of the radiant heat transfer taking place in the furnace.

As the furnace was running with a constant throughput of wire, most of the parameters of the furnace did not vary with time. In order to find the power used in heating the wires in the furnace, the following data was required for each of the wires being processed.

- Material - various types of austenitic stainless steel wire were processed at once. This information was obtained from production data at the factory.

- Diameter - Various gauges of wire were being processed, thus the diameter of each wire was obtained from production data. In addition to this, a sample of each wire was measured using a micrometer.

- Speed - Each size of wire being processed was pulled through the furnace at a different speed. This data was found by measuring the rotational speed of the mandrels which pulled the wires through the furnace.

- Temperature - the temperature in each tube at the beginning and end of each zone was measured using a thermocouple probe. In practice it was found that it was not possible to push the probe down a number of the tubes because they were partially blocked. Such a blockage was due to the lubricating soap present on the wire's surface congealing on the inner surface of the process tube. The set temperatures of each zone were also required, and these were taken from the displays on the controllers located on the side of the furnace.

Finally the ambient temperature in the factory was measured using the thermocouple probe. In addition to the wire data, the power consumed by each zone was measured using kilowatt-hour meters. In this case, just three or four sets of readings were taken from each meter over a three hour period. The time each reading was taken was also noted as in the start-up test. The equipment used is described in the following section.

3.4 EQUIPMENT USED.

This section describes the equipment used to measure the various parameters in both tests.

(i) Power consumption in each zone. - This was measured in both tests using twelve KiloWatt-hour meters on loan from the Yorkshire Electricity Board. The type of meter used was a common type rated at 240 volts A.C., with an accuracy of ±1%. The photograph in figure - (3-3) shows the meters installed on the side of the furnace, and figure (3-4) shows the wiring diagram for each of the meters.

(ii) Temperatures inside tubes. - The probe used to measure the temperatures in the tubes is shown in figure (3-5). The thermocouple used was a Gordon k-type mineral insulated thermocouple with an inconel sheath of 1.5 millimetres diameter, and length of twenty feet. When the thermocouple was inserted into a furnace tube, it was found to buckle, thus the position of the end along the tube could not be accurately determined.

Figure 3-3. Photograph showing the Kilowatt-hour meters installed on the Furnace.

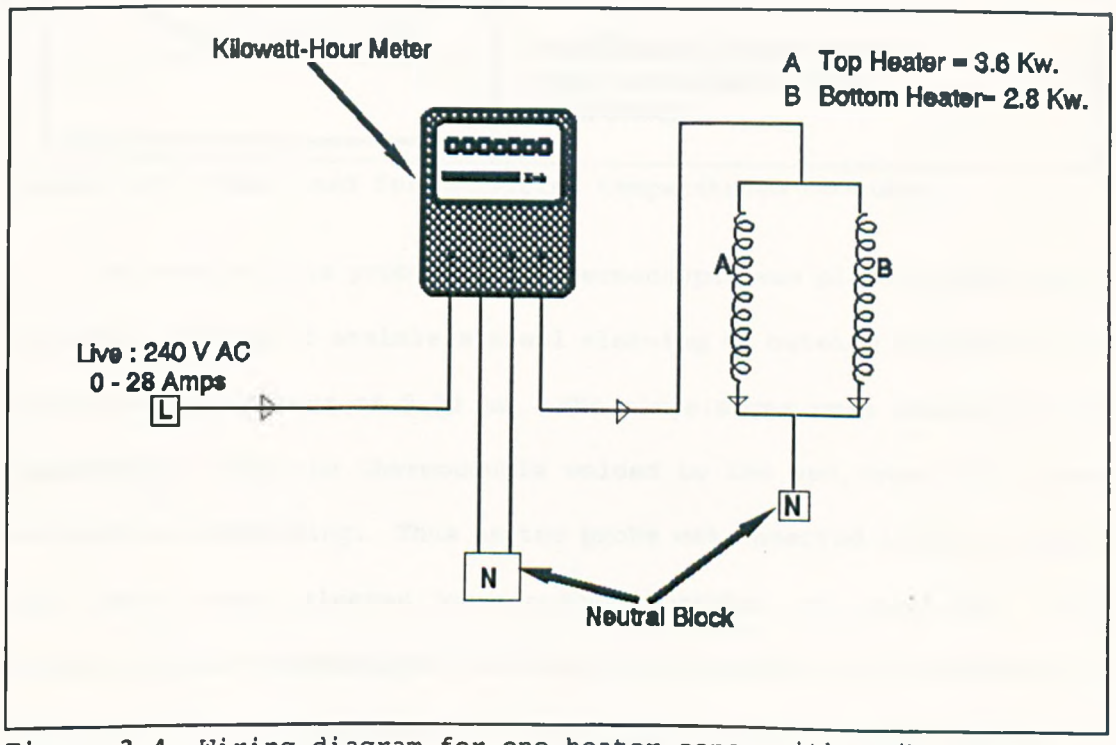

Figure 3-4. Wiring diagram for one heater zone, with KW/hr meter.

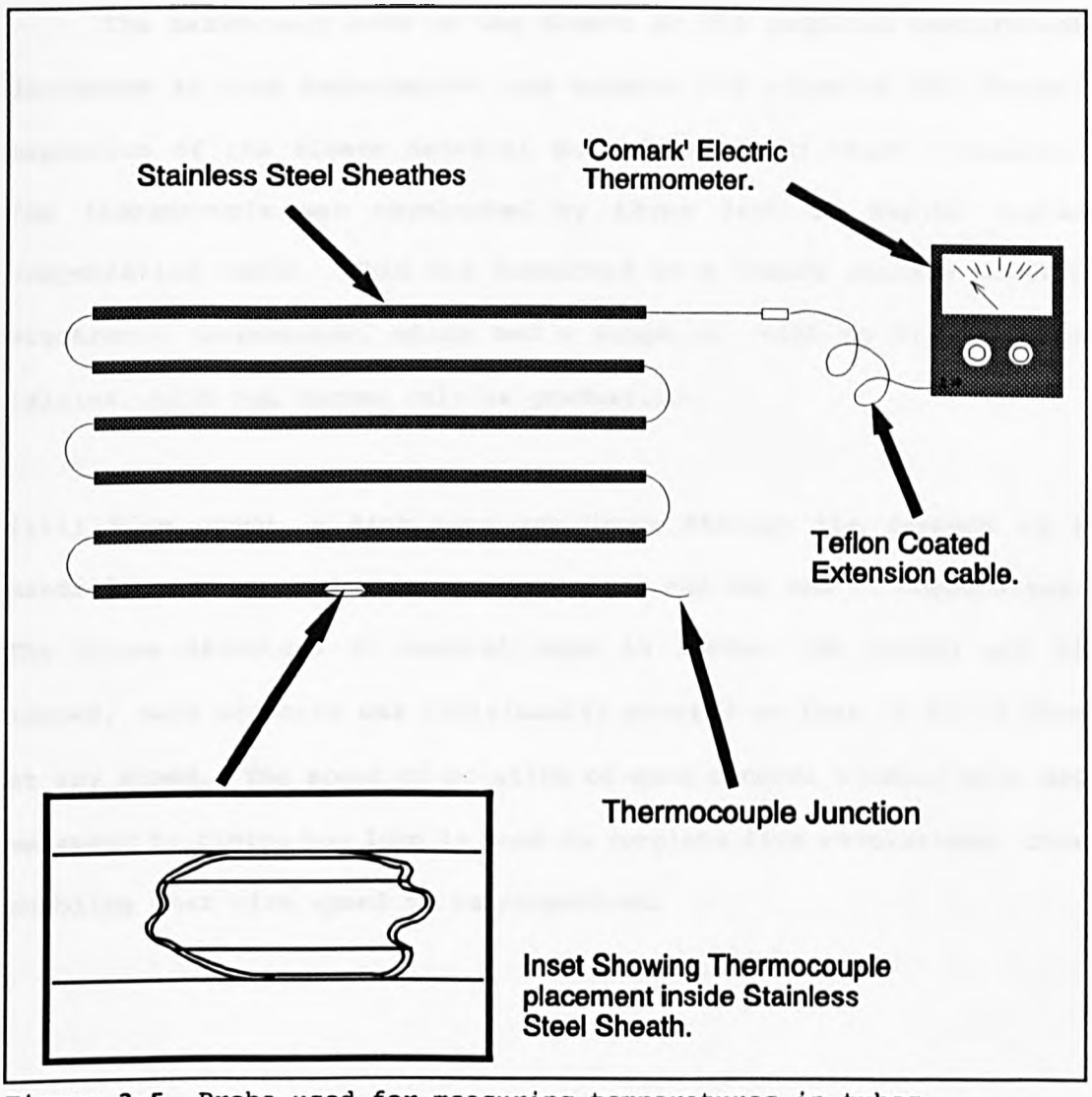

Figure 3-5. Probe used for measuring temperatures in tubes.

To resolve this problem, the thermocouple was placed inside six, one metre lengths of stainless steel sleeving of outside diameter 4.04 mm and wall thickness of 0.38 mm. The six sleeves were placed on the thermocouple, and the thermocouple welded to the end tube with three centimetres protruding. Thus as the probe was inserted into a furnace tube, more outer sleeves were pushed together as required. The position of the thermocouple junction in the furnace was determined by marks put onto the sleeves, which were lined up with a reference point on the outside of the furnace.

The marks were made on the sleeve at the required measurement distances at room temperature, and account was taken of the thermal expansion of the sleeve material when determining these distances. The thermocouple was terminated by three feet of teflon coated compensating cable. This was connected to a Comark battery powered electronic thermometer, which had a range of -120 to 1100 degrees celsius, with one degree celsius graduations.

(iii) Wire speed. - Each wire was drawn through the furnace by a mandrel which rotated at a constant speed and was one of three sizes. The three diameters of mandrel were 16 inches, 18 inches and 22 inches, each of which was individually powered so that it could wind at any speed. The speed of rotation of each mandrel winding wire was measured by timing how long it took to complete five revolutions, thus enabling that wire speed to be determined.

CHAPTER 4. ANALYSIS AND DISCUSSION OF THE EXPERIMENTAL RESULTS FROM THE TESTS CARRIED OUT 'ON-SITE' AT CRITCHLEY, SHARP AND TETLOW.

4.1 PRESENTATION OF THE 'START-UP' TEST RESULTS.

This test was carried out three times, each test lasting approximately two and a half hours. The results presented in this report are from the test carried out on Sunday 1st May 1990, which was the only time that all the heaters were fully operational.

The readings taken from the meters and from the thermocouple probe are shown in Appendix D, tables (D-1.1) to (D-1.3) and (D-2.1) to (D-2.3) respectively. A 'Fortran' computer program was used to convert the Kilowatt-hour readings and times taken into power (Kw), the results from which are shown in tables (D-3.1) to (D-3.3) in Appendix D. Another 'Fortran' program was used to produce the power-time and the temperature-time profiles for each zone which are shown in section 4.7, figures (4-1) to (4-12).

4.2 ANALYSIS OF THE 'START-UP' TEST RESULTS.

The graphs in figures (4-1) to (4-12) show that the power consumed by each zone decreases as the temperature of the zone increases. In general the power consumed became constant for each zone when the set temperature of that zone was reached. This power level could be assumed to be that which was required to keep each zone at its set temperature by compensating for losses of heat from that zone.

These power values for each zone were termed steady state losses, and were determined by averaging the power consumed by each zone when all the zones had reached their set temperatures.

In this case the steady state losses were calculated as the average of the last three power readings for each zone. These heat losses and the total for the whole furnace are shown in Appendix D, table (D-4).

4.3 DISCUSSION OF THE 'START-UP' TEST.

The results from the start-up test analyzed in this report illustrate the power required by each zone in order to heat it to its required operating temperature. The time taken to heat all the zones to their required temperatures was approximately two hours. Whilst the total energy required to heat the furnace zones was not particularly important at this stage, the amount of power which was required to maintain them at their set temperatures was important. The power which was supplied to a particular zone was that which was required to replace the heat losses from that zone. This power was termed the steady state losses of the zone, and was determined as explained in section 4.2.

It is evident from the graphs in figures (4-1) to (4-12), that the furnace did not actually attain steady state conditions whilst readings were being taken. This was due to the fact that the furnace tested was being used in a tight production schedule. This made it necessary to begin wire processing immediately the furnace had reached operating temperature. Therefore the steady state power readings are likely to be subject to error.

However the steady state powers in table (D-4) do indicate some important factors involving losses from the furnace.

- In general the losses from each zone increased with the temperature of the zone. This related to the fact that the higher the temperature of the zone, the greater the temperature difference between it and the environment and hence the larger the heat loss from that zone to the environment.

- The most significant heat losses would be expected from the end zones (zones one and twelve). This is due to the fact that the zones at the end of the furnace have a larger surface area exposed to the environment outside the furnace. Therefore the conduction of heat from these zones to the environment should be higher than from the remainder of the zones. The figure below displays the heat losses from each zone recorded during the start-up test.

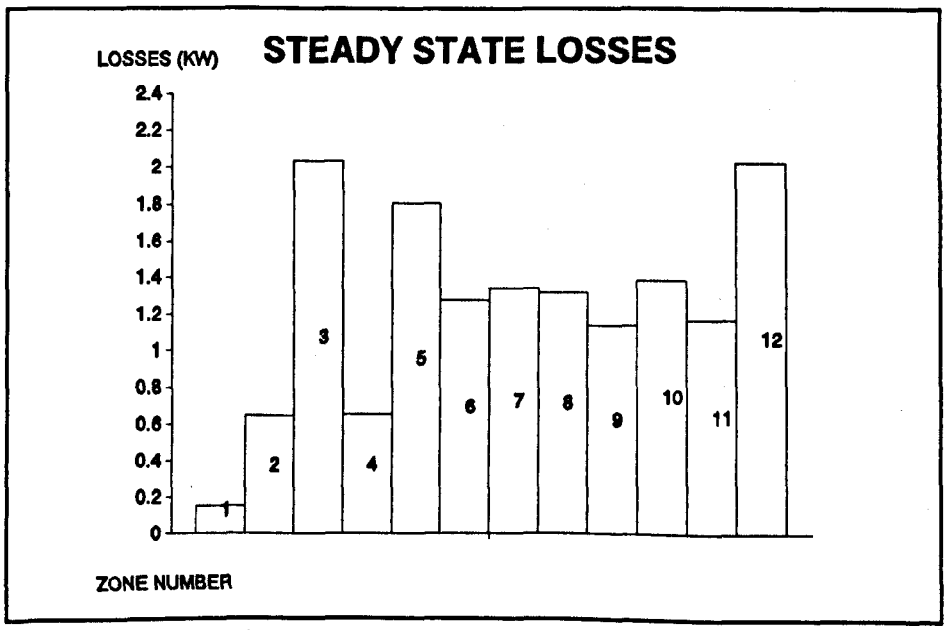

Bar chart showing the heat losses from the twelve zones recorded during the start-up test.

However zone one can be seen to have the lowest losses of all the zones. This was due to the hot furnace gas flowing down the tubes from the 'hot' end of the furnace, from which heat was transferred to zone one, thus replacing much of the heat lost. Conversely it can be seen that zone twelve had the highest losses, which was due in part to the fact that the cold furnace gas entered the furnace in this zone, hence much of the heat supplied to this zone was used to heat the gas.

- Zones three and five appeared to have unexpectedly high losses, for which there was no immediately apparent physical explanation. Hence this was attributed to a malfunction of the temperature controllers or the kilowatt-hour meters in these zones.

4.4 PRESENTATION OF THE RESULTS FROM THE 'RUNNING' TEST.

A number of 'running' tests were carried out on the furnace, each time with a slightly different selection of wires being processed. The most successful test carried out was on 25th May 1990, in which the greatest number of wire temperatures were measured. The results from the remainder of the tests were incomplete, as a large number of the process tubes had become partially blocked, thus preventing temperature measurement in those tubes. The temperature was measured in the tubes for which readings were possible at the end of each heated zone. These are shown along with the set temperature of each zone in tables (D-5.1) to (D-5.3) in Appendix D. Temperature-distance profiles for each tube for which readings were taken are shown in figures (4-13) to (4-22) in section 4.7.

The data for each wire being processed is shown in table (D-6), Appendix D, and this includes the material, diameter and calculated speed for each wire. Finally the Kilowatt-hour meter readings taken during the test for each zone and the time interval between readings are shown in table (D-7), along with the calculated powers for each zone.

4.5 ANALYSIS OF THE RESULTS FROM 'RUNNING' TEST.

The first part of this analysis was to produce an energy balance for each zone, and from this to calculate the following:

(i) The efficiency of each zone.

(ii) The efficiency of the whole furnace.

The basis of this energy balance was to calculate the total energy used to heat the wire in each zone, and to compare this with the energy supplied to each zone. The energy used to heat wire in each zone was the total of the energy used to heat each wire in that zone. The power consumed by one wire as it passes through a zone is given by,

$$\dot{Q}=\dot{M}\cdot\int_{T_i}^{T_o} C(T)\cdot dT \qquad (4\text{-}1)$$

Where,

T_i is the absolute temperature in the tube at the beginning of the zone.

T_o is the absolute temperature in the tube at the end of the zone.

C(T) is the specific heat of the wire material (see appendix C for C(T) expressions).

Equation (4-1) was used in a BASIC programme to evaluate the power used to heat each wire in each zone, and the total power used to heat all the wires in each zone. The results of this program are given in tables (D-8.1) to (D-8.4), appendix D. The values of T_i and T_o used for those tubes for which no temperature measurements were taken, were considered to be equal to those of tubes containing identical wire. In order to find the efficiency of each zone, the total power used to heat wire in each zone was divided by the power supplied to each zone, giving the efficiencies as in table (D-9), appendix D.

In order to find the total efficiency of the furnace, the total power required to heat each wire was determined over the length of the furnace by putting T_i equal to the ambient temperature and T_o equal to the maximum temperature of the wire. The results for this were found using the same BASIC programme as before, but with a slight modification. The results are given in table (D-10). The heat transferred to each wire passing through the furnace was then summated to give the total heat transfer to wire in the furnace,

P_{wire}= 19.432 Kw

The total power supplied to the furnace was calculated by summating the power supplied to each of the heating zones giving,

P_{sup}= 27.803 Kw

Therefore the total efficiency of the furnace was given by

$$\eta_{tot}=\frac{P_{wire}}{P_{supp}}\cdot 100\% = \frac{19.432}{27.803}\cdot 100\% \qquad (4\text{-}2)$$

$$= 69.9\%$$

The expected losses from the furnace during processing of wire was given by,

$$P_{loss}=P_{supp}-P_{wire} \qquad (4\text{-}3)$$

$$= 8.371\ Kw$$

This concluded the energy balance for the running test.

The second part of this analysis deals with the calculation of the theoretical radiative heat transfer using the experimental data from the running test. The basis of this was to consider the radiative heat transfer to a single wire in a single tube. In order to find the radiant heat transfer from the tube to the wire in a particular zone, equation (2-7) was solved numerically using the measured wire temperature in that zone. This was carried out for each of the wires passing through the furnace, and the results summated to give the total heat transferred in that zone. However the exact temperature profile of the wire was not known, and in order to determine it accurately many more temperature measurements would have been required. Thus only the maximum radiative transfer in each zone was calculated, ie at the beginning of each zone where the temperature difference was greatest.

The only temperature data available was the wire temperatures and the set temperature for each zone, therefore it was considered more practical to consider the heat transfer from the tubes to the wires. Because there was no specific data for the temperature profiles of the tubes, the tubes were considered to be isothermal along the length of a particular zone, and at the set temperature of that zone. To reduce the amount of calculations required, the following simplifications were introduced,

- The temperature of all the wires were considered to be the same at a given position along the tubes. Therefore the required wire temperature (T_w) at the beginning of a zone was taken as the average of the measured values of wire temperature at that point. The values of these temperatures are given in table (D-11.1), along with the tube temperatures (T_{ti}).

• The diameter of each wire was taken as the average of all the wires being processed during the test. This diameter was calculated as,

D_w= 1.699 mm.

And the inside diameter of each tube was found from figure (3-1) as,

D_{ti}= 16 mm.

Thus from equation (2-29),

F_{ti-w}=0.1062

Therefore it was possible to consider the radiative transfer to a single wire, and multiply this by the number of wires being heated to determine the total radiative heat transfer in each zone. The emissivities of each surface were required at the relevant temperatures, and these were found using the appropriate emissivity functions in appendix C. The calculated emissivities are shown in table (D-11.1) in Appendix D.

The emissivities, along with the geometrical values required were then substituted into equation (2-5) to give the required thermal resistances R_{ti-w} for each zone, which are shown in table (D-11.2). Equation (2-8) was then used to calculate the black body potential of each surface, and an expression similar to equation (2-7) was used to find the radiant heat transfer Q_{rad} to the wire.

As there were seventeen wires being processed during this test, the total heat transfer to each zone by radiation was then found by

$$Q = 17 \bullet Q_{rad}$$

An example calculation is shown below for zone one.

T_{ti}= 970 K $\epsilon_{ti}(T_{ti})$ = 0.615 D_{ti} = 16 mm.

T_w = 694 K $\epsilon_w(T_w)$ = 0.722 D_w = 1.699 mm.

$A_{ti} = \pi \bullet D_{ti}$ = 50.265 x10^{-3} m^2/metre length

$A_w = \pi \bullet D_w$ = 5.337 x10^{-3} m^2/metre length

and F_{ti-w}= 0.106

Therefore equation (2-5) becomes,

$$R_{ti-w} = \frac{(1-0.106)}{50.3x10^{-3}x0.615} + \frac{1}{50.3x10^{-3}x0.106} + \frac{(1-0.722)}{5.3x10^{-3}x0.722}$$

$$= 271\ m^{-2}$$

And equation (2-1) becomes,

$$q_{rad} = \frac{5.669x10^{-8}\ x\ (970^4-694^4)}{270.95}$$

$$=136.7\ Watts$$

Therefore for all seventeen wires,

$$q_{rad} = 17\ x\ 136.7 = 2.323\ Kw$$

4.6 DISCUSSION OF THE RESULTS FROM THE 'RUNNING' TEST.

The energy balance carried out using data from this test produced the efficiencies of each zone as in table (D-9). As mentioned before, this efficiency was the percentage of the power supplied to a zone which actually goes to heating the wire in that zone. The efficiency of each zone decreased from 77.5% in zone one to -31.8% in zone twelve, the main reasons for this being,

- As the temperature of the wire increased, the amount of heat transferred to the wire in each zone reduced. However the losses in each zone remained constant. Thus the proportion of heat supplied to each zone which constituted the heat loss in that zone increased with wire temperature. Thus the proportion of the heat supplied which was transferred to the wires decreased, so the efficiency decreased.

- The negative efficiencies in zones eleven and twelve were due to the fact that the wires actually lost heat in these zones even though power was supplied to these zones. The most likely cause of this was again the flow of cold furnace gas into the furnace tubes at this end of the furnace. Hence much of the heat supplied here went to heating the gas.

This was supported somewhat by the steady state powers which were found in the start-up test to be higher than the running powers for zones seven to twelve (see tables (D-4) and (D-7) in Appendix D).

Although it has already been established that these steady-state powers were somewhat erroneous, it should be noted that the power supplied with just gas flowing was more than that supplied when gas and wire are flowing in the last six of the zones in the hot end of the furnace. These last six zones therefore provided the 'soaking' region for the wires, by maintaining them at the required soaking temperature, whilst the first six zones were used to heat the wire to the required temperature.

The most unreliable aspect of this experimental work was the temperature data acquired, there being no guarantee that the temperatures measured were those of the wires. This was because it was not possible to attach a thermocouple to the wire. This was highlighted by the fact that the average temperature recorded at the beginning of zone one was 421°C, which signified a rise in the wire temperature of approximately 400°C in the unheated length of tube before the start of the zone. One possible explanation of this was that heat was transferred to the wire from the hot gas, causing this rise in temperature. However a more plausible explanation was that the thermocouple probe was actually measuring the temperature of the gas itself. Obviously any heating effects of the wire due to this hot gas would have to be considered in later work, as well as a method of measuring wire temperature accurately. The overall efficiency of the furnace was the percentage of the total power supplied to the furnace which was used to heat the wire. This was not dependent on the temperatures in each zone, but was calculated using the initial wire temperature (ambient) and the maximum temperature of the wire.

The value of this total efficiency was found to be 69.89% which was lower than the quoted 78% overall efficiency of the furnace.

The total heat loss calculated from the running test of 8.371 Kw in the previous section was much less than the value of 14.964 Kw calculated from the steady-state powers, as shown in appendix D, table (D-4). This bears out the prediction made in earlier discussions that the steady-state powers measured were too high.

The results from the radiative heat transfer calculations for the running test data indicate that the maximum radiative transfer from the tubes to the wires in each zone decreased as the wire temperature increased (see table (D-11.2) in Appendix D). This is due to the decrease in the temperature difference between the tubes and the wires. It should be pointed out that the thermal resistance R_{ti-w} decreased as the temperature of the exchange surfaces increased. This is due to the increase in the emissivities of the surfaces as the surface temperature increases. However in the majority of the zones, the magnitude of the maximum radiative transfer was higher than the transfer required to give the temperature rise measured for each zone (comparing tables (D-8.1) to (D-8.4) and (D-11.2) in Appendix D). This indicates that the calculated values for radiative transfer may have been too high due to inaccuracies in the temperatures used in their calculation. Alternatively the emissivity expressions used in the calculations were not those for the actual surface condition of the wires and tubes. Also the total power used to heat wire in each zone (table D-8.4) may have been slightly higher than was calculated, as the exact properties of the wire material were not known.

4.7 GRAPHS OF RESULTS OBTAINED FROM THE EXPERIMENTAL WORK ON THE FURNACE AT 'CRITCHLEY'S'.

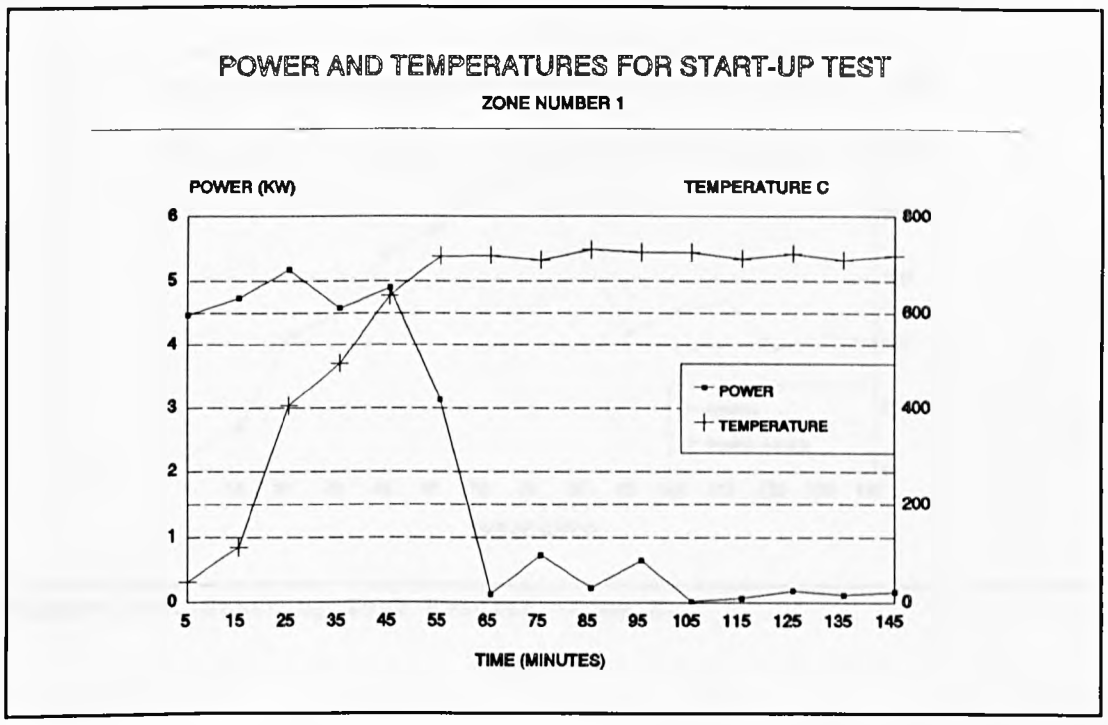

Figure 4-1. Start-up Test Results -Zone 1.

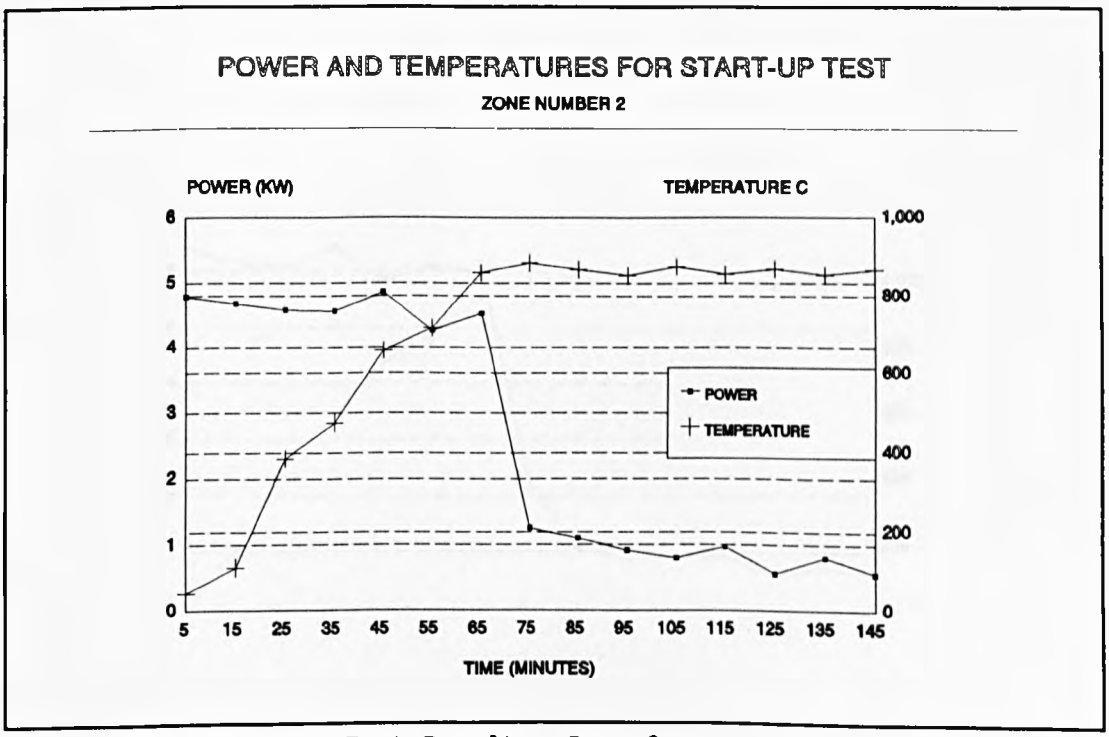

Figure 4-2. Start-up Test Results -Zone 2.

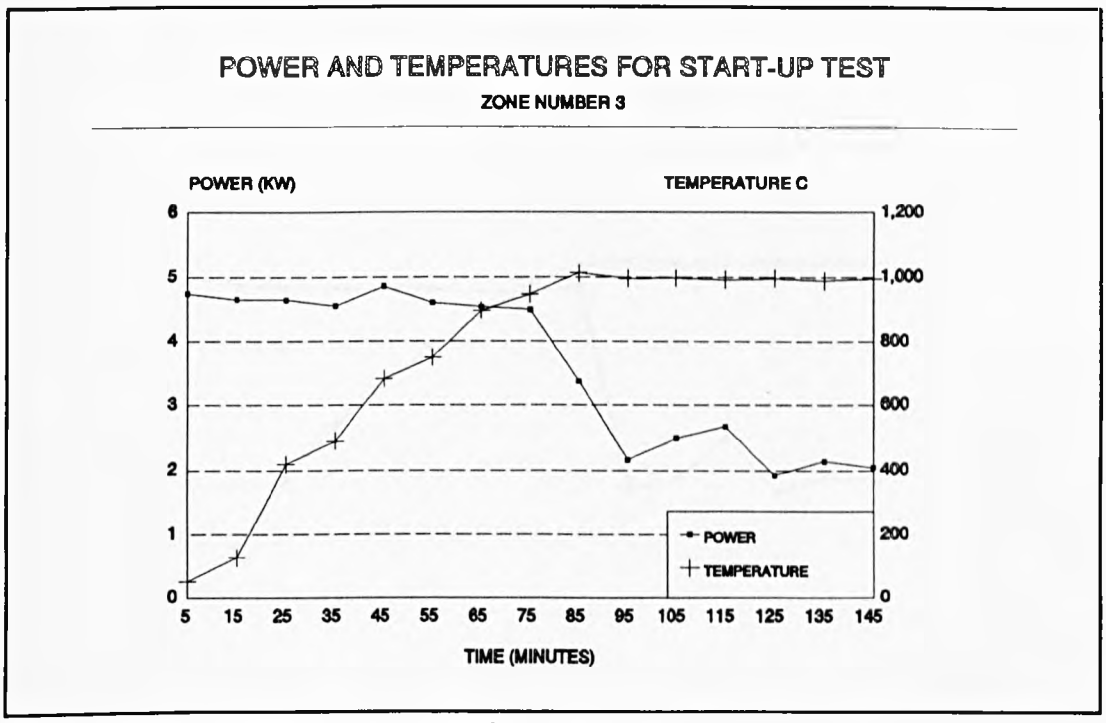

Figure 4-3. Start-up Test Results -Zone 3.

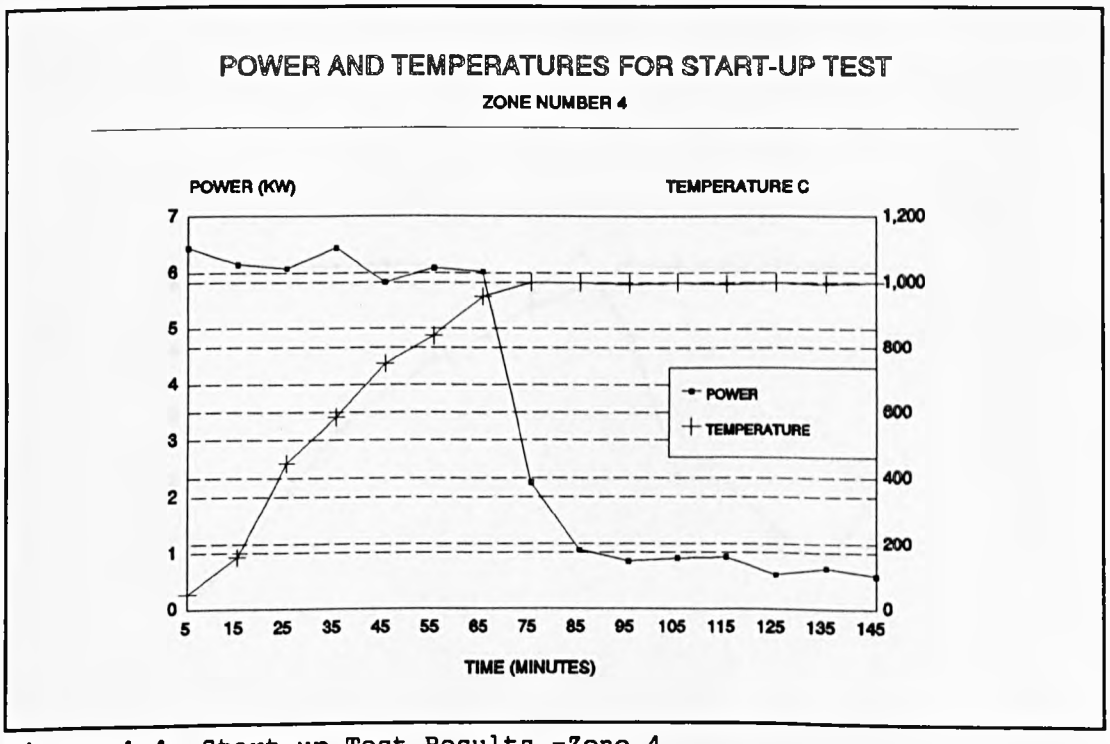

Figure 4-4. Start-up Test Results -Zone 4

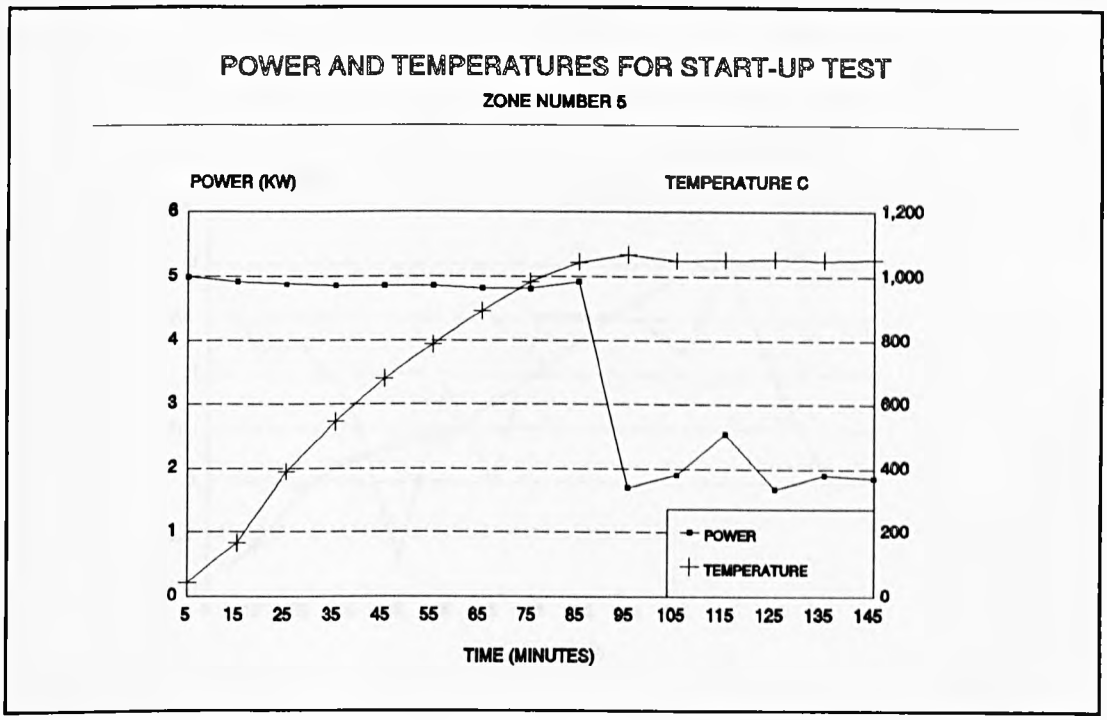

Figure 4-5. Start-up Test Results -Zone 5.

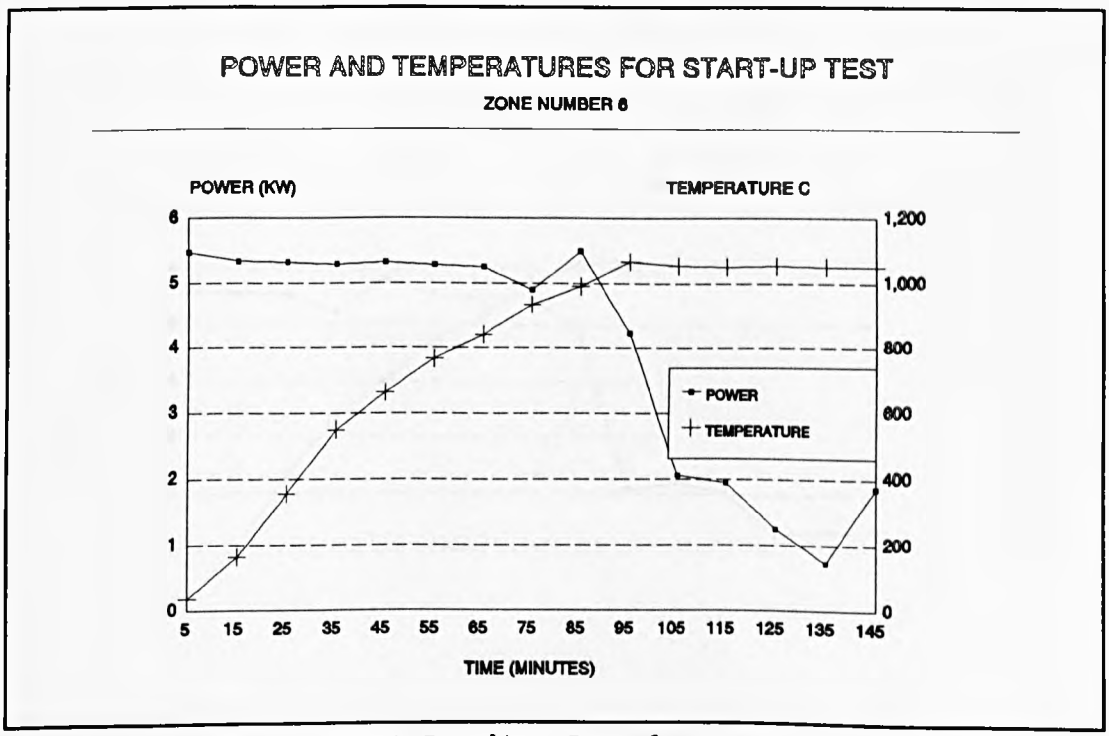

Figure 4-6. Start-up Test Results -Zone 6.

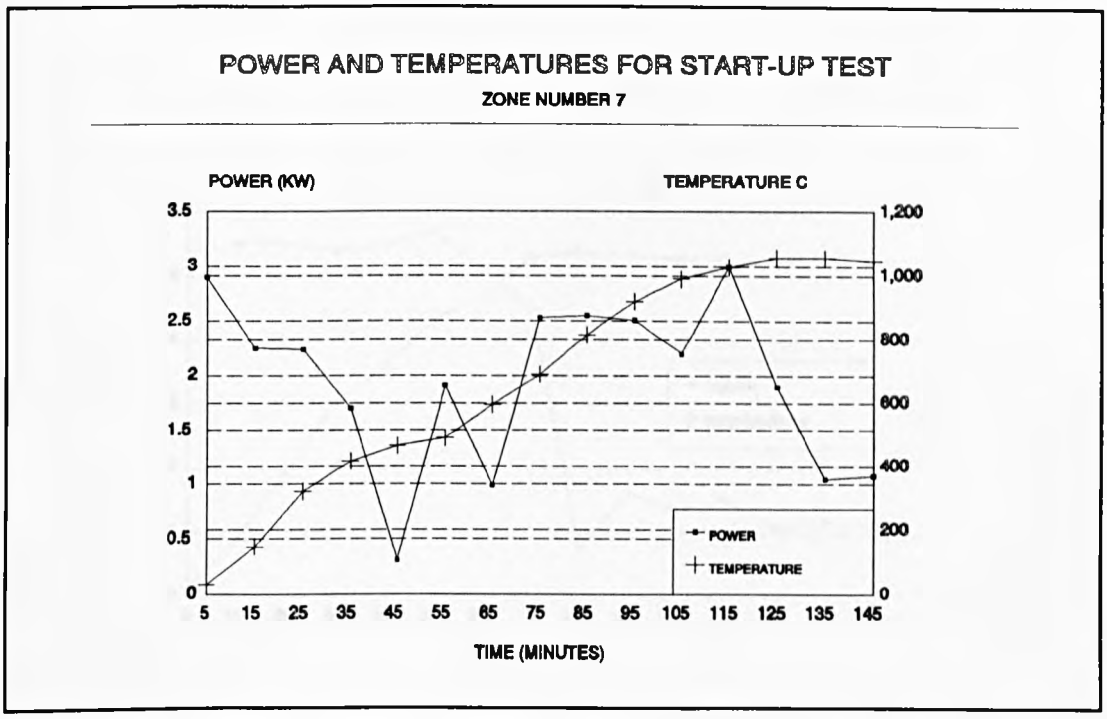

Figure 4-7. Start-up Test Results -Zone 7.

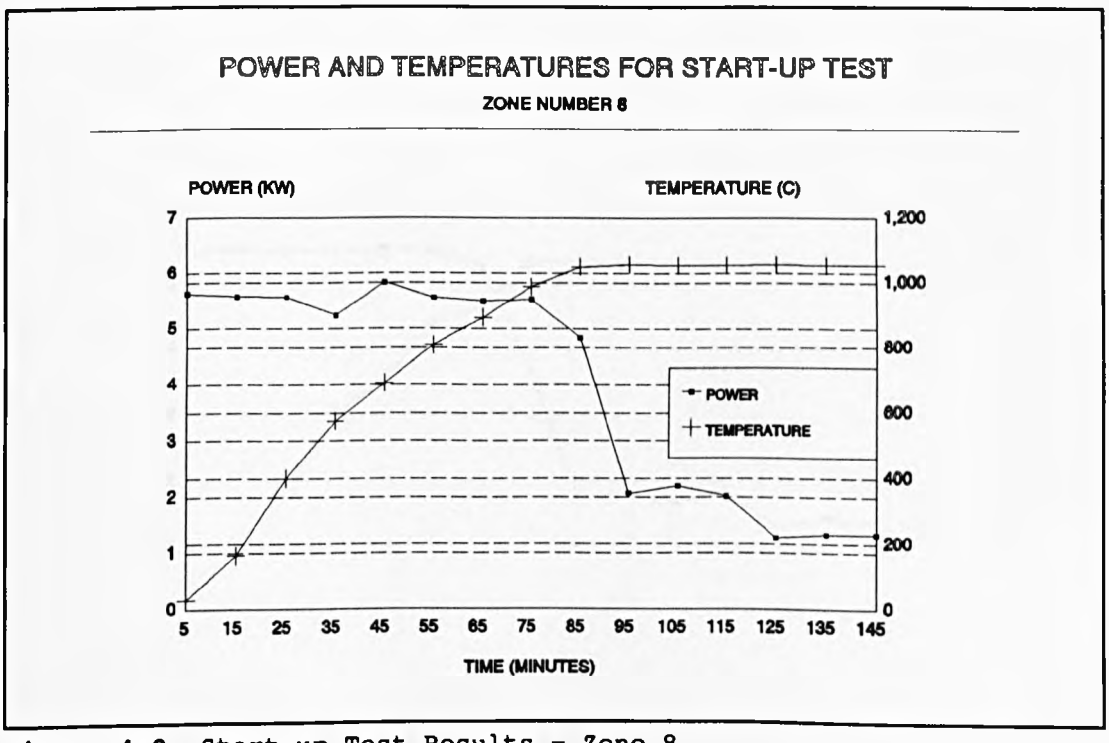

Figure 4-8. Start-up Test Results - Zone 8.

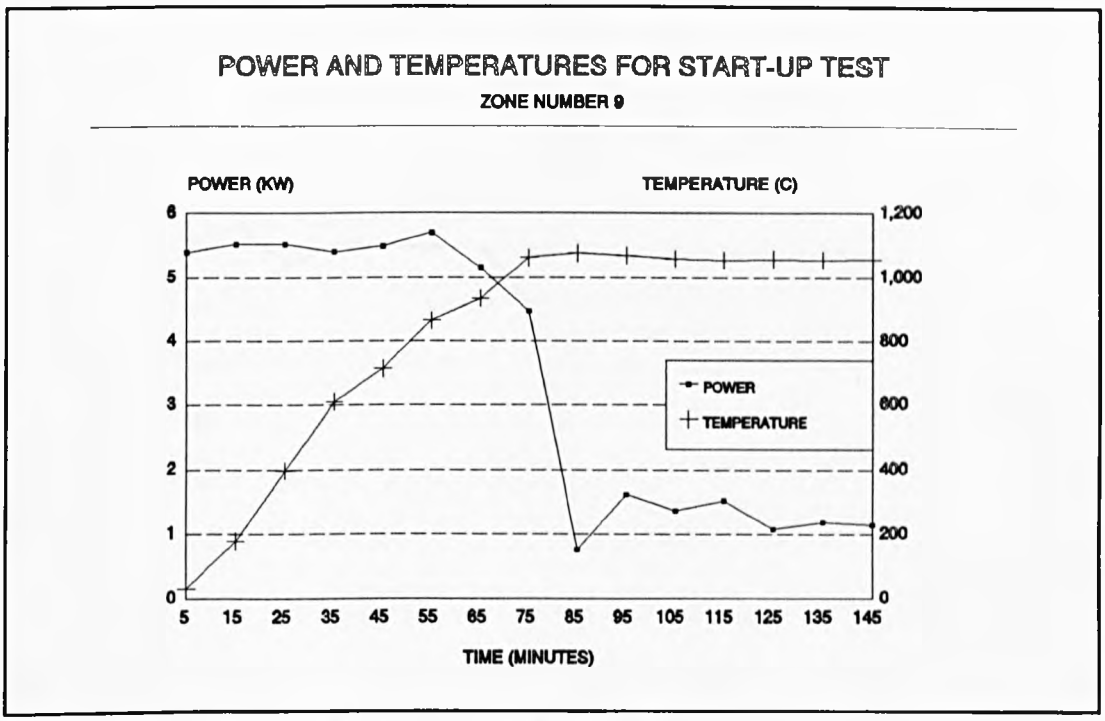

Figure 4-9. Start-up Test Results -Zone 9.

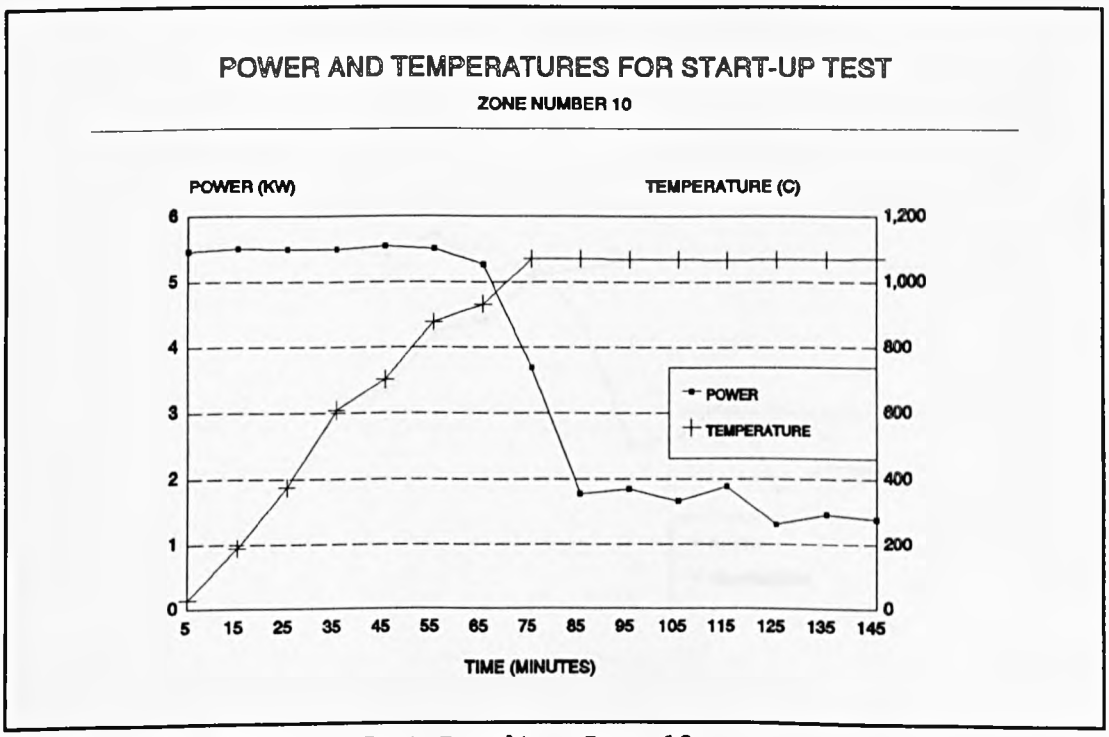

Figure 4-10. Start-up Test Results -Zone 10.

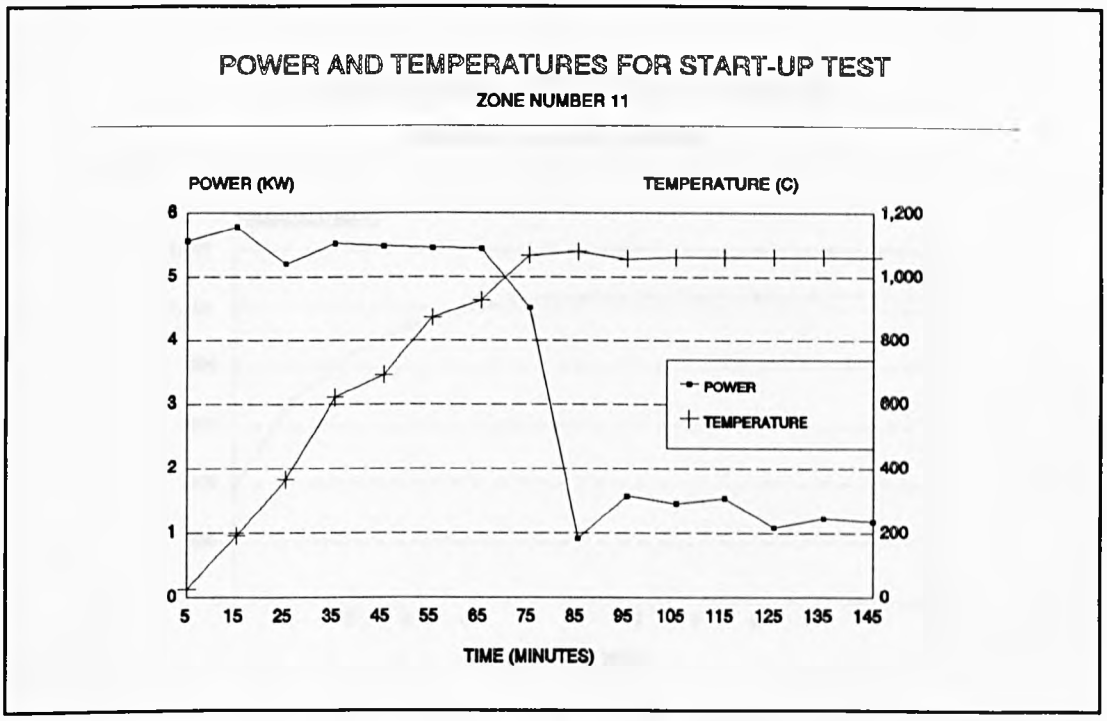

Figure 4-11. Start-up Test Results -Zone 11.

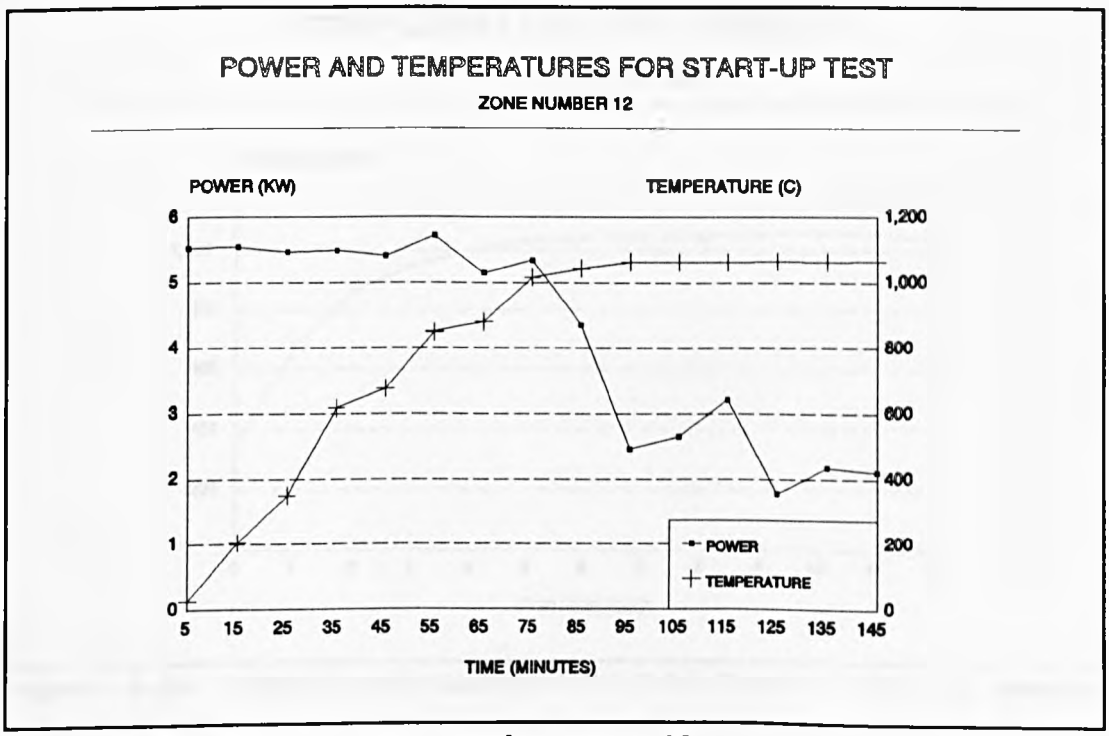

Figure 4-12. Start-up Test Results -Zone 12.

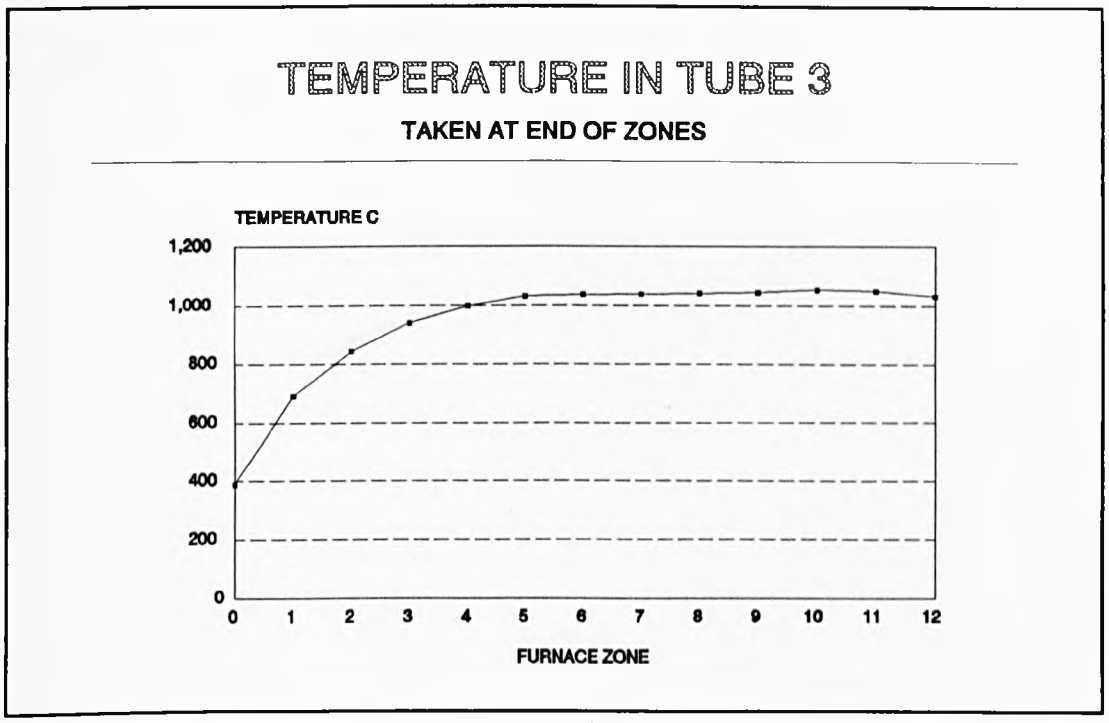

Figure 4-13. Temperatures Measured in Tube Number 3 During Running Test.

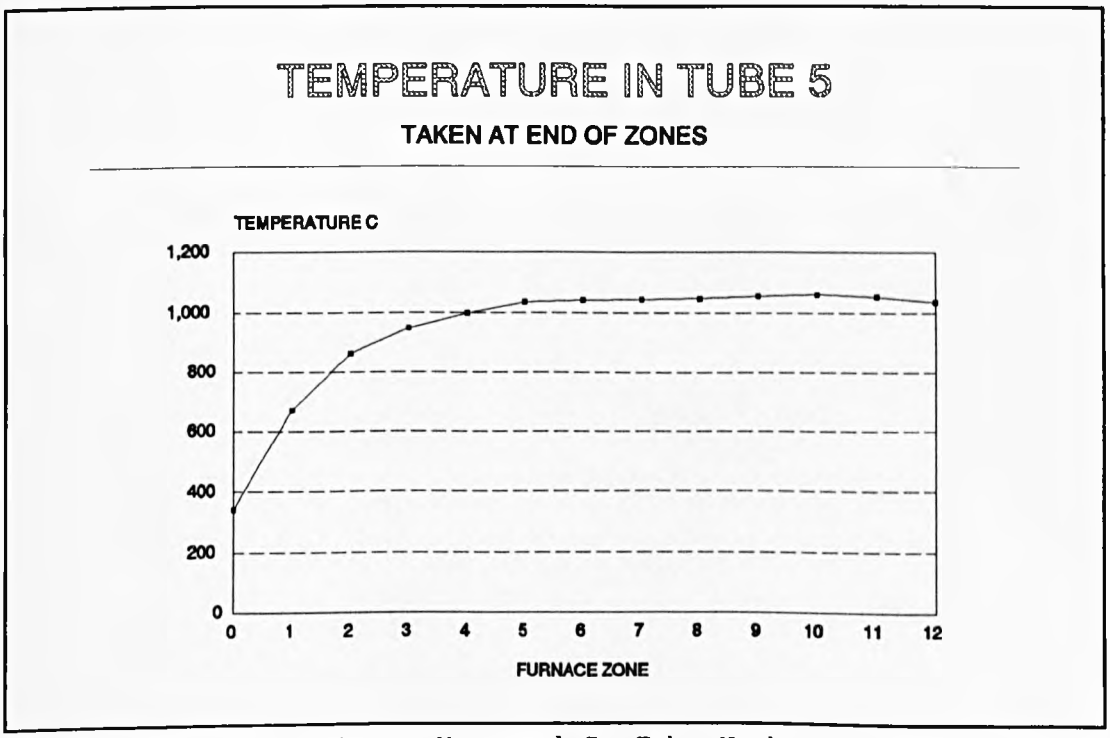

Figure 4-14. Temperatures Measured In Tube Number 5 During Running Test.

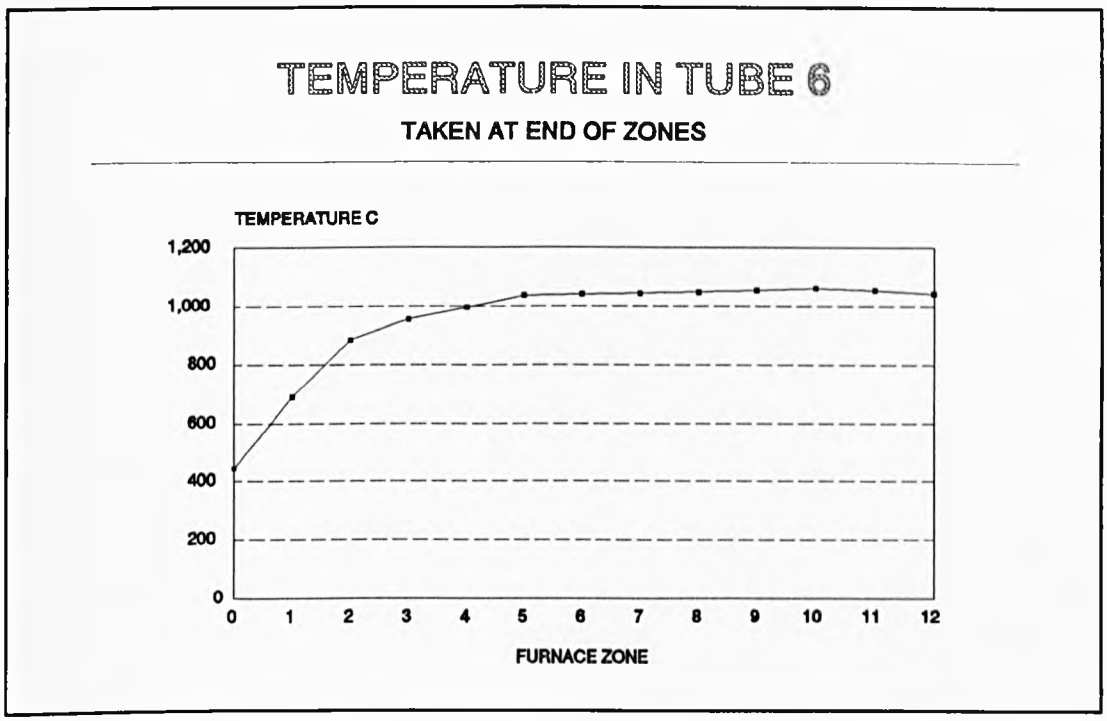

Figure 4-15. Temperatures Measured In Tube Number 6 During Running Test.

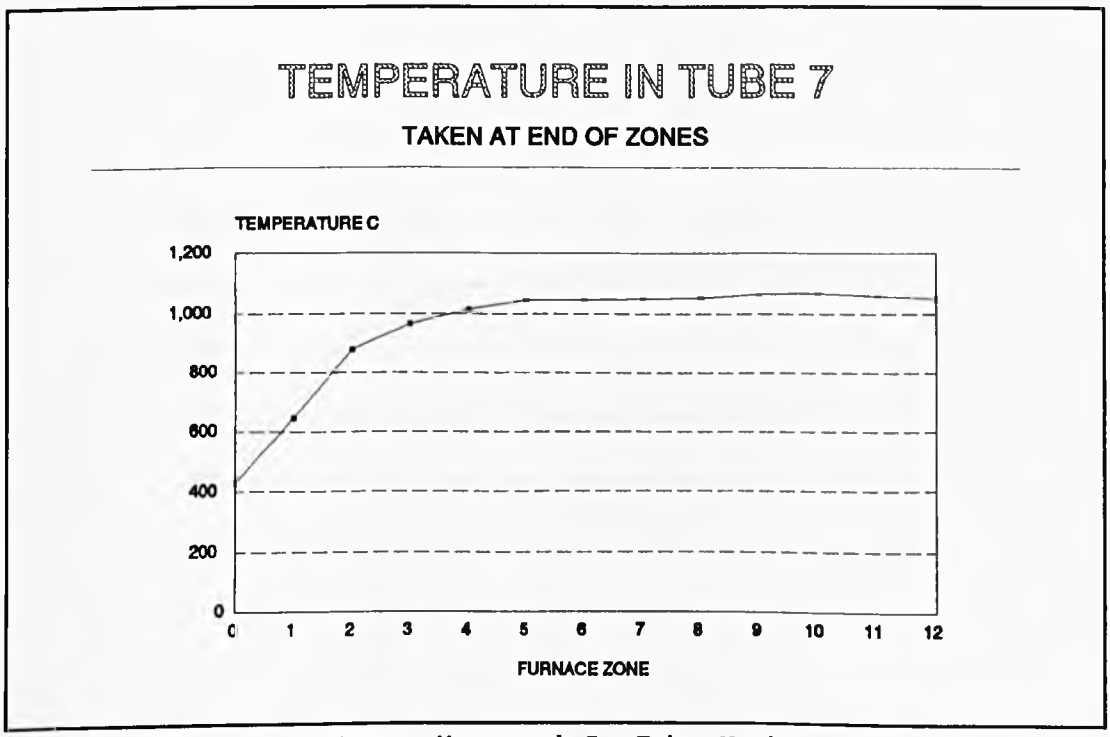

Figure 4-16. Temperatures Measured In Tube Number 7 During Running Test.

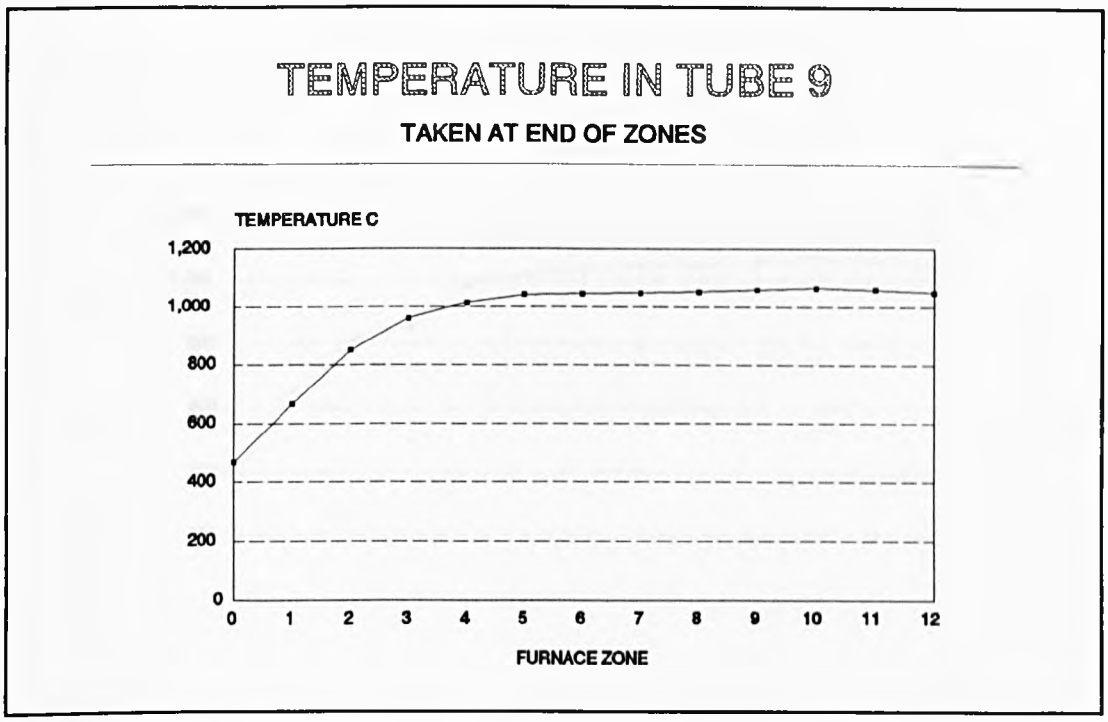

Figure 4-17. Temperatures Measured In Tube Number 9 During Running Test.

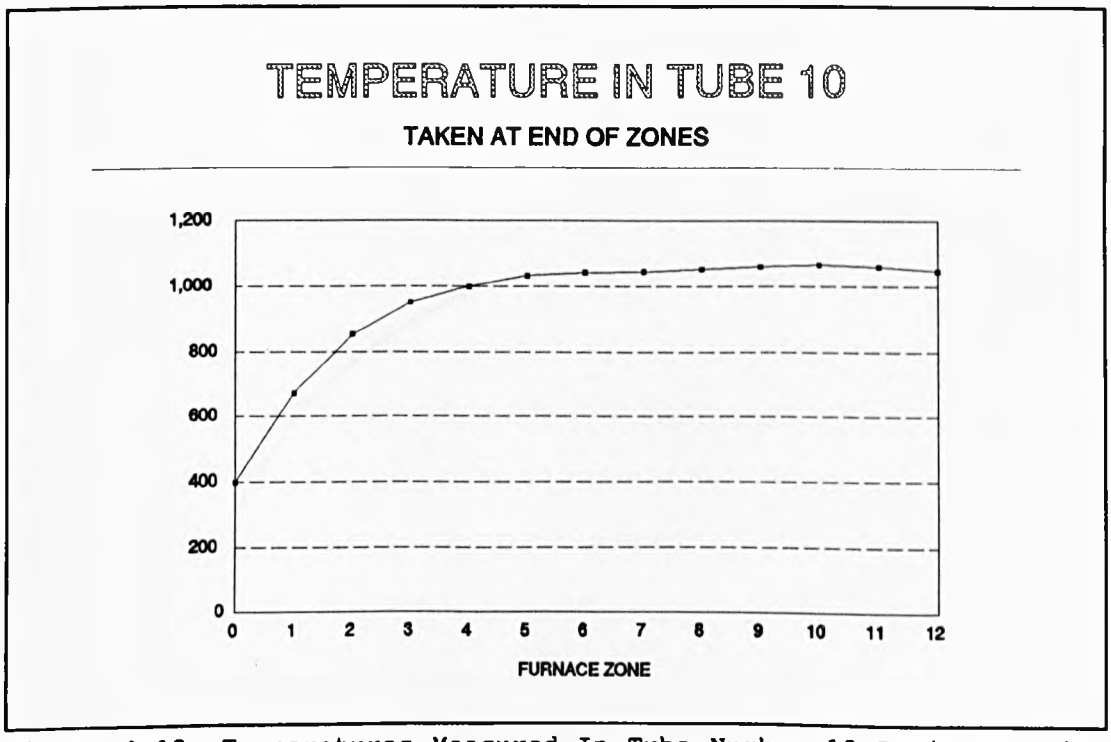

Figure 4-18. Temperatures Measured In Tube Number 10 During Running Test.

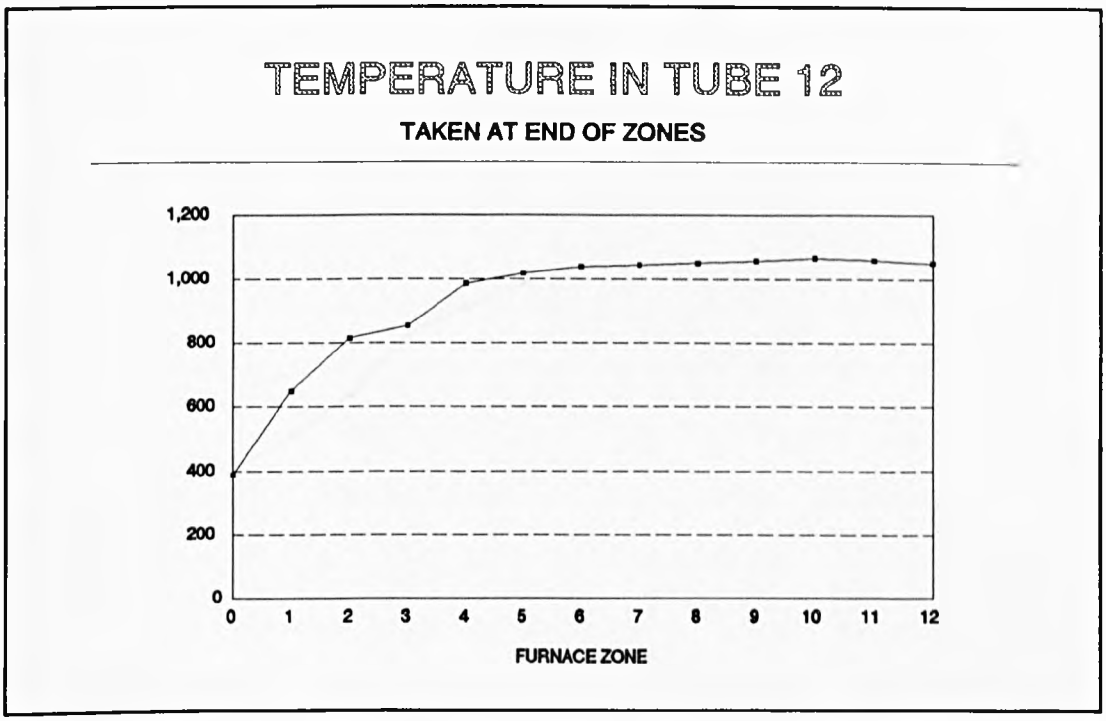

Figure 4-19. Temperatures Measured In Tube Number 12 During Running Test.

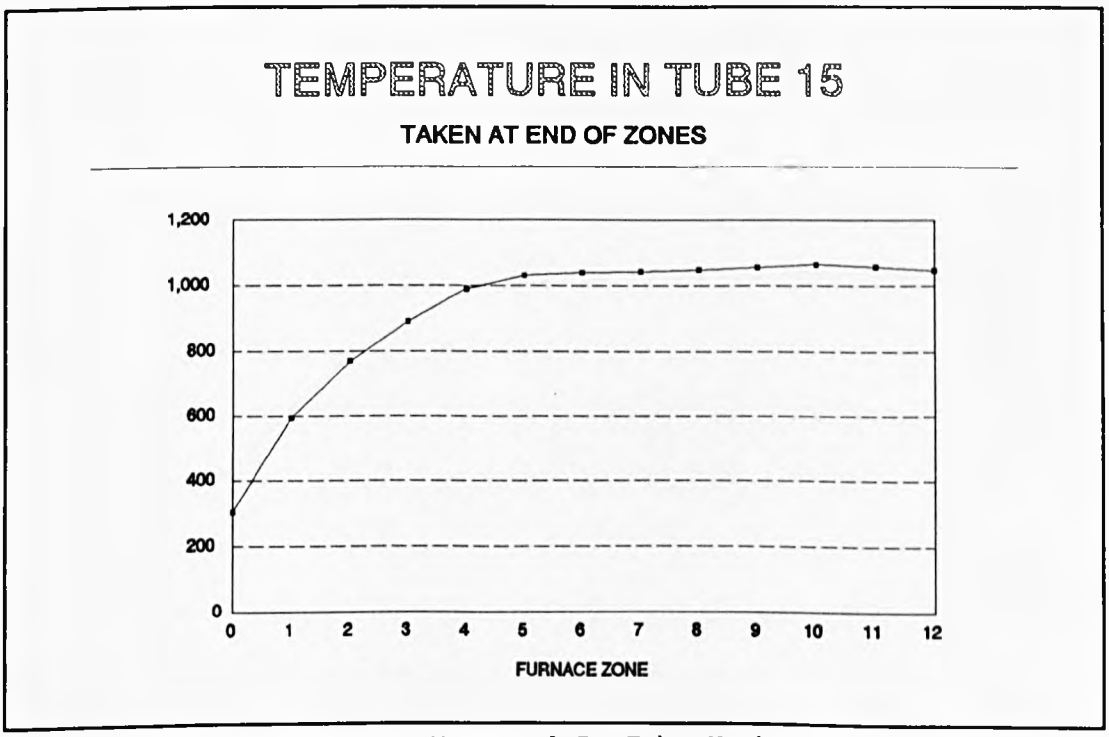

Figure 4-20. Temperatures Measured In Tube Number 15 During Running Test.

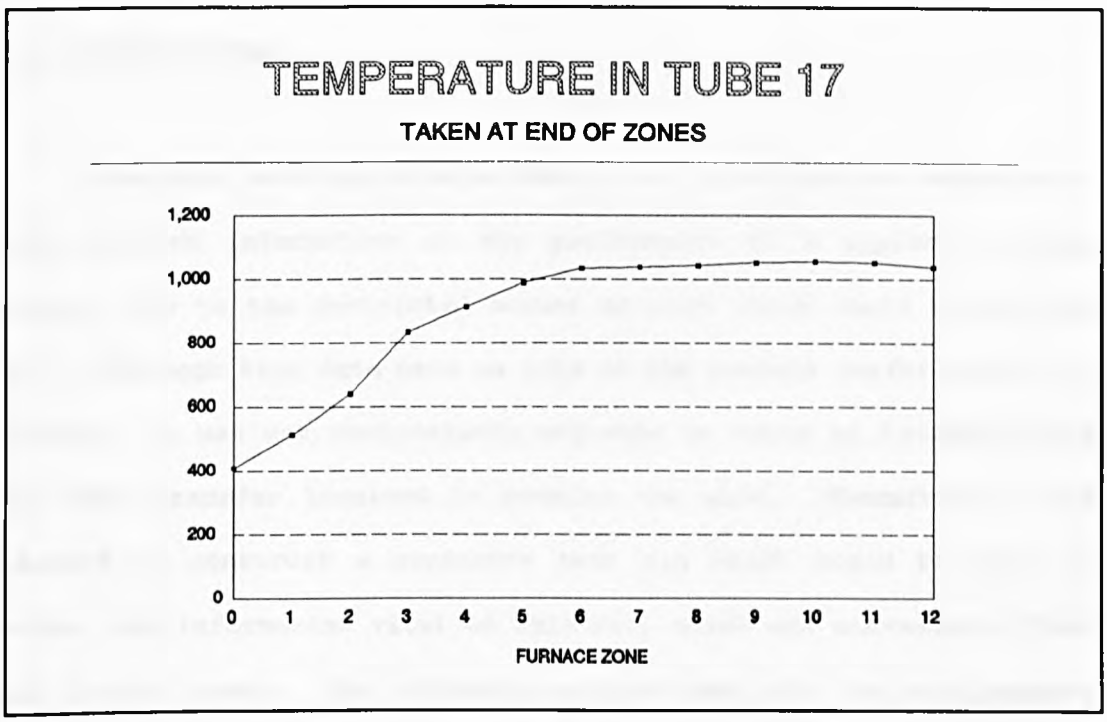

Figure 4-21. Temperatures Measured In Tube Number 17 During Running Test.

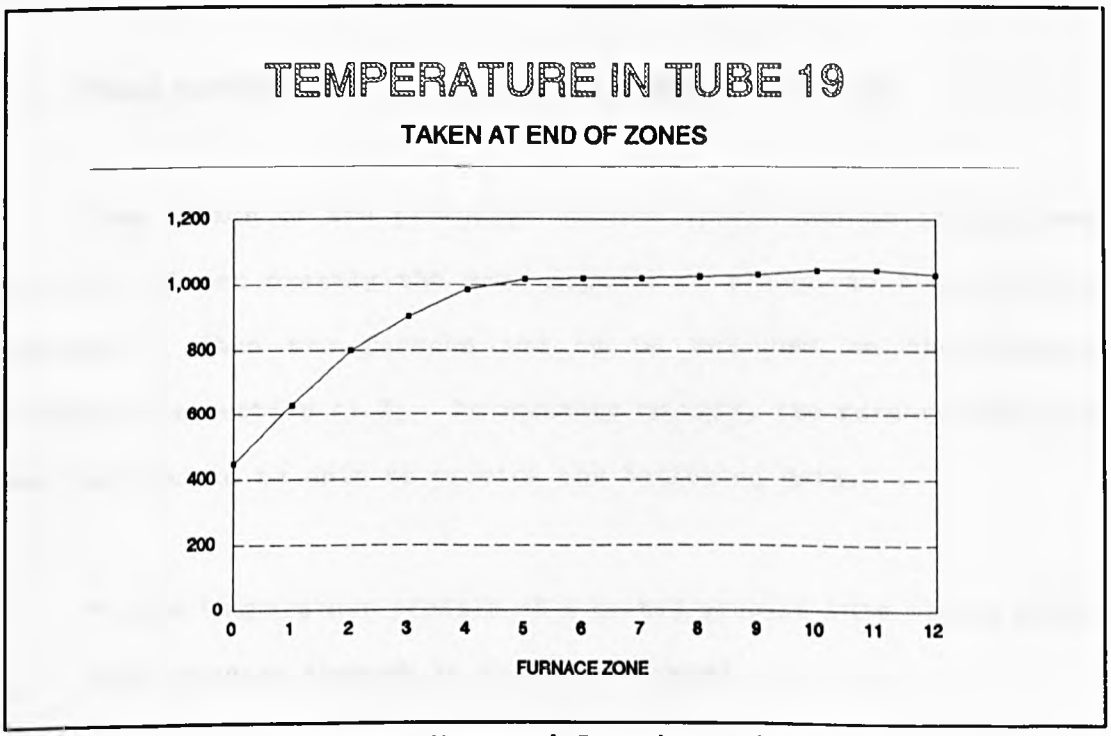

Figure 4-22. Temperatures Measured In Tube Number 19 During Running Test.

CHAPTER 5. DEVELOPMENT OF THE PROTOTYPE FURNACE.

5.1 INTRODUCTION.

The first section on experimental work provided the author with only limited information on the performance of a typical furnace design, due to the restricted amount of work which could be carried out. Although this data gave an idea of the overall performance of a furnace, it was not particularly valuable in terms of investigating the heat transfer involved in heating the wire. Therefore it was decided to construct a prototype test rig which could be used to gather the information vital to this end, which was unavailable from the initial tests. The following sections describe the requirements of the prototype rig, and then go on to explain how the rig was conceived to satisfy these requirements.

5.2 BASIC REQUIREMENTS OF A PROTOTYPE FURNACE TEST RIG.

The design of the prototype furnace itself had to incorporate similar, if not exactly the same aspects of design as the existing furnaces. Thus the furnace had to be designed on the concept described in section (1.3). In addition to this, the furnace designed was required to be able to provide the following data,

- The temperature profile of a heated process tube with a given wire passing through it at a given speed.

- The temperature profile of a given wire passing through a heated process tube at a given speed.

- The power consumed by each heated zone to maintain it at its set temperature, with and without wire passing through the furnace.

The above information was required to be available for a range of wire sizes and speeds, in order to ascertain more accurately the heat transfer mechanisms from the furnace to the wire. Therefore the prototype furnace had to be provided with ;

i). All the services provided to a furnace in its working environment, which comprise,

- A system for winding the wire at variable speeds through the furnace.
- A means to supply one or more process gases to the process tube(s) at variable, and metered amounts.
- A means of cooling the wire from its process temperature to an acceptable level.
- Any safety equipment required, either by the Government's, or the University's health and safety authorities.

ii). A full range of sensors and instrumentation required to extract and record all the required data from the furnace.

5.3 DESIGN AND SPECIFICATIONS OF THE PROTOTYPE FURNACE AND TEST RIG.

5.3.1 Specifications of the Single Tube Prototype Furnace.

The furnace produced was designed and built by Meltech Furnaces to a specification decided upon by Meltech and myself. The specification was based on the criteria given above plus the limitations on space in the laboratory area.

The furnace constructed was a single-tube furnace, with three separately controlled heating zones. A photograph of the furnace is shown in figure (5-1), and the essential dimensions are given in figures (5-2) and (5-3).

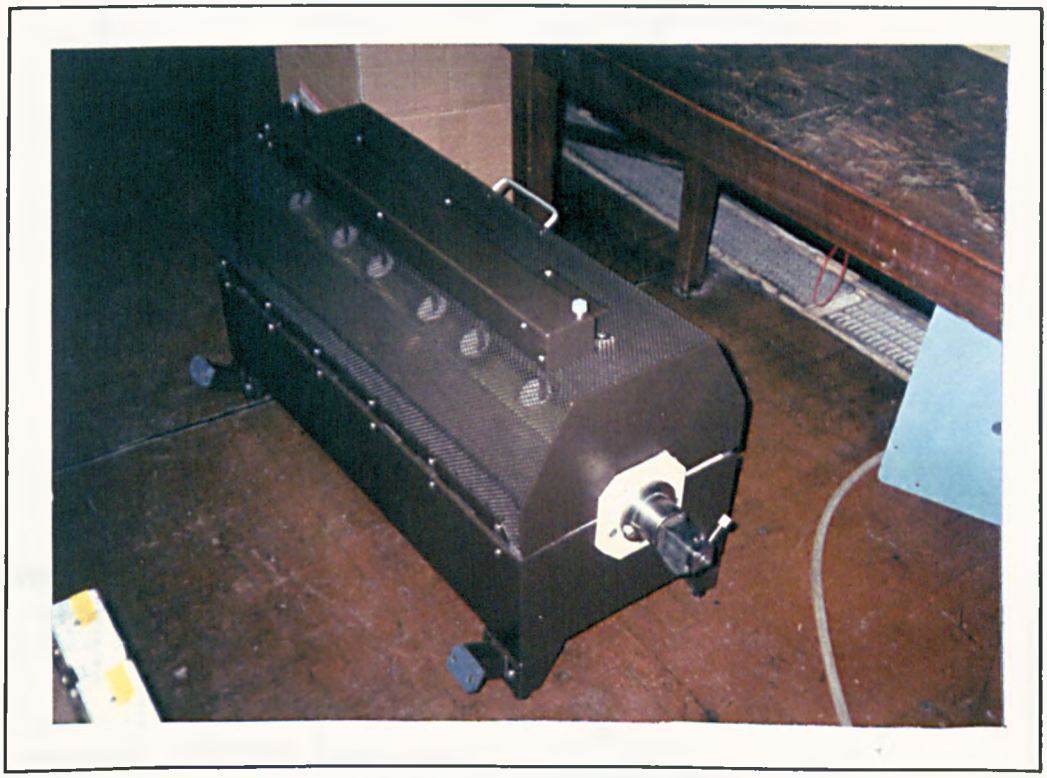

Figure 5-1. A photograph illustrating the prototype furnace as supplied.

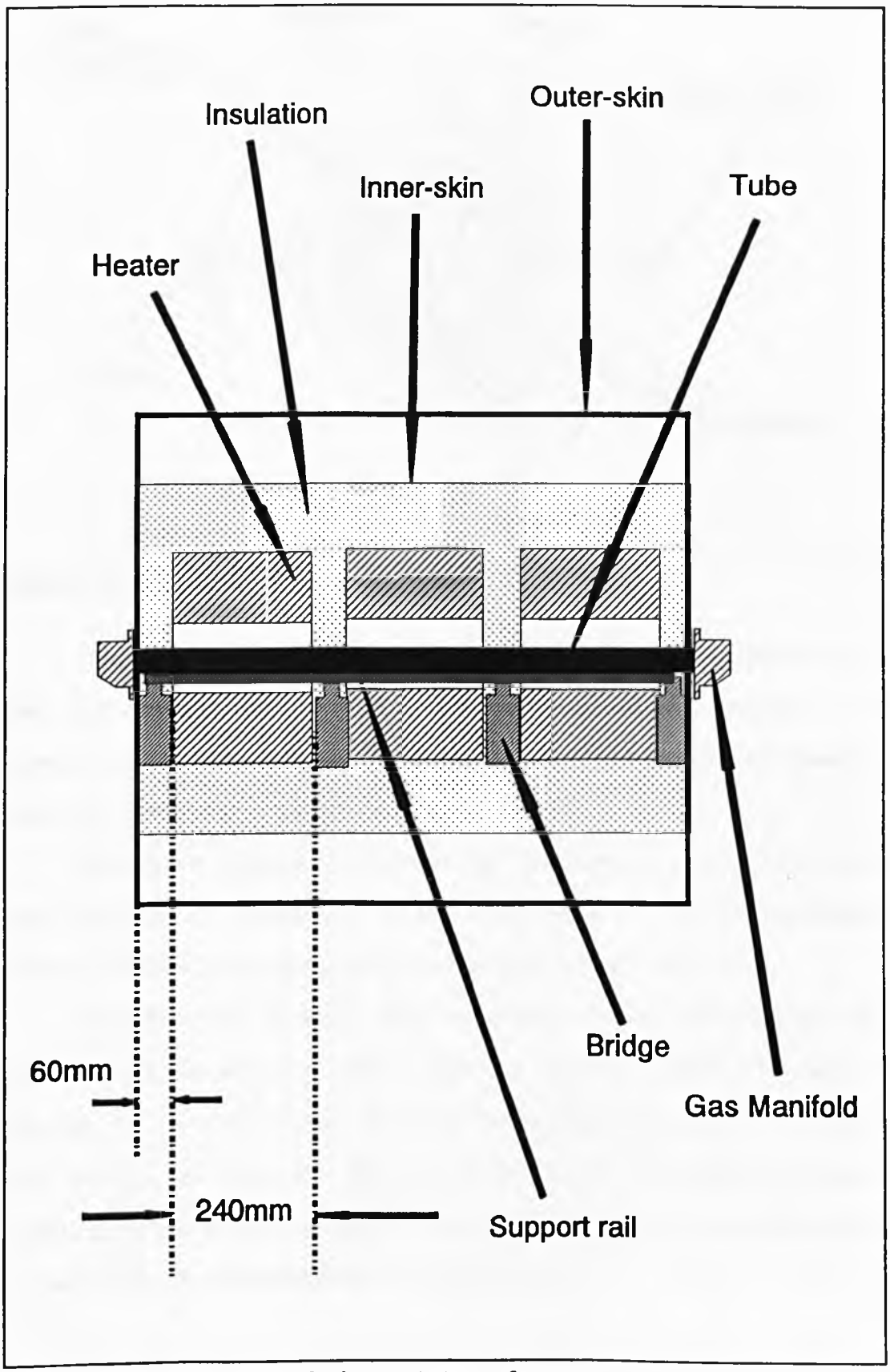

Figure 5-2. Side view of the prototype furnace.

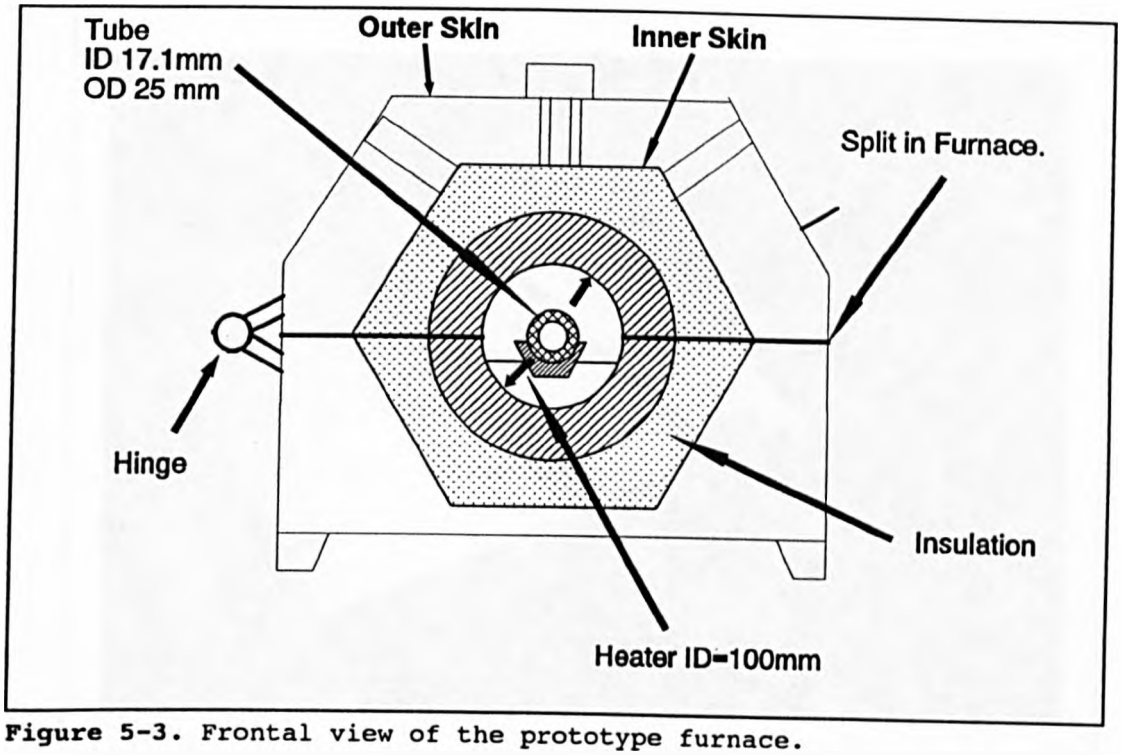

Figure 5-3. Frontal view of the prototype furnace.

The furnace incorporated a single process tube, supported by a rail and bridges and situated inside three cylindrical heaters. The tube, rail, bridges and heater materials were of the type utilized in previous production furnaces.

The space between the heaters and the inner-skin of the furnace was insulated by layers of Ceramic Fibre blanket, and the inner-skin of the furnace was supported within a perforated outer skin.

The heaters in each zone consisted of two semi-cylindrical shells, one on the top and one on the bottom. This allowed the furnace to be split across its horizontal axis, by means of a hinged top half. The top half of the furnace could therefore be opened manually to allow full access to the furnace chamber and process tube, as depicted in the photograph in figure (5-4).

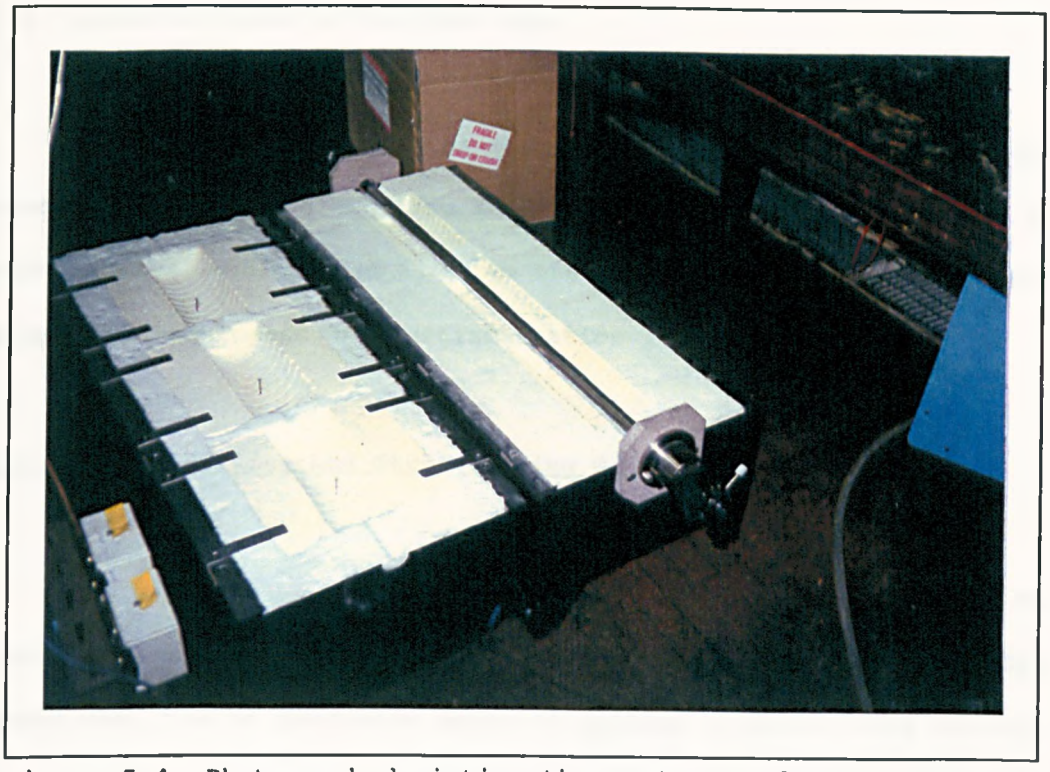

Figure 5-4. Photograph depicting the prototype furnace with the top section opened.

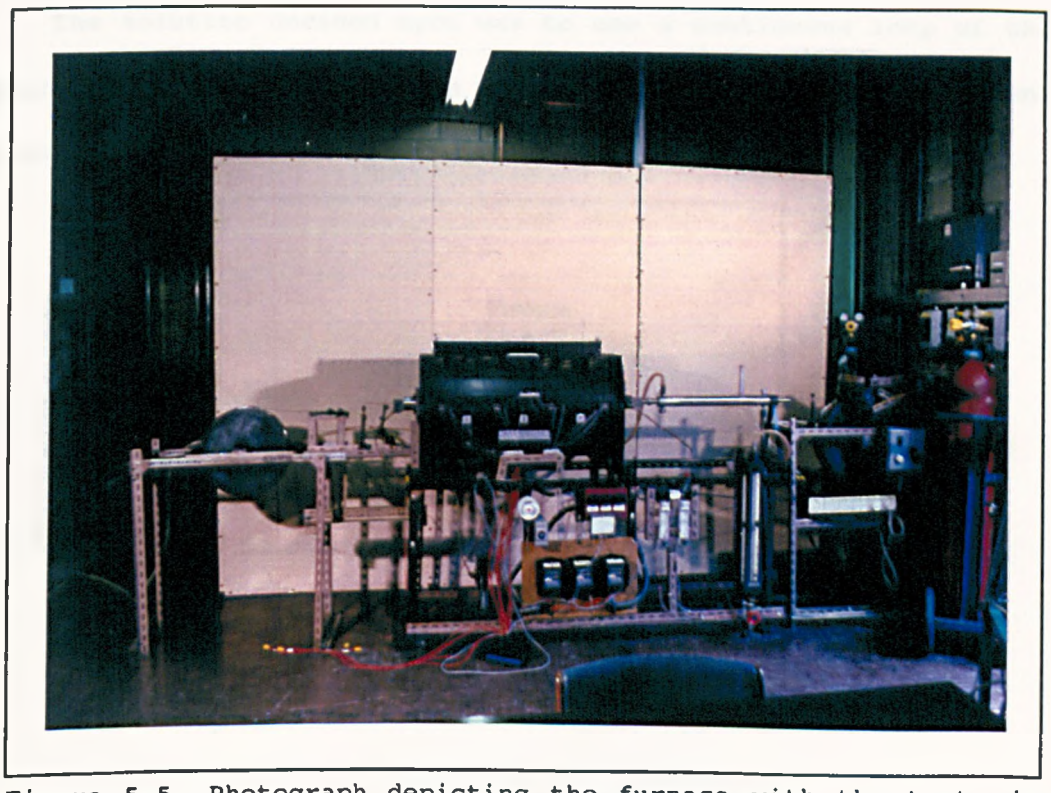

Figure 5-5. Photograph depicting the furnace with the test rig built around it.

5.3.2 Specifications of the Test Rig.

This section discusses the test rig which was built around the furnace to provide the required facilities discussed in section 5.2. The photograph in figure (5-5) shows the rig which was built, with all the required equipment and instrumentation installed.

5.3.2.1 Wire Winding and Straightening Gear.

Wire winding gear used in industry is extremely difficult to obtain, and was also prohibitively expensive for this project. The problem was, how to produce a means of pulling a single wire through the furnace at the required constant speed, without exceeding cost or space limitations.

The solution decided upon was to use a continuous loop of the required wire, stretched between two rollers, one of which was driven, the other kept under tension.

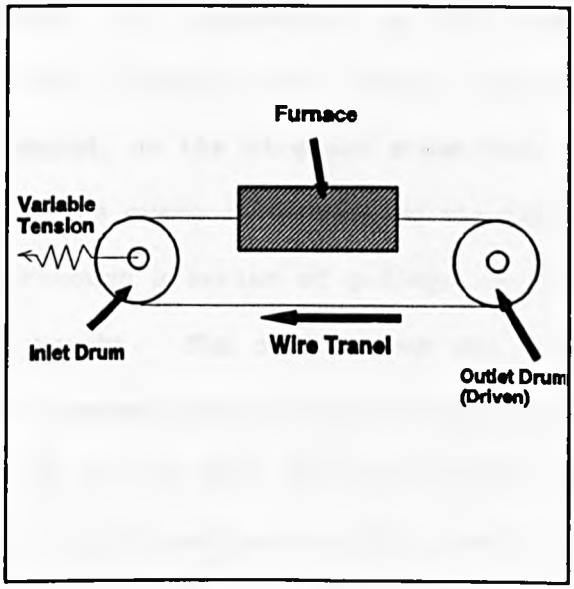

Figure 5-6. Schematic layout of the wire winding system.

The furnace was situated between the two drums, as in the schematic diagram in figure (5-6), so that the wire was pulled through the furnace, passed round the powered drum, and then back under the furnace to the other drum, before re-entering the furnace.

The main problem with this configuration was that the wire needed to be able to cool down to ambient temperature before re-entry into the furnace. The wire of diameter less than 3 mm was found to cool down satisfactorily to ambient temperature in the available time, but wire thicker than 3 mm diameter did not. However it was maintained that the temperature of the wire at the furnace entry was required to be constant so that the wire temperature profile could be found. This constant entry temperature was used as the initial temperature of the wire temperature profile and did not have to be ambient temperature. The tension on the wire inlet drum was adjustable, to keep the wire straight, and central as it passed through the tube, preventing it from touching the inside of the tube. Unfortunately it was found that the tension produced by this caused an unacceptable amount of elongation of the wire at elevated temperatures. This elongation or 'creep' resulted in the wire diameter being reduced, as the wire was stretched, until finally the wire snapped. This was overcome by keeping the inlet drum fixed, and passing the wire through a series of pulleys as in figure (5-7), in order to keep it taught. The outlet drum was driven by a smaller roller, which was pressed onto the wire at the top of the drum the arrangement of which can be seen in figure (5-8). The small roller was driven, via a v-belt and pulleys by a small D.C. motor, whose speed was determined by a D.C. variable controller.

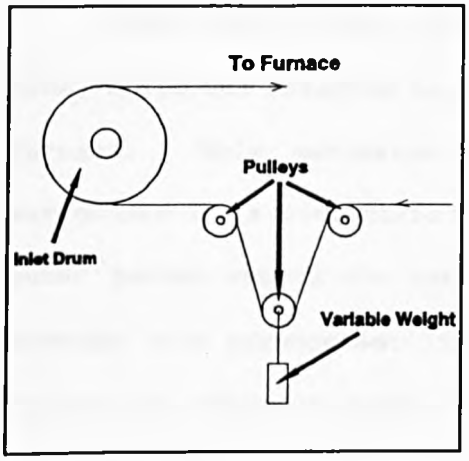

Figure 5-7. Wire tensioning system.

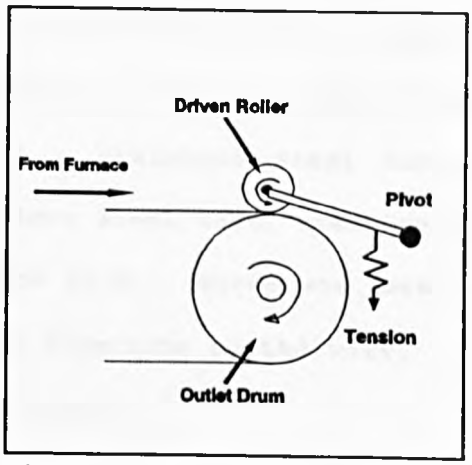

Figure 5-8. Wire driving arrangement.

5.3.2.2 Wire Cooling.

Once the wire had undergone the required annealing process, it was necessary to cool the wire to below its oxidization temperature before it left the reducing atmosphere in the furnace tube.

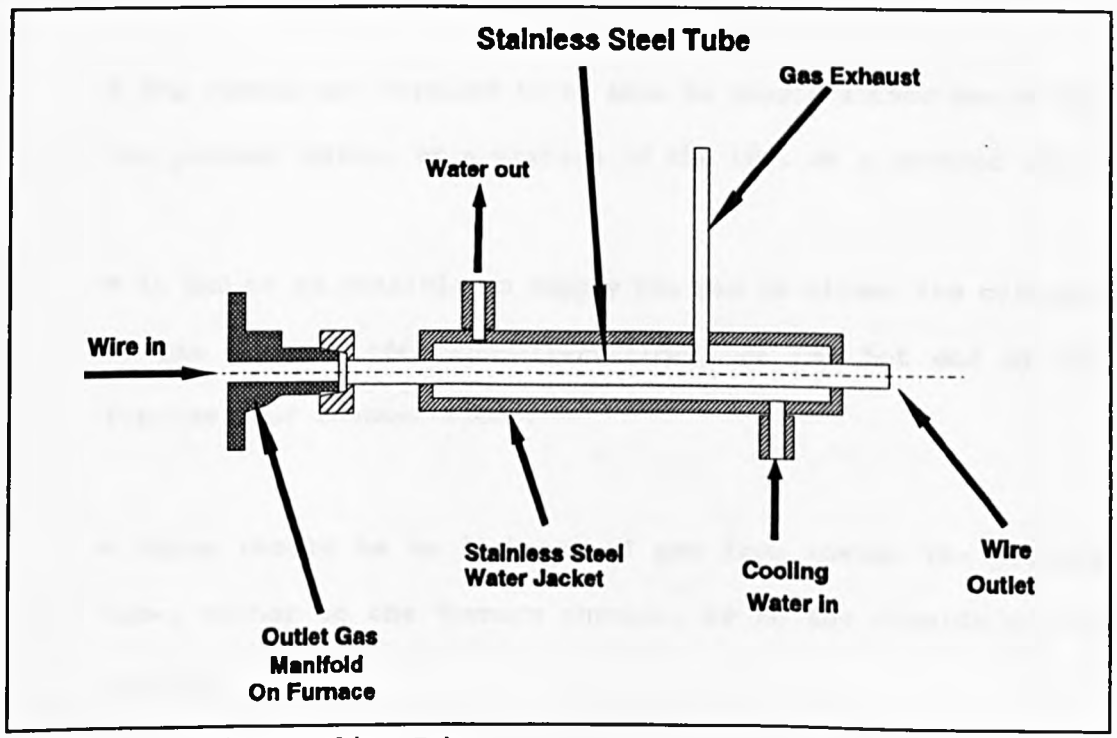

Figure 5-9. Wire Cooling Tube.

This function was carried out by an extension of the process tube, which was attached to the gas manifold at the output end of the furnace. This extension consisted of a Stainless Steel tube, surrounded by a concentric closed Stainless Steel tube, creating a water jacket around the tube as in figure (5-9). Water was passed through this arrangement in the opposite direction to the wire, to provide an effective means of cooling the wire.

5.3.2.3 Process Gas Supply and Safety Equipment.

Because of the high temperatures involved, a reducing gas was required in the process tube, as described in section 5.2. The two main constituents of the furnace reducing gas were Hydrogen and Nitrogen. The gas supply to the process tube must fulfil the following criteria ;

- The system was required to be able to supply either one of the two process gases, or a mixture of the two, at a metered rate.

- It had to be possible to supply the gas to either the cold end of the furnace (for concurrent-flow), or the hot end of the furnace (for counter-flow).

- There should be no leakages of gas from inside the process tube, either to the furnace chamber, or to the outside of the furnace.

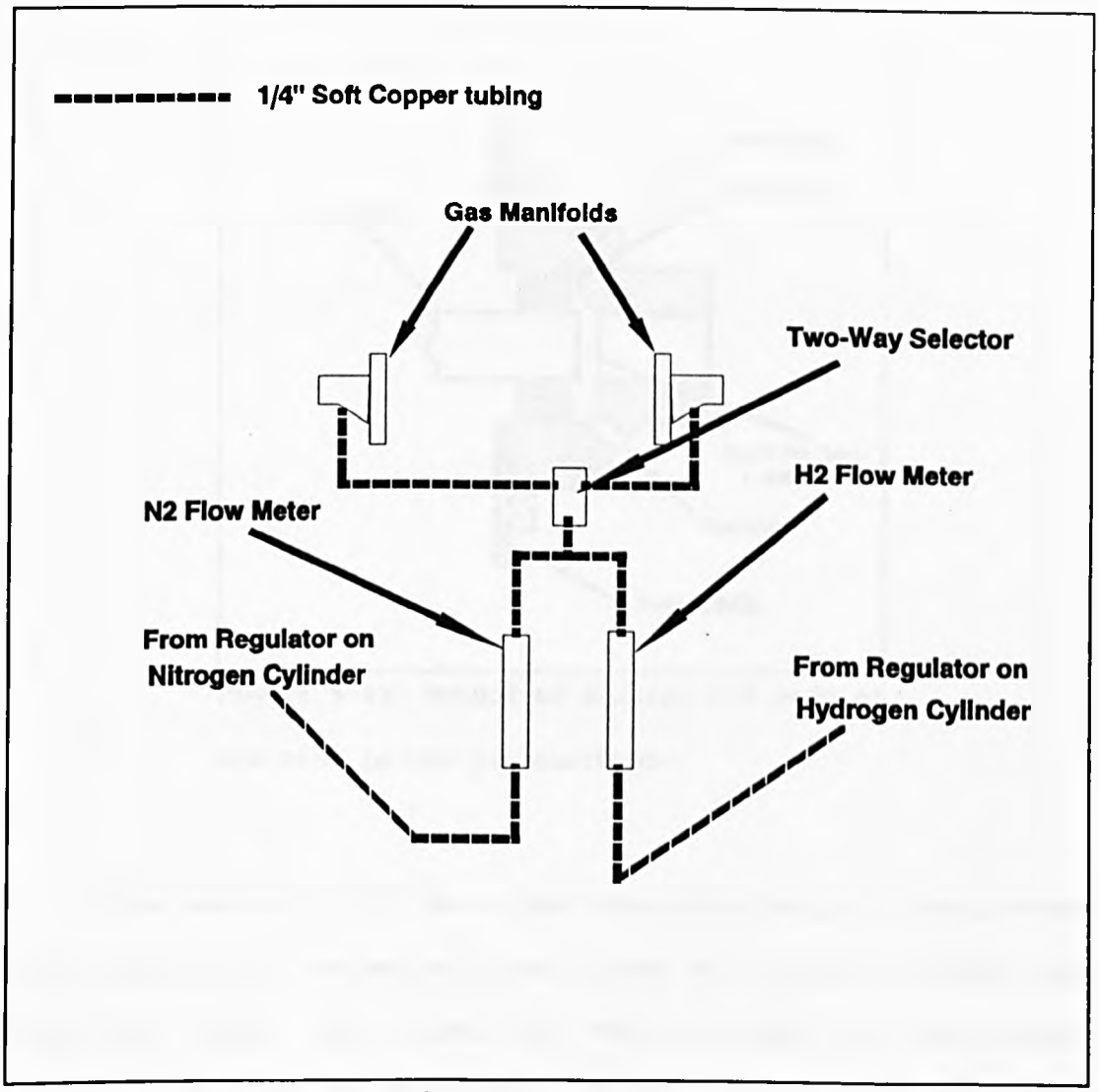

Figure 5-10. A Schematic Diagram of the Reducing Gas Supply.

A schematic diagram is shown in figure (5-10) of a gas supply circuit which satisfies all the above criteria.

The process tube was held in place between the two gas manifolds, and in order to ensure that the tube was free to expand and contract, an effective, but flexible seal was required at these interfaces. This was provided by glands of two types of material, placed alternately in the annular space between the tube and the manifold, as in figure (5-11). This seal was also effective at the high temperatures at which the furnace needs to run.

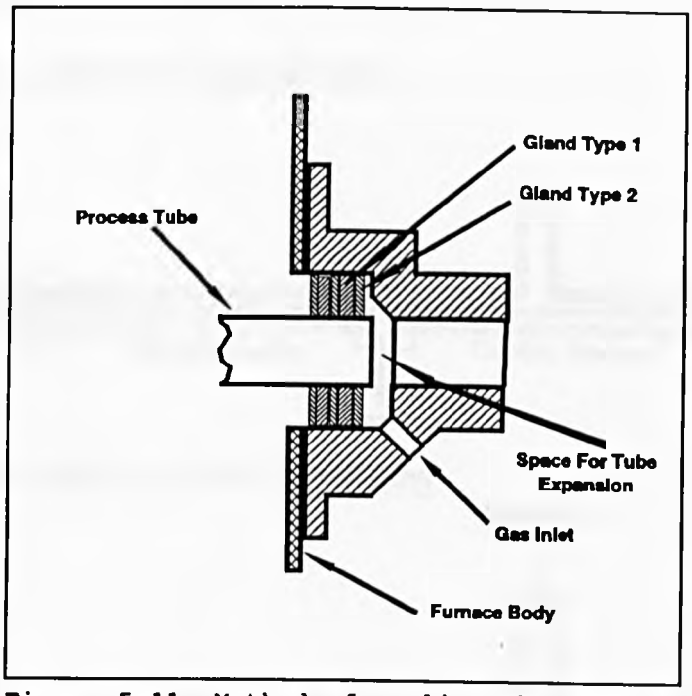

Figure 5-11. Method of sealing the ends of the tube in the gas manifolds.

This sealing system meant that the whole length of the process tube and cooling tube was a single sealed unit, apart from the wire inlet and outlet, gas inlets and the gas outlet on the cooling section. In order to ensure that all the required tube was filled with gas, the various inlets and outlets were blocked off as in figure (5-12), for both types of flow. In order to block the required gas outlets, a wad of ceramic fibre was placed in the tube. Although this did allow a very small amount of gas through, it was found to be very effective for sealing the annular area between the moving wire, and the tube at both ends of the furnace.

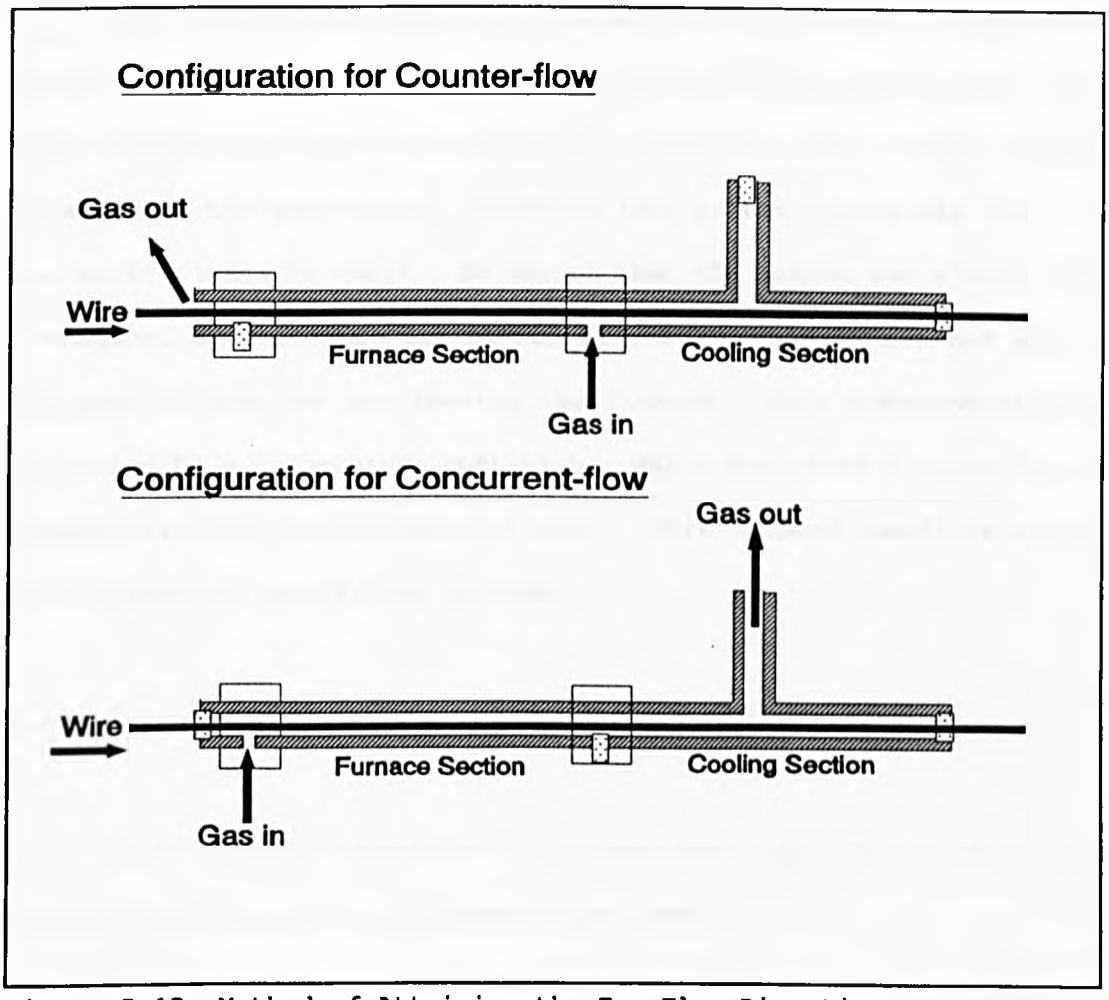

Figure 5-12. Method of Attaining the Two Flow Directions.

In order to work with a highly flammable gas such as Hydrogen in a laboratory environment, it was essential to take the following safety precautions,

- Ensure that no flash-back occurred to the Hydrogen cylinder.

- Ensure that any Hydrogen which left the furnace was burnt off immediately, to prevent a dangerous build-up of the gas in the laboratory.

The first requirement was satisfied by fitting a flash-back arrestor to the outlet of the regulator on the Hydrogen cylinder. The other requirement was fulfilled by placing a lit bunsen burner adjacent to the gas outlet. Hence as long as the bunsen was lit, the gas would always be burnt. To ensure that the bunsen was always lit, a sheathed thermocouple was placed in the bunsen's flame, but not in the path of the hot gas leaving the furnace. This thermocouple was connected to a temperature controller, which activated a siren if its temperature fell below a certain level. This allowed immediate action to be taken to rectify any problem.

5.3.3 Specification of Control System and Instrumentation.

This section describes the equipment used to control the furnace, and the basic instrumentation used.

5.3.3.1 Control System.

The control system was required on the furnace in order to maintain the set temperature in each zone. The system utilised on the prototype was basically the same as that used on a production furnace. A sheathed K-type thermocouple was situated in the centre of each zone, one centimetre above the tube. Each thermocouple was connected to a separate Eurotherm, model 91 PID-ON/OFF, temperature controller. The controller compared the measured temperature of the zone with the set temperature of that zone. It then produced a pulsed output according to the difference in temperatures, and the internal parameters of the controller.

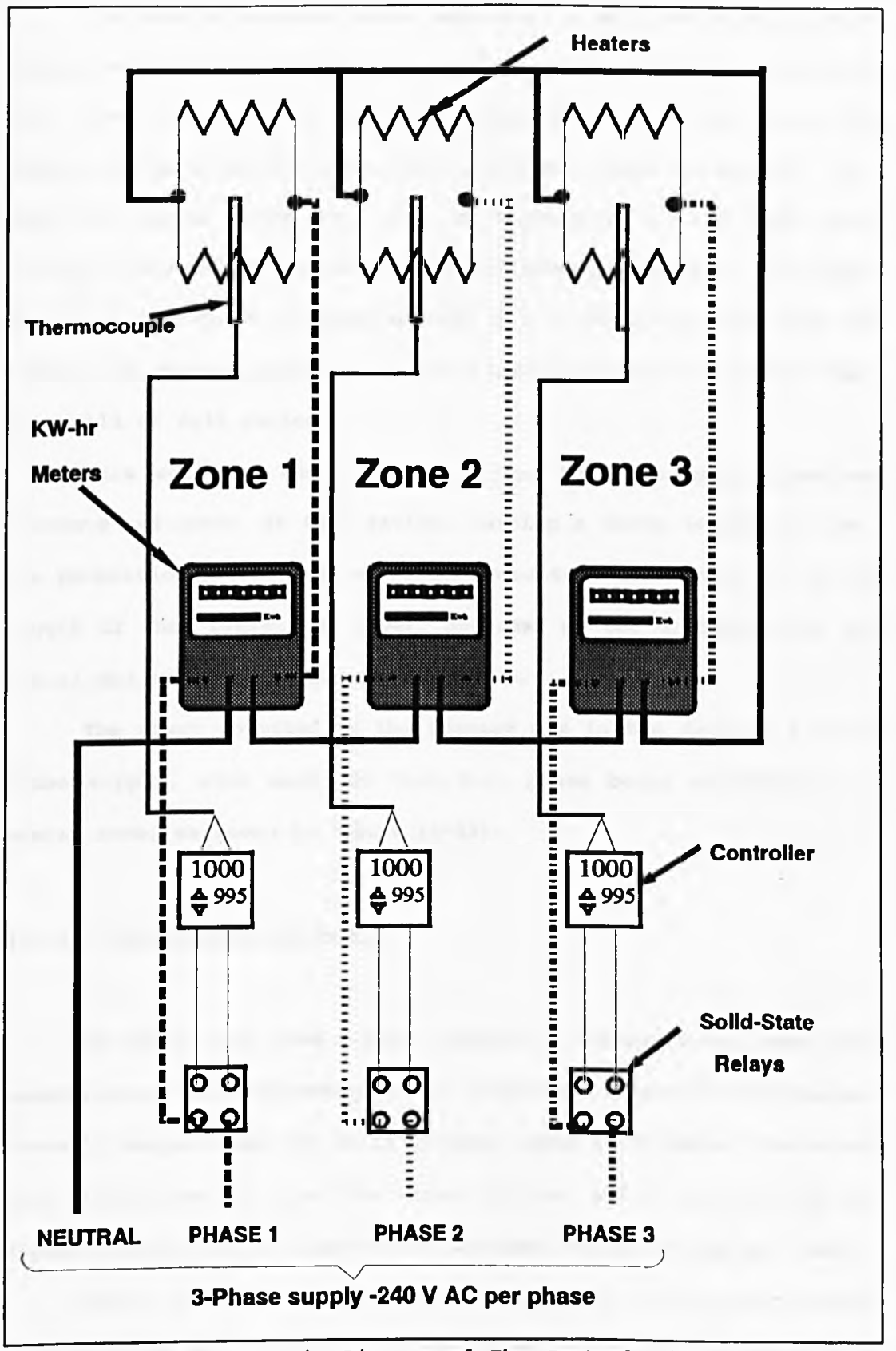

Figure 5-13. A Schematic Diagram of The Control Circuit and Power Supply.

The resulting pulse signal was used to activate a solid state relay, which switched the power supply to the zone's heaters on and off. For instance, if the temperature difference was large, the output signal from the controller would have been constantly 'on', thus the heater would have been on constantly, at its full power rating. However as the temperature difference decreased, the output signal would switch off periodically, for a certain period, thus the heater was only receiving power for a certain proportion of the time, but still at full rating.

This could be summarised by saying that the heater received 'packets' of power at full rating, lasting a given length of time. The proportion of time for which the power to a heater was on, or the length of the 'packet' of power, depended on the difference in the actual and set temperatures of that zone.

The power supplied to the furnace was in the form of a three phase supply, with each 240 Volt A.C. phase being connected to a heater zone, as shown in figure (5-13).

5.3.3.2 Measurement of Power.

As can be seen from circuit diagram in figure (5-13), each zone incorporated a Kilowatt-hour meter. These meters were of the standard domestic single phase 240 Volts AC type, rated 20-80 Amps. The meters were calibrated so that the disc rotated 187.5 revolutions per Kilowatt-hour, and were guaranteed accurate to within one per cent.

Whilst the power to the heater was switched on, the disc rotated at a constant rate, and the numerical display was also incremented at a constant rate.

When the power to the heater was off, the meter stopped. In order to find the power used by the heaters, each meter reading was recorded at ten minute intervals. The average power used by each zone in a given period was found as follows ;

$$P = \frac{\text{Change in Meter Reading (Kw-hour)} * 60}{\text{Time Period (Minutes)}}$$

Unfortunately, this method required regular and accurate reading of the three meters, which was extremely difficult when trying to carry out other measurements on the furnace. A more sophisticated method of recording the zonal powers is described in chapter 6.

5.3.3.3 Measurement of Temperature.

The important temperatures which needed to be recorded on the furnace were those of the process tube. The methods used to record wire temperatures are described in chapter 6.

The main problem in measuring the tubes' temperatures was that of attaching the thermocouple to the tube surface without effecting the temperature of the surface. This necessitated a minimum area of contact between the tube and the thermocouple. Also desirable was a minimum thermocouple wire cross sectional area through which heat could be conducted to or from the surface. Another requirement was that the thermocouples were easily removable when a faulty thermocouple needed to be replaced, or when a different tube was to be used. Most importantly, the thermocouples were required to withstand temperatures of over 1000^{o}C for at least five working hours.

The type of thermocouple used was made from K-type, Chromel-Alumel thermocouple wire, covered with high temperature fibre-glass insulation. The diameter of the thermocouple wires used was 0.3 mm, in a flat pair configuration, with a total insulation thickness of 0.5 mm. The fibre-glass insulation was removed from the last fifteen centimetres of both wires and replaced with high temperature ceramic fibre sleeving on each wire. This provided electrical insulation for the wires at high temperatures, and some protection from deterioration of the wires due to high temperature oxidation. The protruding two wires were then spot welded together, creating a measuring junction, which was in turn spot welded to the inconel tube at the required position.

Unfortunately, the spot welding equipment was not available to carry out the welding required in-situ, so the process tube had to be removed from the furnace, and taken to a separate welding laboratory. This was necessary in order to replace one or more of the thermocouples on the tube.

In order to prevent any of the good thermocouples breaking off the tube, the arrangement needed strengthening. This was achieved by 'stapling' the insulated part of the thermocouple to the tube using a two centimetre length of stainless steel wire, spot welded to the tube on either side of the thermocouple, approximately one centimetre from the junction. This was found to provide a good means of reducing the stress on the joint between the junction and the tube. When all the thermocouples were in place on the tube, it was re-installed onto the furnace, with the thermocouple wires fed between the upper and lower halves of the furnace.

On the outside of the furnace, the thermocouples were connected to extension cable via a multiple connector. The arrangement of the tube thermocouples is illustrated in figure (5-14).

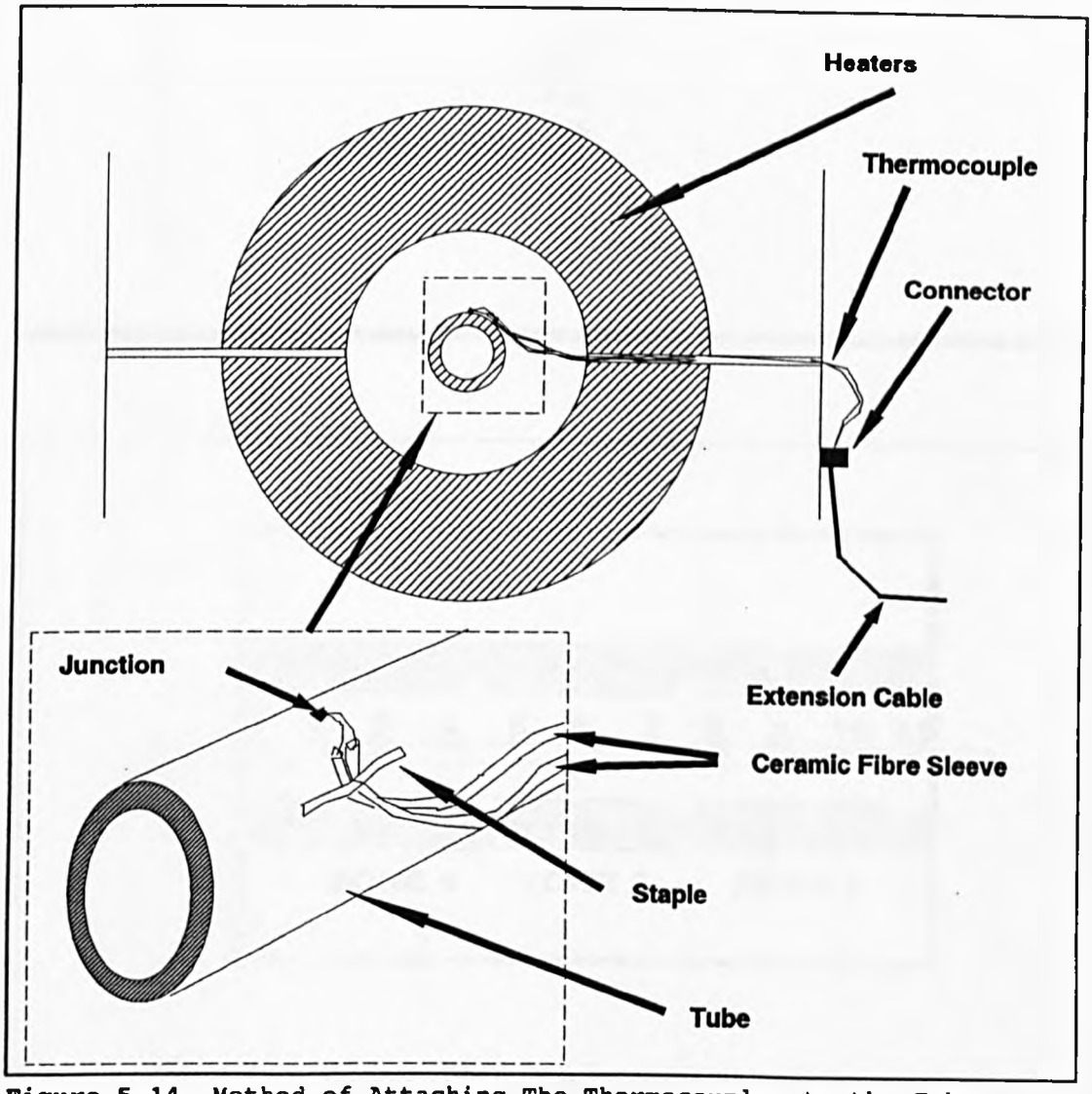

Figure 5-14. Method of Attaching The Thermocouples to the Tube.

In total, eleven thermocouples were placed on the tube, in a straight line on the top of the tube, with a distance of ten centimetres between each.

The distance of each thermocouple from the furnace entrance is given in the table (5-1), whilst figure (5-15) shows how each thermocouple's position relates to the furnace furniture.

Table 5-1. Position of the tube thermocouples.

Thermocouple Number	Furnace Distance mm
1	135
2	235
3	335
4	435
5	535
6	635
7	735
8	835
9	935
10	1035
11	1135

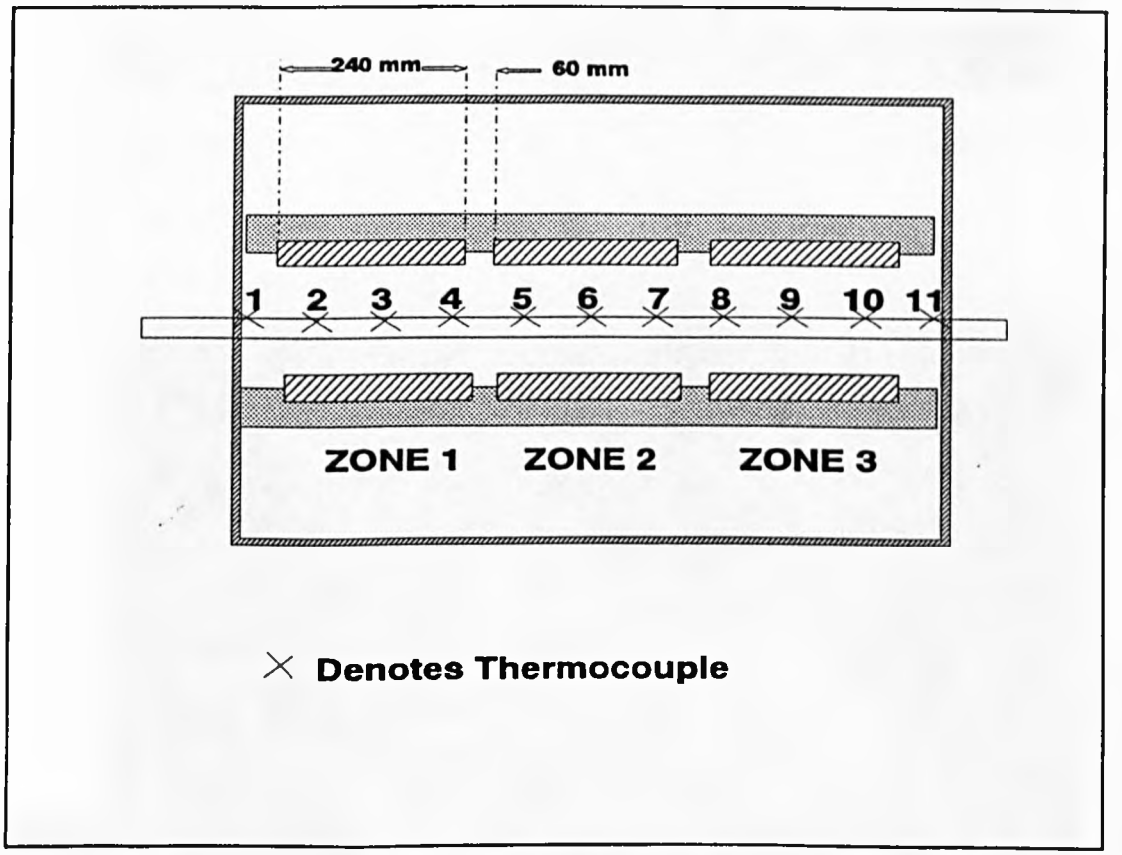

Figure 5-15 Location Of The Thermocouples In Relation To The Furnace Furniture.

The photograph in figure (5-16) depicts the thermocouples attached to the tube.

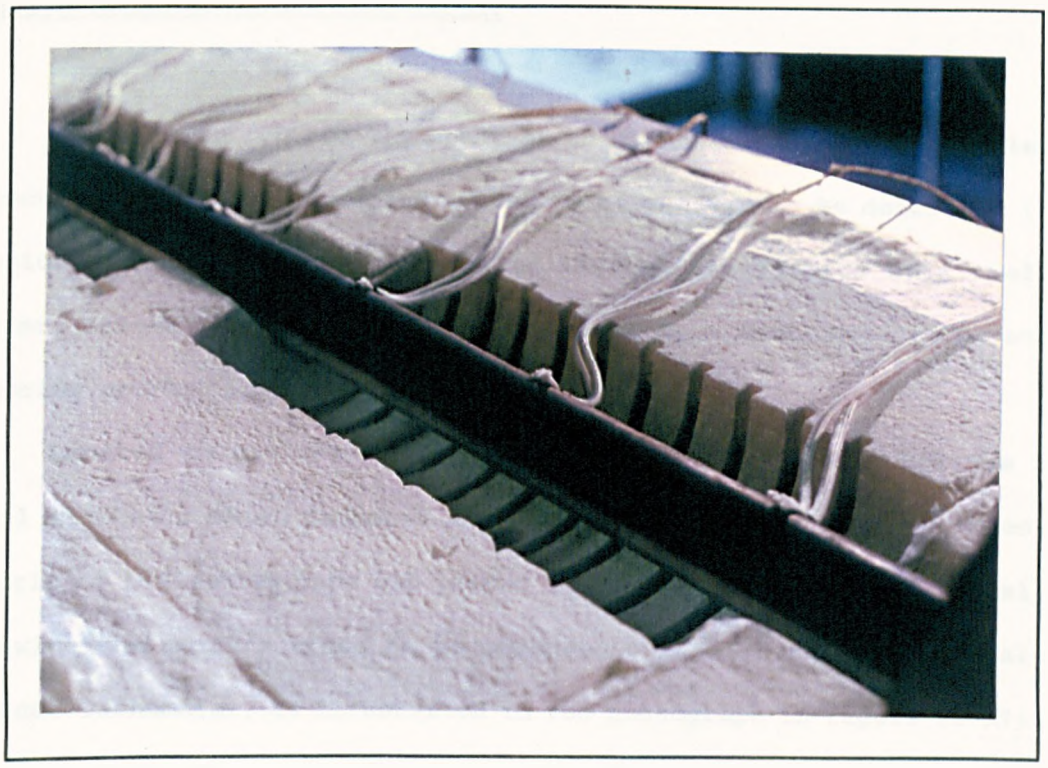

Figure 5-16. Photograph depicting the thermocouples attached to the process tube.

Figure 5-17. Measurement of the motor speed using the digital optical tachometer.

5.3.3.4 Measurement of Wire Speed.

In order to control the speed at which the wire was being pulled through the furnace, the speed needed to be measured. As described in section 5.3.2.1, the wire was pulled through the furnace by a small roller, driven via two pulleys and a V-belt, by a small D.C. motor and reducing gearbox arrangement.

Located on the rear end of the rotor shaft of the motor was a small flywheel, which dampened any fluctuations in the motor's speed. A strip of reflective tape was placed on the outside of this flywheel, allowing the motor's speed to be measured using a hand held Digital-Optical-Tachometer, as illustrated in the photograph in figure (5-17).

In order to ascertain wire speed from the measured speed of the motor, a simple calibration experiment was carried out. The motor was set to its slowest maintainable speed using the variable D.C. controller, and the speed of the roller was measured by timing how long it took to complete twenty revolutions. The roller speed could then be translated to wire speed using the following expression,

$$S = \frac{\pi * ROLLER\ DIAMETER\ (MM)\ *\ ROLLER\ SPEED\ (RPM)}{60} \quad (MM/S)$$

This was repeated at nine regular intervals up to the maximum motor speed, and the results are given below in table (5-2). These results are shown in the graph in figure (5-18), and show the expected linear relationship.

Table 5-2. Results of calibration test for wire speed.

Motor Speed (RPM)	Wire Speed (mm/s)
215	26.9
535	71.4
865	114.2
1158	151.8
1486	193.7
1820	241.6
2130	282.7
2433	314.2
2657	350.8

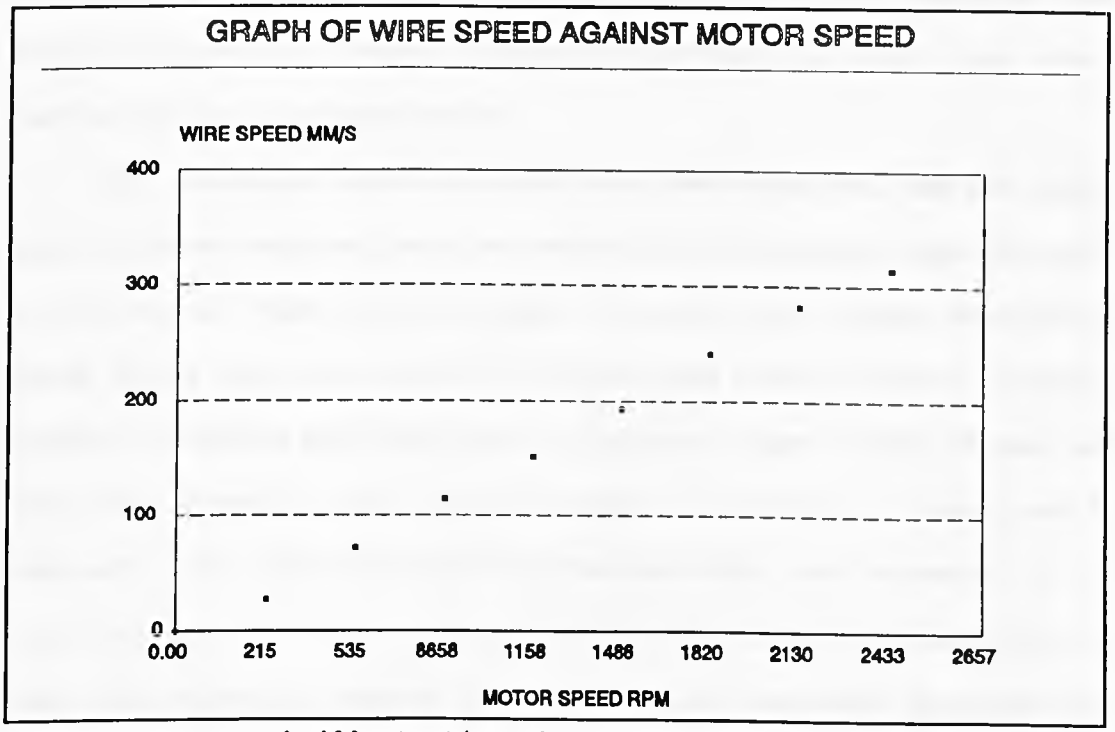

Figure 5-18. Graph illustrating the relationship between motor speed and wire speed.

The required calibration factor was found from the gradient of the best fit line through the points, giving the simple relationship,

$$S\ (MM/S) = 0.132 * MOTOR\ SPEED\ (RPM)$$

This expression was used to determine the wire speed, and to set the motor speed for the required wire speed.

5.3.4 Data Acquisition Using the Orion Data-Logger.

In order to record the temperature data from the thermocouples, a system was required to convert the thermocouple voltages to temperatures, and then to store them for further analysis. The chosen method was to use a piece of equipment known as a data-logger. The data-logger used was a Schlumberger 'Orion' Data-logger, the operation of which is described in Appendix A. The Orion had facilities for logging up to two hundred channels independently, which was quite sufficient for this application.

The extension cables from the tube thermocouples, and any other thermocouples required, were connected to the Analogue Input Circuit of the Orion. This was done using a standard 35303A Input Connector, which plugs onto the end of a 35301A Reed Relay Selector circuit board, accessible from the rear of the data logger. Each channel of the Input Connector had three terminals - H (high), L (low) and G (ground). The positive wire from the extension was connected to H, and the negative wire was connected to both L and G, as described in the Orion Operating Manual [6]. Each input connector provided the connections for twenty thermocouples to twenty channels of the Orion.

The tube thermocouples were connected to the first eleven terminals of an input connector, and this was plugged into the first Reed Relay Selector circuit board. Thus the tube thermocouples occupied the first eleven channels on the Orion.

Information about the method of programming the Orion to log and process data is given in Appendix A and in chapter 6.

CHAPTER 6. EXPERIMENTAL WORK CARRIED OUT ON THE PROTOTYPE FURNACE.

6.1 SETTING UP THE PROTOTYPE FURNACE FOR THE EXPERIMENTAL WORK.

6.1.1 Fitting Wire to the Furnace.

In order to carry out a test on the furnace, it was first necessary to install the required test piece of wire into the furnace. The wire used was supplied by Meltech Furnaces Ltd, and Critchley Sharp and Tetlow Ltd, and was a range of sizes of Austenitic (300 series) Stainless Steel. The selected wire was firstly threaded through a guide at the inlet of the furnace to keep it central in the furnace. It was then threaded through the process tube and the cooling tube, then around the driving drum. The wire was then passed over the straightening/ tensioning pulleys as in the photograph in figure (6-1), before going around the second drum.

The wire was then cut off to the correct length, and the two ends placed in a set of clamps, as illustrated in the photograph in figure (6-2), and then cleaned ready for welding together.

Two methods were used to weld the ends of the wire together. The first method, for wires of 3 mm diameter or less was to use a portable spot-welder with a hand held electrode holder. The welder used was a type TW2 portable spot welder, made by Hirst Electronics and was supplied with a set of small 'remote-initiate' hand-held tongs. The wires were placed in the clamps so that the two ends of the wire were overlapping, and the clamps tightened.

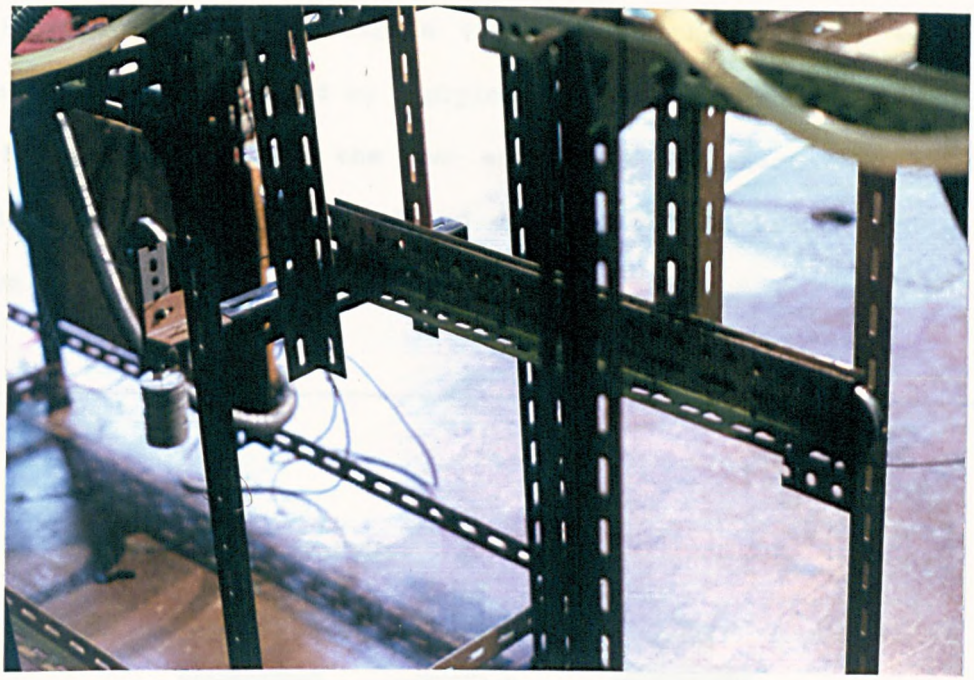

Figure 6-1. A photograph showing the wire on the tensioning pulleys.

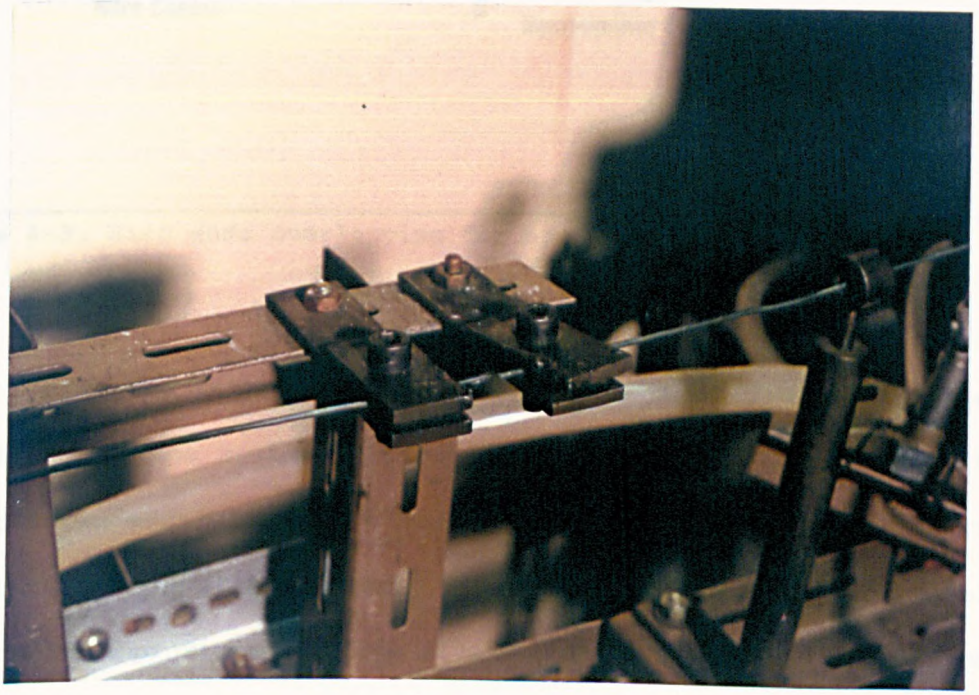

Figure 6-2. A photograph showing the ends of the wire in the clamps, ready for joining.

The electrodes were then held together so that the two wires were between them as in figure (6-3) , and the required welding current was then activated by applying pressure to the trigger on the hand held tongs. Once the two ends were satisfactorily joined together, the weld area was filed down to give a smooth and even surface.

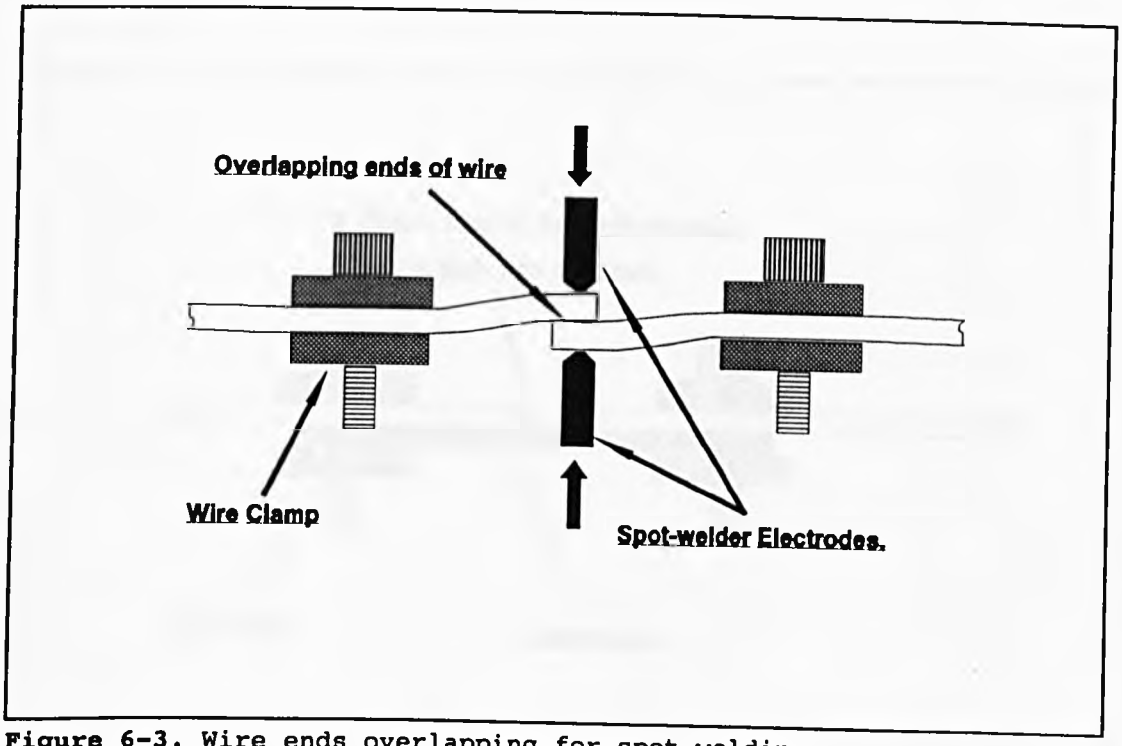

Figure 6-3. Wire ends overlapping for spot welding.

The second method was required for wires of diameter greater than 3 mm, as the spot welder could not supply sufficient power to fuse the two ends together. This method involved using an electric arc welder to join the two ends. The two ends were filed to roughly an angle of approximately forty five degrees. The ends were then put in the clamps so that the two ends formed a 'V' shaped cavity. A strip of Copper was then clamped under the wire, providing a heat sink to prevent the wire from melting.

The 'V' shaped cavity was then filled using the arc-welder with a Stainless Steel filler rod, producing a solid joint as in figure - (6-4). As for the first method, the joint was then filed down to produce a smooth and even finish.

The wire was then in the form of a loop, which could be passed through the furnace to reproduce results that would occur for a continuous length of wire.

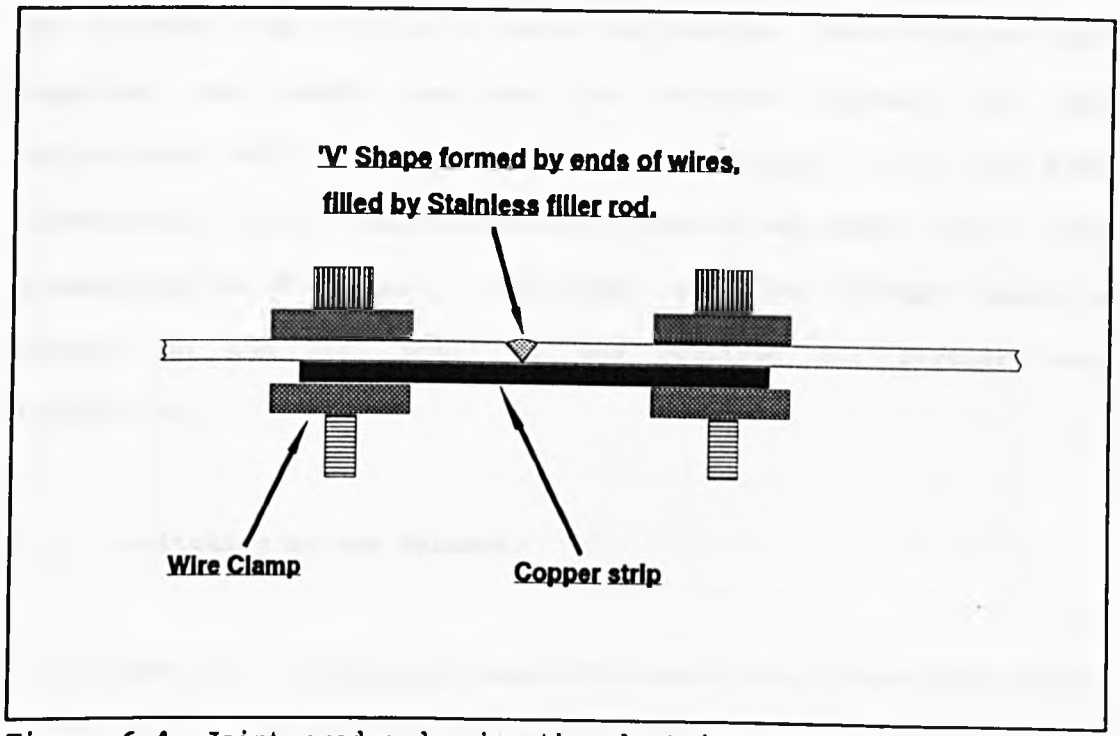

Figure 6-4. Joint produced using the electric arc-welder.

Finally, the annular area between the wire and the tube had to be blocked off at one end of the furnace to provide a seal for the process gas (see section 5.3.2.3).

6.1.2 Setting Up The Instrumentation.

Before switching the furnace on, it was necessary to check all the tube thermocouples for damage, and then to connect the input connectors to the Orion. Once all the required connections had been made, the Orion and the BBC Micro were turned on. The 'BASIC' program with data files containing the required Orion data bases was then run on the BBC. The first effect of this was to ask the user for a name for the disc file in which to store the results. Once this had been supplied, the logger was sent the relevant channel and task definitions, and the logger started. The output of all the tube thermocouples could then be checked in case of any faults such as bad connections or breakages. The logger was then 'Halted' using a command on the BBC, until it was required for further data acquisition.

6.1.3 Switching on the furnace.

Once all the equipment had been checked, the three-phase supply to the heaters and controllers was switched on from a master switch on the laboratory wall. The display on each of the controllers was then illuminated, showing the actual and the set temperature of each zone. The set temperature of each zone could be adjusted to its required value using the set-up keys on the front of the appropriate controller.

The three controllers were then set to 'self tune' in order to provide optimum performance of the furnace.

Before the furnace reached the oxidation temperature of the tubes, the reducing gas supply was introduced to the furnace. The direction selector was set to provide the gas flow in the required direction through the furnace. The flow rate was then adjusted to the required level using the needle valve incorporated in the flow meter. As hydrogen was being used, the bunsen flame was placed at the appropriate point (see section 5.3.2.3) in order to ignite the gas leaving the furnace. The furnace was now ready for experimental work to commence.

6.2 THE 'START-UP' TEST.

This test was carried out in order to establish the 'background' conditions of the prototype furnace. The background conditions comprised the temperature of the tube thermocouples and the power supplied to each of the zones with the furnace switched on, but with no wire flowing through it. The furnace was set up as described in section 6.1 with the set temperature of the three zones at 1000°C, and then switched on. The process gas used in the furnace was Hydrogen, set to flow in a counter-current direction at 1 litre per minute. The data-logger was then operated, the task of which was to scan all the tube thermocouples every thirty seconds. The temperature of each thermocouple was logged at each scan provided that it had increased by more than 1°C since its previous measurement. All the logged data, along with the time at which it was measured was then sent to a data file on the 'floppy' disk drive attached to the BBC Microcomputer. The logged temperatures were also displayed on the monitor of the BBC Microcomputer so that they could be observed as the test proceeded.

In addition to the temperature measurements, the readings from the three Kilowatt-hour meters were required at five minute intervals. These were observed and recorded along with the time of recording. This was continued until all the tube temperatures were observed to have become constant, indicating that the furnace had reached its operating temperature, and could be described to be at 'Steady-state'. When a given tube temperature became constant, its value at each scan was no longer logged, and hence no longer displayed on the monitor. The furnace was considered to have attained steady-state conditions when none of the tube temperature had been displayed on the monitor for a period of one minute or more. The power supplied to each zone was also deemed to have reached its steady-state value at this point. The method of processing and the presentation of the data from this test are included in chapter 7.

6.3 THE 'RUNNING' TEST.

Once the furnace had reached Steady-state conditions as described in the previous section, the 'running' test could be carried out. The object of this test was to assess the tube temperature profile and the power supplied to each zone with wire of a given diameter 'running' at a constant speed through the furnace.

The wire winding motor was switched on and the wire speed determined using the Digital Optical Tachometer as described in section 5.3.3.4. Adjustment of the variable D.C. controller which supplied the motor then provided the required wire speed for the test. Once the wire was 'running', the logger was set to scan and log the tube thermocouples every thirty seconds as for the start-up test.

The readings from the three Kilowatt-hour meters were also recorded every five minutes as described for the start-up test. The tube temperatures and zonal powers were noted when both sets of results had become constant.

Having ascertained that the tube temperatures were constant, the temperature of the wire itself was measured as it passed through the furnace. The methods used for wire temperature measurement are described in the following section.

6.4 WIRE TEMPERATURE MEASUREMENT.

In order to establish the extent of the heat transfer within the furnace, it was necessary to obtain a temperature profile for the wire as it passed through the furnace. Several methods of wire temperature measurement were considered, including the thermocouple probe used for the 'on-site' temperature measurement. The method decided upon however was to use what is known as a 'Sacrificial' thermocouple. Standard high-temperature glass-fibre insulated 'K-type' thermocouple wire was spot-welded at one end to produce the junction. This junction was then attached to the wire itself, and pulled through the furnace.

Because the thermocouple insulation was fibre-glass, with a maximum temperature of approximately 400^{o}C it would have been destroyed when subjected to the temperatures inside the furnace, hence the name 'Sacrificial'. However the insulation was found to remain intact, at least until the end of the last heating zone of the furnace.

Therefore, although a new thermocouple was required for each wire test, this was still a cheap and very effective method of measuring the temperature of the wire.

The output from this thermocouple was passed, via compensating cable, to channel 13 of the Orion. The Orion was programmed to scan this channel every 0.2 seconds, and to log the temperature only when it had changed by more than one degree centigrade since the previous scan. Three different procedures were used to measure wire temperature, these are discussed below.

6.4.1 Wire Temperature Measurement Method A.

This was the method used first, and was the most straightforward of the three. Once the furnace had reached steady state temperature with the wire moving, the logger was halted, and the wire drive switched off. The junction of a pre-prepared sacrificial thermocouple was then spot-welded to the wire at a position just before the entry to the furnace. The photograph in figure (6-5) overleaf depicts the thermocouple welded to the wire just before it enters the furnace. The logger was then re-started, and the wire winder switched on at the same speed as before. The wire then pulled the thermocouple through the furnace, and the thermocouple measured the wire temperature as it was heated. When the thermocouple junction reached the end of the cooling tube, the logger was halted and the wire drive switched off. The thermocouple was then detached from the wire, and removed from the furnace. However when the wire was stopped for thermocouple attachment, the tube temperatures departed from the steady state conditions.

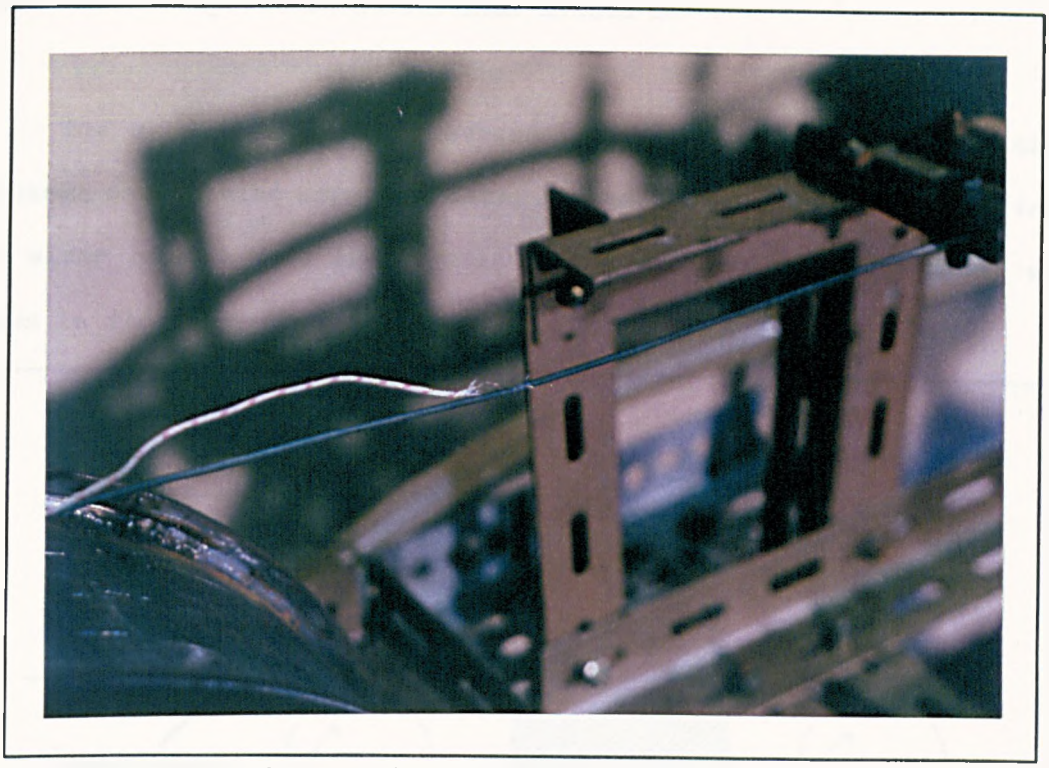

Figure 6-5. A photograph of the sacrificial thermocouple welded to the wire.

Therefore the heat transfer from the tube to the wire would have been different from that which would have occurred had the wire not been stopped. In order to minimize these effects, the period for which the wire was stopped was kept as short as possible. Unfortunately, when the junction was welded to the wire, heat was introduced to the area of wire around the weld. Therefore the wire around the thermocouple junction was not at ambient temperature for at least a minute after the weld took place.

This meant that a 'trade-off' had to be made between speeding up the process, and having the thermocouple at ambient temperature at entry to the furnace. In addition to this, when the wire winder was re-started, it did not reach the required speed immediately, so the wire may not have been at the required speed when it entered the furnace.

6.4.2 Wire Temperature Measurement Method B.

The second method was devised in an attempt to eliminate the problems encountered using the first method. Method B involved having two wires of the same diameter in the furnace at the same time, as shown in figure (6-6) below.

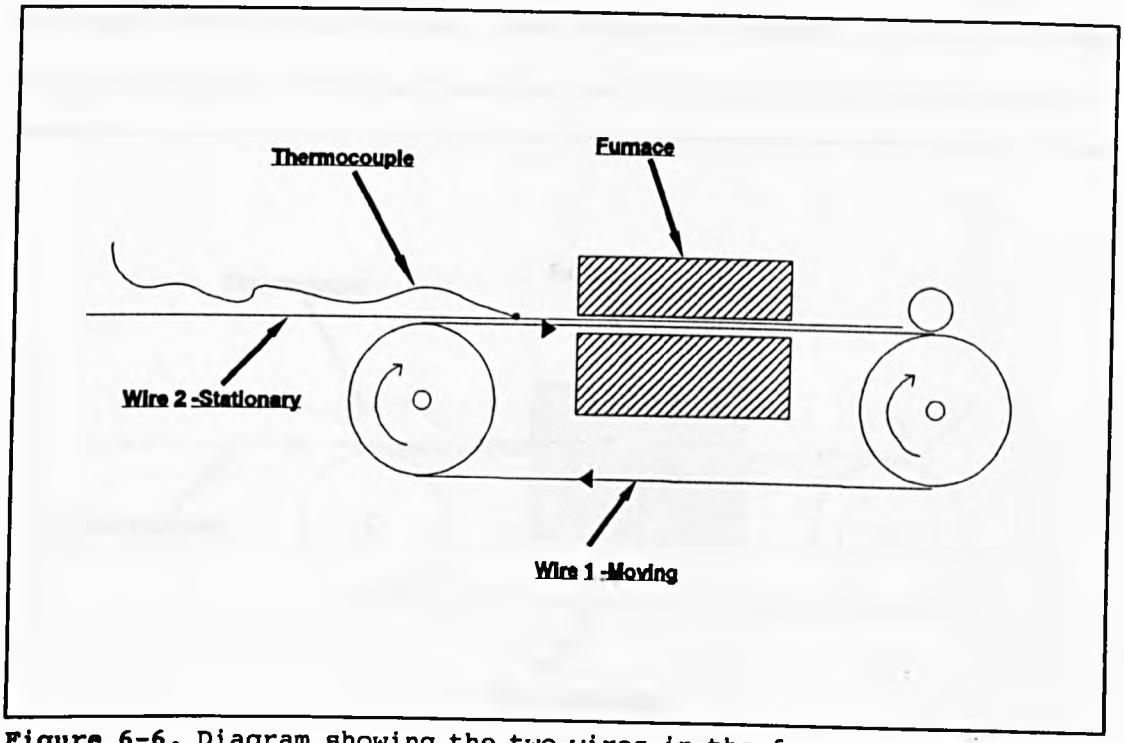

Figure 6-6. Diagram showing the two wires in the furnace, prior to the wire test.

Wire 1 was a loop as before, which was initially moving at the required test speed. Wire 2 was a straight piece of wire, approximately twice the length of the furnace, and was stationary in the process tube, with one end adjacent to the wire winder. Because wire 2 was stationary in the tube, it was assumed to have had a minimal effect on the heat transfer to wire 1 from the tube.

Welded to wire 2, at a distance of approximately thirty centimetres from the furnace entrance, was a sacrificial thermocouple, as used in method A.

Again the thermocouple was connected to channel 13 of the Orion, and logged as before. When the furnace had reached steady-state conditions, wire 1 was cut adjacent to the winding drum, whilst it was still moving.

The end of wire 2 was then immediately placed between the wire roller and the drum, causing it to be pulled through the furnace at the same speed at which wire 1 was originally moving. Thus wire 1 was now stationary, and wire 2 moving, as in depicted in figure (6-7).

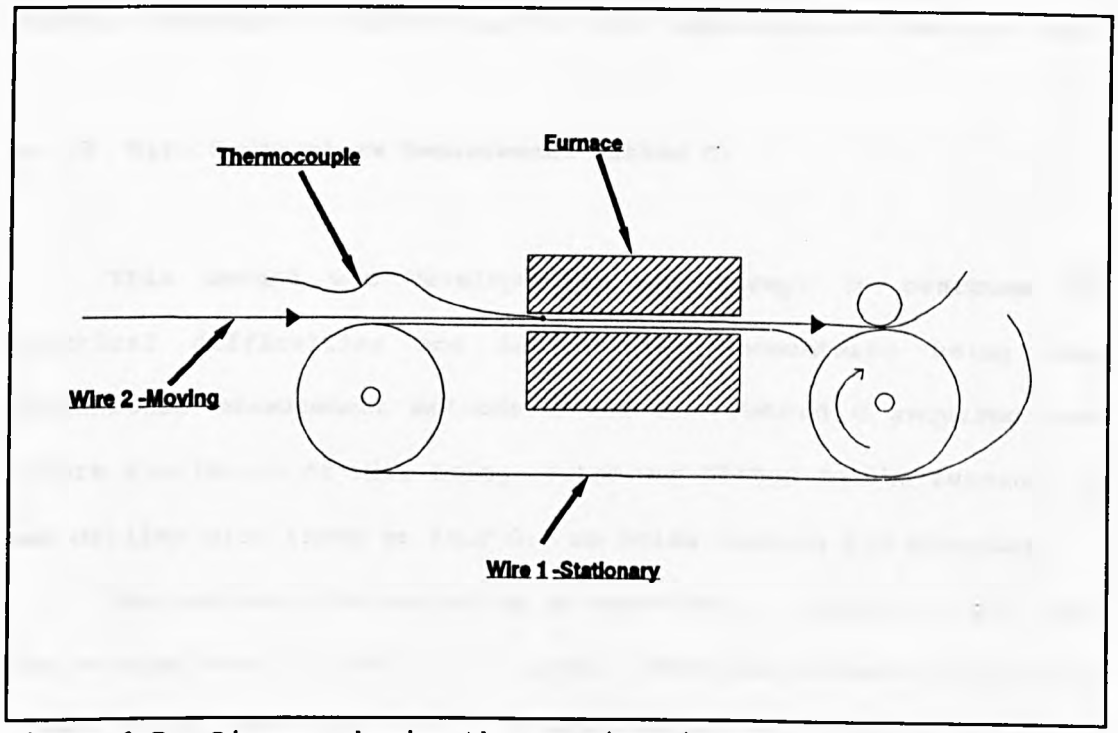

Figure 6-7. Diagram showing the two wires in the furnace -During wire test.

Therefore the thermocouple was passed down the furnace tube in the same manner as in method A, but in this case there was only a minimal theoretical change in the furnace conditions. This could be assumed due to the fact that there was always one stationary wire and one moving wire in the process tube at any one time.

The main problem encountered with this method was in cutting wire 1, and then feeding wire 2 into the wire winder as quickly as possible. This was made more difficult by the tendency of the loose ends of the wires to become entangled with each other and other parts of the furnace. Ideally more than one pair of hands was required to carry out this operation successfully.

Another disadvantage associated with methods A and B was that the thermocouple was welded to the surface of the wire in both cases, and was therefore not measuring the true temperature of the wire core.

6.4.3 Wire Temperature Measurement Method C.

This method was developed in an attempt to overcome the practical difficulties and inaccuracies encountered using wire temperature measurement methods A and B. Method C required that before the length of wire being tested was fitted to the furnace, it was drilled with three or four 0.7 mm holes through its diameter.

The wire was then installed as described in section (6.1.1), and the running test carried out as usual. When the furnace reached its steady state condition, the wire temperature could then be measured. A previously prepared sacrificial thermocouple was connected to the logger in the same manner as before. With the logger operational, the moving wire was examined closely to find one of the previously drilled holes. On finding such a hole, the thermocouple was then inserted into the hole, as shown schematically in figure (6-8), and in the photograph in figure (6-9), just before the entry to the furnace.

The wire then carried the thermocouple through the furnace with the logger recording its temperature as before.

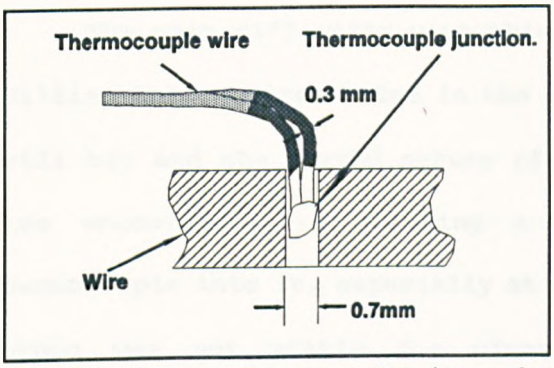

Figure 6-8. Diagram showing the thermocouple in the drilled hole.

This method was more accurate than the others in measuring the actual temperature of the wire because the junction was shielded from most of the radiation from the tube and convection from the gas in the tube. It was also assumed that the thermocouple inserted into a hole in the wire measured its temperature close to its core, rather than on its surface. This method of measuring wire temperature also had the least effect on the steady state tube temperatures and power consumed by the furnace.

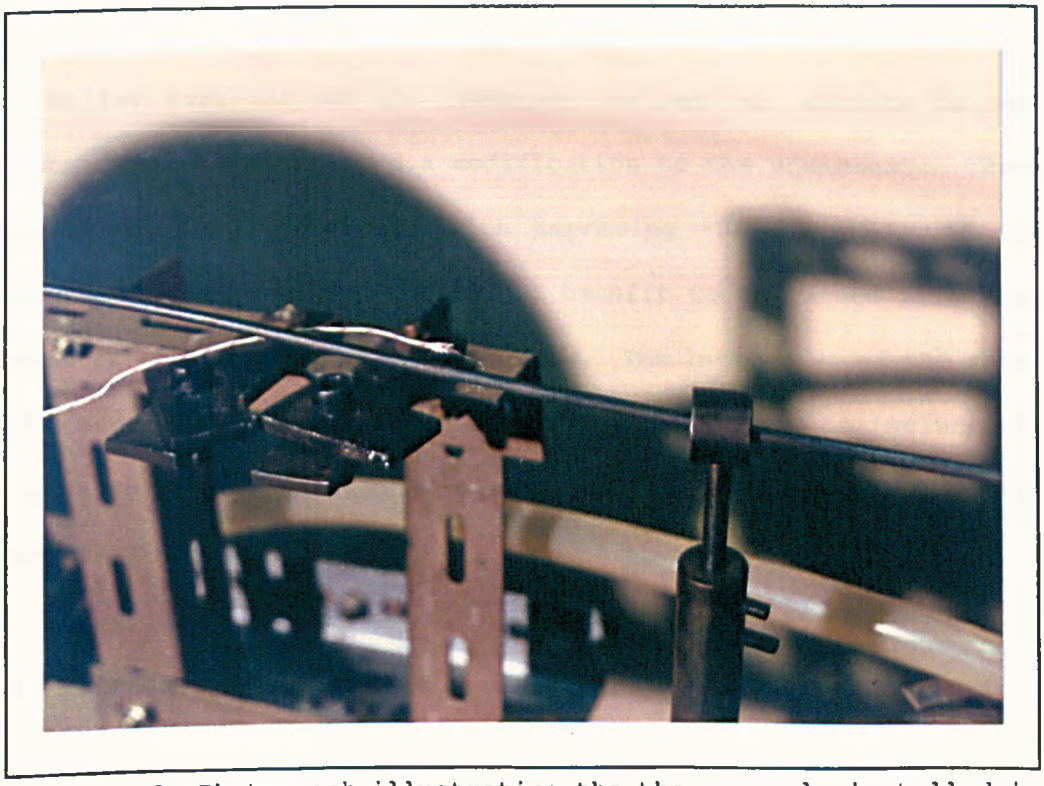

Figure 6-9. Photograph illustrating the thermocouple installed in the drilled hole in the wire.

The main difficulty with this method was the actual process of drilling the required holes in the wire, due to the small size of the drill bit and the curved nature of the wire surface. Problems were also encountered in locating a hole, and fully inserting the thermocouple into it, especially at higher wire speeds. Finally, this method was not viable for wires of diameters less than three millimetres, as the holes made the wire too weak to process without breaking.

The method of processing the data from the wire temperature tests was the same for each method, and is discussed chapter 7.

6.5 IMPROVEMENTS TO MEASUREMENT TECHNIQUES.

Whilst carrying out the tests on the furnace, various factors were observed which required a modification to the equipment. These factors were mostly involved with improving the integrity of the results, but there was some practical benefit to be gained from them in terms of carrying out the experiments. The latter two of the above wire measurement procedures should, strictly speaking, be included in this section - but for reasons of continuity were placed together with the original method (A).

6.5.1 Introduction of a power logging circuit.

Whilst carrying out the tests on the furnace, difficulty was encountered in taking the readings from the three Kilowatt-hour meters at regular intervals due to pressure from other tasks.

Therefore a process was devised whereby the power intake of the three zones could be measured and recorded by the Orion. The power to each heater was regulated by its controller, which sent pulses to the solid state relay, switching the supply on and off as shown in figure (6-10)

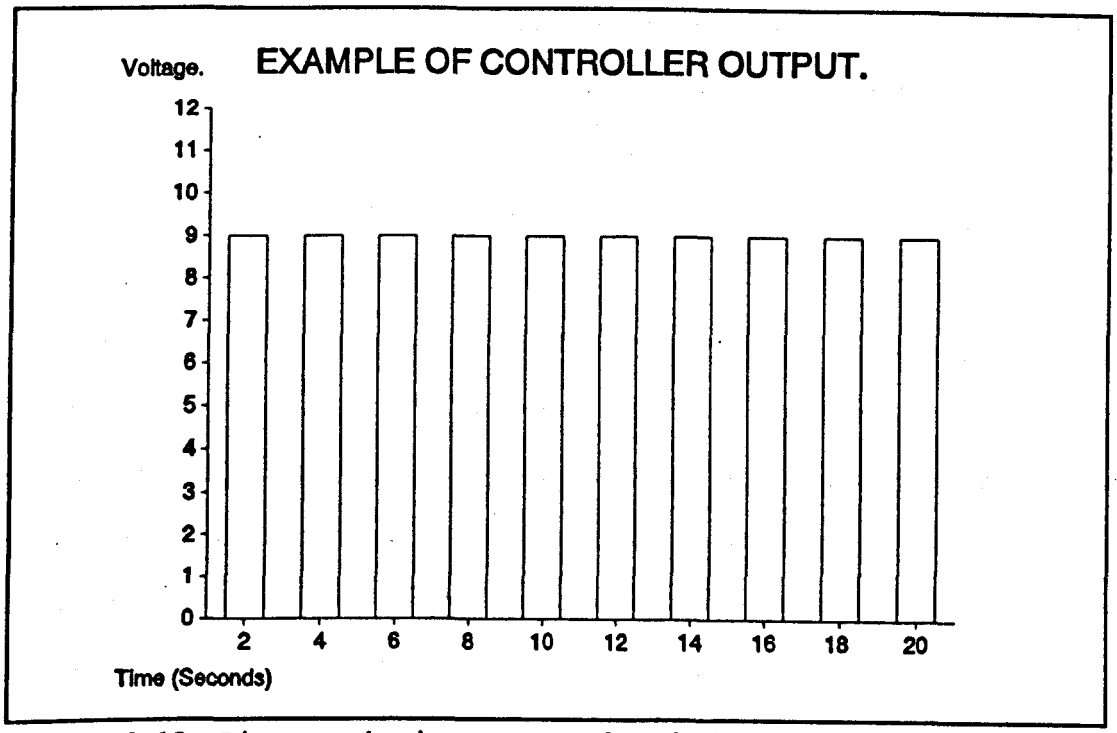

Figure 6-10. Diagram showing an example of the controller output.

If, as shown in the example above the controller pulses on for one second and then off for one second, the power to the heater would be on for fifty percent of the time, and the heater would therefore have been consuming an average of half the full power rating of the heater.

A test was carried out on the three kilowatt-hour meters with the heaters switched on all the time. The disc on each meter rotated 187.5 times for each kilowatt-hour consumed. The time was recorded for the disc to complete ten revolutions on each meter, which translated to a power consumption of 0.0533 Kilowatt-hours.

The time taken to consume this power was found to be 170 seconds, which translated to a maximum power rating for each heater of 1.130 Kw. Thus the above example consumed fifty percent of this value, which is 0.565 Kw. Therefore the actual power consumed by one of the heaters at any time could be calculated from the proportion of the time that the controller's output signal was 'on'. In order to measure this value using the Orion, a 'counter-timer' module was required to count the number of 'on' pulses in a given time period. Unfortunately this module was not available for the Orion, and so another method needed to be developed.

The analogue input circuit of the Orion had an 'average value' option for processing the measured data, which could be used to measure a large number of results, and then to log the average value of these results. By scanning the output signal of the controller ten times per second for twenty seconds, the average value of these results, divided by the controller's output voltage gave the proportion of the time that the signal was 'on'. Using the example in figure (6-10), where the signal was 'on' for one second, and 'off' for one second, the average voltage produced by logging this signal would have been fifty percent of the actual voltage of the signal. This was the same as the proportion of the maximum power rating of that heater which was being consumed. Unfortunately the output signal from the controllers was not a consistent voltage as required for this method, so a constant voltage had to be supplied which could be switched on and off by the controller signal.

An amplified switching circuit was constructed as in figure - (6-11) for each of the controllers.

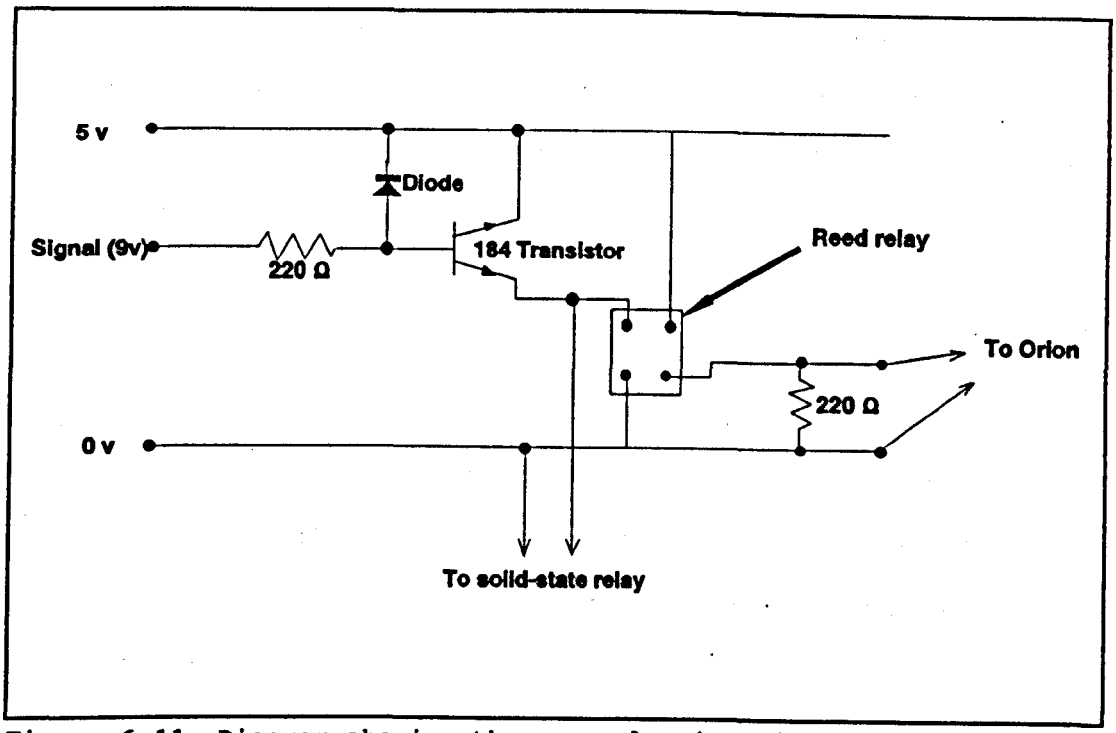

Figure 6-11. Diagram showing the power logging circuit developed.

The output signal from the controller was increased using the amplifying circuit, whose output signal was then used to operate the solid state relay for the heater. The output also operated a reed relay, which switched on and off a constant voltage supply to the logger input. A stabilized voltage supply unit giving 5 volts with an accuracy of 0.5 percent was used to provide the constant voltage.

Therefore the average voltage logged for the example in figure (6-10) would have been 2.5 volts, which signified a power consumption of fifty percent of the total rating.

Three of the circuits shown in figure (6-11) were assembled and tested, and each of these was then connected into one of the control circuits of the furnace. The outputs from the circuits connected to zones 1 to 3 were measured by channels 21 to 23 of the data logger respectively. Channels 21 to 23 were defined as voltage inputs on the Orion, and were programmed to scan all three channels at a rate of ten scans per second for twenty seconds, at two minute intervals.

The power being consumed by a particular zone at the time of logging could then be found from the logged average value of the scans. If the average value was found to be 2.3 volts, the power would be found as follows,

$$Q = \frac{2.3}{5.0} \times 1130 = 520 Watts \qquad (6\text{-}1)$$

This method was compared with the Kilowatt-hour meter readings recorded over a period of 30 minutes, and the results were found to be within five percent. This method was considered to be more accurate than a manual reading of the meters.

6.5.2 Introduction of a triggering mechanism for wire temperature logging.

The results of a wire temperature measurement test consisted of a data file containing the temperatures measured by the wire thermocouple and the time at which the temperature was recorded (see section 7.3.3). In order to calculate the relevant distance of the thermocouple along the furnace, the time at which the thermocouple entered the furnace was required. Initially this was found from an examination of a hard copy of the results. The object of this was to identify the first increase in temperature, which then would signify that the thermocouple had entered the furnace.

However this method was difficult because of the fact that there was a hydrogen flame at the inlet to the furnace, which affected the temperature prior to furnace entry.

Therefore a method had to be found to link the resulting temperature/time data to real time occurrences during the experiment. This was achieved by connecting a manually operated trigger circuit to channel 30 of the Orion, as illustrated in figure (6-12) below.

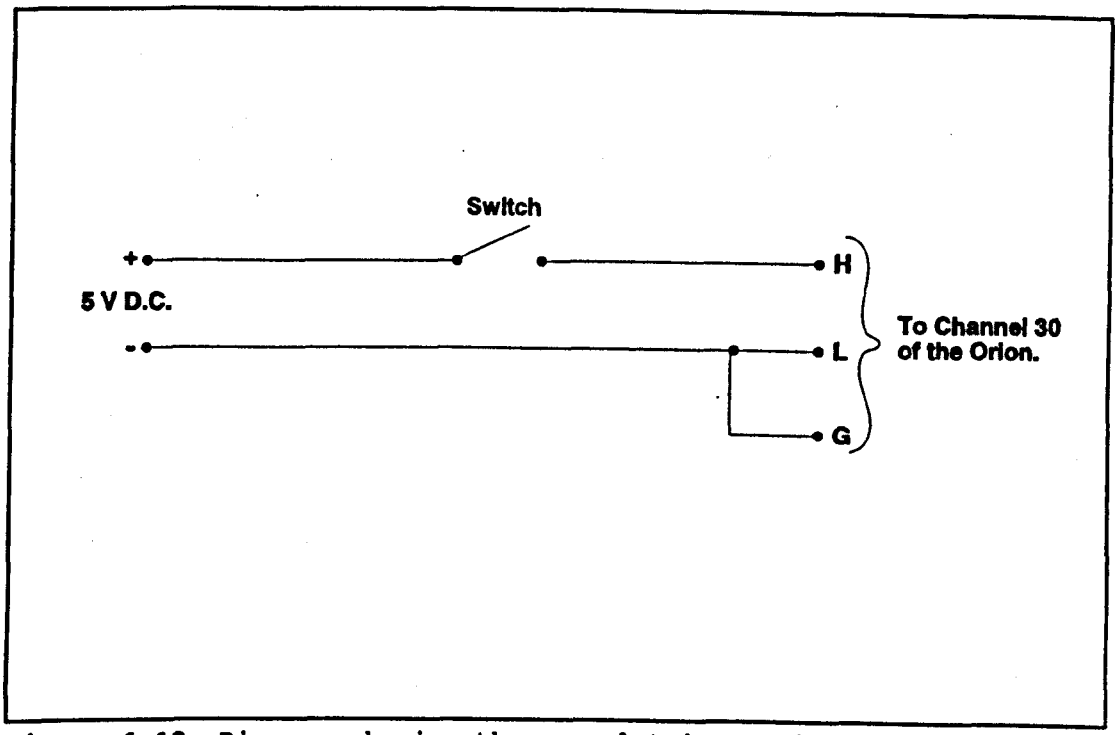

Figure 6-12. Diagram showing the manual trigger circuit.

The Orion was programmed to scan channel 30 at the same time as the wire thermocouple channels, and to log the value only if there was a change of more than one volt. Therefore when the trigger was switched on or off, the value of channel 30 was recorded with the wire temperature for the time at which it was activated.

The trigger was switched manually when the thermocouple junction passed the entrance to the furnace, and again when it passed a viewing window between the furnace and the cooling tube, resulting in two 'markers' being written to the data file with the other temperature data logged.

These two markers were then found on a hard copy of the data file, indicating the entry and exit time of the thermocouple junction, as illustrated in figure (6-13) below,

```
16:09:16.8
013 0026.5
D
16:09:17.0
013 0032.4    030 005.00 -WIRE ENTRY TIME/TEMP.
D
.
.
* THERMOCOUPLE IN FURNACE *
.
.
.
16:32:21.2
013 0897.2
D
16:32:21.4
013 0896.3    030 000.00 -WIRE EXIT TIME/TEMP
D
16:32:21.6
013 890.2
D
```

Figure 6-13. Finding wire entry and exit points from the data.

Once these points had been found, the temperature distance profile could be determined as in section 7.3.3. Although this procedure relied on human reactions to define the point of entry of the thermocouple, it was still more satisfactory than the method previously used, as described earlier in this section.

6.5.3. Change in the diameter of the wire roller.

Whilst carrying out wire tests, it was found that the motor speed was uneven at low wire speeds (up to 30 mm/s), which caused some uncertainty in the results. The method found to overcome this problem was to replace the driven wire roller (100 mm diameter) with a smaller one (50 mm diameter).

In doing so, the motor's speed was doubled for a given wire speed, providing the flywheel with more inertia, which gave it a more constant speed. The calibration factor from motor speed (RPM) to wire speed (mm/s) which was discussed in section 5.3.3.4 and found to be 0.132, had to be changed to half this value ie 0.066, which was then used in subsequent experiments.

CHAPTER 7. PRESENTATION AND DISCUSSION OF RESULTS FROM THE TESTS ON THE PROTOTYPE FURNACE.

7.1 INTRODUCTION.

The first section of this chapter contains a summary of the actual tests carried out on the prototype. The next section describes the methods used to process the various results in order to present them. This is followed by the presentation and discussion of all the results, and then a presentation of the results chosen for further analysis.

7.2 SUMMARY OF THE TESTS CARRIED OUT USING THE PROTOTYPE FURNACE.

The tests were carried out on the prototype furnace over a period of approximately eight months. There were two types of experiment carried out, the first of which was the start-up test as described in section (6.2). The results for one of the start-up tests carried out are presented and discussed in section (7.4).

The second type of experiment carried out was a running test, where a wire was passed though the furnace at a given speed , as described in section (6.3). The running tests presented are those for which a full set of data was available (ie. steady state zonal powers and tube temperatures, and the temperature of the wire as it passed through the furnace). The tests were carried out on Austenitic Stainless steel wire of two, three or four millimetres diameter and the wire speeds used were approximately fifteen, thirty, forty-five and sixty millimetres per second.

7.3 METHOD OF PROCESSING THE RESULTS FOR ANALYSIS.

All the results logged from a particular test were stored in a data file on the 'floppy' disk drive of the BBC micro. These files contained the tube temperatures, the wire temperatures, any 'markers' from the trigger circuit, the zonal powers along with the time at which each of them was logged. Figure (7-1) illustrates an example of part of a hard copy of a typical data file containing all the above results. The following three sub-sections describe how the particular types of data were processed from the data file.

7.3.1 Tube Temperatures.

The tube temperatures were measured by eleven thermocouples on the tube surface, as described in section (5.3.3.3). These thermocouples were connected to channels one to eleven respectively of the Orion, and a typical output is shown in figure (7-1) part (i).

The first scan (at 12:55:40.5) logged the temperature of all the thermocouples (in degrees centigrade) as shown. The next scan, thirty seconds later, only logged some of the tube temperatures - those which had changed by one degree or more since the last scan. This reduced the amount of data space required for all the results, and also made it easier to see when a particular temperature had become steady.

A temperature was deemed to have become steady after it had not been logged for two scans (ie one minute) at which point the last recorded temperature was recorded as the steady temperature. This method was used to find the steady temperature of all the tube thermocouples either for the start-up test or for a running test.

```
12:55:40.5                                                          )
001 0027.94  002 0168.78  003 0183.05  004 0174.71                  )
005 0129.06  006 0139.51  007 0143.20  008 0150.98                  )
009 0168.75  010 0103.39  011 0020.31                               )
D                                                                   ) (i)
12:56:10.5                                                          )
003 0189.10  004 0181.12  006 0148.60  009 0172.31                  )
010 0110.11                                                         )
D
12:57:00.5                                                      )
021 5.00100  022 5.02200                                        ) (ii)
023 5.00010                                                     )
D
.
.
.
12:57:01.2                    )
013 0028.33                   )
D                             )
12:57:01.6                    )
013 0032.45                   ) (iii)
D                             )
12:57:01.8                    )
013 0045.22  030 5.00100      )
D                             )
.
.
.
12:57:21.4                    )
013 0897.2                    )
D                             )
12:57:21.6                    )
013 0891.2   030 0.000010     ) (iv)
D                             )
12:57:21.8                    )
013 0882.4                    )
D                             )
.
```

Figure 7-1. An Example Of A Data File Containing Results From A Running Test.

7.3.2 Steady State Power.

The power at any given time was calculated from the average voltages logged by channels twenty-one to twenty-three at that time. From figure (7-1), part (ii), the average voltages at the start of the test (12:57:00.5) were all equal to five volts.

This signified that all three zones were running at full power at this point in time (see section 6.5.1). the values of channels twenty-one to twenty-three were logged every two minutes, and the power consumed by each zone could then be calculated from these values using equation (6-1).

7.3.3 Wire Temperature.

The Orion scanned the temperature of the wire thermocouple ten times per second during the running test. The temperature of this thermocouple was not logged before the thermocouple entered the furnace because the Orion was programmed to log it only if there was a change of more than one degree centigrade. Once the temperature of the wire thermocouple began to increase, it was logged as in figure (7-1), part (iii), as channel thirteen.

The value of the trigger (channel thirty) was logged at 12:57:01.8, and this time was then considered to be the point at which the wire thermocouple entered the furnace. The temperature measured by the wire thermocouple was then logged every 0.2 seconds whilst it passed through the furnace. Figure (7-1), part (iv), shows that the trigger (channel 30) is again logged at 12:57:21.8, which was then taken as the time at which the thermocouple passed the viewing window at the end of the furnace.

Once the inlet and outlet times of the thermocouple had been recorded, the data for channel 13, and the times recorded were copied to a separate file. This file was then edited, removing all the data before and after the wire thermocouple was in the furnace.

This modified data file, containing the wire temperature data and times recorded, was then copied to a file on a PRIME file-store. This was carried out using a program which caused the BBC microcomputer to emulate a dumb terminal on the PRIME network.

The BBC microcomputer could then be connected to the PRIME network, and logged in to a personal file-store, to which the data file was then copied directly from the BBC's disk drive.

In order to produce a profile of the wire's temperature against distance along the furnace, the time of the first result (ie at point of entry) was set to zero. The times for the remainder of the wire temperature measurements were then set relative to the time of thermocouple entry to the furnace. This provided the time that the thermocouple had been present in the furnace when each measurement was taken. The distance along the furnace at which the each wire temperature reading was taken was then found by multiplying the time in the furnace by the speed of the wire. The wire temperature profile could then be plotted on the same axes as the tube temperature profile to provide a comparison between wire and tube temperature at any point along the furnace.

7.4 PRESENTATION AND DISCUSSION OF THE RESULTS FROM THE START-UP TEST.

The start-up test has been described in section (6.2), and was carried out in order to establish the 'background' conditions for the furnace, at operating temperature, but with no wire passing through it. All the tests were carried out with all three heated zones set to one thousand degrees centigrade. The process gas was Hydrogen, flowing at one litre per minute in a counter-current direction. The measured powers and temperatures during the start-up test are presented in the graph in figure (7-2) below.

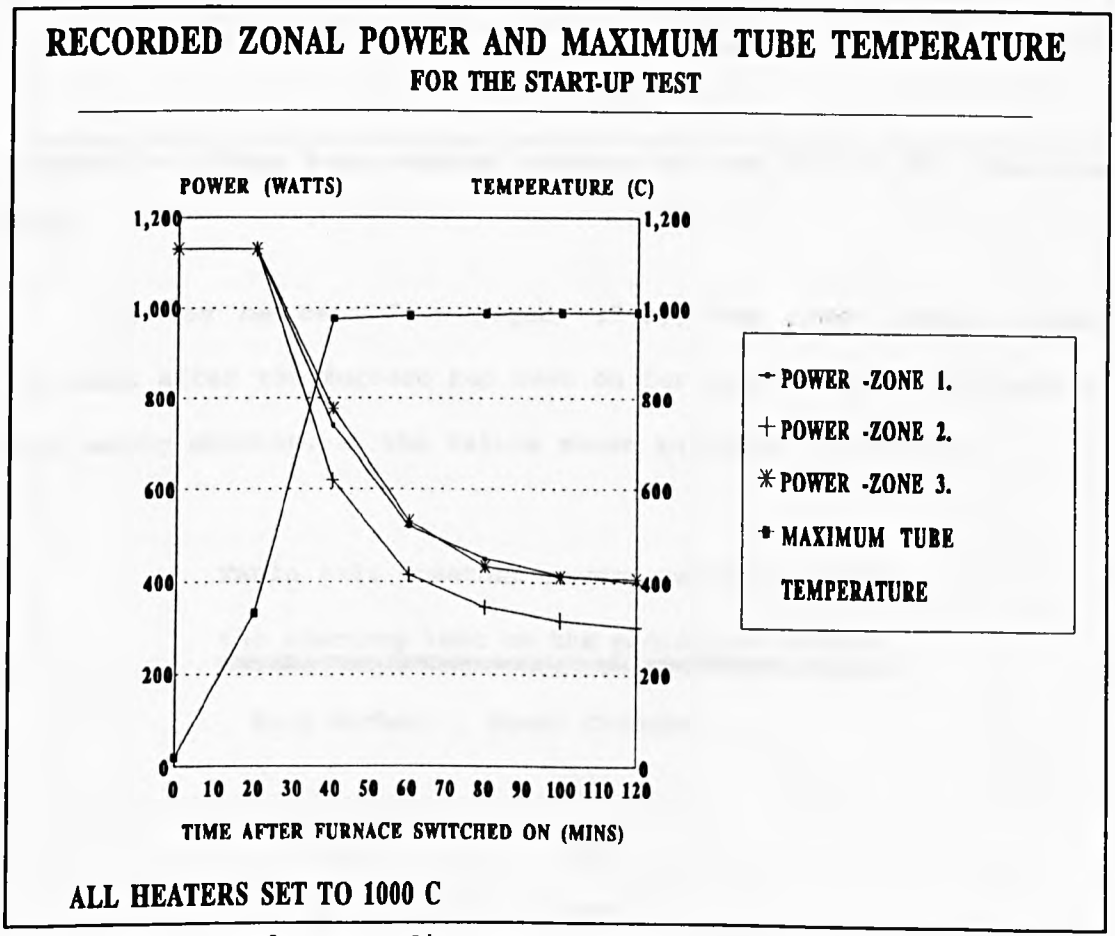

Figure 7-2. Results From The Start-up Test.

The temperatures of the eleven tube thermocouples recorded once the furnace had attained steady state are presented in figure (7-3) below.

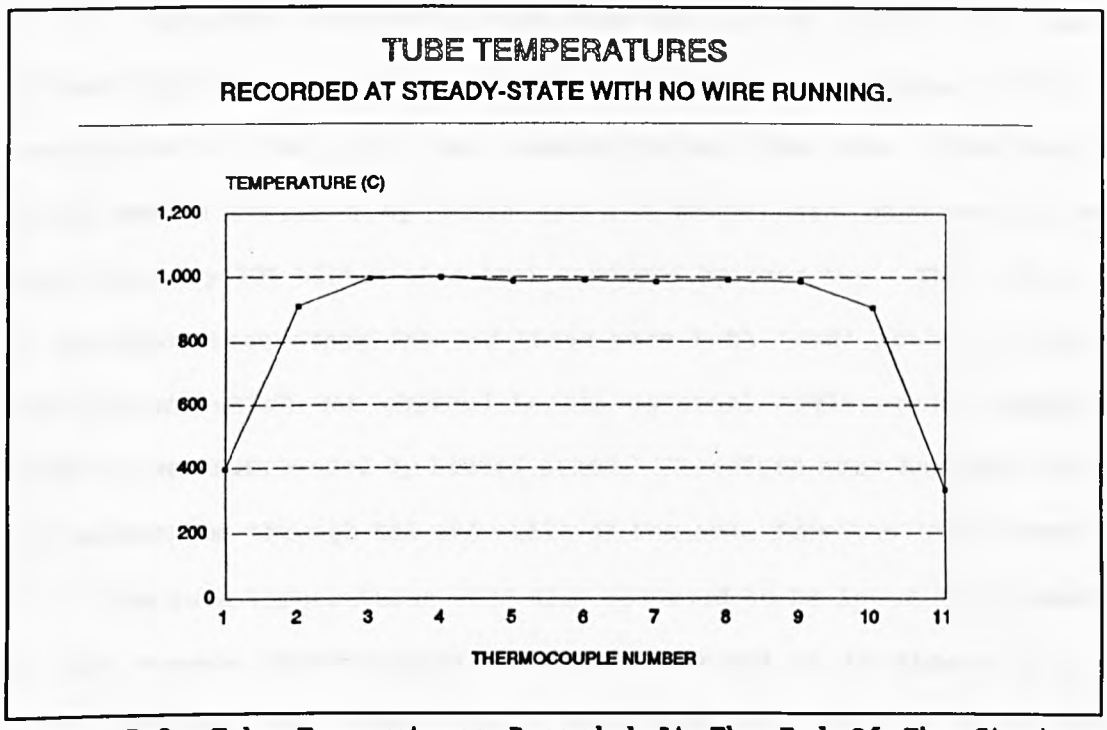

Figure 7-3. Tube Temperatures Recorded At The End Of The Start-up Test.

As can be seen from Figure (7-2), the zonal powers became constant after the furnace had been on for approximately one hundred and twenty minutes, at the values shown in table (7-1) below.

Table 7-1. Constant powers recorded during the start-up test on the prototype furnace.

Zone Number.	Power Consumed
1	400
2	303
3	408

The steady-state powers recorded for the three zones as shown in table (7-1) represent the power consumed by each zone in order to maintain the furnace at the steady state temperatures shown in figure (7-3). The power consumed in each zone was used to replace heat lost through furnace's insulation to the outside of the furnace, and heat transferred to the process gas passing through the tube. The steady state powers consumed by zones one and three were observed to be approximately 30% higher than that consumed by zone two. This was due to the fact that zones one and three were both 'end' zones -ie they had one end which was exposed to the external environment, whereas zone two was surrounded by heated zones. Therefore more heat was lost via conduction through the end walls of the zone from the 'end' zones.

The tube temperatures were also observed to be lower at the ends of the furnace (thermocouple numbers 1,2,10 and 11 in figure (7-3)) which suggests that conduction of heat must have occurred along the tube out of the furnace. This conduction was caused by the temperature gradient dT/dX along the tube as it passes through the ends of the furnace, which may be clearly seen in the tube temperature profile in figure (7-3). The conduction along the process tube from both zones 1 and 3 to the outside of the furnace were found using the Fourier equation to be 15 Watts. The temperature gradient of the tube in zone 2 was negligible, hence there was considered to be no conduction taking place along the tube in this zone.

The process gas entered the tube at slightly higher than ambient temperature in the 'hot' end of the furnace. A small amount of heat was therefore used to heat this cold gas as it entered the furnace at the end on zone three. Hence the tube temperatures at this end of the furnace were slightly lower than those at the other end.

This was also evident from the power supplied to zone three, which was slightly higher than that supplied to zone one.

The results from this test provided the 'background' conditions for the furnace, which could then be compared with the results from the running tests.

7.5 PRESENTATION AND DISCUSSION OF RUNNING TEST RESULTS.

The results presented in this section are those from the running tests successfully carried out on the prototype furnace. The results are presented in groups of tests carried out on the same wire size at approximately the same speed. The graphs presented show the wire and tube temperature profiles for each test in a particular group, accompanied by a table showing the precise details of each test, and the zonal powers recorded. All the tests were carried out with the heaters in each zone set to a thousand degrees centigrade, and a process gas of Hydrogen flowing at one litre per minute, in the opposite direction to the wire (counter-current).

7.5.1 Results For 2 mm Wire At Approximately 30 mm/s.

The tests carried out with these conditions are shown in detail in table (7-2), and the resulting temperature profiles are presented in figure (7-4).

The first test presented was carried out using method A to measure the wire temperature, which involved stopping the wire and welding the thermocouple to it.

TABLE 7-2.

TEST NO.	WIRE SPEED (MM/S)	METHOD OF WIRE TEMP. MEASUREMENT	POWER (W) 1	2	3	TOT.
1.1	30	A	525	347	464	1336
1.2	30	B	739	430	433	1602
1.3	30	B	684	439	368	1491

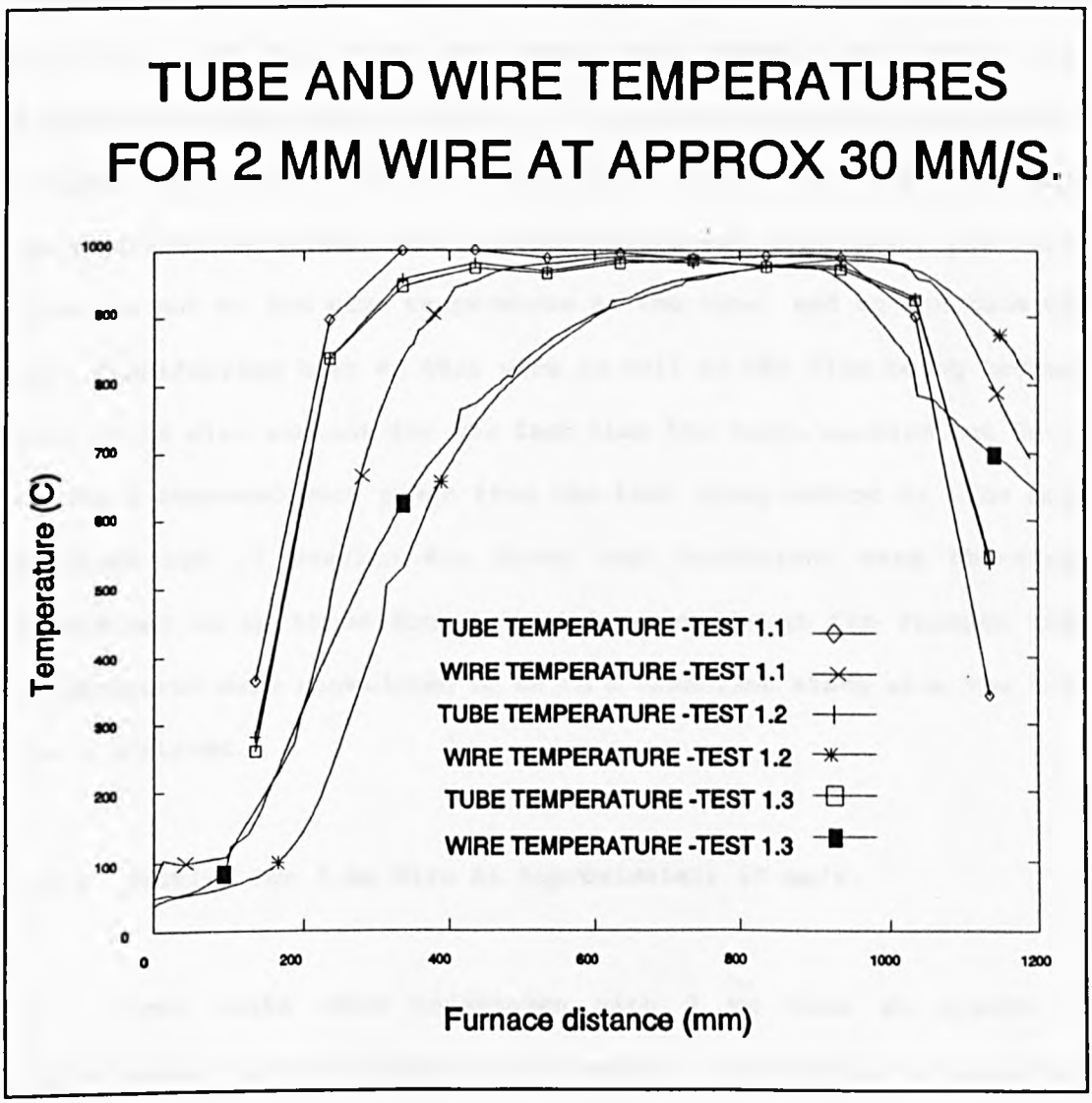

Figure 7-4.

The fact that the furnace conditions changed whilst the wire was stopped is evident from comparing the tube temperature profile from test 1.1 with those of tests 1.2 and 1.3.

The tube temperatures were higher for test 1.1 than for the other two tests. The wire temperature profile from test 1.1 was observed to have begun at a higher temperature than the other two tests, which was caused by the heat added to the wire by the thermocouple welding process.

The wire temperature for test 1.1 was also observed to have increased more rapidly than for tests 1.2 and 1.3. This was due to the fact that the other two tests were carried out using wire temperature measurement method B. The wire temperature measurement methods were described in section 6.4. When the first wire was stopped and the second wire started during the wire test, the first wire was not at the same temperature as the tube, and so the tube was also transferring heat to this wire as well as the wire being tested. This would also account for the fact that the tests carried out using method B consumed more power than the test using method A. The most reliable set of results for these test conditions were therefore considered to be those from test 1.1, even though the furnace tube temperatures were considered to be in a transient state when the test was undertaken.

7.5.2 Results For 2 mm Wire At Approximately 60 mm/s.

Three tests were undertaken with 2 mm wire at speeds of approximately sixty millimetres per second, the details of which are shown in table (7-3).

The results from these tests are displayed in figure (7-5), comprising the wire temperature and tube temperature profiles for each test.

Table 7-3.

TEST NO.	WIRE SPEED (MM/S)	METHOD OF WIRE TEMP. MEASUREMENT	POWER (KW) 1	2	3	TOT.
2.1	61	A	938	839	686	2463
2.2	60	B	837	591	520	1948
2.3	60	B	785	569	505	1859

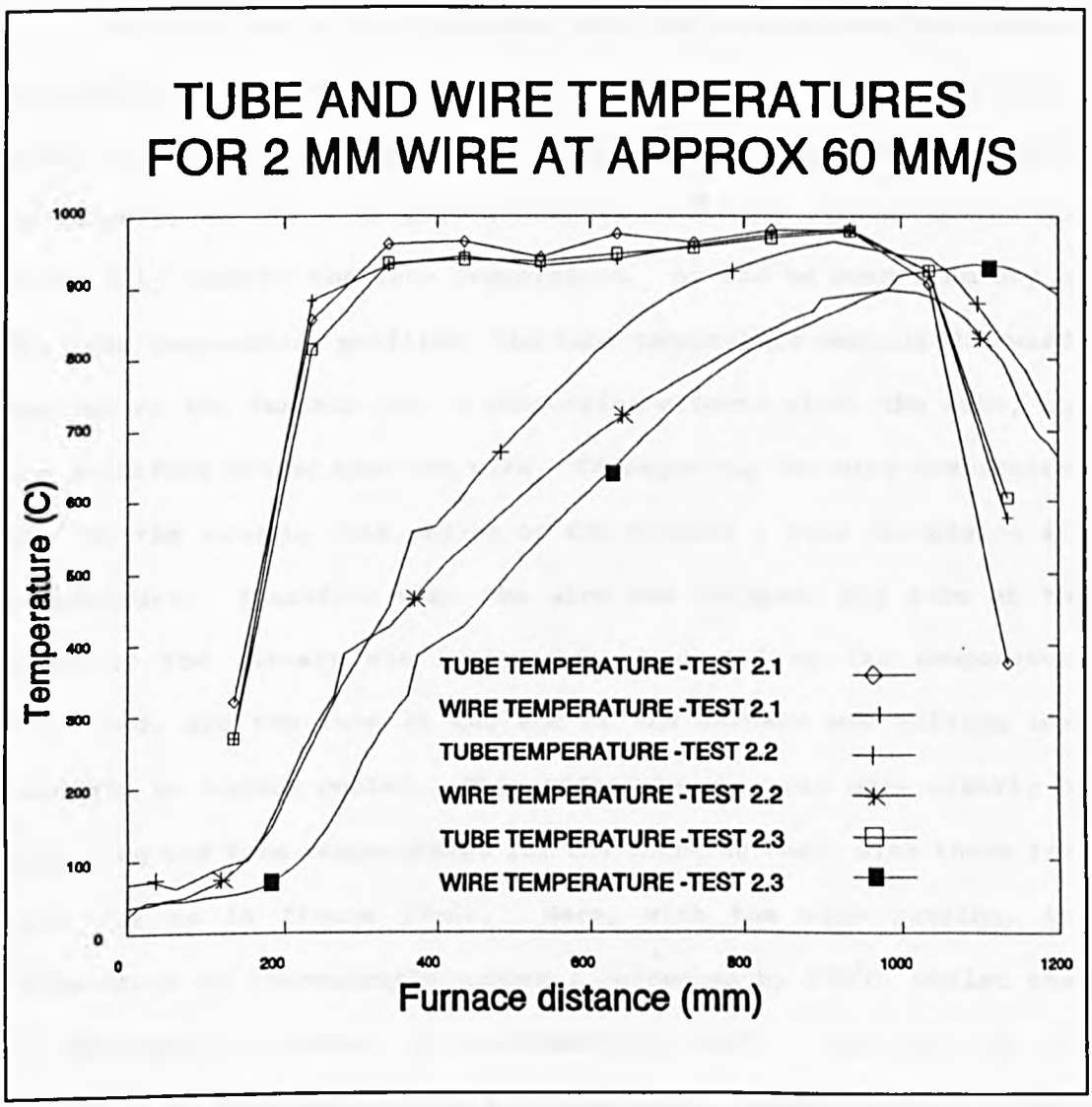

Figure 7-5.

The tube temperature profile for test 2.1, which was carried out using wire temperature measurement method A, was again observed to be higher than the tube temperature profiles for tests 2.2 and 2.3.

This illustrates the fact that the tube temperatures changed when the wire was stopped using method A, and were therefore no longer at steady state.

What should be noted from the tube temperature profiles is that when the wire was stopped, the tube temperature at the start of the furnace increased, whilst those at the end of the furnace actually decreased.

This was due to the fact that when the wire entered the furnace at ambient temperature, heat was transferred from the hot tube to the wire, causing the temperature of the tube to decrease at this point. Conversely, as the wire passed down the furnace, it was heated and eventually reached the tube temperature. As can be seen from any of the tube temperature profiles, the tube temperature decreased towards the end of the furnace due to conduction effects along the tube, and was therefore cooler than the wire. Consequently the wire transferred heat to the tube in this region of the furnace , thus increasing its temperature. Therefore when the wire was stopped, the tube at the start of the furnace was losing less heat and so its temperature increased, and the tube at the end of the furnace was gaining less heat and so became cooler. This effect may be seen more clearly by comparing the tube temperatures for the start-up test, with those from test 2.2 as in figure (7-6). Here, with the wire running, the temperature of thermocouple number 1 decreased by 150^{o}C, whilst that of thermocouple number 11 increased by 220^{o}C. The rest of the thermocouple temperatures did not show such a marked change as these two end thermocouples. This was because the end thermocouple positions were not in direct view of the heaters, and so did not receive any heat via radiation but via conduction along the tube.

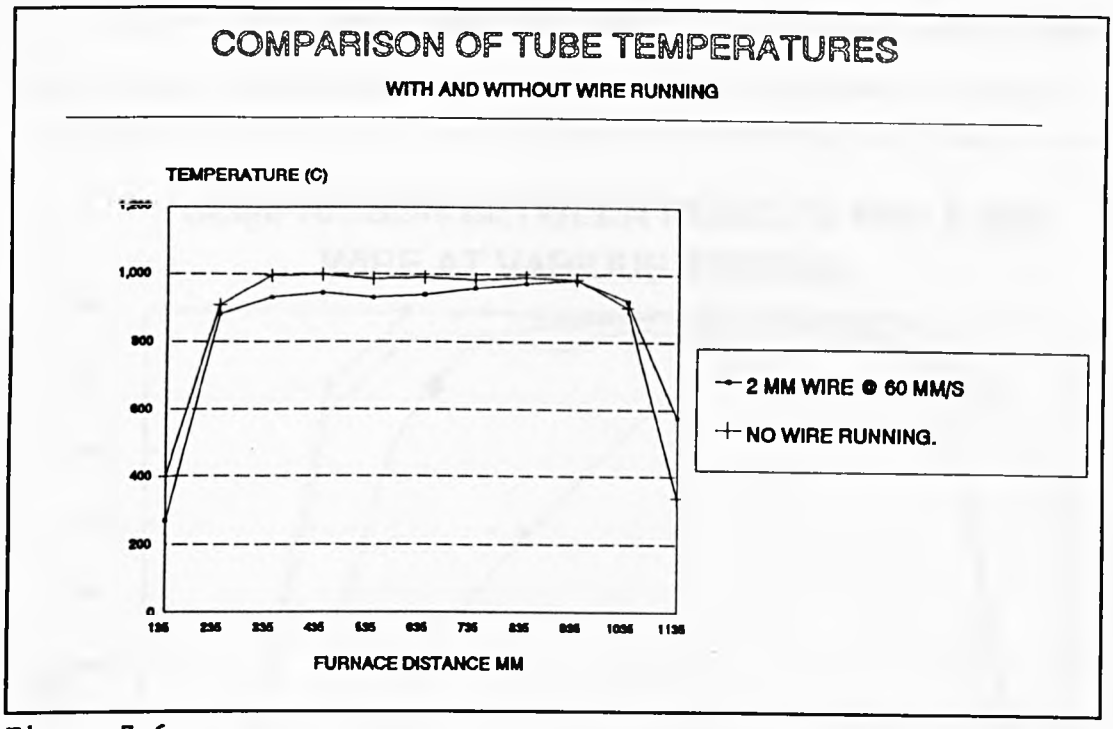

Figure 7-6.

Therefore when the wire entered the furnace and heat was transferred from the tube to the wire, very little heat was conducted along the tube to thermocouple position 1, hence the temperature dropped accordingly. The temperature at thermocouple position 11 increased sharply for the same reason - as the wire was already hot by the time it reached this point in the furnace, heat was transferred to this region of the tube by conduction along the tube and by radiation from the wire. Tests 2.2 and 2.3 were carried out using method B to measure wire temperature, and the same observations can be made about the resulting wire temperature profiles as for the previous set of tests.

The results from test 2.1 were chosen to be the most reliable because the tube was only transferring heat to the wire whose temperature was being measured, and not to a second wire as in test 2.2 and 2.3.

Figure (7-7) below shows the result from the two tests chosen for 2 mm wire at speeds of thirty and sixty millimetres per second.

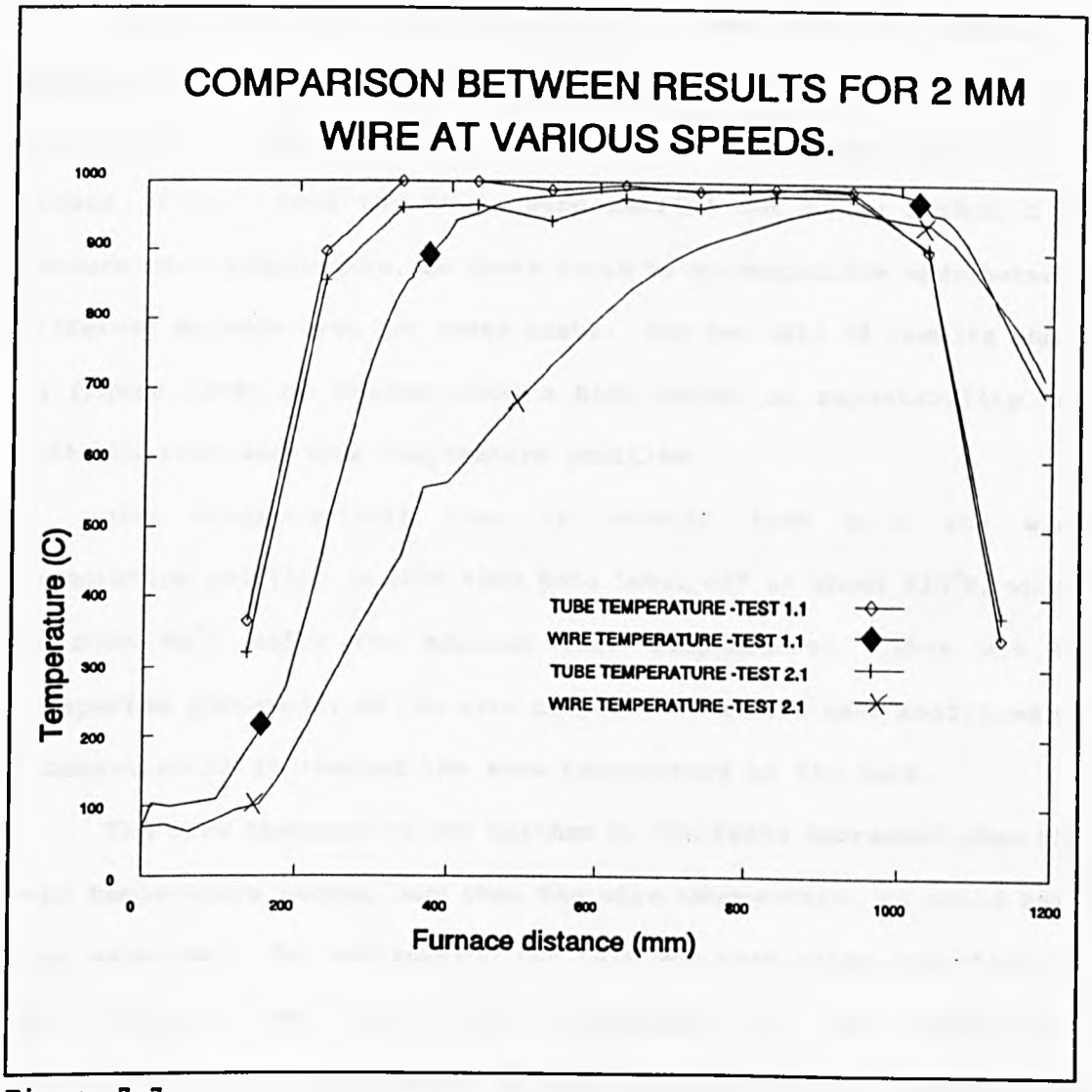

Figure 7-7

As can be observed, the temperature of the wire increased more rapidly with distance along the furnace for the test carried out with the lower wire speed. This was due to the fact that the wire was at a given position in the furnace for a longer period of time when a lower wire speed was utilised. Therefore more heat was transferred to the wire at a given position, providing a greater increase in wire temperature at that position.

7.5.3 Results For 3 mm Wire At Approximately 15 mm/s.

Two tests were carried out on 3 mm wire at speeds of approximately 15 millimetres per second and these are detailed in table (7-4). The resulting temperature profiles are presented in figure (7-8). Both the tests were carried out using method C to measure wire temperature, so there could be no comparison made between different methods used for these tests. The two sets of results shown in figure (7-8) do however show a high degree of repeatability for both the tube and wire temperature profiles.

One characteristic that is evident from both the wire temperature profiles is that they both level off at about 910°C, which is some 80°C below the maximum tube temperature. This was an unexpected phenomena, as the wire temperature should have continued to increase until it reached the same temperature as the tube.

The wire temperature for neither of the tests decreased when the tube temperature became less than the wire temperature, as would have been expected. The explanation for this was that after some time in the furnace, the fibre glass insulation of the sacrificial thermocouple on the wire became so badly damaged that the thermocouple wires were allowed to touch, creating 'parasitic' junctions.

These parasitic junctions would have caused the temperature to have been measured at points along the furnace other than at the end of the thermocouple. This phenomena was found to be limited to tests carried out at speeds of approximately 15 mm/s.

This could be accounted for by the fact that the thermocouple was exposed to the high temperatures in the furnace for a longer period of time than when higher speeds were used.

After the wire tests had been carried out, the thermocouple insulation was examined, and was found to have deteriorated to a larger extent than for the tests carried out at higher speeds.

Table 7-4.

TEST NO.	WIRE SPEED (MM/S)	METHOD OF WIRE TEMP. MEASUREMENT	POWER (KW) 1	2	3	TOT.
3.1	14.8	C	754	363	326	1443
3.2	15.0	C	789	354	333	1476

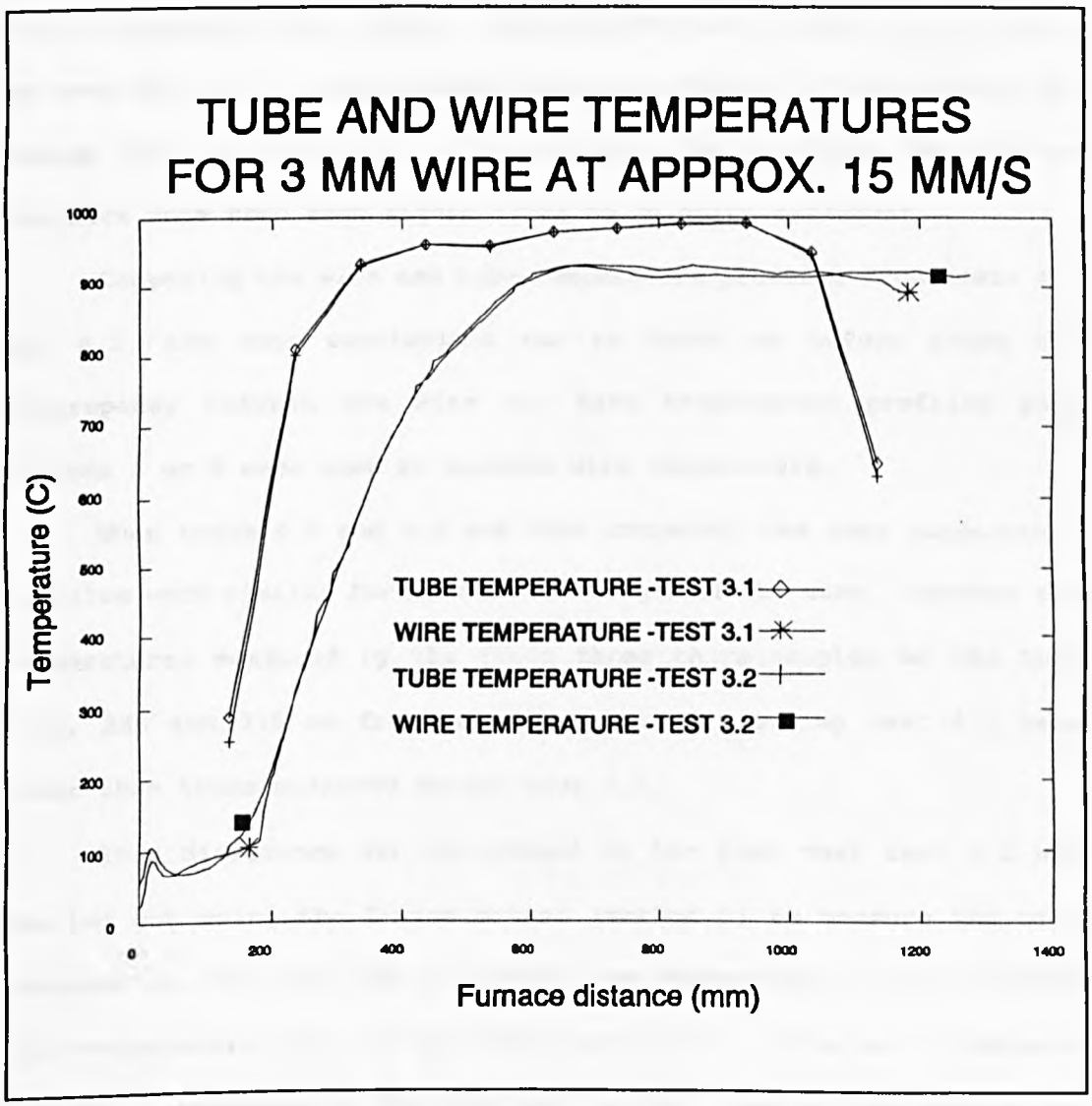

Figure 7-8.

The results of test 3.2 were chosen to represent 3 mm wire at 15 mm/s as its measured speed was 15 mm/s.

7.5.4 Results For 3 mm Wire At Approximately 30 mm/s.

The three tests undertaken with these conditions are detailed in table (7-5) below, and the resulting temperature profiles are presented in figure (7-9).

Each of the tests were carried out using a different method for wire temperature measurement. From observation of table (7-5) it may be seen that all the wire speeds were approximately 30 millimetres per second (over a range of ± 8 %), however the resulting temperature profiles were seen from figure (7-9) to be quite different.

Comparing the wire and tube temperature profiles from tests 4.1 and 4.2, the same conclusions can be drawn as before about the discrepancy between the wire and tube temperature profiles when methods A or B were used to measure wire temperature.

When tests 4.2 and 4.3 are then compared, the tube temperature profiles were similar for most of the length of the tube. However the temperatures measured by the first three thermocouples on the tube (135, 235 and 335 mm from the furnace inlet) during test 4.2 were lower than those measured during test 4.3.

This difference was attributed to the fact that test 4.2 was carried out using the 2-wire method (method B) to measure the wire temperature, and that the wire which was stopped had not yet reached tube temperature when the test was carried out. This would indicate that the temperature of the tube was 'pulled' down in the part of the tube where the wire was coldest -ie at the inlet to the furnace.

Table 7-5.

TEST NO.	WIRE SPEED (MM/S)	METHOD OF WIRE TEMP. MEASUREMENT	POWER (KW) 1	2	3	TOT.
4.1	27.9	A	857	415	452	1725
4.2	32.5	B	889	641	509	2039
4.3	30.0	C	880	615	509	2004

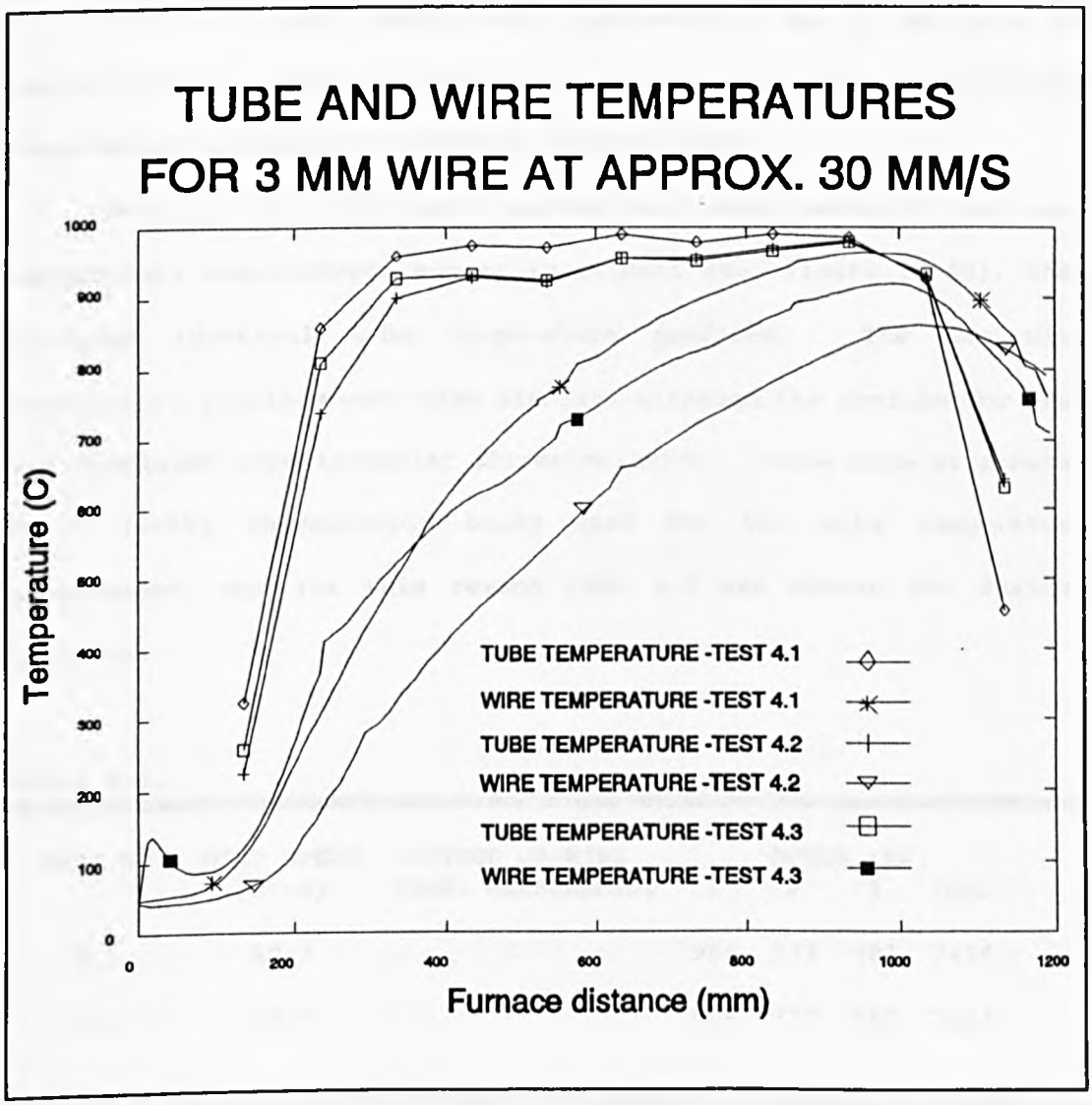

Figure 7-9

Test 4.3, which was carried out using method C was assumed to have produced the most accurate set of results, and was therefore chosen for further analysis.

The peak in the wire temperature profile at the start of the furnace was attributed to the fact that the wire thermocouple temperature was influenced by the Hydrogen flame as it entered the furnace.

7.5.5 Results For 3 mm Wire At Approximately 40 mm/s.

The two tests which were carried out on 3 mm wire at approximately 40 mm/s are detailed in table (7-6) and the resulting temperature profiles are shown in figure (7-10).

Both of the tests were carried out using method C for wire temperature measurement, and as is evident from figure (7-10), they produced identical tube temperature profiles. The two wire temperature profiles were also similar, although the profile for test 5.1 displayed some irregular characteristics. These were attributed to a faulty thermocouple being used for the wire temperature measurement, and for this reason test 5.2 was chosen for further analysis.

Table 7-6.

TEST NO.	WIRE SPEED (MM/S)	METHOD OF WIRE TEMP. MEASUREMENT	POWER (KW) 1	2	3	TOT.
5.1	40.3	C	956	777	681	2414
5.2	40.5	C	956	777	681	2414

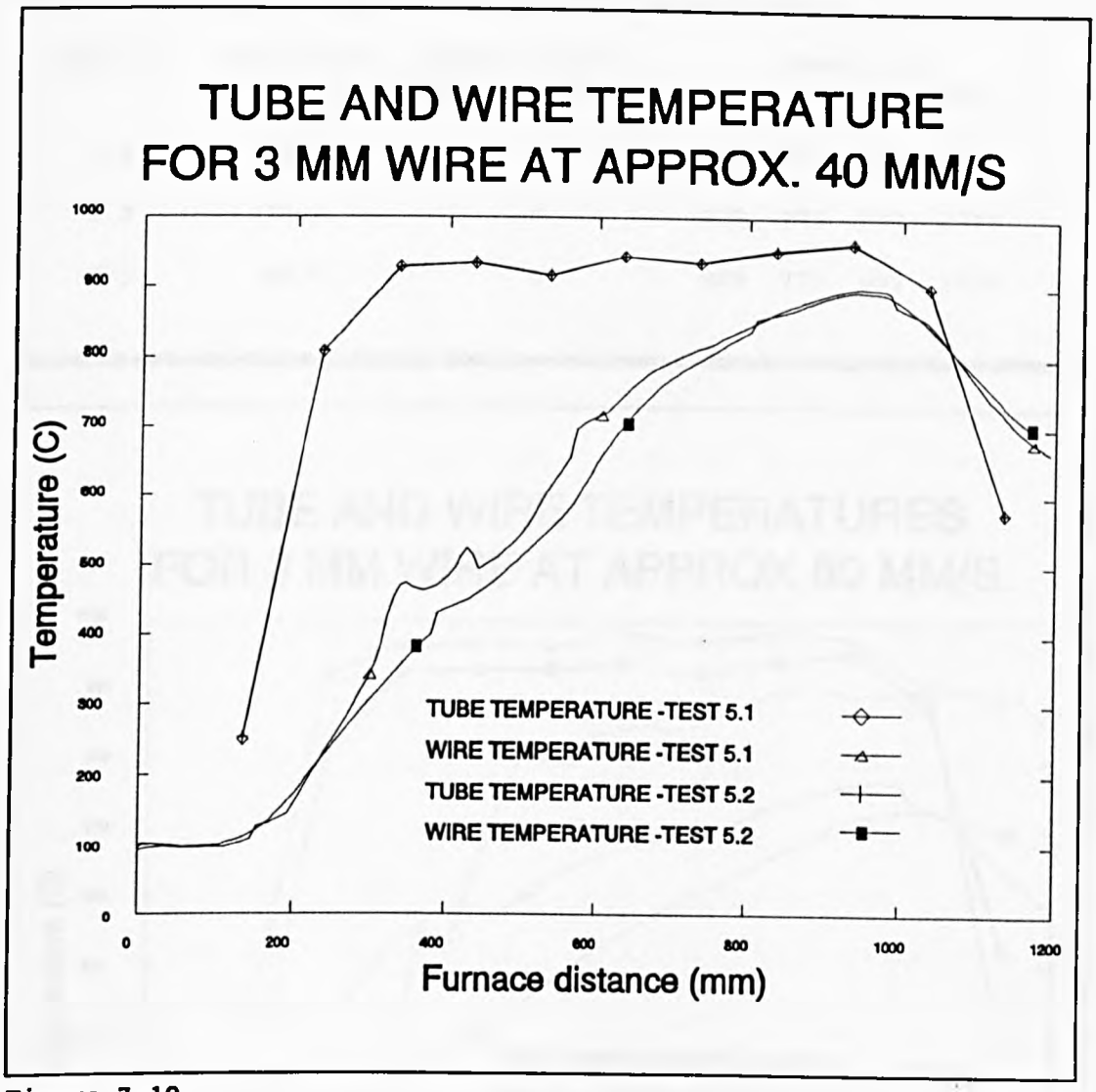

Figure 7-10.

7.5.6 Results For 3 mm Wire At Approximately 60 mm/s.

The details of the three tests carried out on 3 mm wire at speeds of approximately 60 mm/s are presented in table (7-7) and the resulting temperature profiles shown in figure (7-11).

Test 6.1 was carried out using method A to measure the wire temperature. The resulting wire temperature profile was considered unacceptable as it showed the wire temperature fluctuating as it increased. This was attributed to a faulty wire thermocouple being used.

Table 7-7.

TEST NO.	WIRE SPEED (MM/S)	METHOD OF WIRE TEMP. MEASUREMENT	POWER (KW) 1	2	3	TOT.
6.1	66.1	A	1111	852	685	2648
6.2	58.8	C	909	770	697	2376
6.3	55.6	C	909	770	697	2376

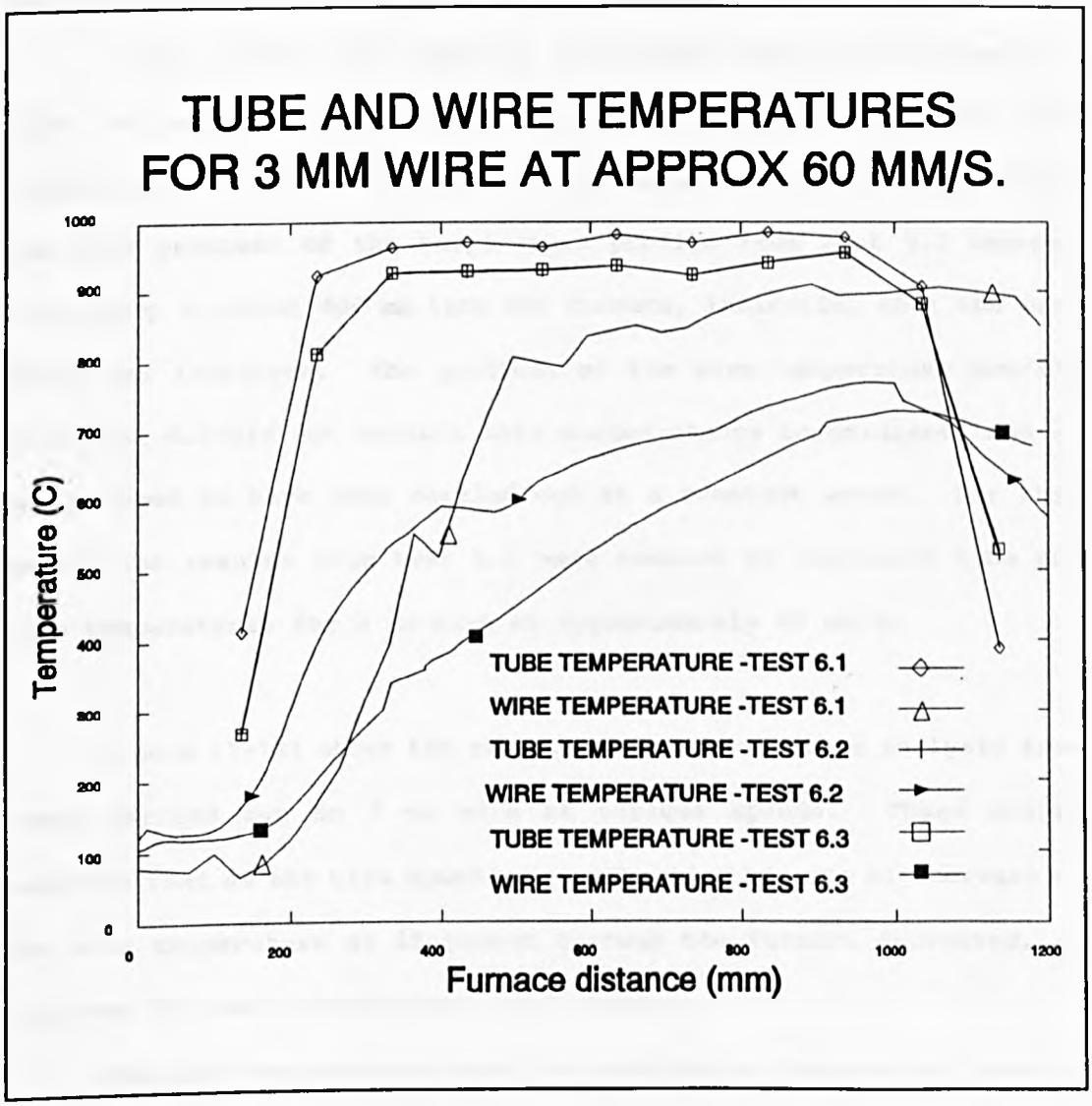

Figure 7-11.

Tests 6.2 and 6.3 were undertaken with similar conditions producing identical tube temperature profiles.

However the resulting wire temperature profiles displayed a considerable difference between the heating characteristics of the wire in the two tests. Examination of figure (7-11) indicates that the wire temperature profile from test 6.2 showed a rapid rise in the wire temperature during the first heating zone of the furnace. This could have been caused by the wire being stopped or slowed down for a short period of time during the wire temperature measurement.

A drop in the wire speed in this region would have caused the wire to receive more heat at a given position, therefore its temperature would have increased to a greater extent at that position. The wire gradient of the temperature profile from test 6.2 becomes less steep at about 400 mm into the furnace, indicating that the wire speed had increased. The gradient of the wire temperature profile from test 6.3 did not exhibit this marked change in gradient, and so was assumed to have been carried out at a constant speed. For this reason the results from test 6.3 were assumed to represent tube and wire temperatures for 3 mm wire at approximately 60 mm/s.

Figure (7-12) shows the results chosen for further analysis from tests carried out on 3 mm wire at various speeds. These graphs indicate that as the wire speed was increased, the rate of increase of the wire temperature as it passed through the furnace decreased, as observed for tests carried out on 2 mm wire.

The tube temperatures were also observed to decrease as the wire temperature increased. This was due to the fact that the faster the wire was travelling, the colder it was at any give point along the furnace.

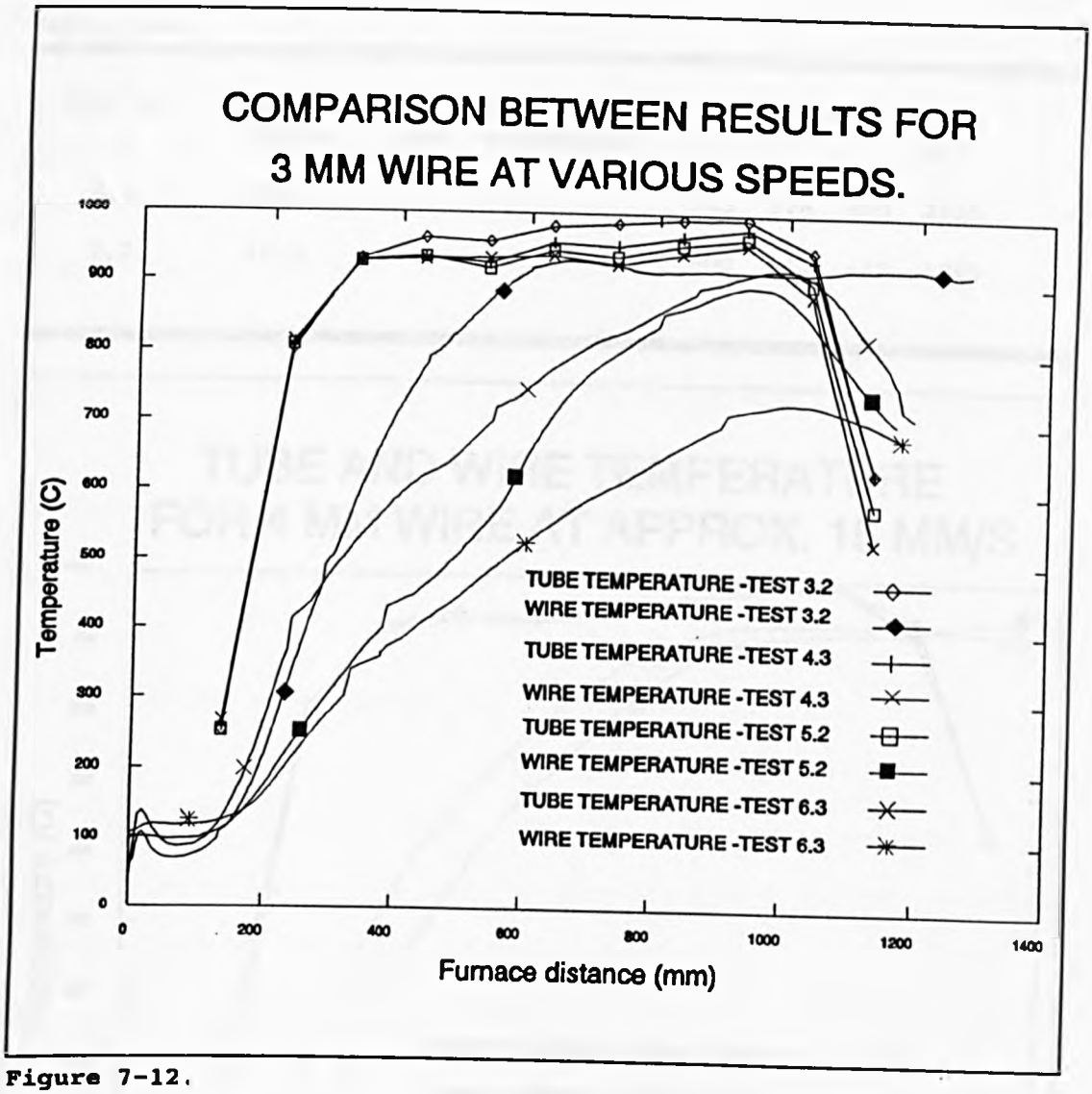

Figure 7-12.

Therefore the heat energy transferred from the tube per second increased due to the increase in the temperature difference between the wire and the tube. This increase in heat transfer from the tube to the wire caused the tube temperature to decrease when the wire speed was increased.

7.5.7 Results For 4 mm Wire At Approximately 15 mm/s.

Table (7-8) contains the details of the two tests carried out on 4 mm wire at approximately 15 mm/s, and the resulting wire and tube temperature profiles are shown in figure (7-13).

Table 7-8.

TEST NO.	WIRE SPEED (MM/S)	METHOD OF WIRE TEMP. MEASUREMENT	POWER (KW) 1	2	3	TOT.
7.1	13.3	C	985	574	500	2059
7.2	15.0	C	900	543	426	1869

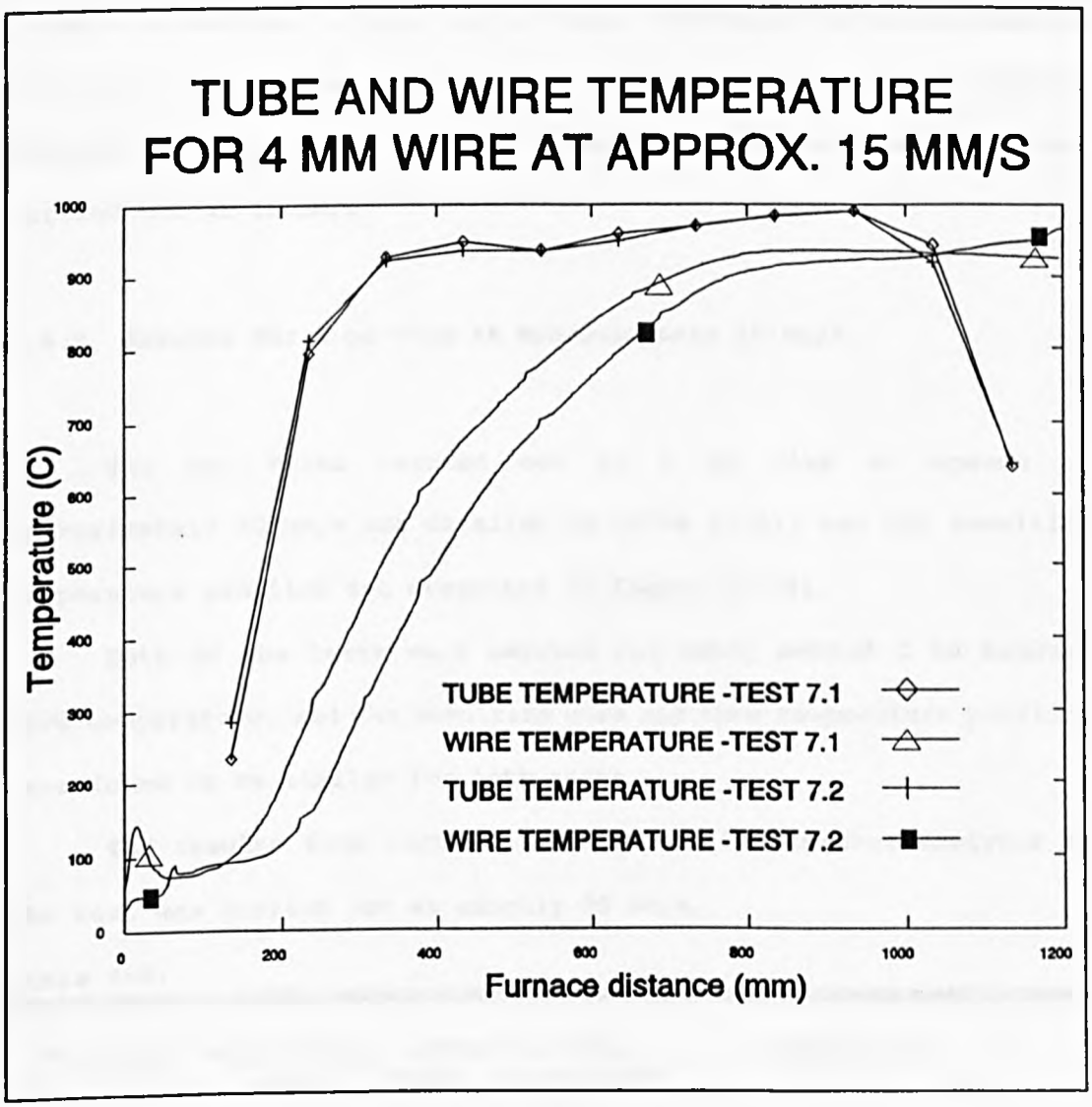

Figure 7-13.

Both of the tests were carried out using method C to measure wire temperature, and the resulting tube temperature profiles were the same.

The two wire temperature profiles were also found to be fairly similar except that the wire temperature for test 7.1 increased more quickly than that for test 7.2. This was expected as a slower speed was measured for the wire in test 7.1, which would cause the wire temperature to increase more quickly. Both of the wire temperature profiles exhibit the same characteristic as described for 3 mm wire at 15 mm/s in section 7.3 and this is again attributed to disintegration of the thermocouple insulation. Although both tests provided acceptable results, test 7.2 was chosen for further analysis as it was carried out at 15 mm/s.

7.5.8 Results For 4 mm Wire At Approximately 30 mm/s.

The two tests carried out on 4 mm wire at speeds of approximately 30 mm/s are detailed in table (7-9), and the resulting temperature profiles are presented in figure (7-14).

Both of the tests were carried out using method C to measure wire temperature, and the resulting wire and tube temperature profiles were found to be similar for both tests.

The results from test 8.2 were chosen for further analysis as the test was carried out at exactly 30 mm/s.

Table 7-9.

TEST NO.	WIRE SPEED (MM/S)	METHOD OF WIRE TEMP. MEASUREMENT	POWER (KW) 1	2	3	TOT.
8.1	27.7	C	1037	827	698	2562
8.2	30.0	C	951	718	627	2296

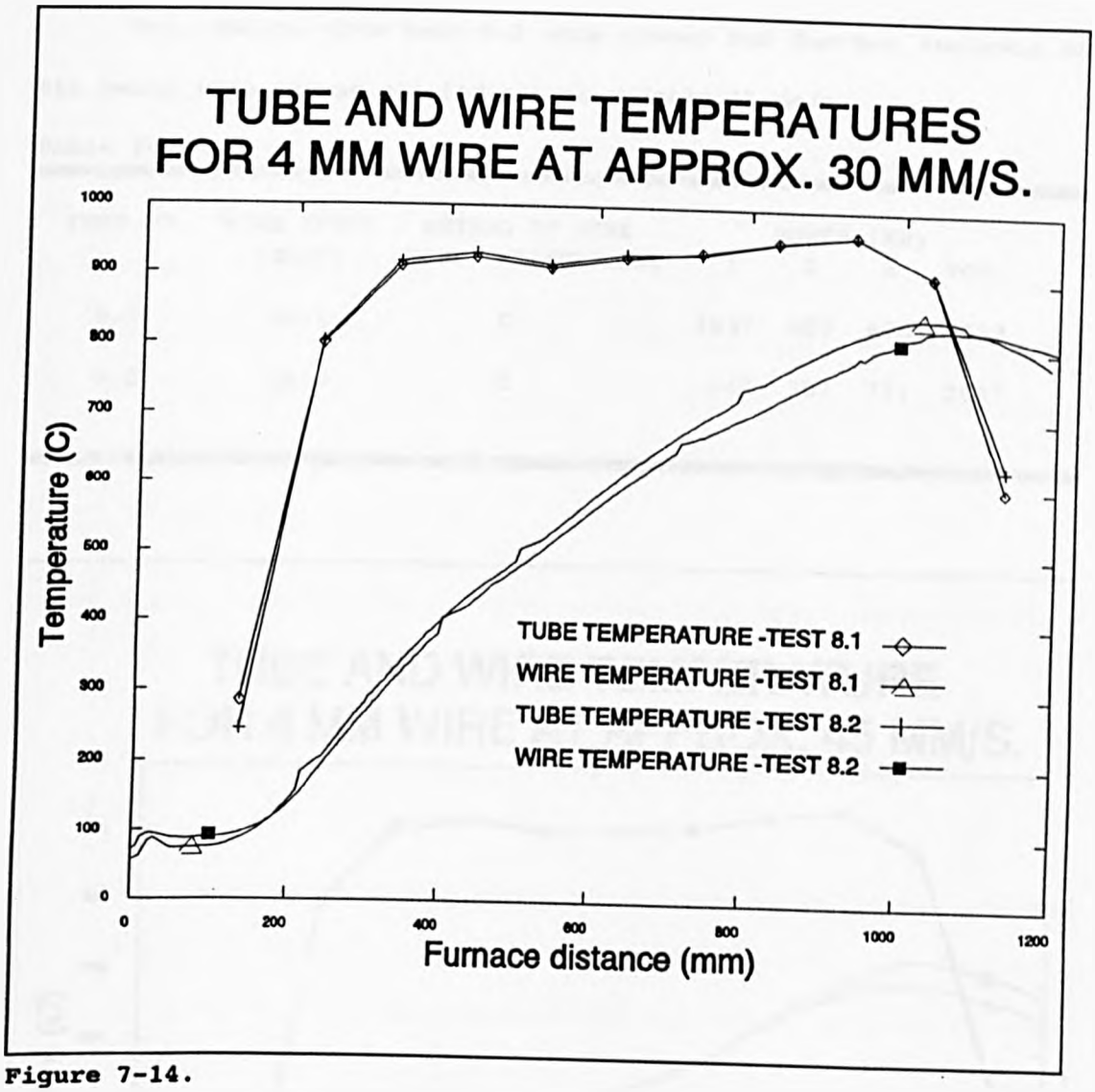

Figure 7-14.

7.5.9 Results For 4 mm Wire At Approximately 45 mm/s.

The two tests which were carried out on 4 mm wire at speeds of approximately 45 mm/s are detailed in table (7-10), and the resulting wire and tube temperature profiles are shown in figure (7-15).

Both tests were carried out using method C to measure wire temperature giving very similar tube temperature profiles. The wire temperature profiles presented were also found to be very close, rising at roughly the same rate, and peaking at the same distance along the furnace.

The results from test 9.2 were chosen for further analysis on the basis that it was carried out at exactly 45 mm/s.

Table 7-10.

TEST NO.	WIRE SPEED (MM/S)	METHOD OF WIRE TEMP. MEASUREMENT	POWER (KW) 1	2	3	TOT.
9.1	45.2	C	1037	827	698	2562
9.2	45.0	C	949	787	771	2507

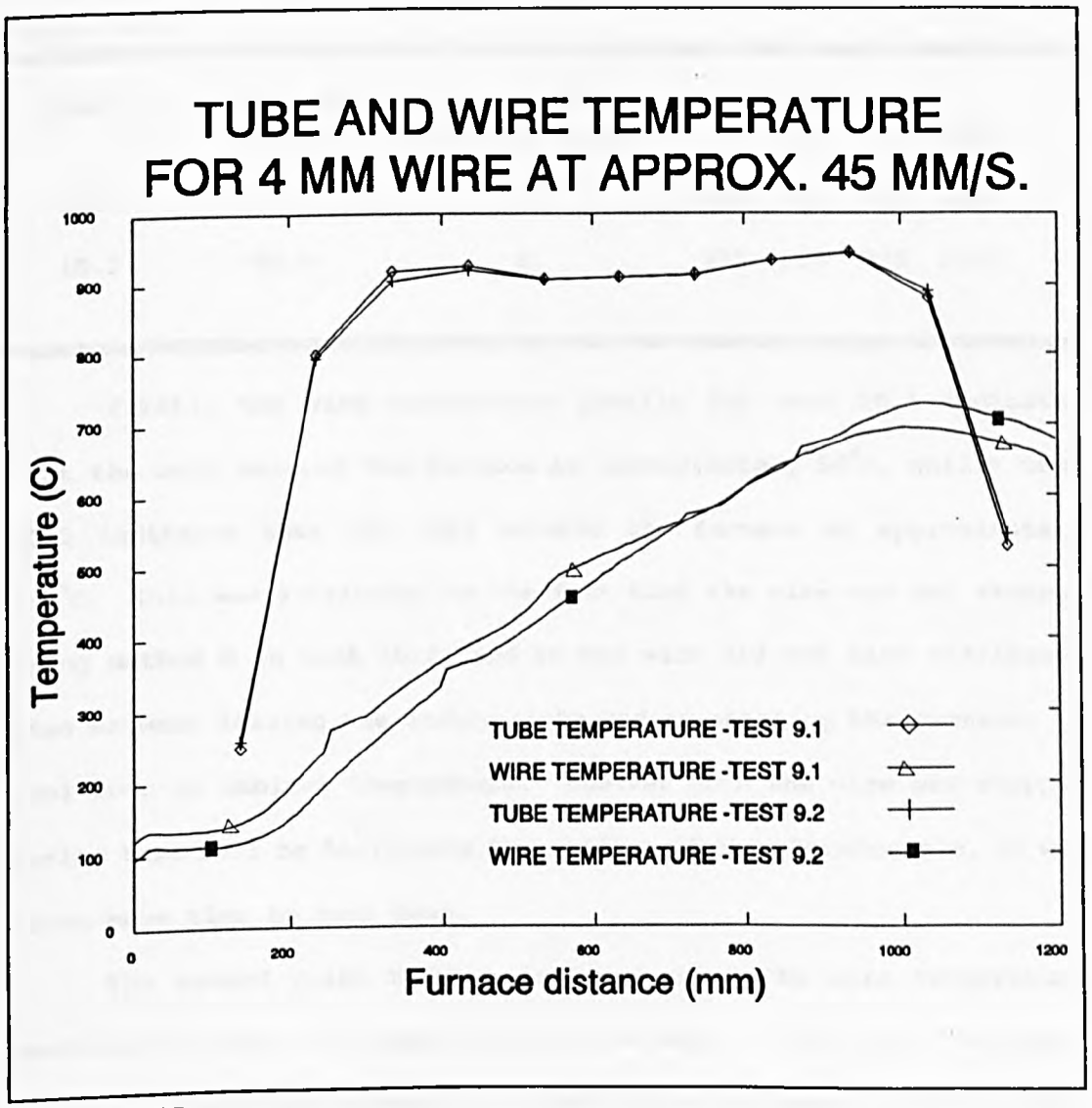

Figure 7-15.

7.5.10 Results For 4 mm Wire At Approximately 60 mm/s.

The two tests carried out on 4 mm wire at approximately 60 mm/s are detailed in table (7-11) and the resulting temperature profiles are shown in figure (7-16). Test 10.1 was carried out using method A to measure wire temperature and the effect of stopping the wire for thermocouple welding can be seen by the increased tube temperatures compared to test 10.2. The wire temperature profiles for the two tests show marked differences.

Table 7-11.

TEST NO.	WIRE SPEED (MM/S)	METHOD OF WIRE TEMP. MEASUREMENT	POWER (KW) 1	2	3	TOT.
10.1	56.7	A	1029	931	877	2837
10.2	60.0	C	975	809	773	2557

Firstly the wire temperature profile for test 10.1 indicates that the wire entered the furnace at approximately 50°C, whilst test 10.2 indicates that the wire entered the furnace at approximately 150°C. This was attributed to the fact that the wire was not stopped using method C in test 10.2, and so the wire did not have sufficient time between leaving the cooling tube and re-entering the furnace, to cool down to ambient temperature. However when the wire was stopped during test 10.1 to facilitate the welding of the thermocouple, it was given more time to cool down.

The second point that was noticed about the wire temperature profiles was that the temperature of the wire in test 10.1 increased sharply between approximately 200 and 350 mm and again between about 600 and 700 mm from the furnace inlet.

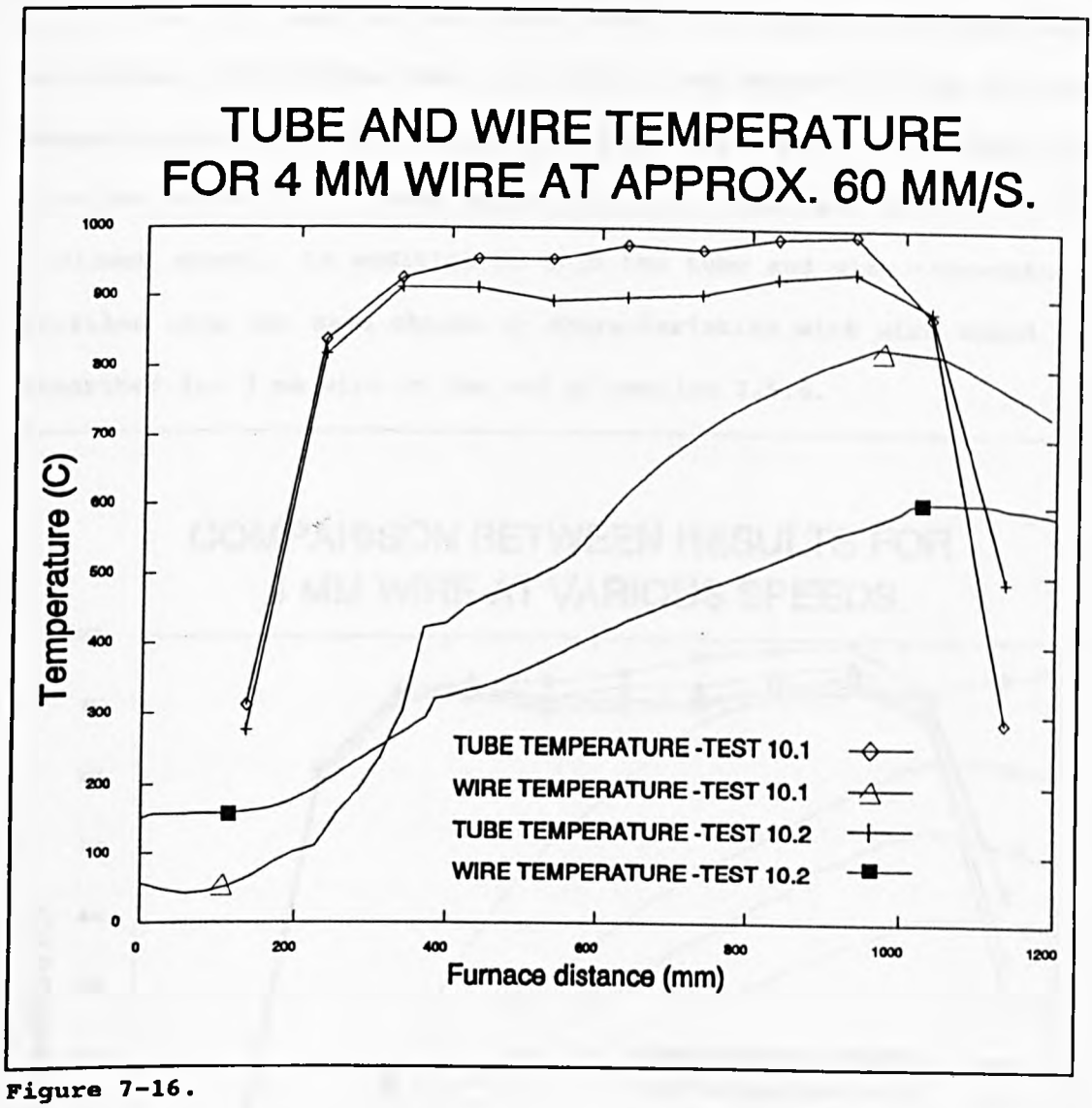

Figure 7-16.

These changes in the expected shape of the wire temperature profile were due to fluctuations in the wire speed during the wire temperature measurement, as explained in section 7.5.6. The results from test 10.2 were therefore chosen for further analysis.

Figure (7-17) overleaf shows the results chosen for further analysis from tests carried out on 4 mm wire at various speeds, the data for which is given in tables (7-8) to (7-11). The wire temperature profiles indicate that the temperature of the wire when it entered the furnace increased as the wire speed decreased.

This was due to the fact that the faster the wire was travelling, the shorter the time that it was exposed to the ambient temperature outside the furnace before re-entering it. Therefore the wire was cooled to a lesser extent than if it had been travelling at a slower speed. In addition to this the tube and wire temperature profiles show the same change in characteristics with wire speed as described for 3 mm wire at the end of section 7.5.6.

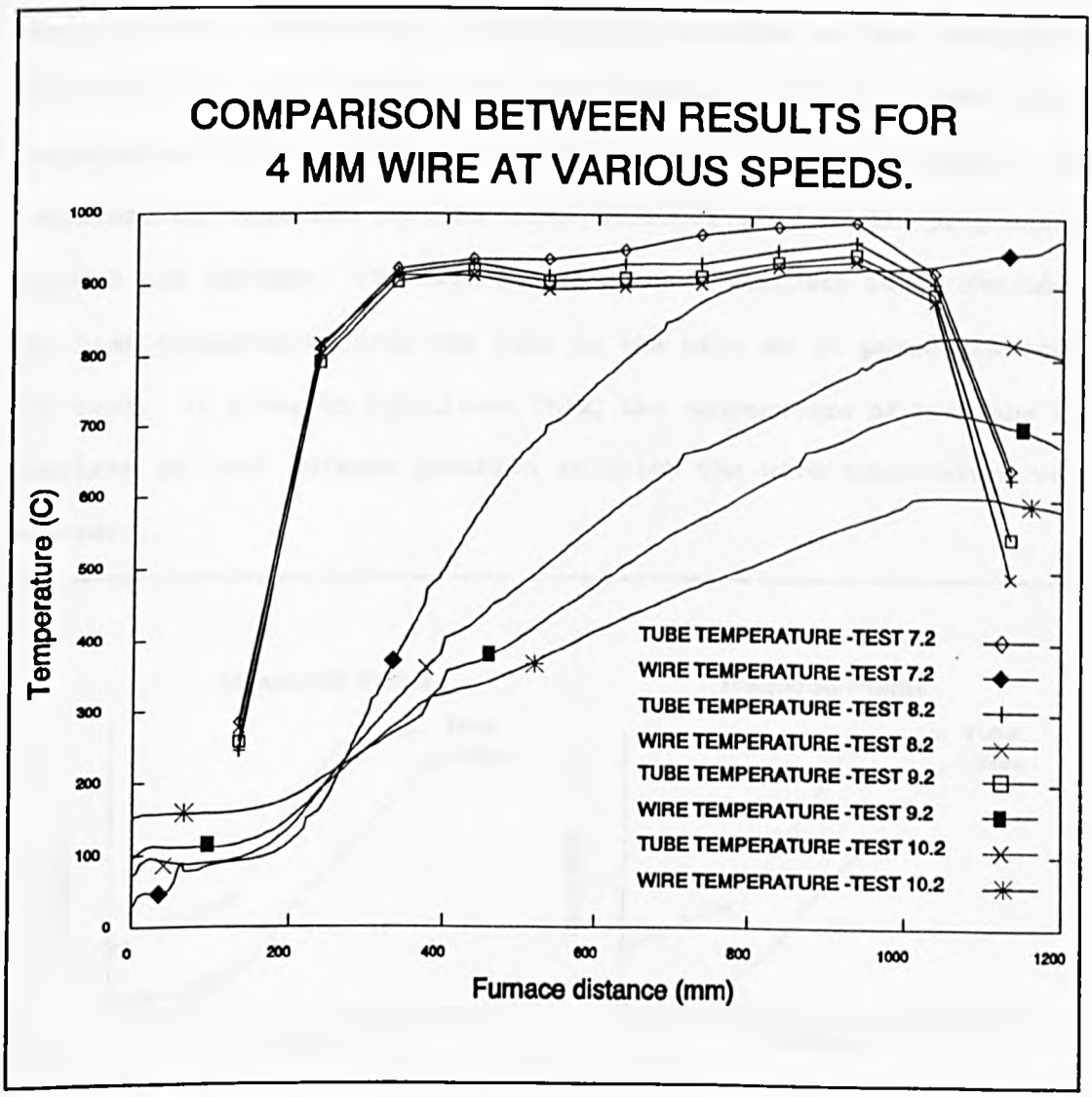

Figure 7-17.

CHAPTER 8. ANALYSIS OF EXPERIMENTAL RESULTS TAKEN ON THE PROTOTYPE FURNACE.

8.1 PROCESSING OF TEMPERATURE DATA FOR ANALYSIS.

The data presented in the previous section consisted of the tube and wire temperature profiles recorded for various wire sizes and speeds. The tube temperature data presented was made up of the temperatures of eleven tube thermocouples situated at ten centimetre intervals on the furnace tube (see section 5.3.3.3). The wire temperature data presented consisted of a larger number of temperatures measured by the wire thermocouple as it progressed through the furnace. The main object of this analysis is to consider the heat transferred from the tube to the wire as it passes through the tube. In order to facilitate this, the temperature of the tube is required at each furnace position at which the wire temperature was recorded.

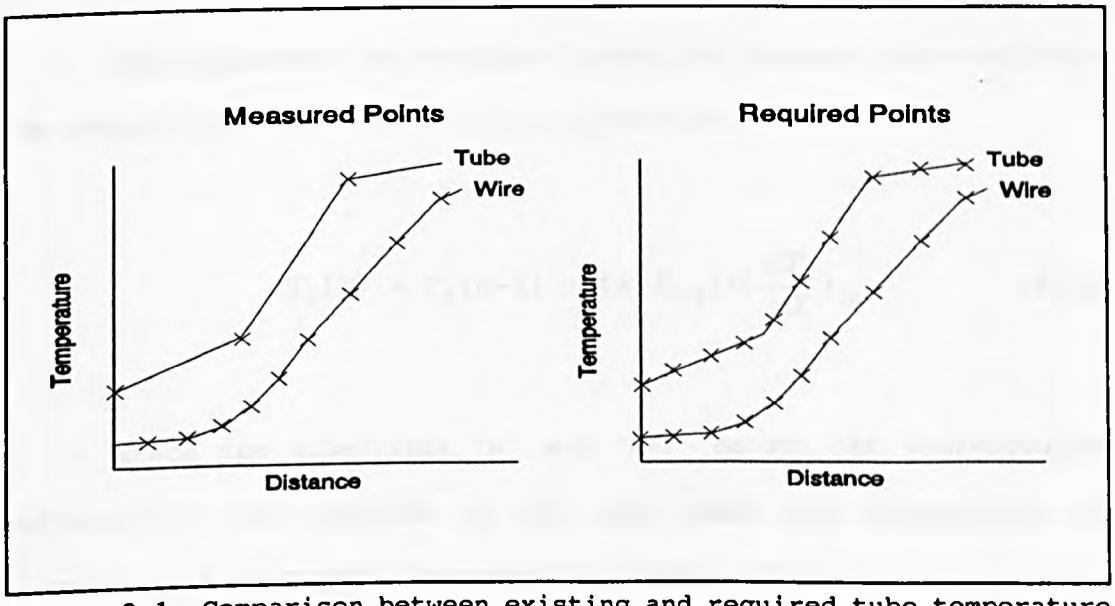

Figure 8-1. Comparison between existing and required tube temperature data.

Figure (8-1) illustrates the comparison between the present, measured temperatures, and the temperatures required for analysis.

In order to obtain the tube temperature at each wire temperature measurement position, the change in tube temperature between each tube thermocouple was assumed to be linear. Thus the temperature of the tube at any position along its length could be determined using linear interpolation between the two adjacent tube thermocouple temperatures.

The gradient of the tube temperature profile could then be determined at a given point along the tube by dividing the temperature difference of the two adjacent tube thermocouples by the distance between the thermocouples, as shown in figure (8-2). Hence the gradient of the tube temperature profile at position x in figure (8-2) was determined by;

$$\left(\frac{dT_t}{dx}\right)_n = \frac{T_t(n) - T_t(n-1)}{X_n - X_{n-1}} \qquad (8\text{-}1)$$

The temperature at position X along the furnace tube could then be determined using the following expression;

$$T_t(X) = T_t(n-1) + (X - X_{n-1}) \cdot \left(\frac{dT_t}{dX}\right)_n \qquad (8\text{-}2)$$

Where the subscripts 'n' and 'n+1' denote the thermocouples adjacent to the position on the tube where the temperature was required. A 'FORTRAN' sub-program was then written to calculate the required tube temperatures using the theory described above. The first task of the sub-program was to input the eleven tube thermocouple temperatures for the appropriate test.

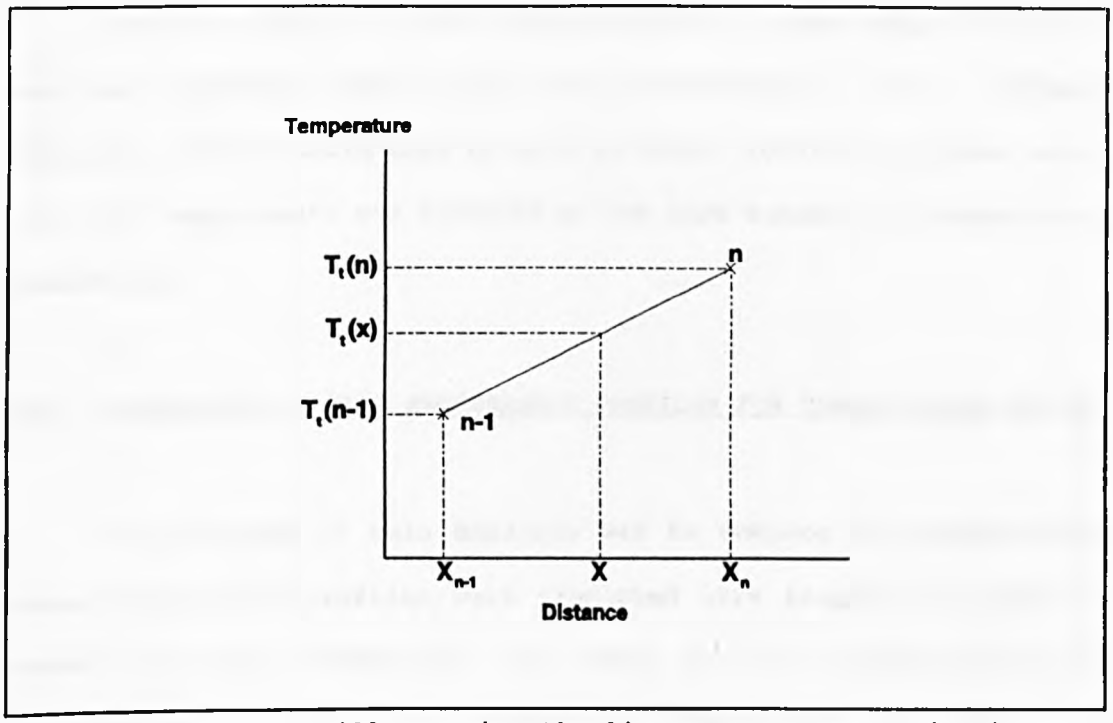

Figure 8-2. Diagram illustrating the linear temperature rise between two tube thermocouples.

In addition to these, the temperature of the tube at the input end (X=0) was estimated and supplied. The sub-program then calculated the temperature gradients between all the known tube temperatures. Following this, the wire temperature profile was read from the appropriate data file.

The distances at which wire temperatures were recorded were then used to calculate the corresponding tube temperatures at those distances using the procedure described above. Twelve tube temperatures were initially known, and so eleven tube temperature gradients could then be calculated.

The temperature gradient utilized to calculate tube temperature at a given tube distance X was that between the two thermocouples adjacent to the position at distance X. For example, to find the tube temperature at X=300 mm, the gradient used would be that between thermocouples 2 and 3.

This was due to the fact that X=300 lay in the range 235 to 335 mm, the respective positions of tube thermocouples 2 and 3. The sub-program produced could then be used in other 'FORTRAN' programs where the tube temperature was required at the wire temperature measurement positions.

8.2 CORRECTION OF WIRE TEMPERATURE PROFILES FOR THERMOCOUPLE ERROR.

The purpose of this analysis was to compare the experimental wire temperature profiles with predicted wire temperature profiles under identical conditions. In order for the experimental wire temperature profiles to be compared accurately with any theoretical results, they had to be corrected for any measurement error.

The theoretical installation error introduced when measuring wire temperature with a thermocouple is discussed in Appendix F. Thus each of the experimental wire temperature profiles presented in section (7.5) had to be corrected accordingly. The model discussed in Appendix F required the tube temperature and the indicated wire thermocouple temperature at a given position to calculate the actual wire temperature at that position.

Due to the large amount of wire temperature data recorded during each experiment on the prototype furnace, a computer program was required to calculate the corrected wire temperature at each position. The computer program developed was written in 'FORTRAN', and was used to calculate the 'corrected' wire temperature at each wire temperature measurement point for each test carried out. The first task of the computer program was to read the wire and tube temperature data for a test from the appropriate data files.

The tube temperature at each of the wire temperature measurement points was then determined using the sub-program developed in section 8.1. The thermocouple installation error at each wire temperature measurement position was then calculated from the indicated wire temperatures and the calculated tube temperatures at these positions. The thermocouple installation error was calculated using an algorithm identical to that developed in Appendix F2. Thus the 'corrected' wire temperature profile was produced from a given wire and tube temperature profile. Corrected wire temperature profiles were then produced for each of the experimental wire temperature profiles presented in section 7.5. These are shown in figures (8-8) to (8-17) in section 8.6.1 at the end of this chapter.

8.3 USING RADIANT HEAT TRANSFER THEORY TO PREDICT THE WIRE TEMPERATURE PROFILE FOR A GIVEN TUBE TEMPERATURE PROFILE.

The theory outlined in chapter 2 describes how heat is transferred from the tube to the wire via radiation. In order to produce a theoretical wire temperature profile for a given set of tube temperatures, it was necessary to consider discrete elements of the wire as it passed through the furnace. Each wire element considered was of length dX and was associated with an adjacent tube element of the same length. This arrangement is shown for a single element in figure (8-3). The tube and wire temperatures are shown to increase over the length of the element dX. The elemental length dX used was considered small enough to assume that the average difference in wire and tube temperatures was equal to the difference at the beginning of the element ie $T_t(X)-T_w(X)$.

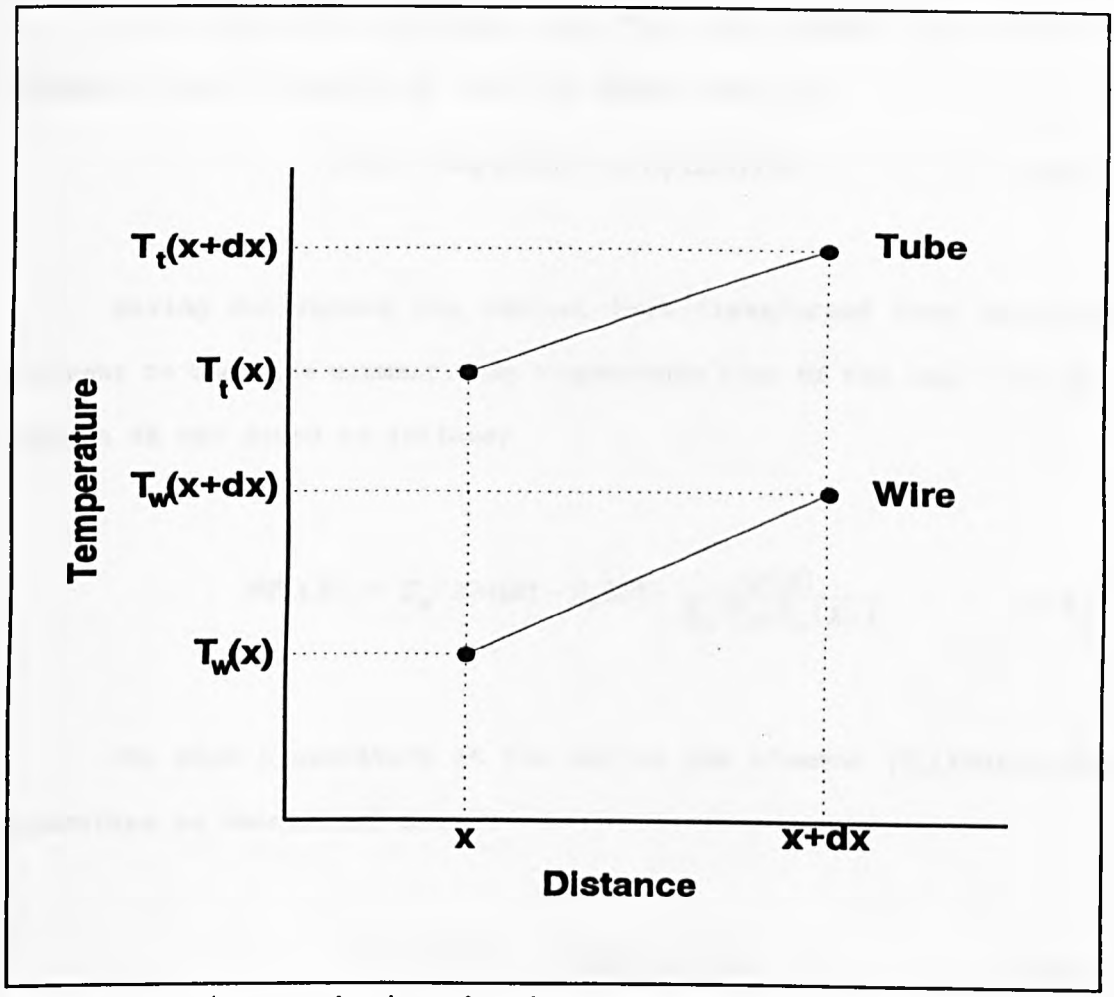

Figure 8-3 Diagram showing the characteristics of a wire and a tube element.

The radiant heat transfer per unit area from the tube to the wire can then be determined using the radiant heat transfer equation (equation (2-7)) as follows;

$$q(X) = R_{tw} \cdot \sigma \cdot (T_t(X)^4 - T_w(X)^4) \qquad (8\text{-}3)$$

Where R_{tw} is the resistance to radiant heat transfer between the tube and the wire which was found in section 2.2 to be;

$$R_{tw} = \frac{1}{\frac{1}{\epsilon_w(T_w(X))} + \frac{A_w}{A_t} \cdot \left(\frac{1}{\epsilon_t(T_t(X))} - 1\right)} \qquad (8\text{-}4)$$

The total heat radiated from the tube element to the wire element, both of length dX was then determined as;

$$Q(X) = A_t \cdot q(X) = \pi \cdot D_t \cdot dX \cdot q(X) \qquad (8\text{-}5)$$

Having determined the radiant heat transferred from the tube element to the wire element, the temperature rise of the wire over the length dX was found as follows;

$$dT_w(X) = T_w(X+dX) - T_w(X) = \frac{Q(X)}{\dot{m}_w \cdot C_w(T_w(X))} \qquad (8\text{-}6)$$

The wire temperature at the end of the element ($T_w(X+dX)$) can therefore be determined from;

$$T_w(X+dX) = T_w(X) + dT_w(X) \qquad (8\text{-}7)$$

This temperature is then used as the initial wire temperature at the beginning of the next wire element. Using the preceding equations, and the required tube temperatures, it is possible to determine the theoretical temperature profile of a wire of given diameter as it progresses through the furnace at a given speed. A computer program was written in 'FORTRAN' to produce such a theoretical wire temperature profile given the initial wire temperature and the tube temperature profile.

Figure (8-4) shows the algorithm used to determine the temperature of each wire element along the furnace.

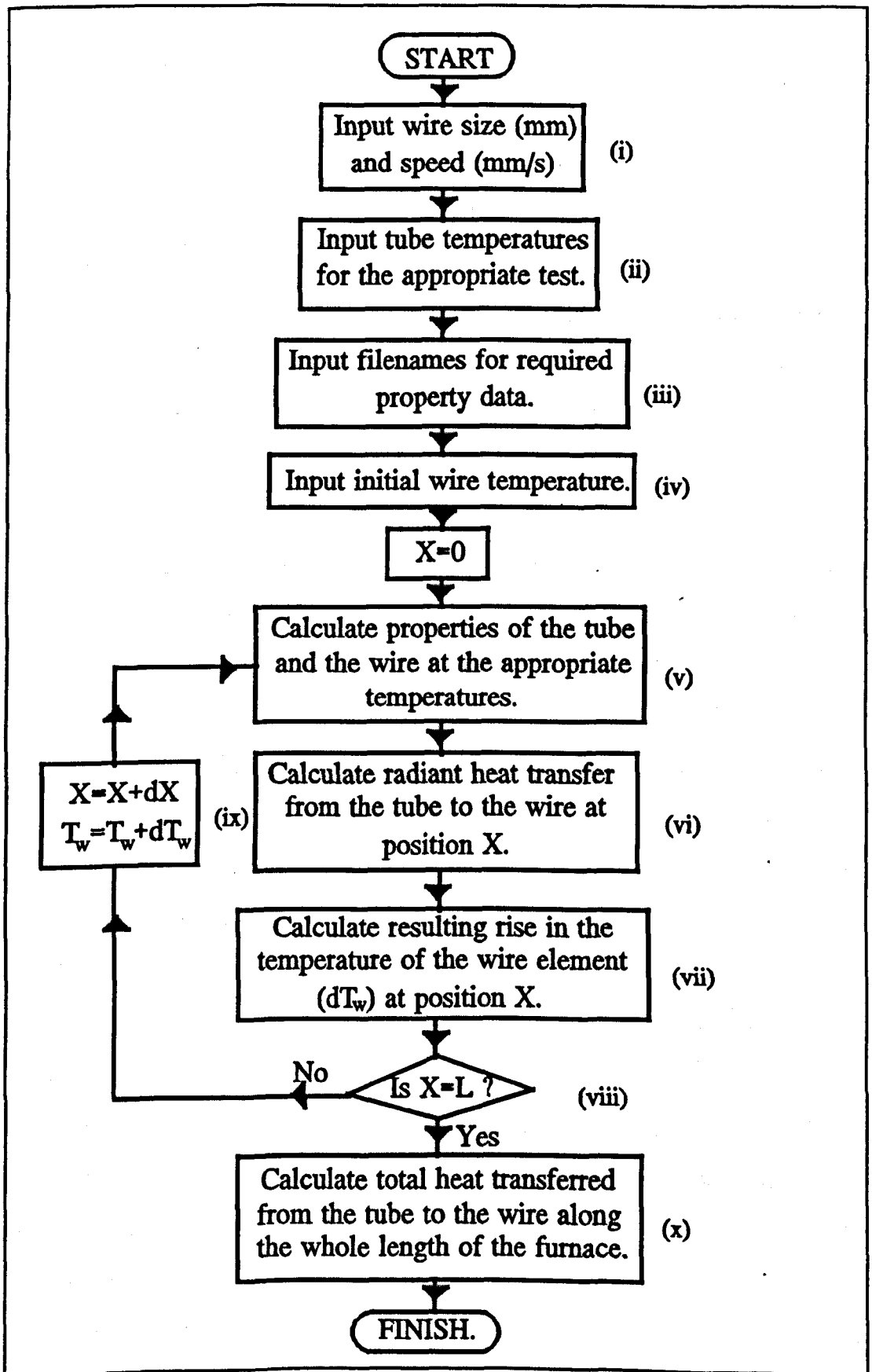

Figure 8-4. Diagram Showing flow chart of radiation calculation.

The following paragraphs describe in detail each of the numbered sections in figure (8.4).

(i) This section requires the input of the diameter and speed of the wire for which the theoretical temperature profile is required.

(ii) This section of the program requires the input of the temperatures of the eleven tube thermocouples, and the estimated tube temperature at the entry end of the furnace. From these twelve tube temperatures the tube temperature at any position along the tube's length can be determined using the procedure outlined in section (8.1).

(iii) In order to calculate the radiant heat transfer to the wire and the resulting temperature change of the wire, various property values are required for the tube and the wire. These properties are needed at the appropriate wire or tube temperature. Polynomial equations relating the required property of a material to its temperature can be found in appendix C, and the coefficients for these equations stored in data files. This section of the program required the input of the names of such files for each of the required properties.

(iv) The inlet temperature of the wire is supplied in this section of the program.

(v) This section calculates the appropriate properties of the wire and tube using the polynomial coefficients from the specified files. The temperatures at which they are determined are those at the beginning of the wire and tube element for which the calculations are being carried out.

(vi) The radiant heat transferred from the tube element to the wire element is calculated in this part of the computer program. Equations (8-3) to (8-5) are used in this calculation, substituting the appropriate property values obtained in the previous part of the program.

(vii) The radiant heat transfer to the wire element at position X results in a change in the temperature of the wire element $dT_w(X)$. The heat transfer, mass flow rate of the wire and the temperature dependent specific heat of the wire are substituted into equation (8-6) to provide the temperature rise of the wire in that element.

(viii) At this point in the program it is determined whether the wire element being considered as it progresses through the furnace had reached the end of the furnace. This is determined by whether or not the distance of the element along the furnace, X is equal to the furnace length, L.

(ix) If the wire element is still in the furnace, then this section of the program is carried out. Here the position of the element X is incremented by its length dX, and the initial temperature of the wire element at its new position set to initial temperature plus the temperature rise of the element at the old position.

(x) When the wire element has passed through to the end of the tube, the total heat transferred to the wire element from the tube is calculated. This is obtained by adding the heat transfer to the element at each position along the furnace, giving the total amount of heat radiated to the wire from the tube as it travel the whole length of the furnace.

Hence the predicted wire temperature profile can be produced from the tube temperature profile and the initial wire temperature.

8.3.1 Comparison Of Wire Temperature Profiles Predicted From Radiant Heat Transfer With Experimental Results.

In order to verify the model described in the preceding section, it was necessary to compare the results with the experimental results. The ten sets of experimental results shown in table (8-1) were chosen in section 7.5 from those carried out for further analysis. The tube temperatures were supplied to the computer program in turn for each of the tests in table (8-1).

Table 8-1

Test Designation Number	Wire Size (mm)	Wire Speed (mm/s)	Wire Entry Temperature(K)
1.1	2	30.0	339
2.1	2	61.0	339
3.2	3	15.0	326
4.3	3	30.0	307
5.2	3	40.0	368
6.3	3	55.6	380
7.2	4	15.0	294
8.2	4	30.0	343
9.2	4	45.0	369
10.2	4	60.0	429

In addition to the tube temperature profile, the wire data was entered for each test. This data consisted of the size, speed and inlet temperature of the wire, as depicted in table (8-1). The predicted wire temperature profiles could therefore be considered to be for the precise furnace and initial wire conditions under which the experimental wire results were measured.

The wire used in the experimental work was Austenitic Stainless Steel, 300 series, the equations for the relevant properties of which are given in Appendix C.

The material of the furnace tube through which the wire passed was Inconel, type 'X'. The equations for the relevant properties of this material are also given in Appendix C.

When the prediction program was operational, the names of the files containing the relevant property equation data were supplied. The results of this prediction program are presented and discussed in the following section.

8.3.2 Discussion Of The Wire Temperature Profiles Predicted For Radiant Heat Transfer.

The wire temperature profiles predicted from radiant heat transfer to the wire are presented in figures (8-18) to (8-27) in section (8.6.2). Each of the predicted wire temperature profiles were plotted along with the corrected wire temperature profile for the associated experiment, as found in section 8.2. From the graphs presented, it is evident that the wire temperatures predicted from radiant heat transfer only do not rise as steeply as the corrected wire temperature profile for the experiment carried out under identical conditions. From this it is evident that the heat being transferred to the wire in the experimental tests was greater than that predicted to be transferred by radiant heat transfer only. In order to investigate the situation further, another mode of heat transfer had to be considered from the tube to the wire in addition to thermal radiation.

8.4 PREDICTING THE TEMPERATURE PROFILE OF THE WIRE DUE TO COMBINED RADIATION AND CONVECTION.

The previous section described the operation of a computer algorithm for predicting the temperature profile of the wire as it passed through the furnace. This model only considered the heat transferred to the wire by thermal radiation. As discussed in section 8.3.2, the theoretical radiative heat transfer to the wire was not sufficient to heat the wire at the rate determined from the experimental work. Appendix E describes the theory used to determine the forced convective heat transfer between the tube and the wire. The nature of the Hydrogen flow through the tube was found in section E2 to be laminar. Having determined this, a method of calculating the convective heat transferred to the wire was devised as described in section E3. In short, the forced convection from the tube to the wire can then be found from the diameter and temperature of the two surfaces. A short algorithm was added to the prediction program discussed in the previous section to calculate the convection from the tube to the wire. This algorithm calculates the convection from the tube to the wire element at a given position using the wire and tube temperature at the beginning of the element.

Initially the mean temperature of the Hydrogen was calculated from the wire and tube temperatures using equation (E-12), Appendix E. The thermal conductivity of Hydrogen was then determined at this temperature from the polynomial equation in appendix C. The convective heat transfer coefficient from the tube to the gas was then found by substituting the thermal conductivity, the Nusselt number (from equation (E-9)) and the hydraulic diameter (from equation (E-7)) into equation (E-6).

Equation (E-13) was then utilised to determine the convection from the tube to the wire element at a given position. The radiation and convection to the wire element at a given position were then added, and the temperature rise of the element at the given position was then calculated from the combined radiative and convective heat transfer to the element. The wire temperature profile was then predicted for a given set of tube temperatures and an initial wire temperature in the same manner as for radiative heat transfer only as in section 8.3.

8.4.1 Comparison Of Wire Temperature Profiles Predicted From Combined Heat Transfer With Experimental Results.

In order to verify the model for combined heat transfer to the wire, it was necessary to compare the predicted wire temperature profile with the corresponding experimental wire temperature profile.

The predicted wire temperature profiles were found using the tube temperatures for the experiments listed in table (8-1), section 8.3.1. The required information for predicting the wire temperature profiles was supplied in the same manner as for the radiative prediction program. The resulting predicted wire temperature profiles were then plotted alongside the corrected experimental wire temperature profile for the experiment in which the tube temperatures were measured. These graphs are shown in figures (8-28) to (8-37) in section (8.6.3) at the end of this chapter.

8.4.2 Discussion Of The Wire Temperature Profiles Predicted For Combined Radiant and Convective Heat Transfer.

The predicted wire temperature profiles determined from the tube temperature profiles in table (8-1), section 8.3.1 are presented in the graphs in figures (8-28) to (8-37) in section 8.6.3. In addition to the predicted wire temperature, each graph also shows the experimental tube temperature profile and the corrected experimental wire temperature profile for the given test. In general the predicted wire temperature profiles compare extremely well with their corresponding corrected experimental wire temperature profiles.

However some of the experimental results do exhibit some deviation from the predicted wire temperature profiles. These deviations were attributed to errors involved in the experimental measurement of the wire temperature profiles, which are discussed in section 7.5.

The prediction model used to calculate the wire temperature profile due to combined heat transfer from the tube to the wire was considered to be accurate when compared with the experimental results.

This model was then developed into a more practical form, so that the wire temperature profile could be determined not from the tube temperatures, but from the temperature of the heaters themselves. This process is discussed in the following section.

8.5 DETERMINING THE HEAT TRANSFER FROM THE HEATERS TO THE WIRE.

8.5.1 Introduction.

The previous section (8.4) described a model which predicted the temperature profile of a wire of a given size travelling at a given speed from a set of measured tube temperatures. A more useful model was required which would predict the wire temperature profile from the temperatures of the heaters. This section describes the theory required to predict the heat transfer from the heaters to the wire, and the application of such theory to model the prototype furnace being used.

8.5.2 Theory required to predict the heat transfer from the heaters to the wire.

In order for heat from the heaters to reach the wire, it must first pass through the process tube, which fully encloses the wire in the furnace. Figure (8-5) depicts the exchange surfaces involved in the heat transfer from the heaters to the wire.

A major assumption made here was that the thermal resistance of the tube wall is negligible, therefore there is negligible temperature differential between its inner and outer surfaces, hence the tube is given the temperature T_t as follows,

$$T_{to} = T_{ti} = T_t \qquad (8\text{-}8)$$

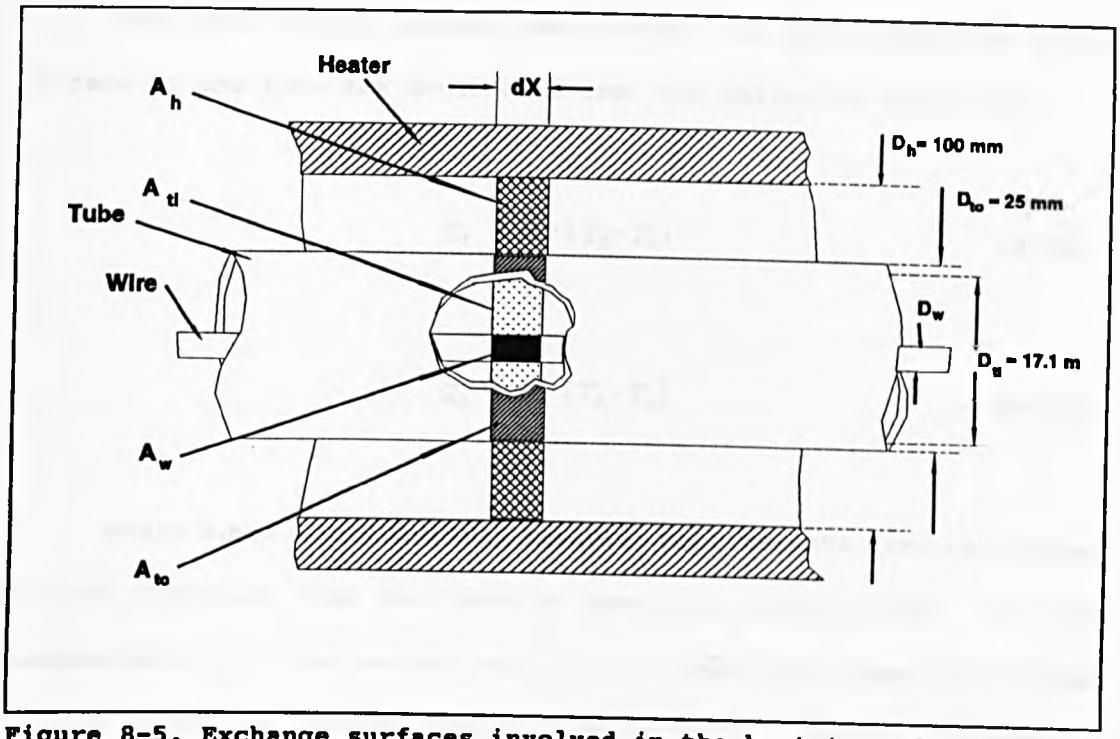

Figure 8-5. Exchange surfaces involved in the heat transfer from the heaters to the wire.

In addition to this, it was also assumed that the tube exchanges heat only with the wire and the heater. Therefore all the heat transferred to the outer surface of the tube from the heaters is transferred from the inner surface of the tube to the wire. The axial conduction of heat along the tube was considered in chapter 7, section (7.4), and found to be negligible when compared with the radiant heat transfer to the tube. Therefore it follows that all the radiant heat reaching the outer surface of the tube is radiated from the inner surface of the tube. This is depicted by,

$$Q = q_1 \cdot A_h = q_2 \cdot A_{ti} \qquad (8\text{-}9)$$

The heat flux q_1 leaving the heater, and q_2 leaving the inner surface of the tube are determined from the following equations,

$$q_1 = h_1 \cdot (T_h - T_t) \qquad (8\text{-}10)$$

$$q_2 = h_2 \cdot (T_h - T_w) \qquad (8\text{-}11)$$

Where h_1 and h_2 are the heat transfer coefficients from the heater to the tube and from the tube to the wire respectively. If the temperature T_h of the heater and T_w of the wire are known at a given point x along the furnace, then T_t must be found in order to ascertain the heat transfer at that point. Substitution of equations (8-10) and (8-11) into equation (8-9) yields the following expression,

$$A_h \cdot h_1 \cdot (T_h - T_t) = A_{ti} \cdot h_2 \cdot (T_t - T_w) \qquad (8\text{-}12)$$

Rearranging equation (8-12) then yields the following equation for T_t,

$$T_t = \frac{A_h \cdot h_1 \cdot T_h + A_t \cdot h_2 \cdot T_w}{A_h \cdot h_1 + A_t \cdot h_2} \qquad (8\text{-}13)$$

Therefore in order to find the tube temperature at a given point, the heat transfer coefficients h_1 and h_2 were required.

The heat transfer from the heater to the tube was considered to be via radiation only. Forced convection is considered to be negligible, as there was no gas flowing in the space between the heaters and the tube. The tube was situated in the centre of the cylindrical heaters, therefore the configuration was that of two concentric cylinders. This configuration was analyzed in chapter 2, and the radiant heat transfer from the heaters to the tube may be written as,

$$Q = \frac{A_h \cdot \sigma \cdot (T_h^4 - T_t^4)}{\frac{1}{\varepsilon_h(T_h)} + \frac{A_t}{A_h}\left(\frac{1}{\varepsilon_t(T_t)} - 1\right)} \qquad (8\text{-}14)$$

From which the following heat transfer coefficient was then developed,

$$H_1 = \frac{A_h \cdot \sigma \cdot (T_h + T_t) \cdot (T_h^2 + T_t^4)}{\frac{1}{\varepsilon_h(T_h)} + \frac{A_t}{A_h}\left(\frac{1}{\varepsilon_t(T_t)} - 1\right)} \qquad (8\text{-}15)$$

Therefore the heat transfer from the heaters to the tube is given by,

$$Q_1 = H_1 \cdot (T_h - T_t) \qquad (8\text{-}16)$$

The heat transfer from the tube to the wire was considered in the previous section to be due to combined radiation and convection.

In order to find the heat transfer from the tube to the wire, the combined heat transfer coefficient H_2 is required such that,

$$Q_2 = H_2 \cdot (T_t - \overline{T}) \qquad (8\text{-}17)$$

The forced convection from the tube to the wire was found in Appendix E to be given by,

$$Q_c = H_c \cdot (T_t - T_f) \qquad (8\text{-}18)$$

Where H_c is given by,

$$H_c = \frac{A_{ti} \cdot N_{u_t} \cdot K_f(T_f)}{D_h} \qquad (8\text{-}19)$$

Where $K_f(T_f)$ is the thermal conductivity of Hydrogen at the gas temperature T_f, Nu_t is the Nusselt number from the tube to the gas (Equation (E-9)), and D_h the hydraulic diameter of the tube and the wire (Equation (E-7)).

The gas temperature was found using equation (E-12) in Appendix E. The surface area A_{ti} being considered here was the area of the element of length dX on the tube surface, given by,

$$A_{ti} = \pi \cdot D_{ti} \cdot dX \qquad (8\text{-}20)$$

The radiant heat transferred from the tube to the wire was found from the theory in section 2 to be given by,

$$Q_r = \frac{A_{ti}\cdot\sigma\cdot(T_t^4-T_w^4)}{\frac{1}{\varepsilon_t(T_t)}+\frac{A_w}{A_t}\left(\frac{1}{\varepsilon_w(T_w)}-1\right)} \qquad (8\text{-}21)$$

Rearranging equation (8-21) yields the following,

$$Q_r = H_r\cdot(T_t-T_w) \qquad (8\text{-}22)$$

Where the radiative heat transfer coefficient is given by,

$$H_1 = \frac{A_{ti}\cdot\sigma\cdot(T_t+T_w)\cdot(T_t^2+T_w^4)}{\frac{1}{\varepsilon_t(T_t)}+\frac{A_w}{A_t}\left(\frac{1}{\varepsilon_w(T_w)}-1\right)} \qquad (8\text{-}23)$$

Therefore the total heat transferred from the tube element to the wire element is given by,

$$Q = Q_c+Q_r = H_c\cdot(T_t-T_f) + H_r\cdot(T_t-T_w) \qquad (8\text{-}24)$$

The combined heat transfer coefficient H_2 may then be written as,

$$H_2 = H_c + H_r \qquad (8\text{-}25)$$

The combined heat transfer from the tube to the wire is thus given as,

$$Q=H_2\cdot(T_t-\bar{T}) \qquad (8\text{-}26)$$

Where $\bar{T}$ is the effective temperature of the gas and the wire. The value of $\bar{T}$ at a given point is found from the gas temperature T_f and the wire temperature T_w at that point using the following expression,

$$\bar{T} = \frac{H_c\cdot T_f + H_r\cdot T_w}{H_c + H_r} \qquad (8\text{-}27)$$

Thus the two heat transfer coefficients H_1 and H_2 can be determined. The tube temperature T_t is then required from equation (8-13) in order to calculate the heat transfer to the wire. However equation (8-13) requires the calculation of the heat transfer coefficients, which in turn require the temperature dependent properties of the tube to be calculated from the tube temperature. Therefore an iterative procedure is required in order to find the tube temperature T_t at a given point. Initially the tube temperature at the given point was 'guessed' as the average of the heater temperature and the wire temperature at that point as follows,

$$T_t'(x) = \frac{T_w(x) + T_h(x)}{2} \qquad (8\text{-}28)$$

The heat transfer coefficients H_1 and H_2 were then calculated on the basis of the estimated tube temperature $T_t'(x)$ using equations (8-16) to (8-26). The tube temperature resulting from these heat transfer coefficients was then calculated using equation (8-13) and the resulting temperature compared with the estimated value.

If there was a difference of more than 1% between the estimated and the calculated tube temperatures then it was necessary to re-calculate the tube temperature. The tube temperature was re-estimated as the average value of the original estimated tube temperature and the calculated value as follows,

$$T_t'(x) = \frac{T_t'(x) + T_t(x)}{2} \qquad (8\text{-}29)$$

The heat transfer coefficients were again calculated using equations (8-16) to (8-26) and the tube temperature was then re-calculated using equation (8-13). This process was continued until the difference between the estimated and the calculated tube temperatures was less than 1%. Having determined the tube temperature at the required position X, the heat transfer from the heater to the wire element at X could then be determined using equation (8-16)

8.5.3 Computer Simulation Of Heat Transfer From The Heater To The Wire.

In order to calculate the heat transfer to the wire from the heater, and thus its temperature profile as it passed through the furnace tube, a computer simulation was required.

The furnace used for the experimental work consisted of three separate cylindrical heater elements surrounding the process tube. The total length of the three heaters was 1 Metre, beginning at a distance of 135 mm from the furnace inlet as in figure (8-6) below,

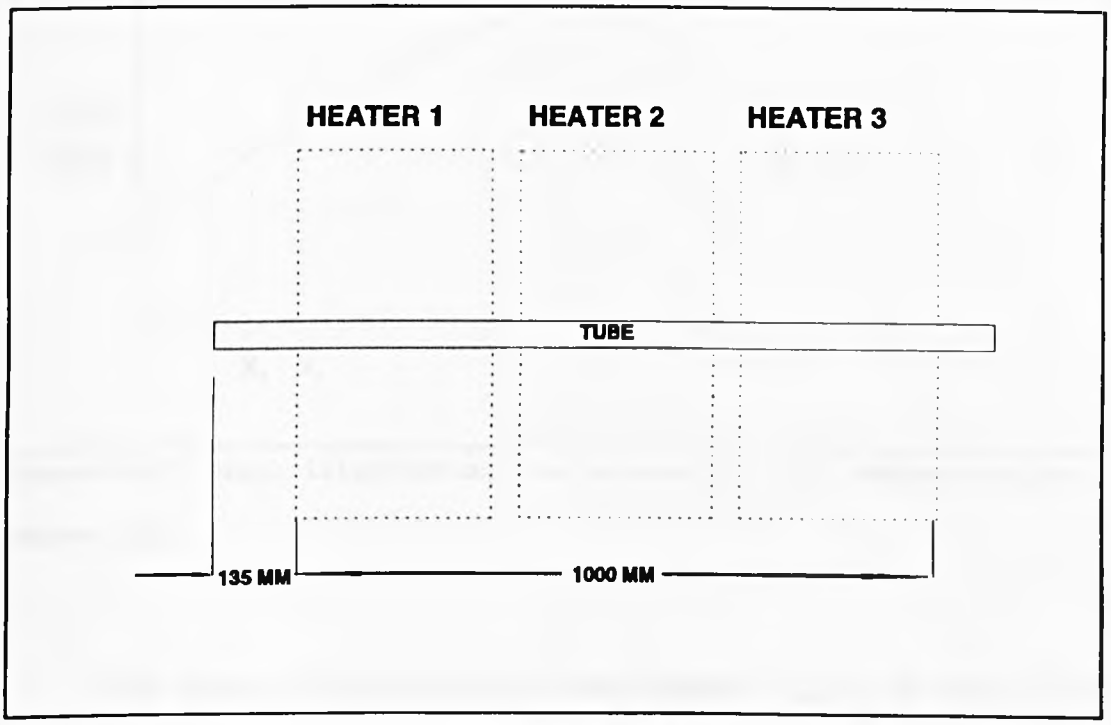

Figure 8-6. Diagram showing the layout of the heaters in relation to the process tube.

Heating of the wire was only considered in the length of tube which was actually inside the heaters for the purposes of this model. In addition the gaps between the heating zones on the furnace were considered as part of the heaters themselves, thus the length of each heater was 333 mm.

As in the earlier models, an element dX was considered as it progressed through the furnace. Figure (8-7) shows the wire element progressing from position X_1 to X_2, a distance dX, and its temperature changing from $T_w(X_1)$ to $T_w(X_2)$.

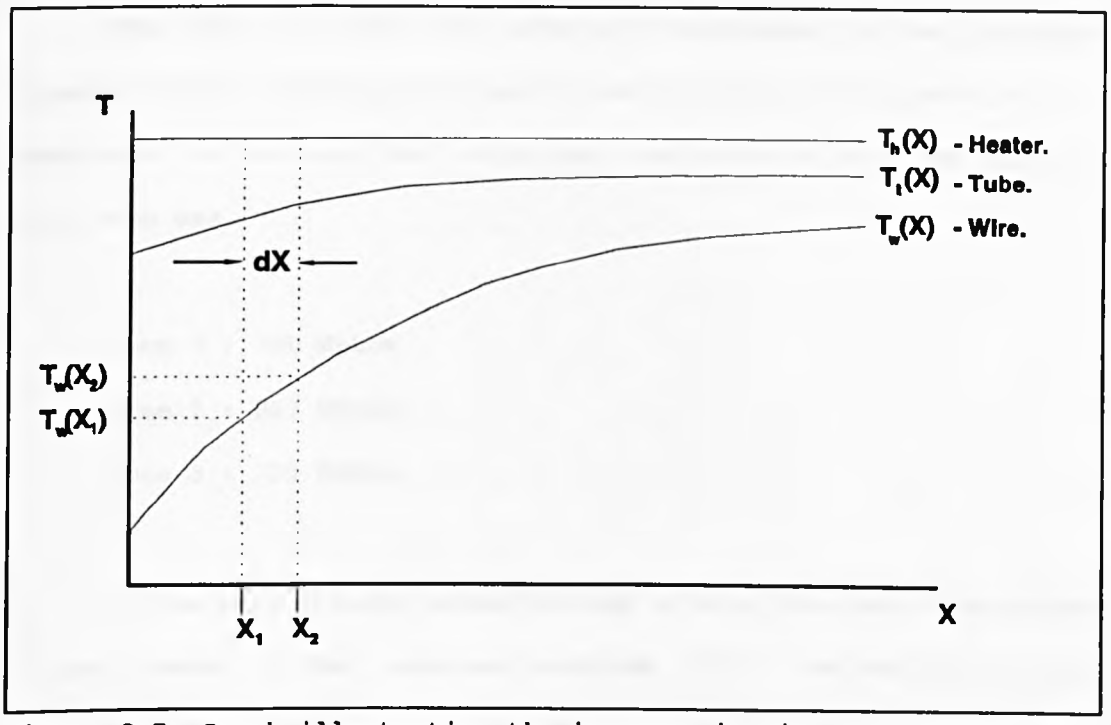

Figure 8-7. Graph illustrating the increase in wire temperature over length dX.

The change in temperature of the element $dT_w(X_1)$ is due to the heat transferred to it at position X_1 as defined by equation,

$$dT_w(X_1) = \frac{Q(X_1)}{\dot{m} \cdot C(T_w(X_1))} \qquad (8\text{-}30)$$

Where m is the mass flow rate of wire through the furnace in Kg/s, and $C(T_w(X_1))$ the specific heat of the wire. Thus the temperature rise of the wire element is calculated as it progresses through the furnace to provide the wire temperature profile.

The tube temperature was also calculated at each position to provide the tube temperature profile. The heaters used on the prototype furnace had a maximum power rating of 1.13 Kw each.

The heat losses from each zone were determined for the prototype furnace in the start-up test, and given in table (7-1), section 7.4. Therefore the maximum heat which was available to heat the wire in each zone was,

Zone 1 : 730 Watts

Zone 2 : 827 Watts

Zone 3 : 722 Watts

As the wire element passed through a zone, the heat transferred to the element in that zone was summated, and at the end of the zone the total was compared with the maximum heat transfer for that zone. If the total exceeded the maximum, then the rate of heat transfer at each elemental position in that zone was recalculated. This time the heat transfer at each position was reduced by a factor F_q as follows,

$$Q(X) = F_q \cdot Q(X) \qquad (8\text{-}31)$$

Where,

$$F_q = \frac{Q_m(Z)}{Q_t(Z)} \qquad (8\text{-}32)$$

Where $Q_m(Z)$ was the maximum heat transfer from the heater in zone number Z, and $Q_t(Z)$ was the total calculated heat transfer in zone number Z. The required thermophysical properties of the exchange surfaces were calculated as described in section 8.3.

The computer program was written in 'FORTRAN' programming language using the 'Prospero Fortran' compiler on a PC.

8.5.4 Results From The Computer Simulation Of The Heat Transfer From The Heaters To The Wire.

The computer simulation model was tested by running it with the wire sizes and speeds of the experimental results which were analyzed, and are shown in table (8-1) below.

Table 8-2

Test Designation Number	Wire Size (mm)	Wire Speed (mm/s)	Wire Temperature At 135 mm.(K)
1.1	2	30.0	427
2.1	2	61.0	345
3.2	3	15.0	368
4.3	3	30.0	382
5.2	3	40.0	371
6.3	3	55.6	384
7.2	4	15.0	343
8.2	4	30.0	355
9.2	4	45.0	376
10.2	4	60.0	423

For each of the tests, the temperature of the three heaters was the same as those of the heaters in the prototype furnace during the experimental tests, ie at 1000°C. The initial temperature of the wires used to start the simulation for a particular test was the wire temperature at a distance of 135 mm from the furnace inlet measured during that test. The simulated tube and wire temperature profiles are plotted alongside the experimental results in figures (8-38) to (8-47), in section (8.6.4).

8.5.5 Discussion Of The Results From The Computer Simulation Of The Heat Transfer From The Heaters To The Wire.

The graphs in figures (8-38) to (8-47) illustrate the experimental and predicted wire and tube temperature profiles for the tests in table (8-2). The theoretical simulation model described in section 8.5.3 was observed to have predicted accurately the temperature profiles of the wire, when compared with the associated experimental wire temperature profiles. The main discrepancy in the predicted wire temperature profiles was found to be that the predicted wire temperature did not 'peak' at some point along the furnace, and then decrease, as was exhibited by the experimental results.

This was attributed to the fact that the conduction of heat along the tube was not considered by the simulation model when calculating the tube temperature profiles. Therefore at the 'hot' end of the furnace, the predicted tube temperature remained at, or close to, the heater temperature, rather than decreasing, as occurred with the experimental tube temperature profiles. Therefore the predicted wire temperature continued to increase, or else remained constant, rather than decreasing, as was found with the experimental wire temperature profiles.

The tube temperature profiles which were predicted using the simulation model were all found to be of the same general shape as the corresponding experimental tube temperature profiles, except that they did not exhibit the drop in tube temperature towards the ends of the furnace, which was attributed to conduction of heat along the tube.

Overall the simulation model was considered to have accurately predicted the wire temperature profiles, when compared with the experimental results. The errors which were regarded to have been caused by the conduction of heat along the tube were considered to be acceptable. The prototype furnace was relatively short in length when compared with the majority of wire annealing furnaces. Therefore the errors discussed in this section were considered to have been even less significant when using this theoretical simulation model to predict the wire temperature profiles in larger scale furnaces.

8.6 PRESENTATION OF GRAPHS DISPLAYING ANALYTICAL RESULTS.

8.6.1 Corrected experimental wire temperature profiles.

The graphs in this section depict the measured or 'indicated' wire temperature profiles from the tests carried out, which were chosen for further analysis in section 7.5. Also presented in each graph is the corrected wire temperature profile for each test, calculated as described in section 8.2

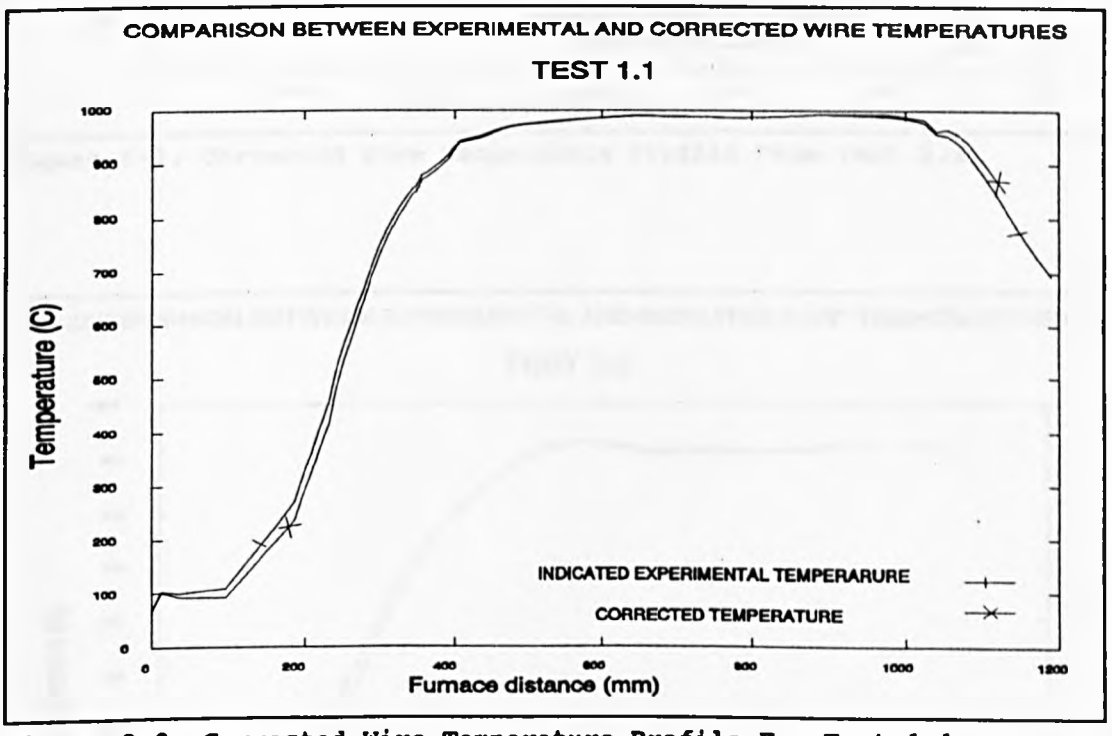

Figure 8-8. Corrected Wire Temperature Profile For Test 1.1.

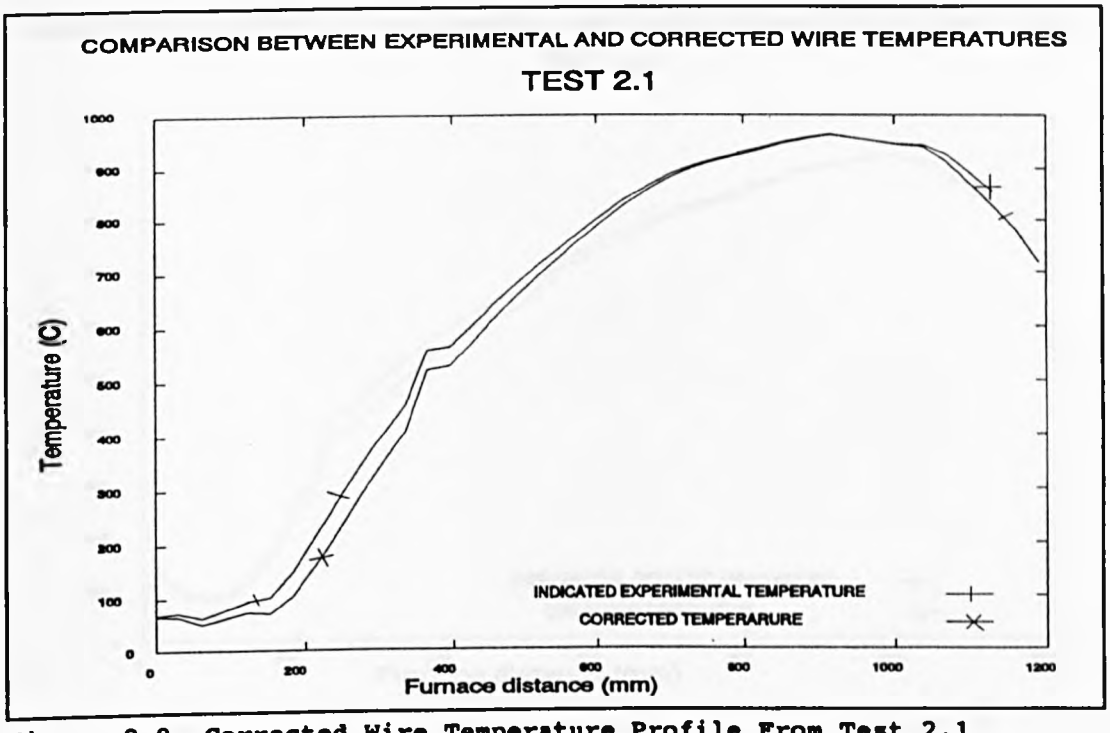

Figure 8-9. Corrected Wire Temperature Profile From Test 2.1

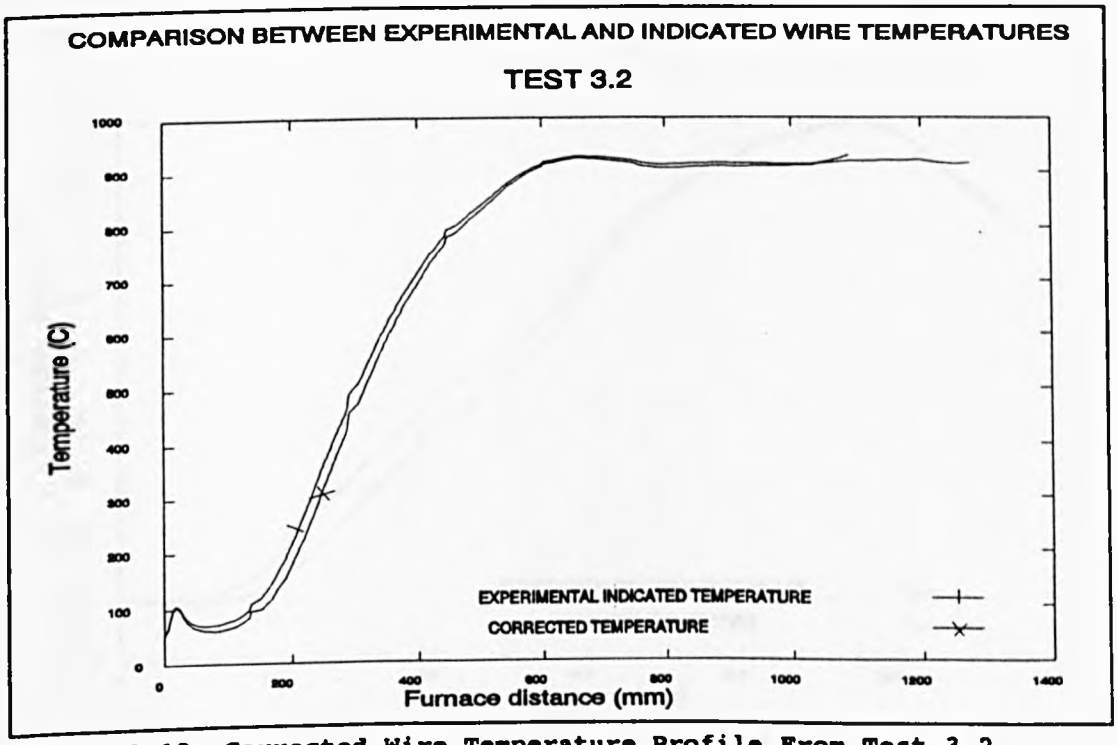

Figure 8-10. Corrected Wire Temperature Profile From Test 3.2

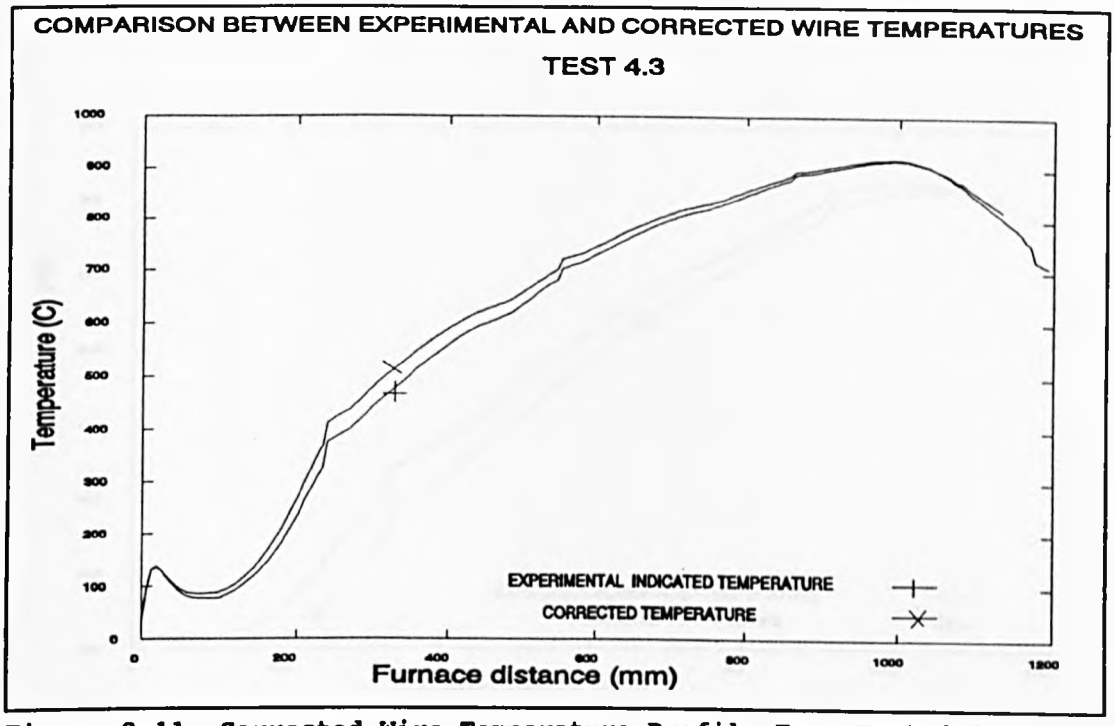

Figure 8-11. Corrected Wire Temperature Profile From Test 4.3

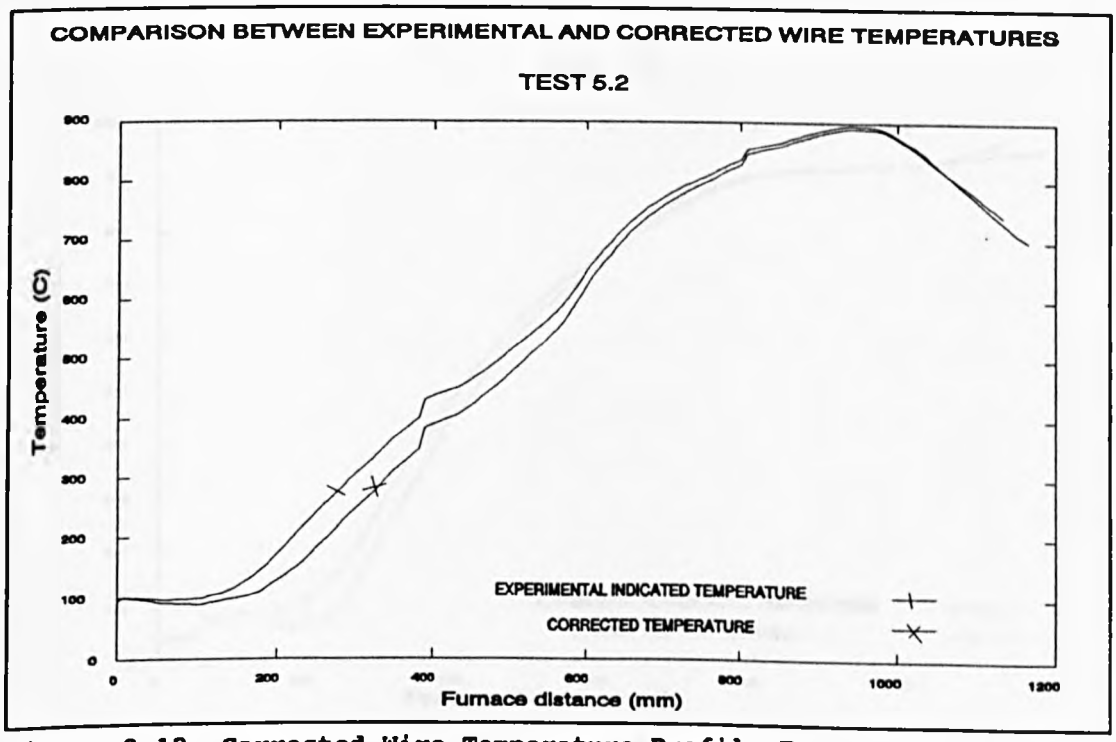

Figure 8-12. Corrected Wire Temperature Profile From Test 5.2

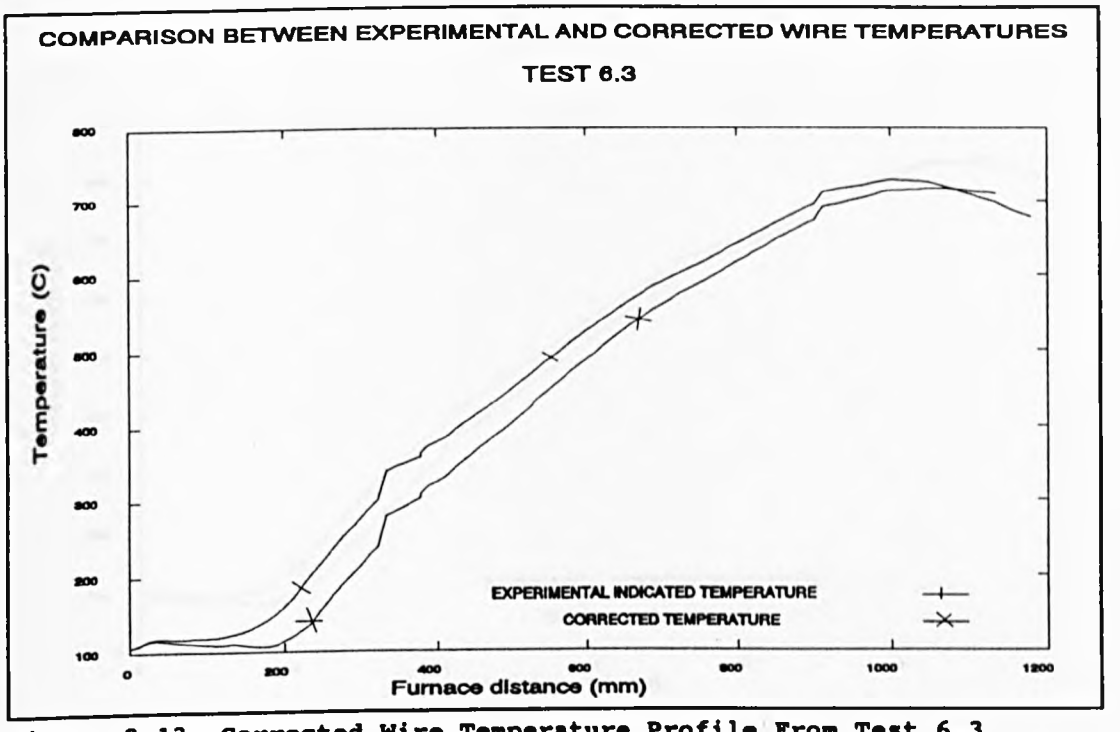

Figure 8-13. Corrected Wire Temperature Profile From Test 6.3

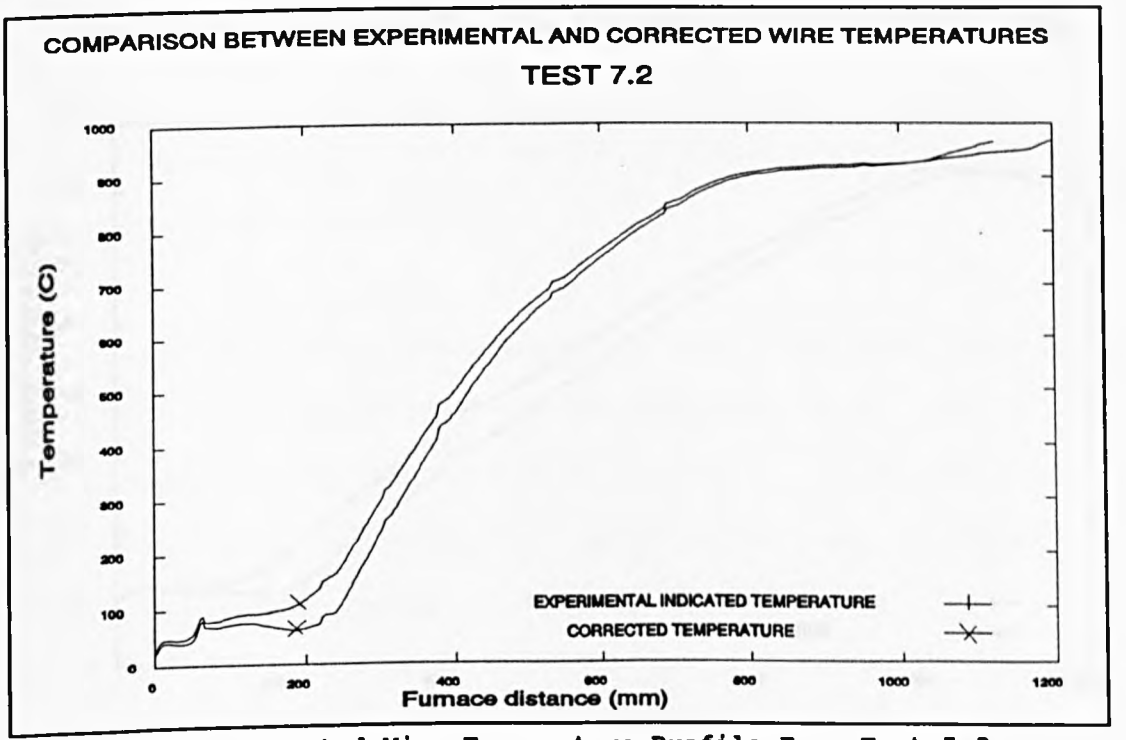

Figure 8-14. Corrected Wire Temperature Profile From Test 7.2

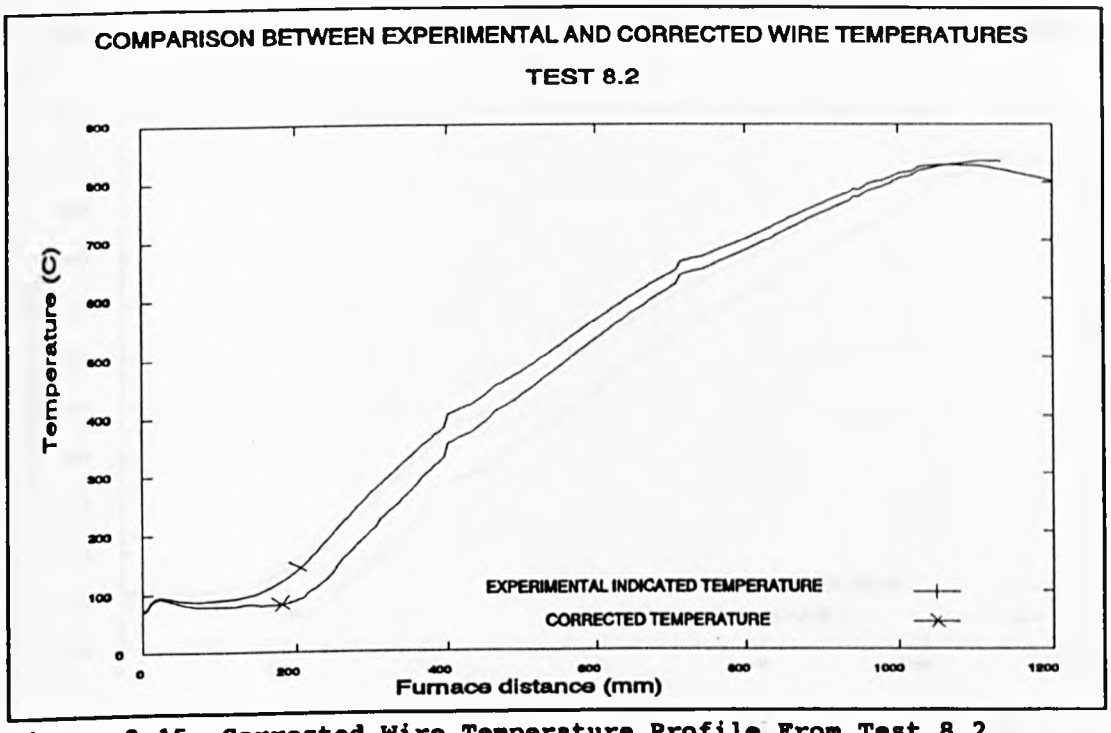

Figure 8-15. Corrected Wire Temperature Profile From Test 8.2

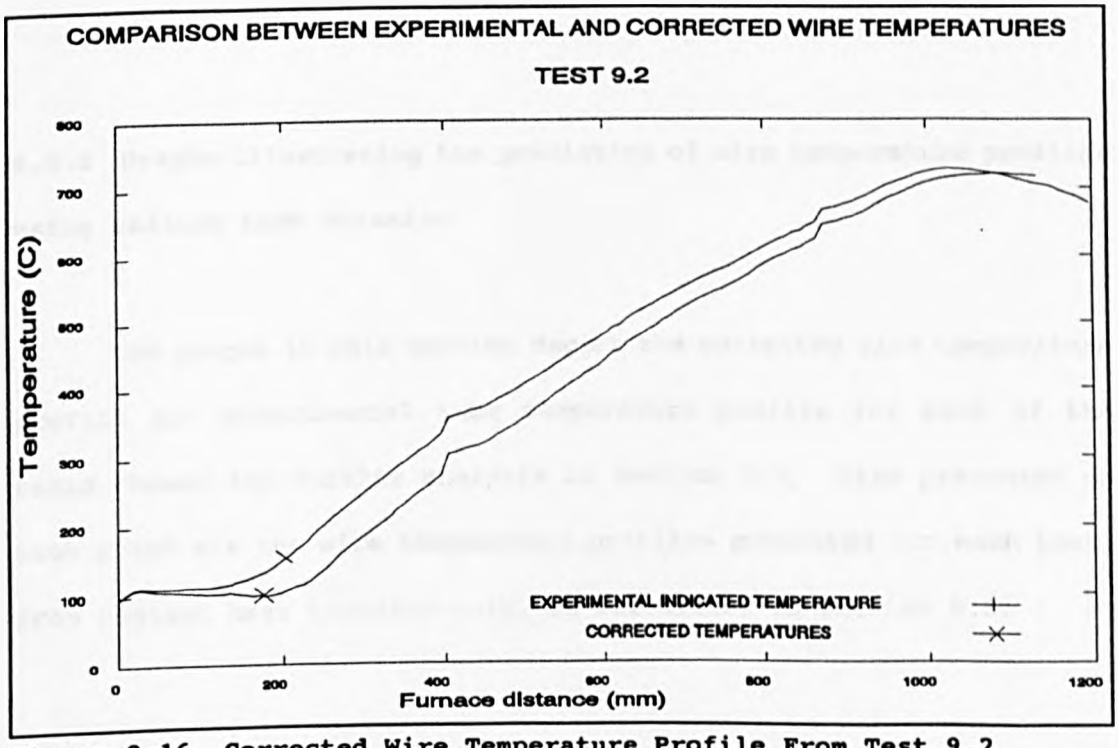

Figure 8-16. Corrected Wire Temperature Profile From Test 9.2

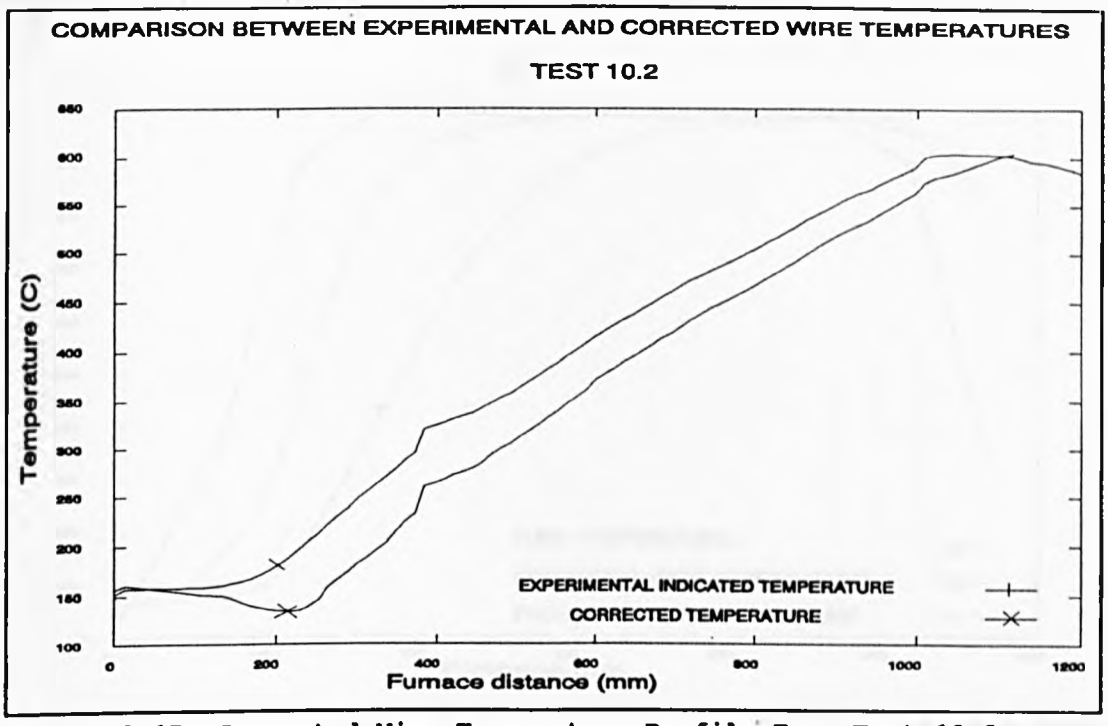

Figure 8-17. Corrected Wire Temperature Profile From Test 10.2

8.6.2 Graphs illustrating the prediction of wire temperature profiles using radiant heat transfer.

The graphs in this section depict the corrected wire temperature profile and experimental tube temperature profile for each of the tests chosen for further analysis in section 7.5. Also presented on each graph are the wire temperature profiles predicted for each test, from radiant heat transfer only, as calculated in section 8.3.

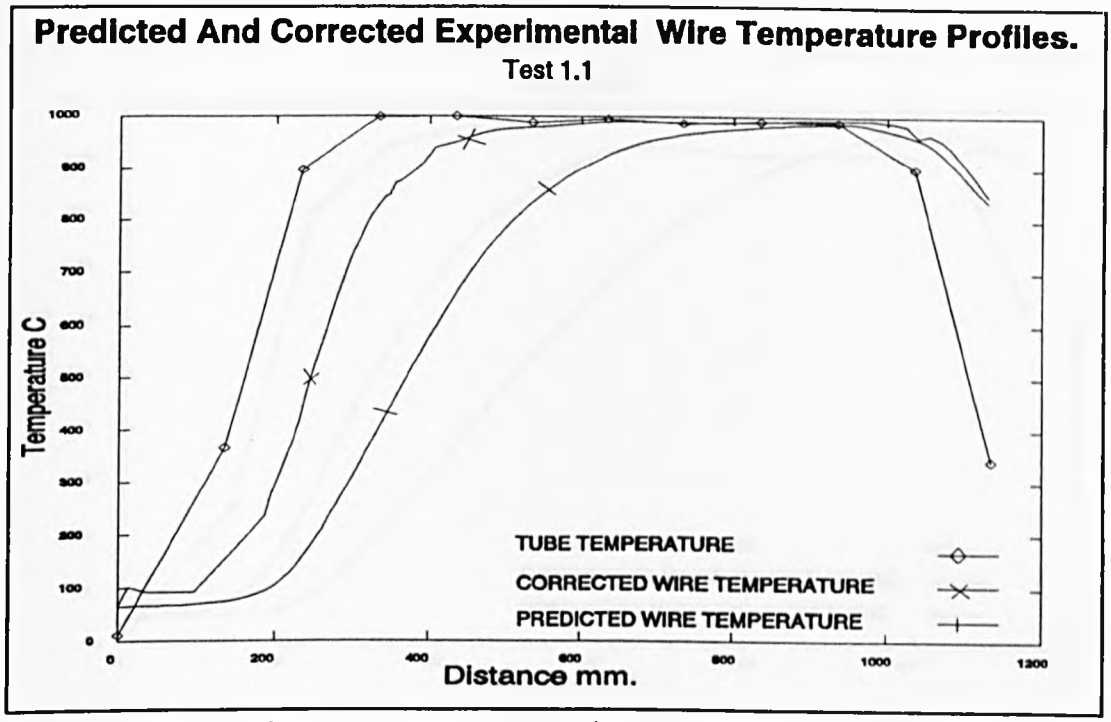

Figure 8-18. Wire temperature profile predicted from radiant heat transfer for test 1.1

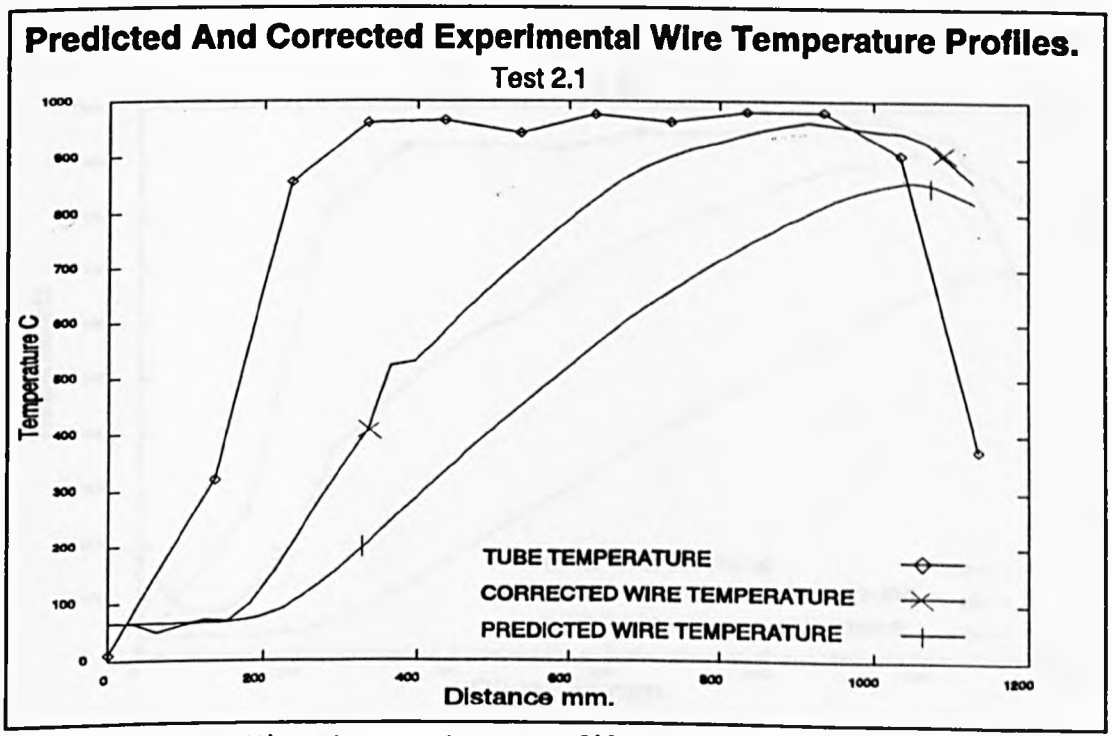

Figure 8-19. Wire temperature profile predicted from radiant heat transfer for test 2.1

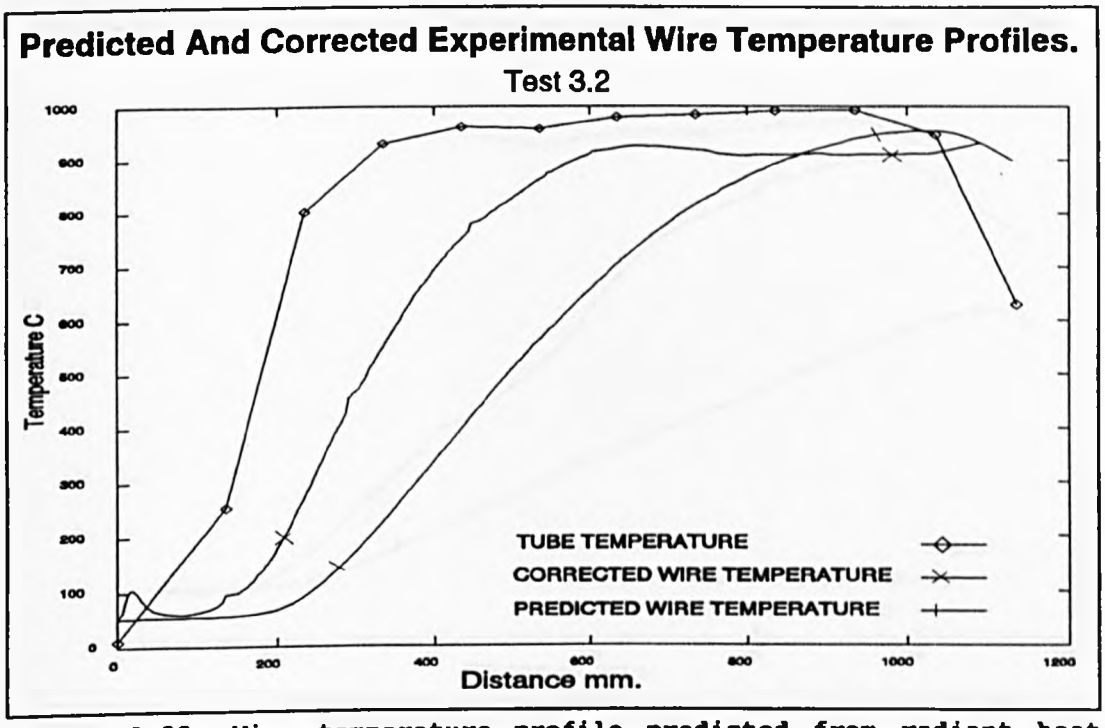

Figure 8-20. Wire temperature profile predicted from radiant heat transfer for test 3.2

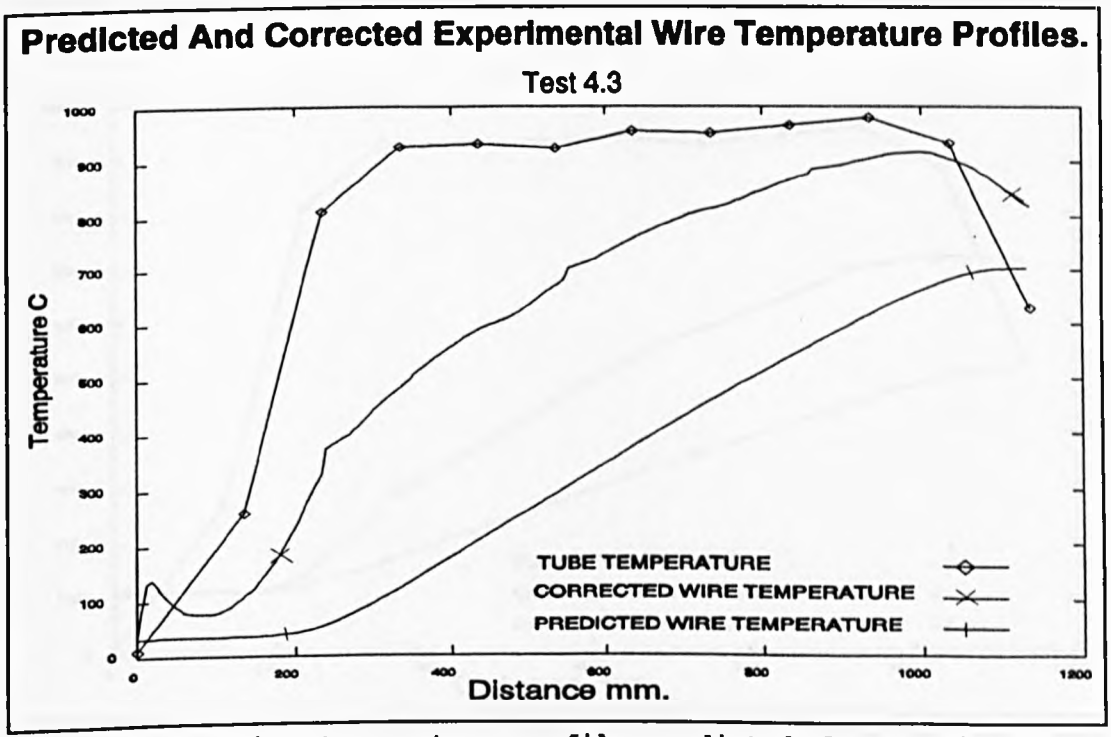

Figure 8-21. Wire temperature profile predicted from radiant heat transfer for test 4.3

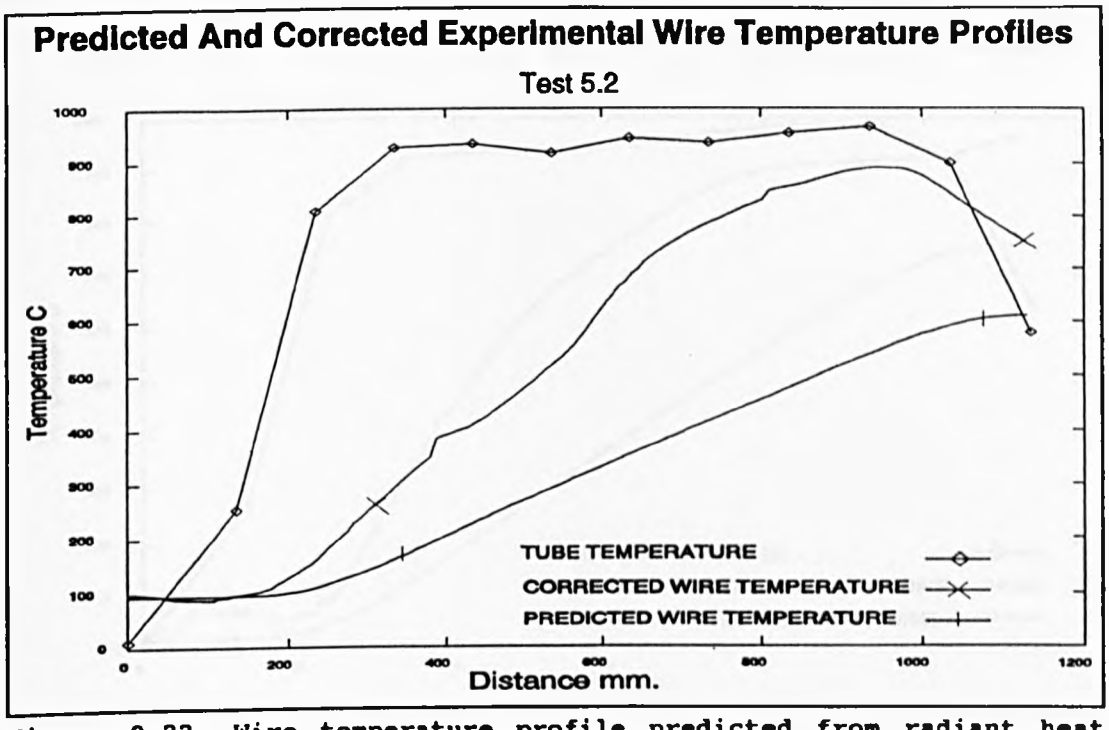

Figure 8-22. Wire temperature profile predicted from radiant heat transfer for test 5.2

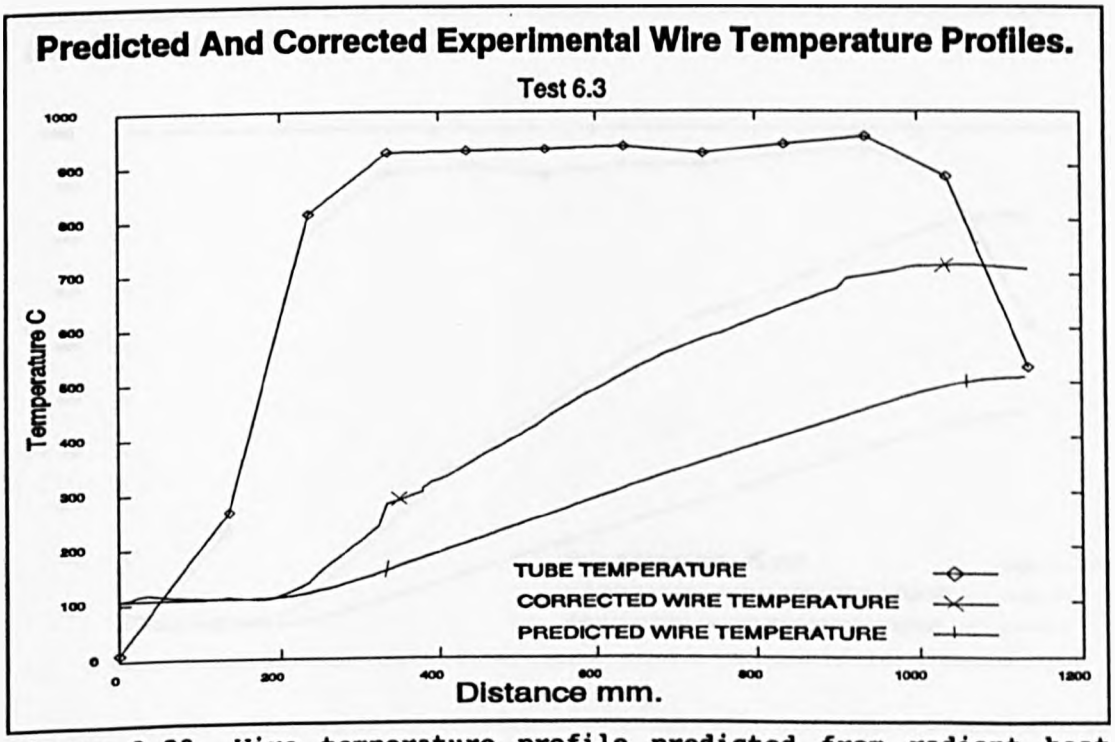

Figure 8-23. Wire temperature profile predicted from radiant heat transfer for test 6.3

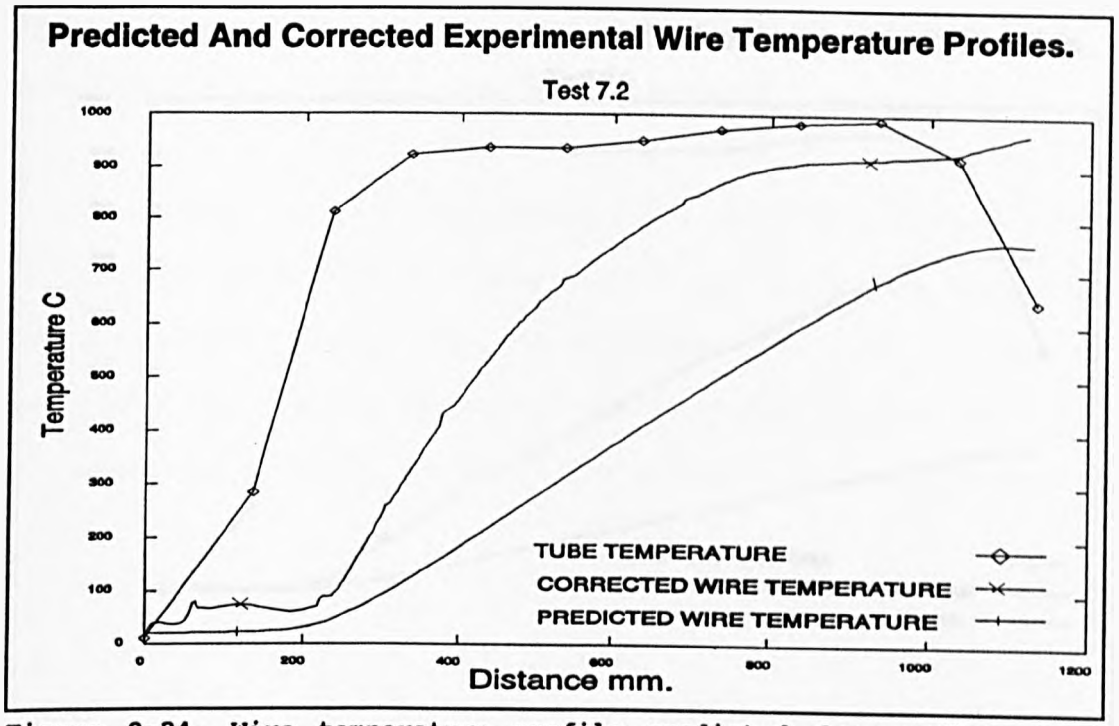

Figure 8-24. Wire temperature profile predicted from radiant heat transfer for test 7.2

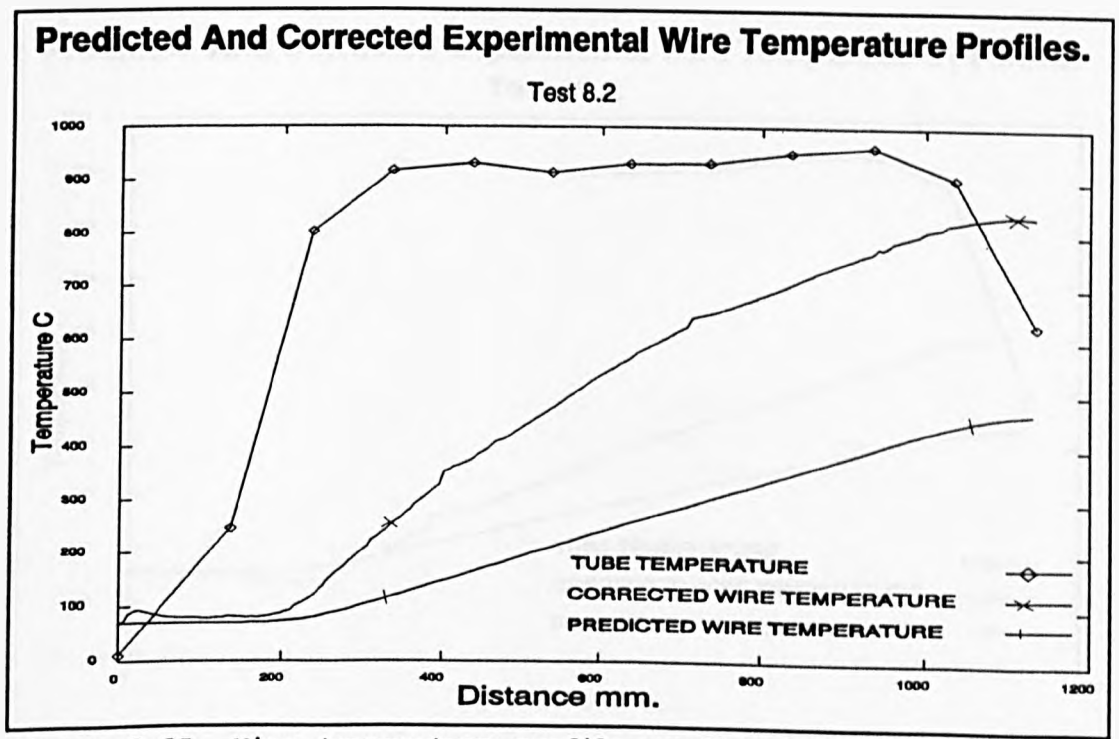

Figure 8-25. Wire temperature profile predicted from radiant heat transfer for test 8.2

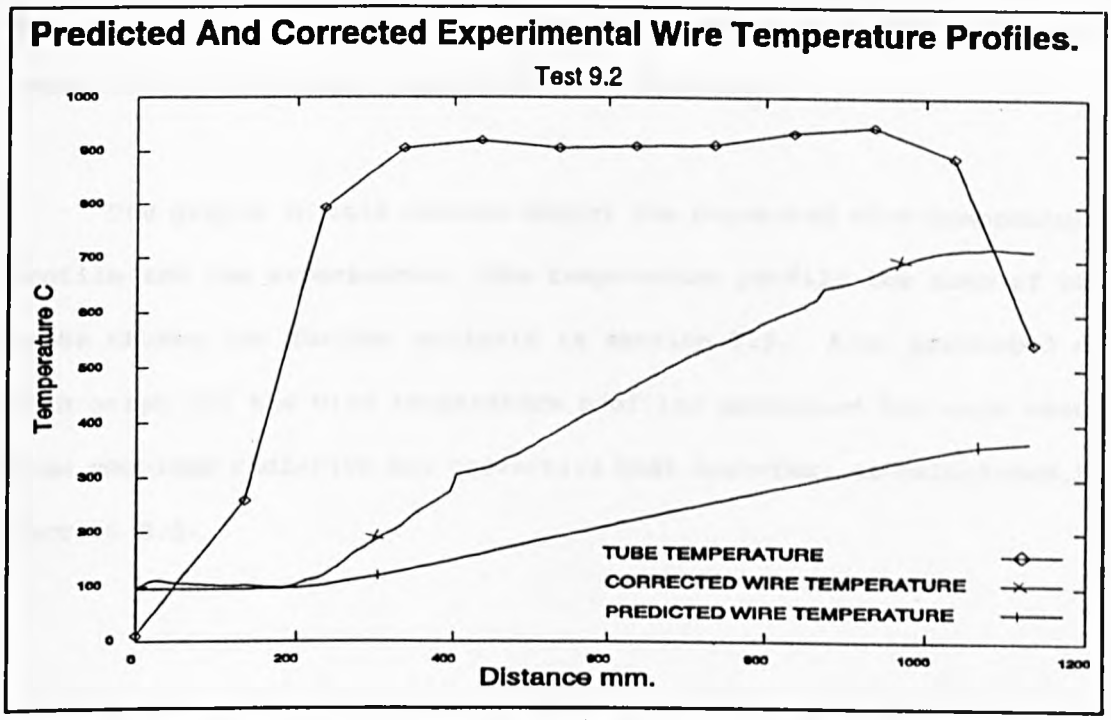

Figure 8-26. Wire temperature profile predicted from radiant heat transfer for test 9.2

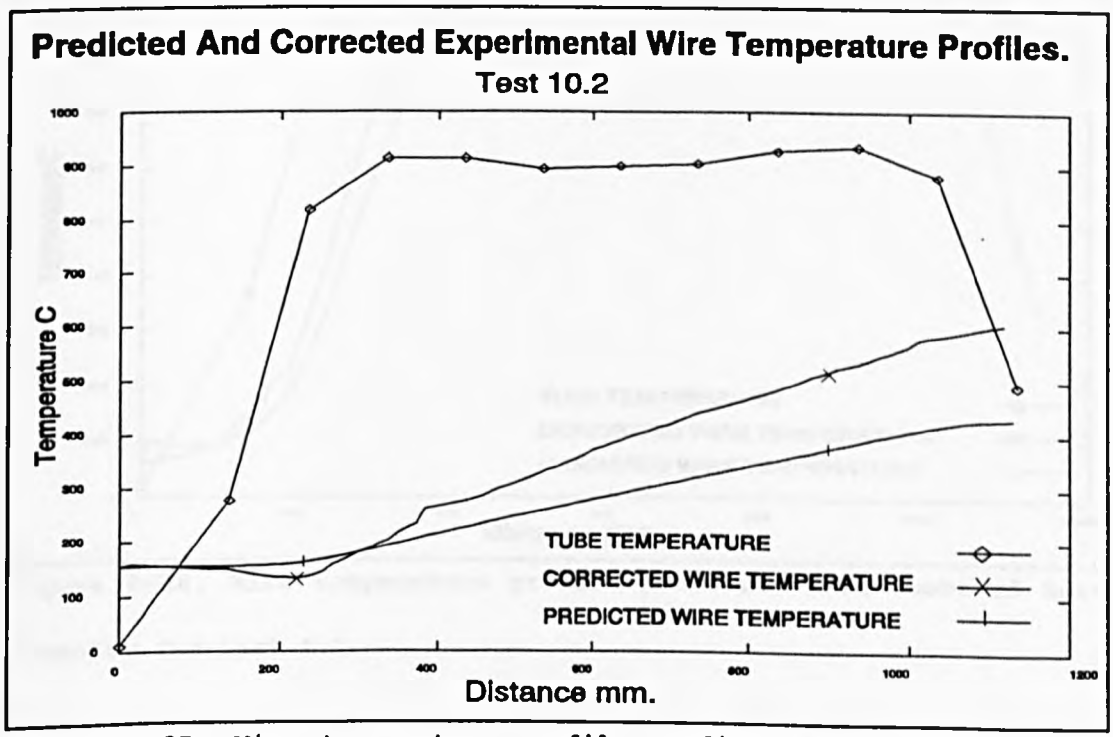

Figure 8-27. Wire temperature profile predicted from radiant heat transfer for test 10.2

8.6.3. Presentation of wire temperature profiles predicted using combined radiative and convective heat transfer.

The graphs in this section depict the corrected wire temperature profile and the experimental tube temperature profile for each of the tests chosen for further analysis in section 7.5. Also presented on each graph are the wire temperature profiles predicted for each test, from combined radiative and convective heat transfer, as calculated in section 8.3.

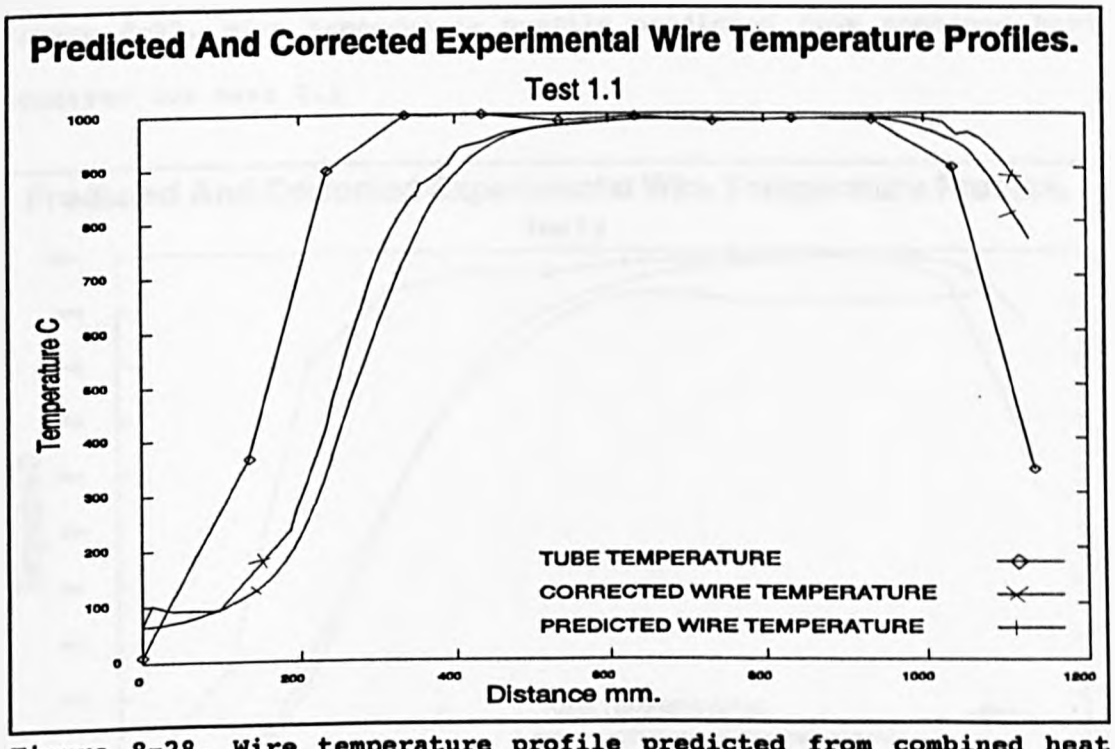

Figure 8-28. Wire temperature profile predicted from combined heat transfer for test 1.1

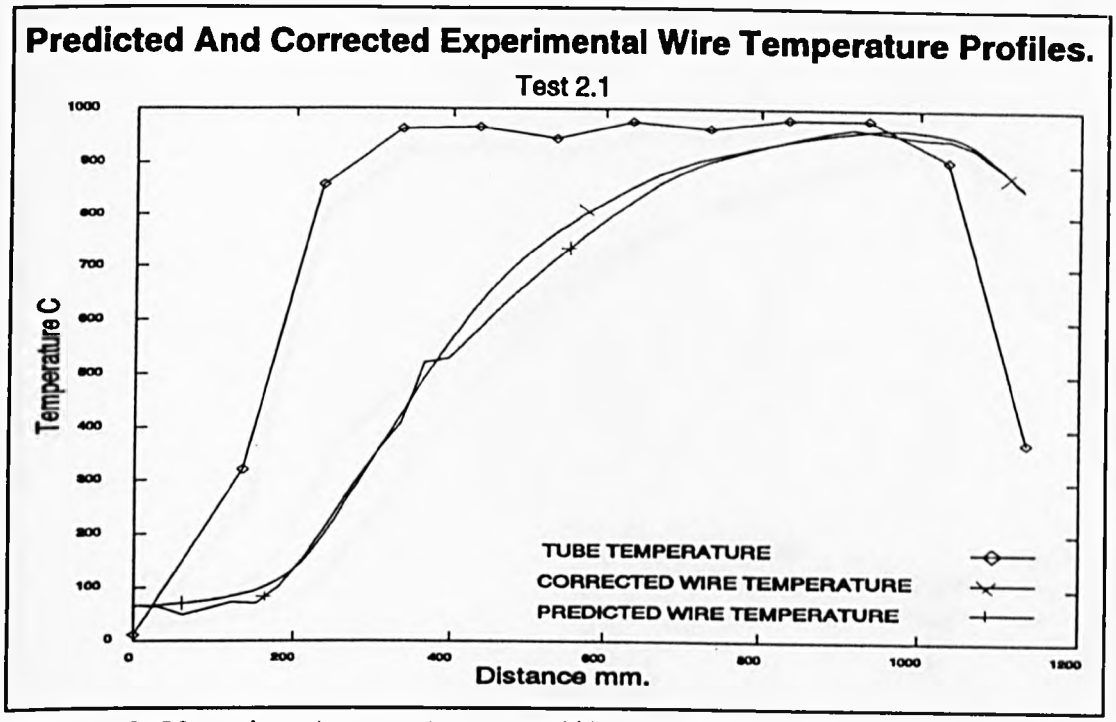

Figure 8-29. Wire temperature profile predicted from combined heat transfer for test 2.1

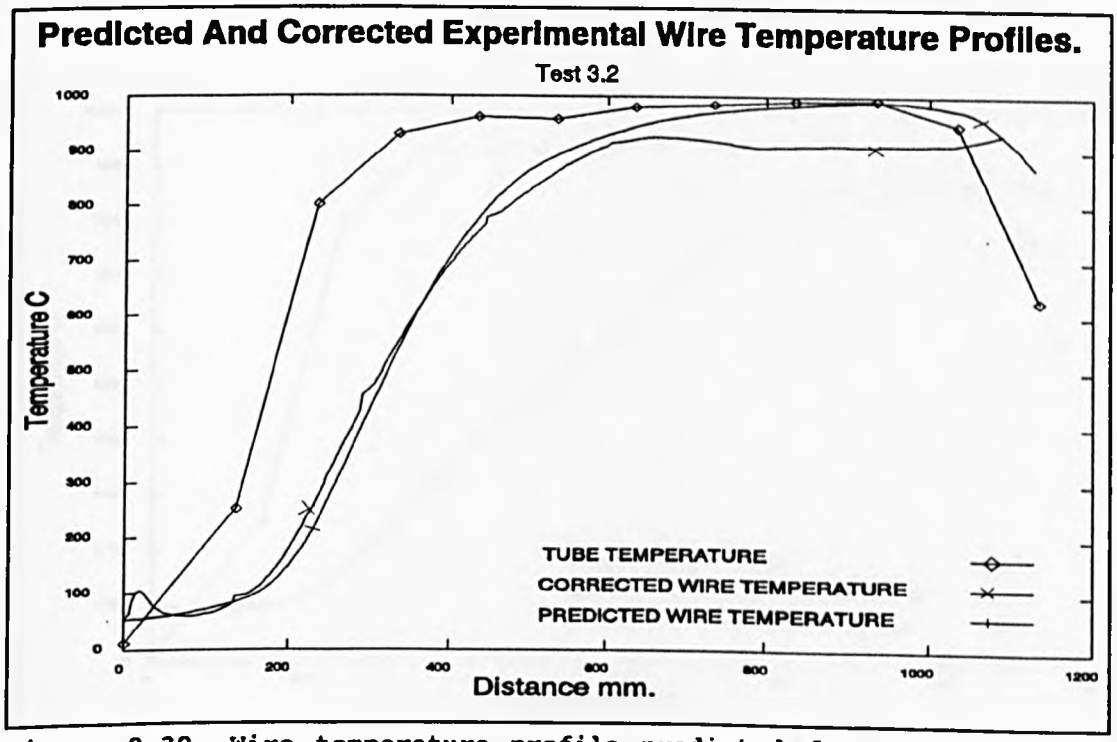

Figure 8-30. Wire temperature profile predicted from combined heat transfer for test 3.2

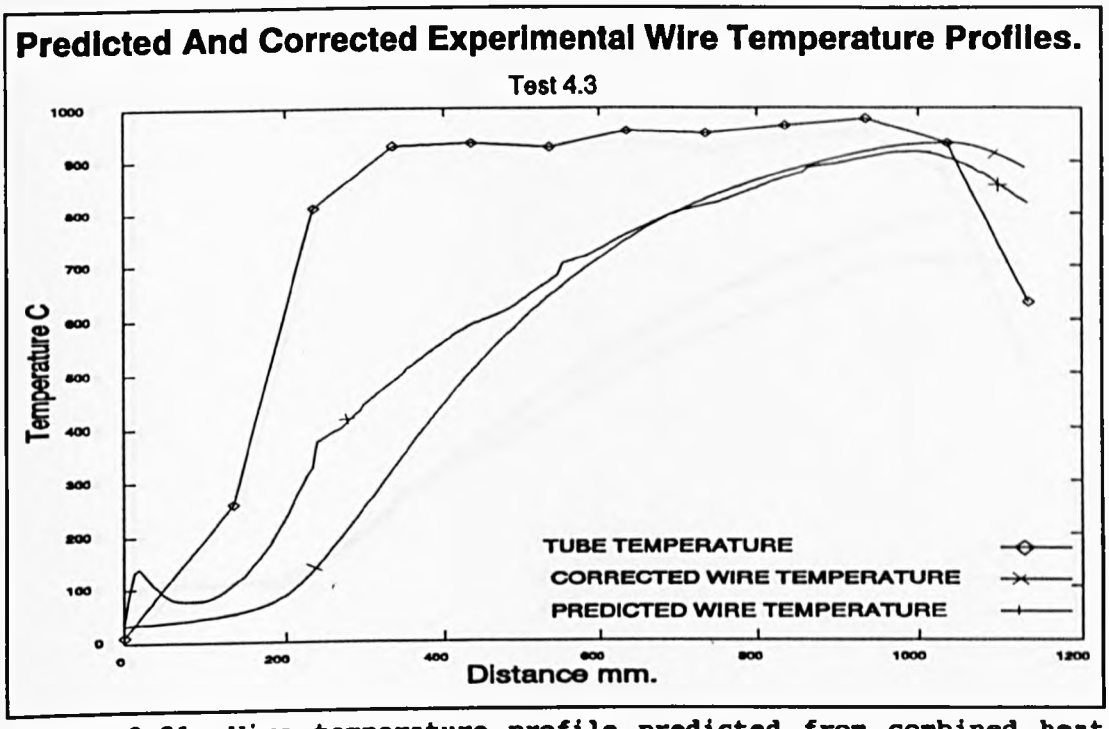

Figure 8-31. Wire temperature profile predicted from combined heat transfer for test 4.3

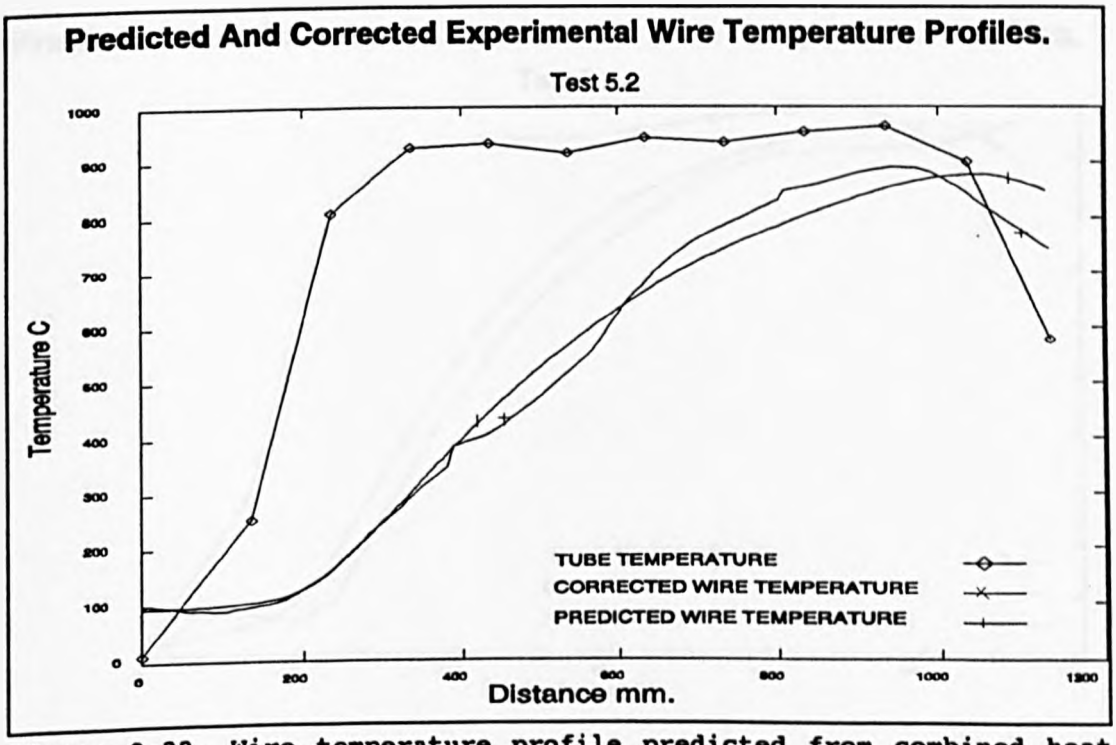

Figure 8-32. Wire temperature profile predicted from combined heat transfer for test 5.2

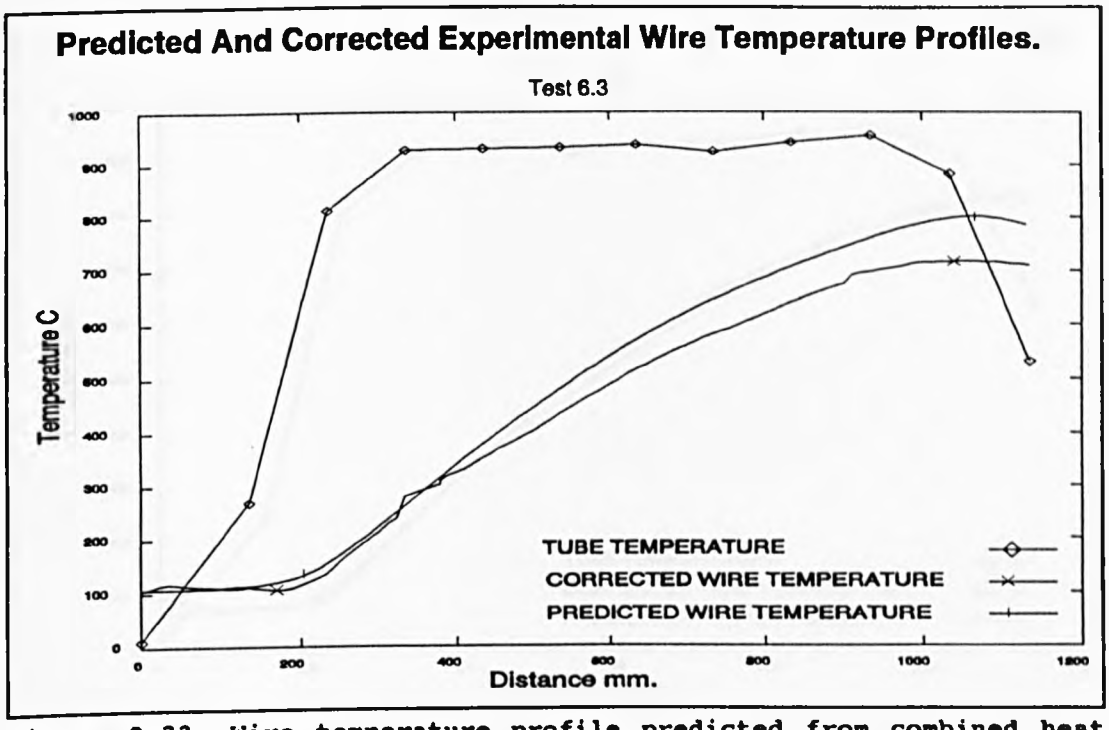

Figure 8-33. Wire temperature profile predicted from combined heat transfer for test 6.3

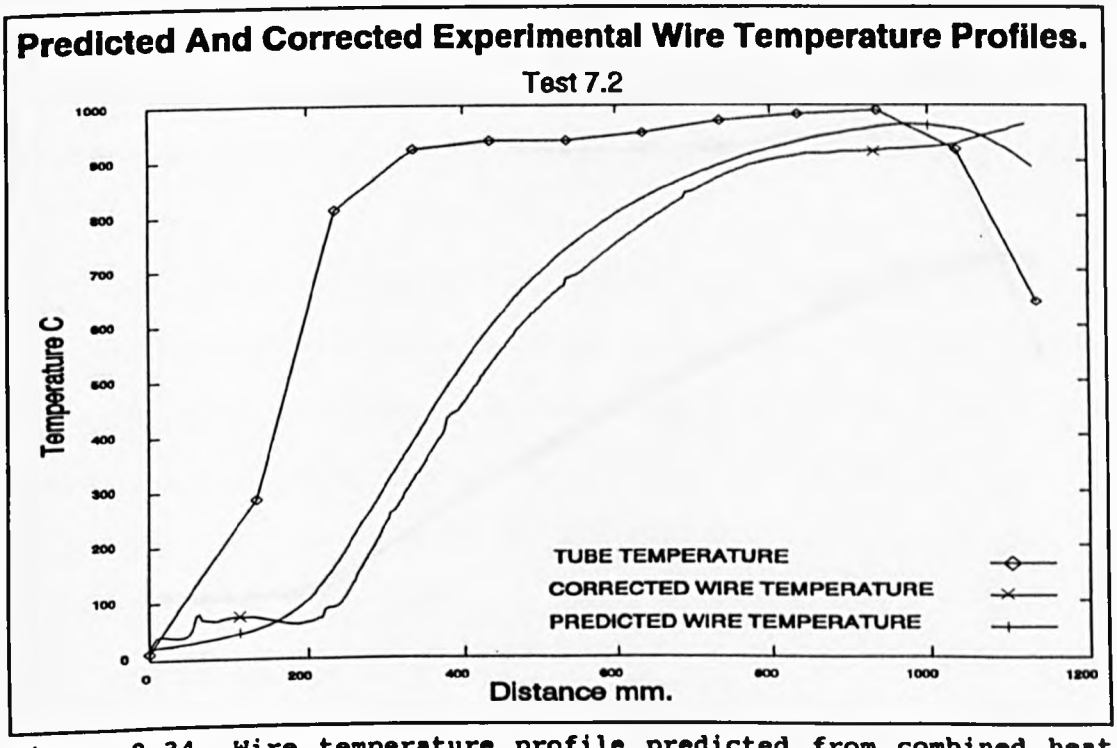

Figure 8-34. Wire temperature profile predicted from combined heat transfer for test 7.2

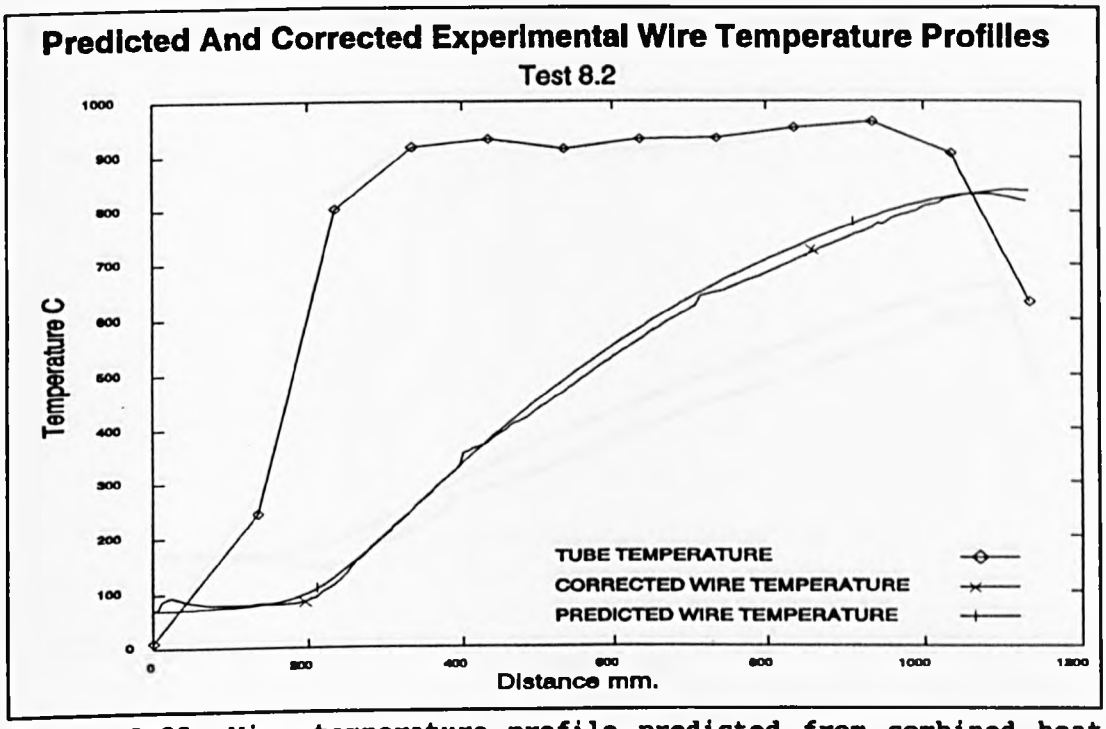

Figure 8-35. Wire temperature profile predicted from combined heat transfer for test 8.2

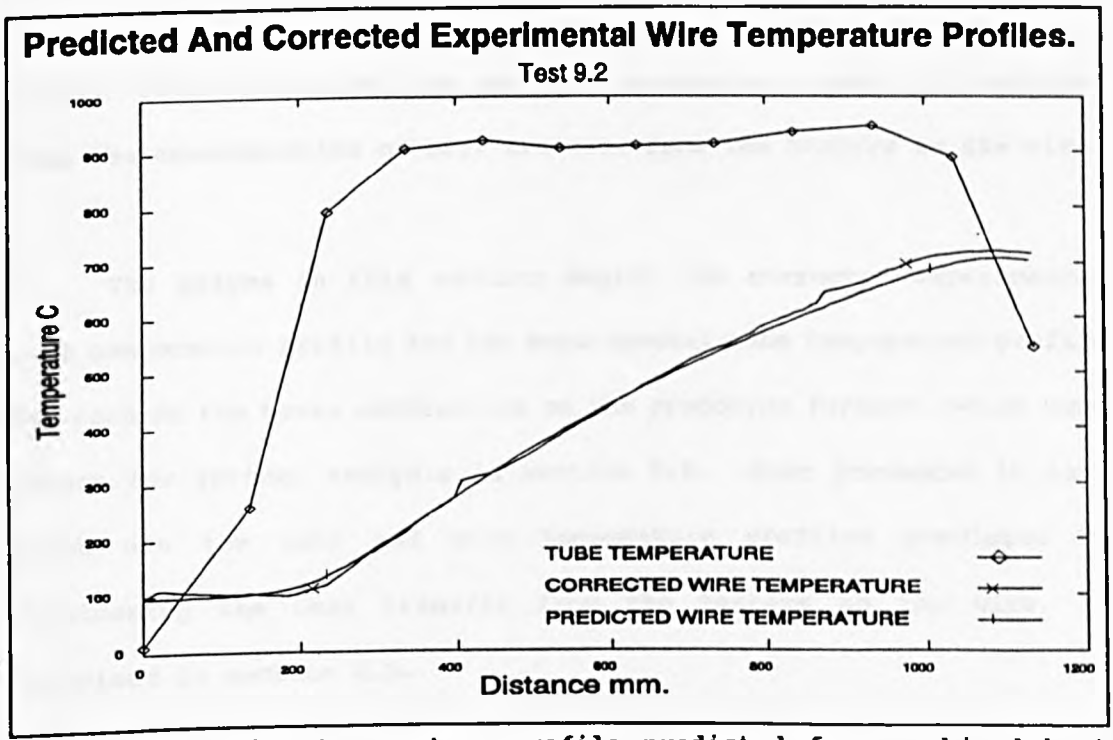

Figure 8-36. Wire temperature profile predicted from combined heat transfer for test 9.2

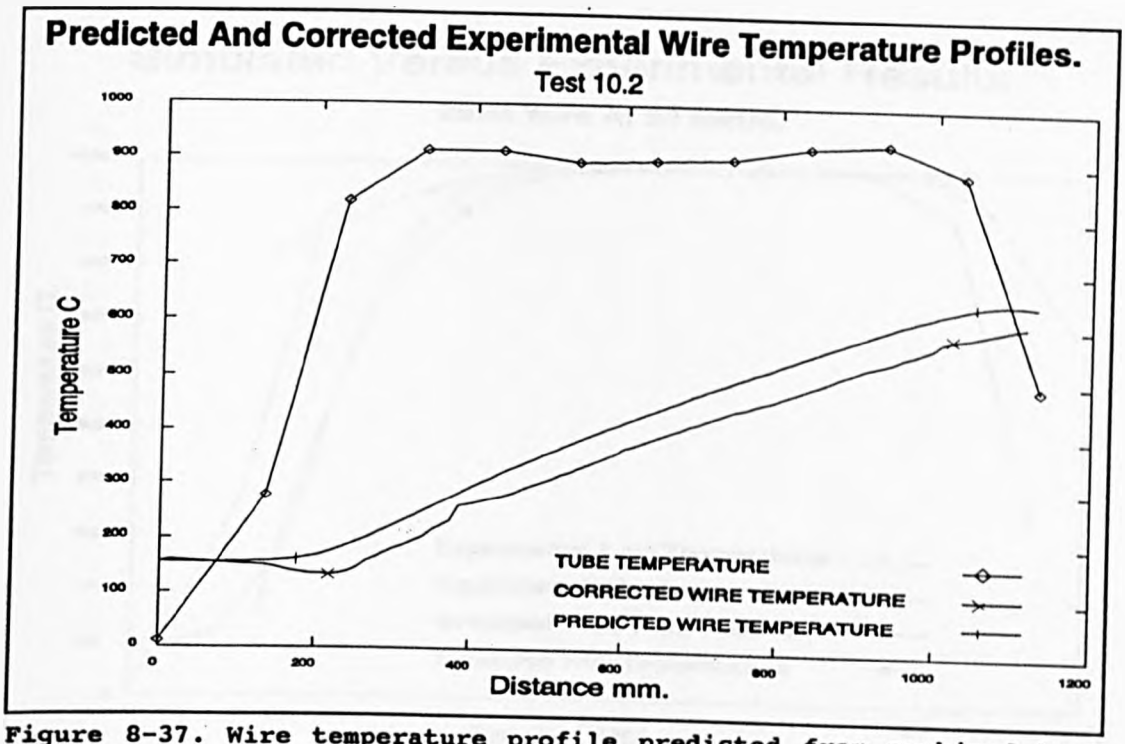

Figure 8-37. Wire temperature profile predicted from combined heat transfer for test 10.2

8.6.4. Presentation of wire and tube temperature profiles predicted from the consideration of heat transfer from the heaters to the wire.

The graphs in this section depict the corrected experimental wire temperature profile and the experimental tube temperature profile for each of the tests carried out on the prototype furnace, which were chosen for further analysis in section 7.5. Also presented in each graph are the tube and wire temperature profiles predicted by considering the heat transfer from the heaters to the wire, as described in section 8.5.

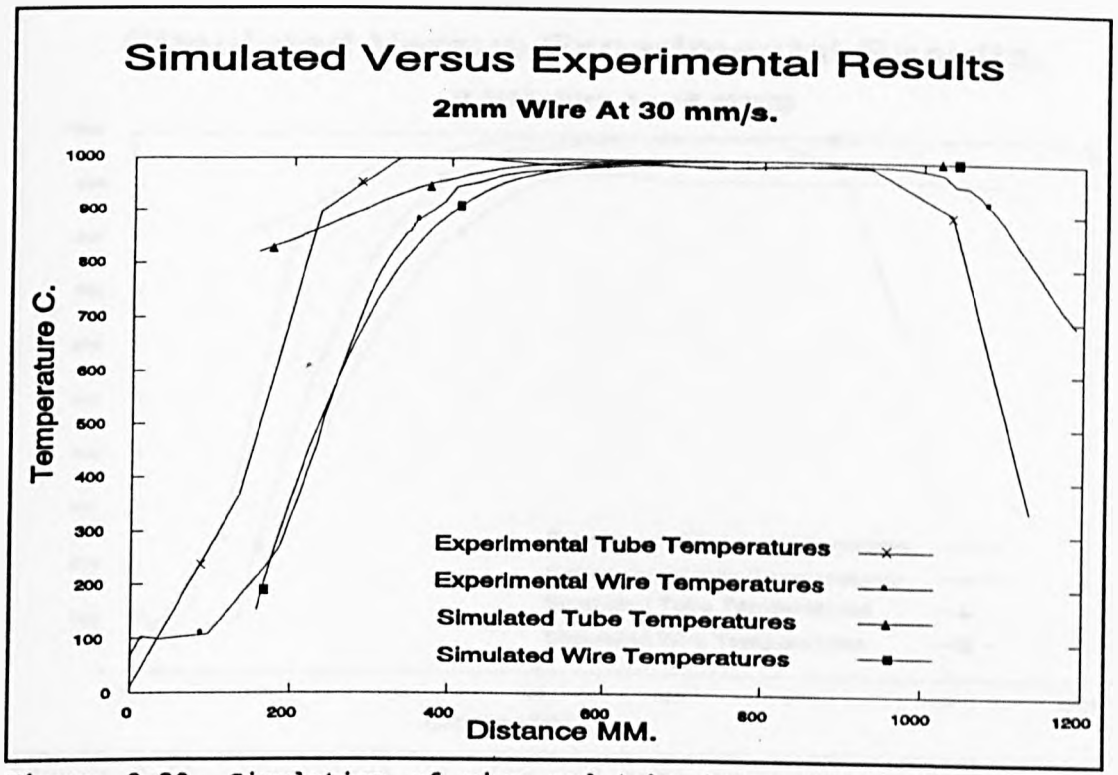

Figure 8-38. Simulation of wire and tube temperatures from heater temperatures of 1000°C compared with experimental results from test 1.1

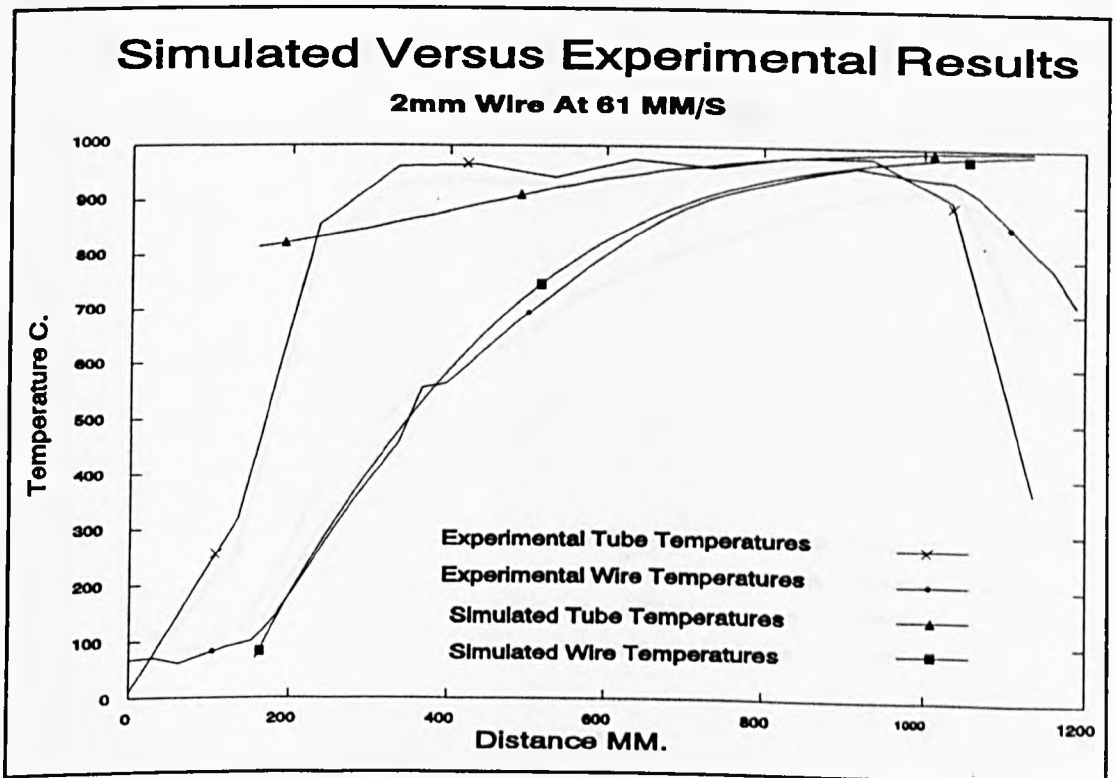

Figure 8-39. Simulation of wire and tube temperatures from heater temperatures of 1000°C compared with experimental results from test 2.1

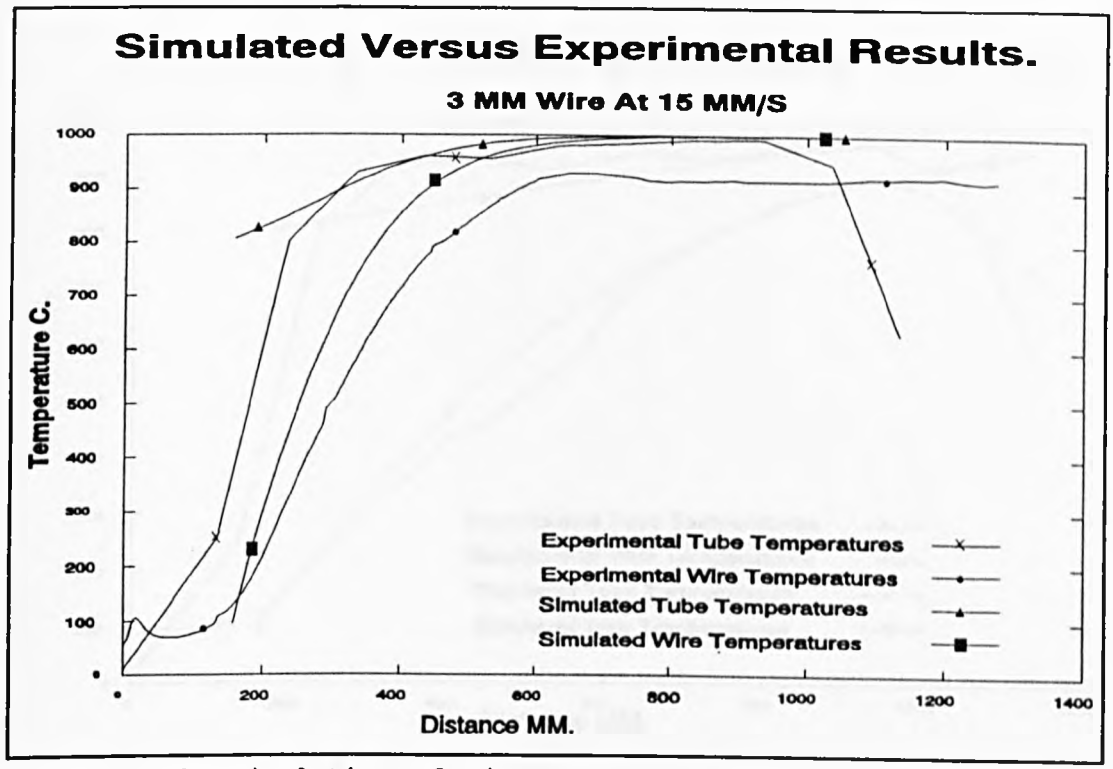

Figure 8-40. Simulation of wire and tube temperatures from heater temperatures of 1000°C compared with experimental results from test 3.2

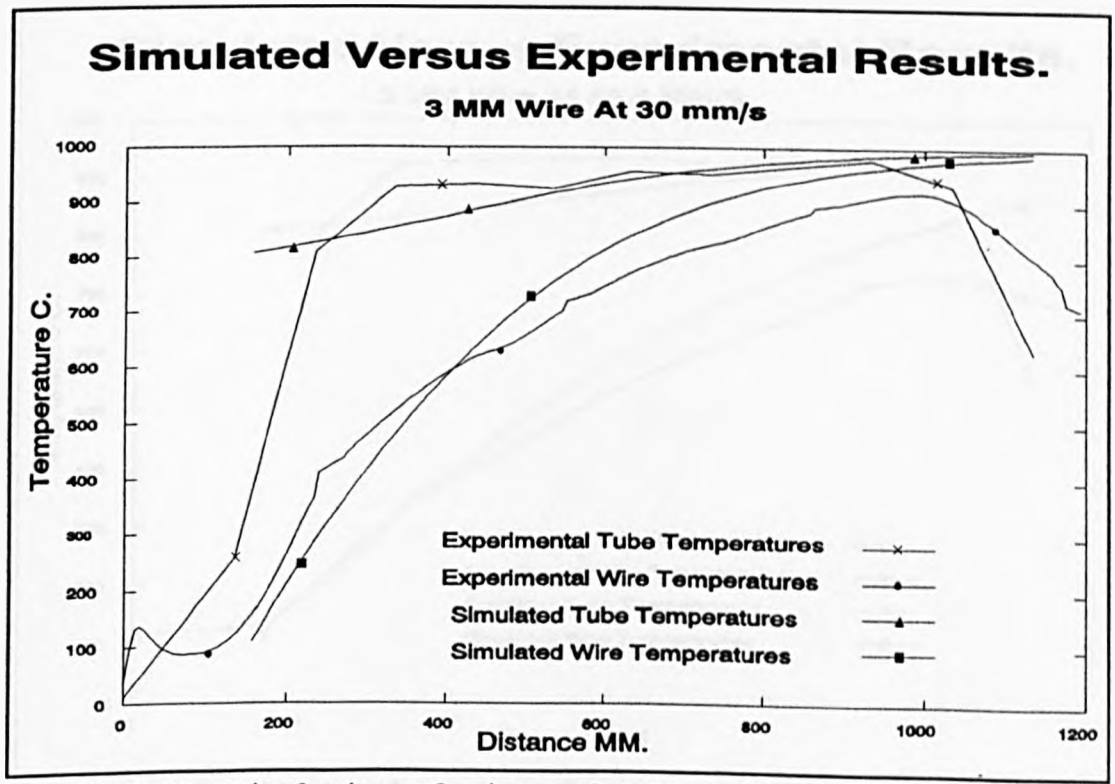

Figure 8-41. Simulation of wire and tube temperatures from heater temperatures of 1000°C compared with experimental results from test 4.3

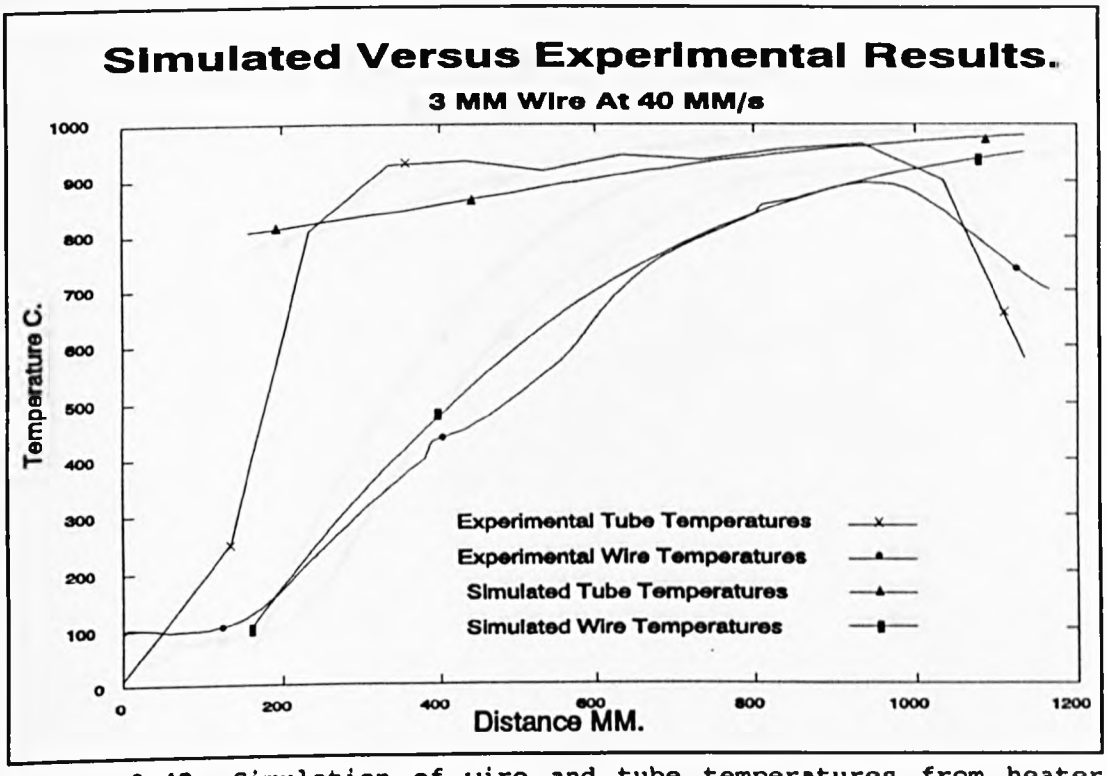

Figure 8-42. Simulation of wire and tube temperatures from heater temperatures of 1000°C compared with experimental results from test 5.2

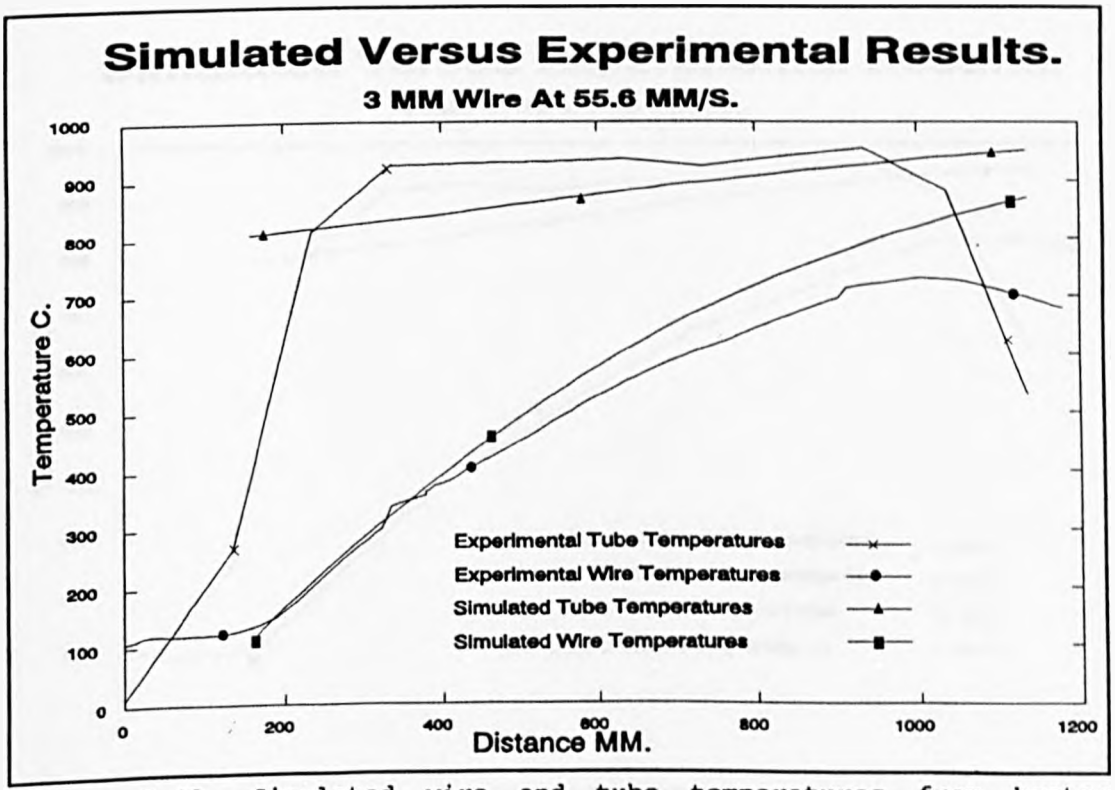

Figure 8-43. Simulated wire and tube temperatures from heater temperatures of 1000°C compared with experimental results from test 6.3

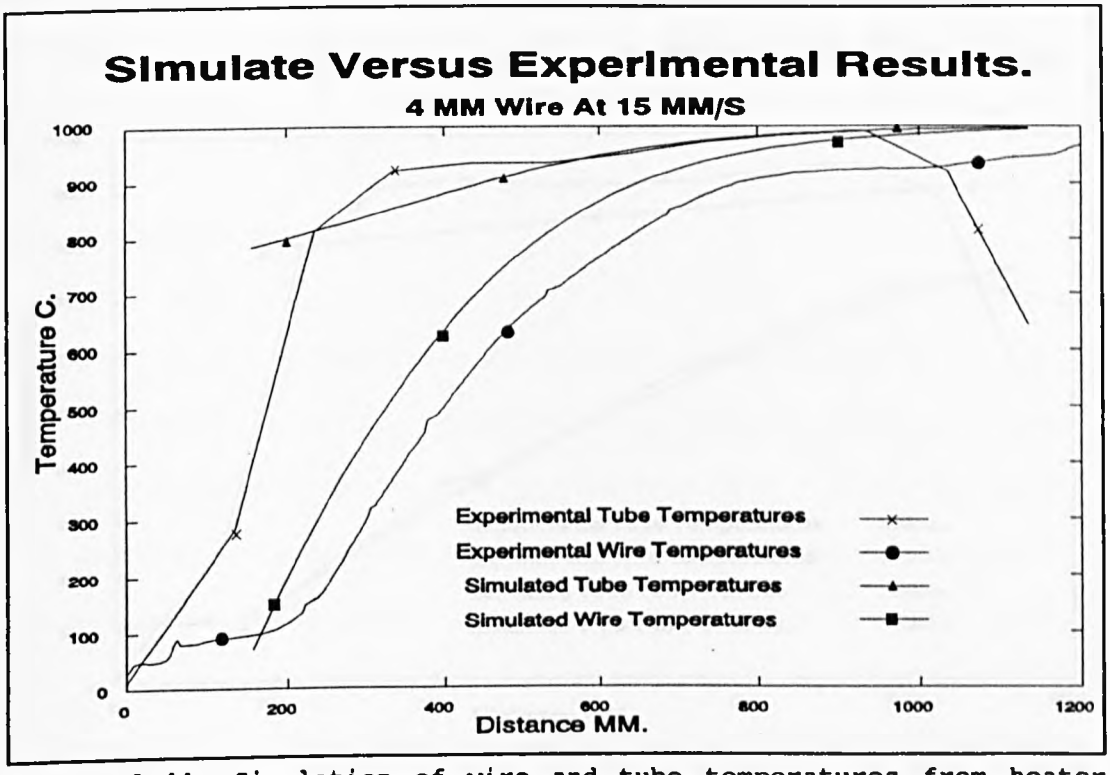

Figure 8-44. Simulation of wire and tube temperatures from heater temperatures of 1000°C compared with experimental results from test 7.2

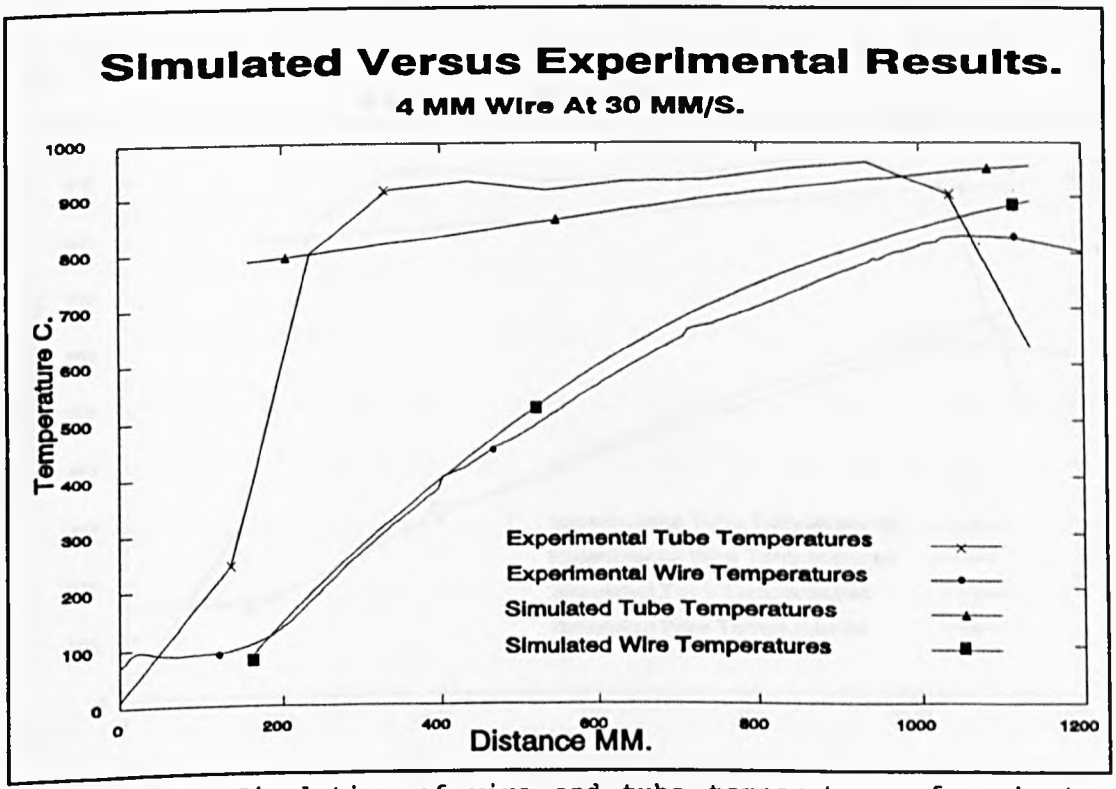

Figure 8-45. Simulation of wire and tube temperatures from heater temperatures of 1000°C compared with experimental results from test 8.2

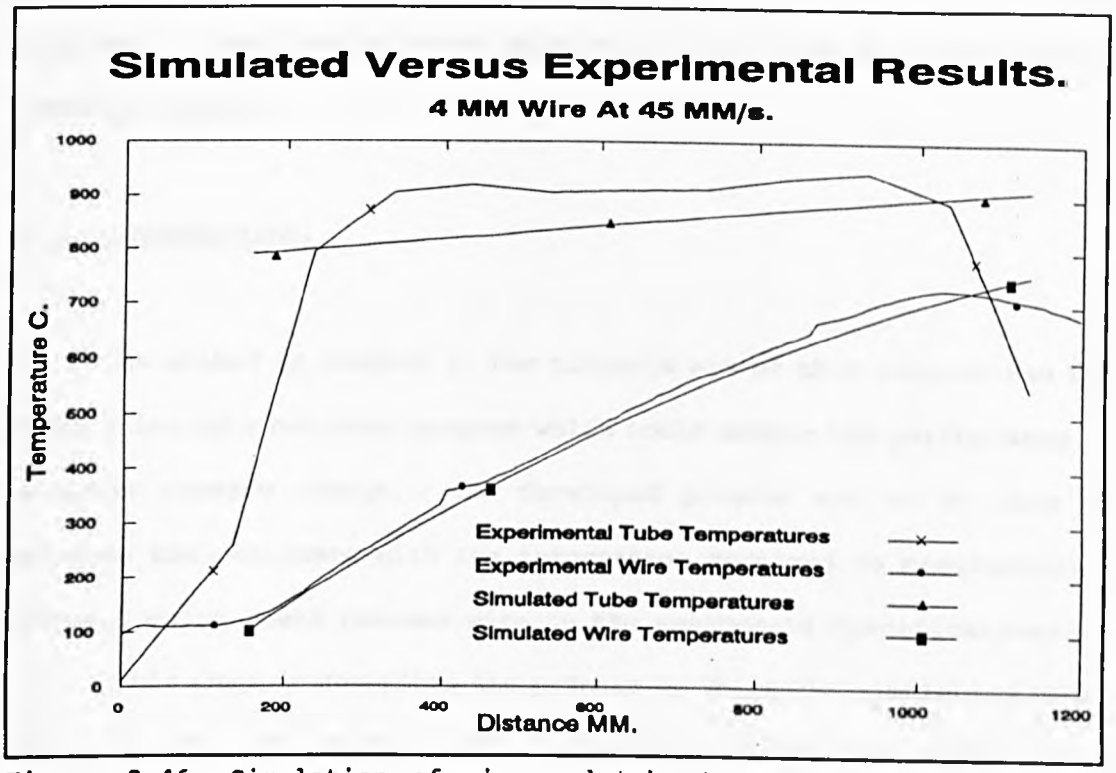

Figure 8-46. Simulation of wire and tube temperatures from heater temperatures of 1000°C compared with experimental results from test 9.2

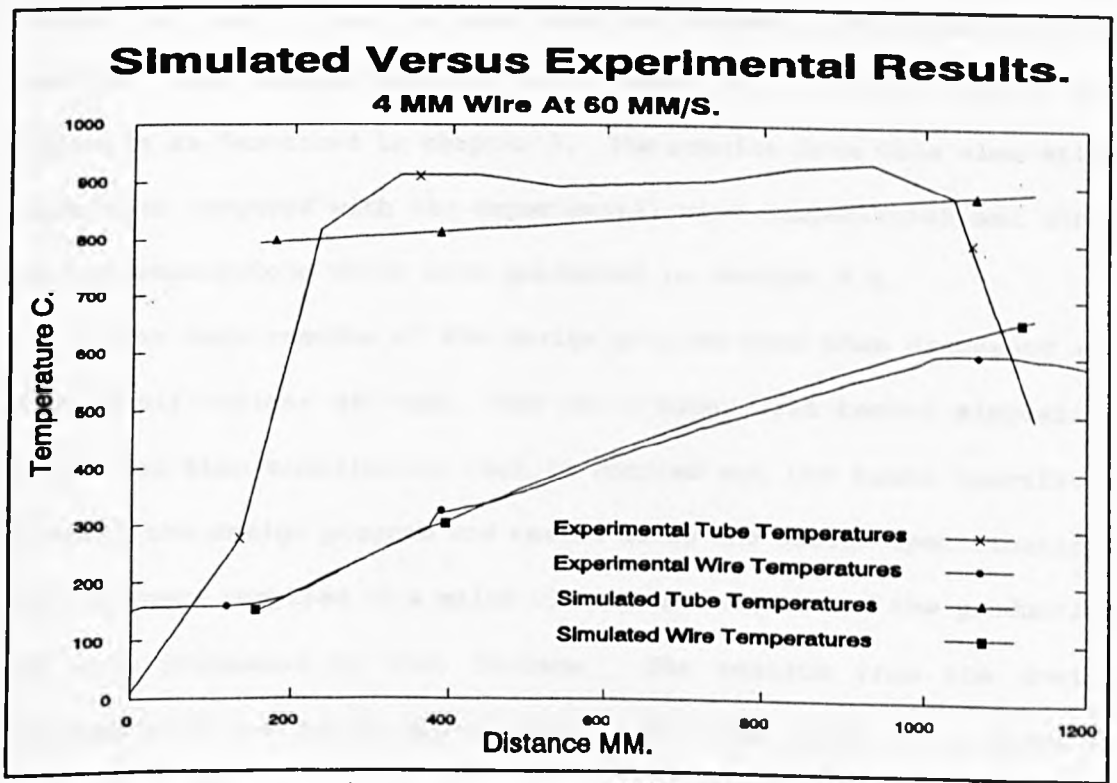

Figure 8-47. Simulation of wire and tube temperatures from heater temperatures of 1000°C compared with experimental results from test 10.2

CHAPTER 9. DEVELOPMENT OF THE PREDICTION MODEL INTO A TOOL FOR USE IN FURNACE DESIGN.

9.1 INTRODUCTION.

As stated in chapter 1, the ultimate aim of this project was the production of a computer program which could assess the performance of a given furnace design. The developed program was to be able to provide the designers with the information required to manufacture a furnace which could process wire to the customer's specifications.

This chapter describes the process by which the simulation model for a single tube furnace with cylindrical heaters was modified to simulate a multi-tube furnace with flat heater panels. The resulting model was tested using the wire data and furnace dimensions from the running test carried out on the furnace at Critchley, Sharp and Tetlow's as described in chapter 3. The results from this simulation were then compared with the experimental wire temperatures and zonal power consumptions which were presented in section 4.4.

The requirements of the design program were then discussed and the specifications set out. The multi-tube, flat heater simulation model was then modified so that it carried out the tasks specified. Finally the design program was tested using the design specifications of a furnace supplied to a major wire manufacturer, and the production of wire processed by that furnace. The results from the design program were then analyzed and compared with the actual performance of that furnace.

9.2 APPLICATION OF THE PREDICTION MODEL TO A FURNACE WITH MULTIPLE TUBES AND WITH FLAT TOP AND BOTTOM HEATER PANELS.

The majority of the wire annealing furnaces manufactured by Meltech are of the general form as described in chapter 1, part 3. The arrangement of the array of tubes is either that of a flat row, or two staggered rows as shown in figure (2-1), section 2.2. The prediction model devised in section 8.5 considered the heat transfer from cylindrical heaters to a single concentric process tube, and from that tube to the wire flowing through it. This model was then verified using experimental results as described in section 8.6. This section describes the modifications to the prediction model required for it to be able to predict the temperature profiles of the wires passing through a multi-tube furnace. Figure (2-1) in section 2.2 depicts two rows of tubes situated between two heater panels, and the dimensions given to the arrangement. The radiant heat transfer from the heaters to a tube on the top row was considered in chapter 2, and the designation of the exchange surfaces is illustrated in figure (2-4) in section 2.2. The radiant heat transfer from the two heaters (surface h) to the outside surface of a tube on the top row (surface to) may be given as,

$$Q_{h\text{-}to} = \frac{\sigma \cdot (T_h^4 - T_t^4)}{\frac{(1-\varepsilon_h(T_h))}{A_h \cdot \varepsilon_h(T_h)} + \frac{1}{A_h \cdot F_{h\text{-}to}} + \frac{(1-\varepsilon_{to}(T_t))}{\varepsilon_{to} \cdot A_{to}}} \qquad (9\text{-}1)$$

Where $F_{h\text{-}to}$ was the configuration factor from the exchange area on the two heaters to the exchange area on the outer surface of a tube on the top row, and is given by,

$$F_{h\text{-}to} = \frac{Z_{hA}\cdot F_{hA\text{-}to} + Z_{hB}\cdot F_{hB\text{-}to}}{Z_{hA}+Z_{hB}} \qquad (9\text{-}2)$$

Where $F_{hA\text{-}to}$ and $F_{hB\text{-}to}$ are the configuration factors from exchange areas on the top and bottom heaters respectively to the exchange area on a tube on the top row, which were found in section 2.2 to be given by,

$$F_{hA\text{-}to} = \left(\frac{r_{to}}{Z_{hA}}\right)\cdot\tan^{-1}\left(\frac{Z_{hA}}{a_1}\right) \qquad (9\text{-}3)$$

$$F_{hB\text{-}to} = \left(\frac{r_{to}}{Z_{hB}}\right)\cdot\tan^{-1}\left(\frac{Z_{hB}}{2\cdot a_2}\right) \qquad (9\text{-}4)$$

The variables Z_{hA} and Z_{hB} are the width of the areas on the top and bottom heaters respectively which exchange heat with a tube on the top row and were found in section 2.2. The area of the heaters which exchanges heat with the tube was found in section 2.2 to be given by,

$$A_1 = 2\cdot(Z_{hA}+Z_{hB})\cdot dX \qquad (9\text{-}5)$$

Equation (9-1) considers the radiant heat transfer between the heaters and a single tube on the top row. Due to the symmetry of the arrangement, the configuration factors and exchange areas were considered to be identical for heat transfer to a tube on the bottom row.

The exchange of heat between the top and bottom heaters was considered to be negligible as the temperature differential between them was relatively small compared with that between the heaters and the tubes. It was also assumed that there was no heat exchanged between one process tube and any of the other process tubes in the system. This was due to the fact that the process tubes were all at approximately the same temperature, and also because the configuration factor from one tube to another was minimal compared with that from the heaters to a tube.

The heat transfer coefficient for radiation from the heaters to a tube was found using equation (9-1) to be,

$$H_{ht} = \frac{A_h \cdot \sigma \cdot (T_h^2+T_t^2) \cdot (T_h+T_t)}{\left(\frac{1}{\varepsilon_h(T_h)}-1\right) + \left(\frac{1}{F_{h-to}}\right) + \frac{A_h}{A_{to}}\left(\frac{1}{\varepsilon_{to}(T_t)}-1\right)} \qquad (9\text{-}6)$$

Therefore the radiant heat transfer from the heaters at temperature T_h (K) to a given tube at temperature T_t (K) was determined by,

$$Q_{h-t} = H_{ht} \cdot (T_h - T_t) \qquad (9\text{-}7)$$

The computer program devised in section 8.5 was then modified so that the radiation was calculated from flat heater panels at local temperature $T_h(X)$ to a tube at local temperature $T_t(X)$. This was carried out by using equations (9-2) to (9-7) to calculate the radiant heat transferred to the tube from the heaters instead of the original equations, (8-14) to (8-27).

Having done this, the computer program could be modified so that it calculated the heat transfer from the heaters to each tube in the furnace, and from each tube to the wire passing through it.

In order to calculate the configuration factors and exchange areas, the dimensions of the furnace and the tubes were required as in figure (9-1). Following this the number of heating zones (NZ), and their length (LZ) was required, as well as the number of process tubes (NT). Finally the material, diameter, process speed and initial temperature of the wire passing through each of the tubes was required. The program then calculated the heat transfer to each of the wires from the heaters at their initial temperatures at the start of heater zone 1 in the same manner as described in section 8.5. The temperature rise of each of the wires over the elemental length dX was then calculated as before to provide the initial temperatures of the wires at the next position along zone 1.

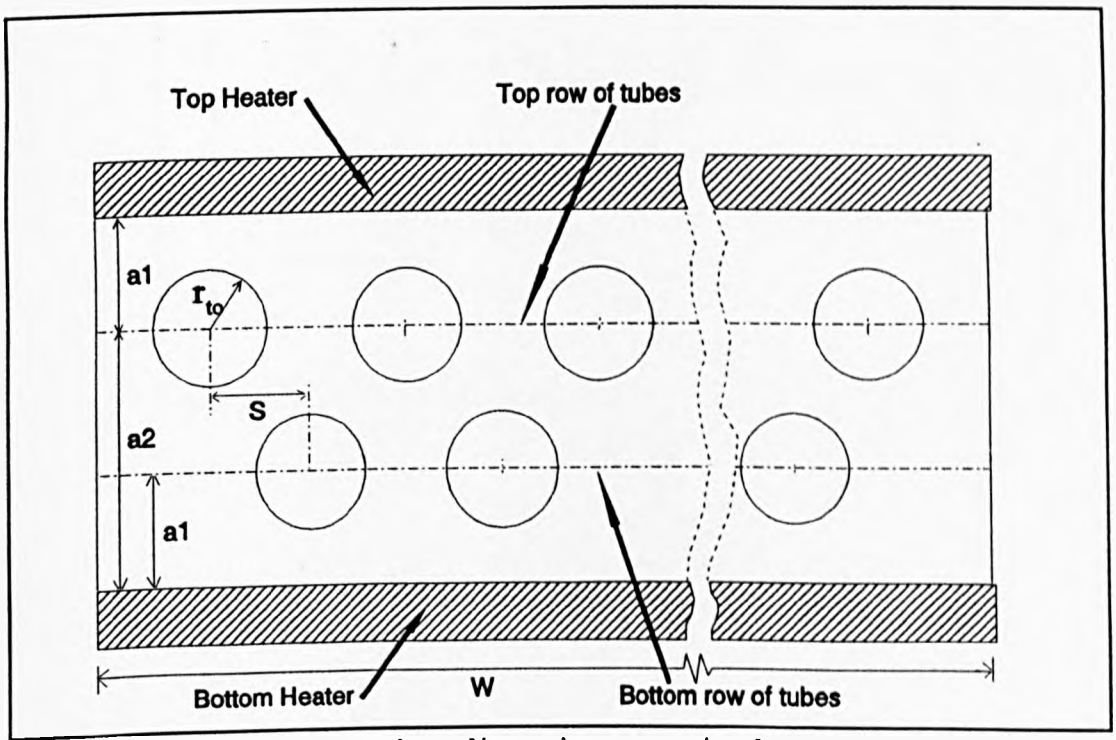

Figure 9-1. Furnace chamber dimensions required.

This was continued in order to provide temperature profiles for all the wires as they progressed along zone one, summating the heat transfers occurring to provide the total for that zone. If the total heat transfer from a given zone exceeded the maximum power rating of the heaters in that zone, then the heat transfers were re-calculated as described in equations (8-30) and (8-31) in section (8.5). The heat transfers in the next zone along the furnace were then calculated in the same manner. This was repeated for all the heater zones of the furnace whose performance was being predicted. Figure (9-2) overleaf illustrates the basic algorithm used in this program.

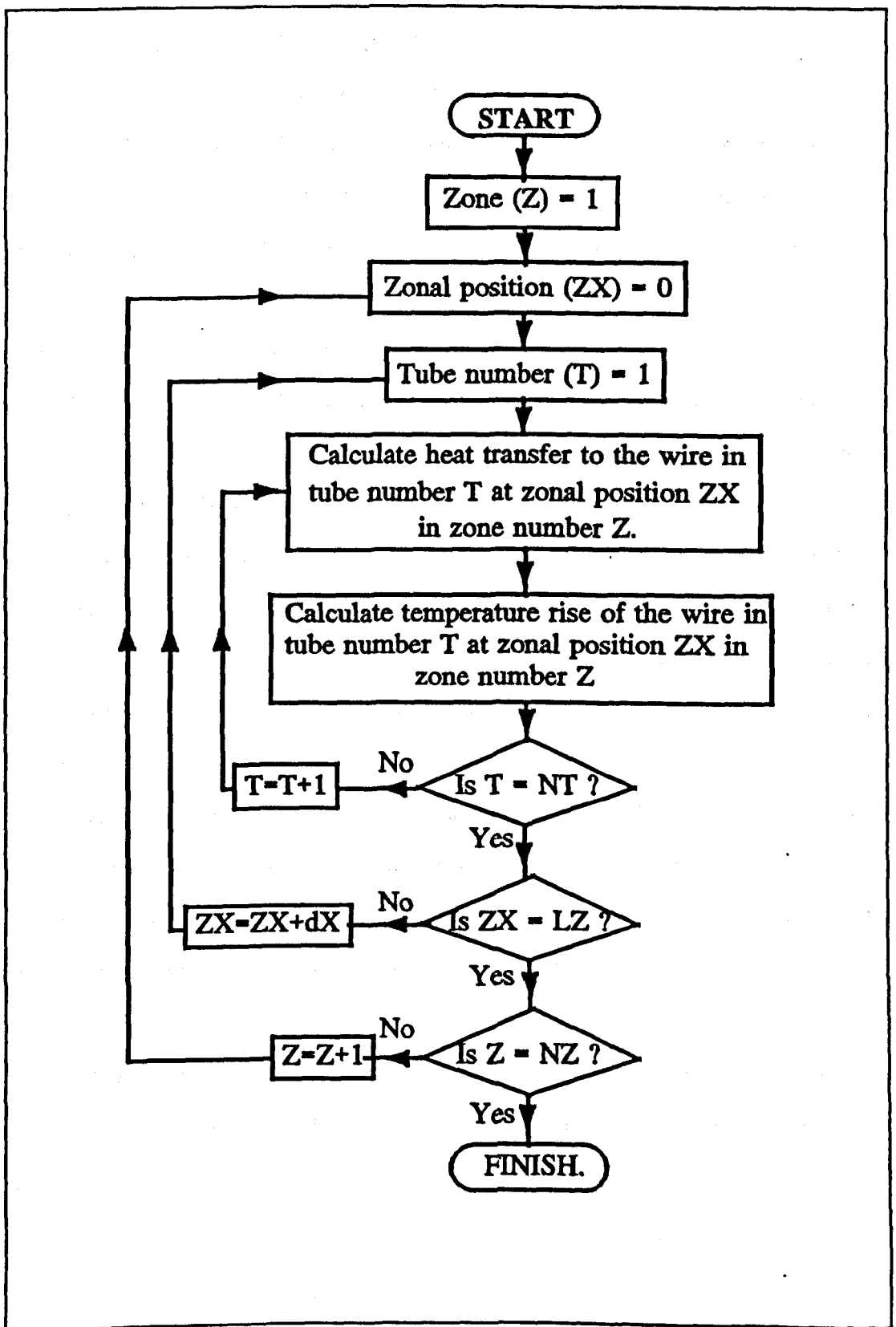

Figure 9-2. Basic algorithm used to calculate the temperature profile of wires passing through a multi-tube furnace.

9.3 PREDICTION OF WIRE TEMPERATURES AND ZONAL POWERS FOR THE CRITCHLEY, SHARP AND TETLOW FURNACE.

The computer program outlined in the previous section was written in 'FORTRAN' programming language using the 'Prospero' compiler on a personal computer. In order to test the algorithms used and the code written, the program was run using the dimensions and production data of a furnace the performance of which had been investigated. The furnace in question was number four furnace at Critchley, Sharp and Tetlow, which is described in section 3.1. The dimensions of the furnace which were required for the prediction model are given in table (9-1) overleaf.

Each of the heating zones had a maximum rating of 6.4 Kilowatts, and the set temperature of the zones were as in table (9-2) overleaf. The material, diameter and speed recorded during the running test for the wire in each of the process tubes is shown in table (D-6) in appendix D.

The properties used were the same as those used for the predictions in the previous section, except for the emissivity of the heater panels, which was found from [7] to be approximately 0.15 throughout the temperature range being used.

The wire and furnace data was then supplied to the prediction program, the results from which are presented in the following section.

Table 9-1. Dimensions of the 'Critchley' furnace which were required for the simulation model.

Number of process tubes. (NT)	19
Number of heating zones. (NZ)	12
Length of each heating zone in mm. (LZ)	418
Width of each heating zone in mm.	660
Height between top and bottom heaters in mm. (a_1+a_2)	124
Distance between axes of the top and bottom rows of tubes in mm. (a_2-a_1)	36
Internal diameter of process tubes in mm (D_{ti})	16
External diameter of process tubes in mm (D_{to})	25

Table 9-2. Set temperatures of the 12 heating zones on the 'Critchley' furnace.

Zone Number.	1	2	3	4	5,6	7-12
Set temperature (K)	970	1122	1240	1272	1322	1323

9.4 PRESENTATION OF AND DISCUSSION OF THE PREDICTED RESULTS FOR THE 'CRITCHLEY' FURNACE.

The wire and furnace data presented in the previous section was used in the simulation program discussed in section 9.2 to predict the temperature profile of each wire as it passed through the furnace, and the power consumed by each zone. As can be seen from table (D-6) in Appendix D, three sizes of wire were being processed in the furnace at the time that the running test was being carried out. The predicted wire temperatures at the end of each zone for wire sizes of 1.22, 1.7 and 2.13 mm are illustrated in the graphs in figures (9-3), (9-4) and (9-5) respectively. Illustrated on the same graphs are the temperatures measured in tubes with the same size wire flowing in them, as presented in appendix D, tables (D-5.1) to (D-5.3).

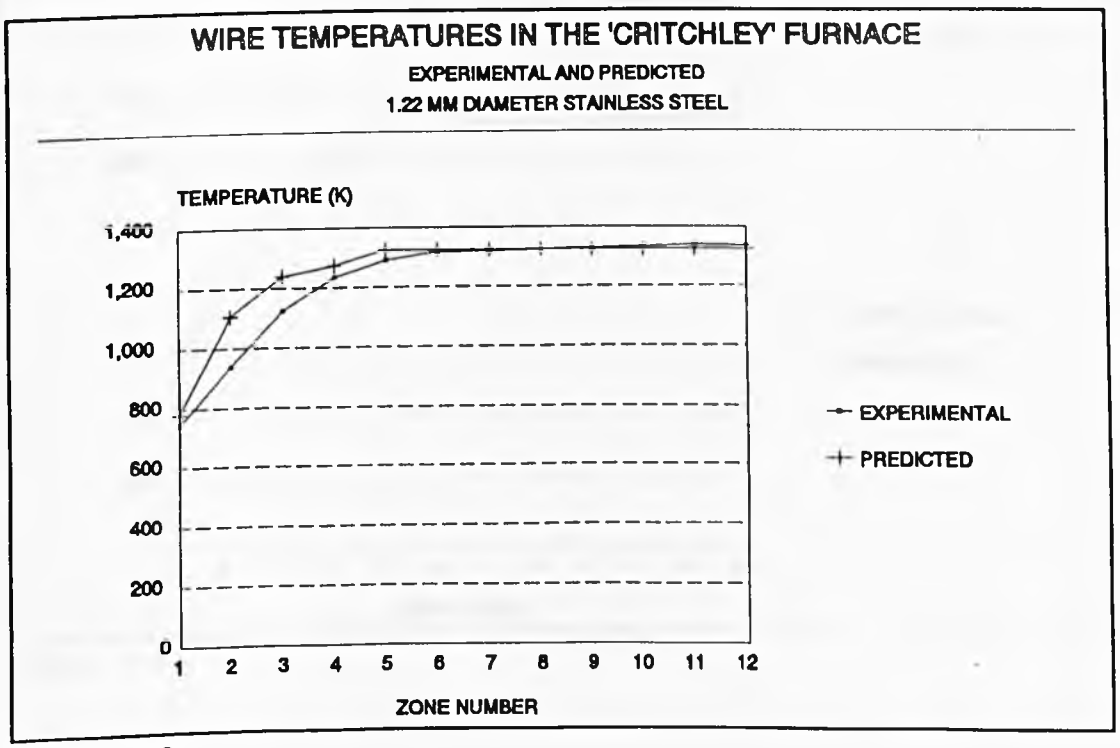

Figure 9-3.

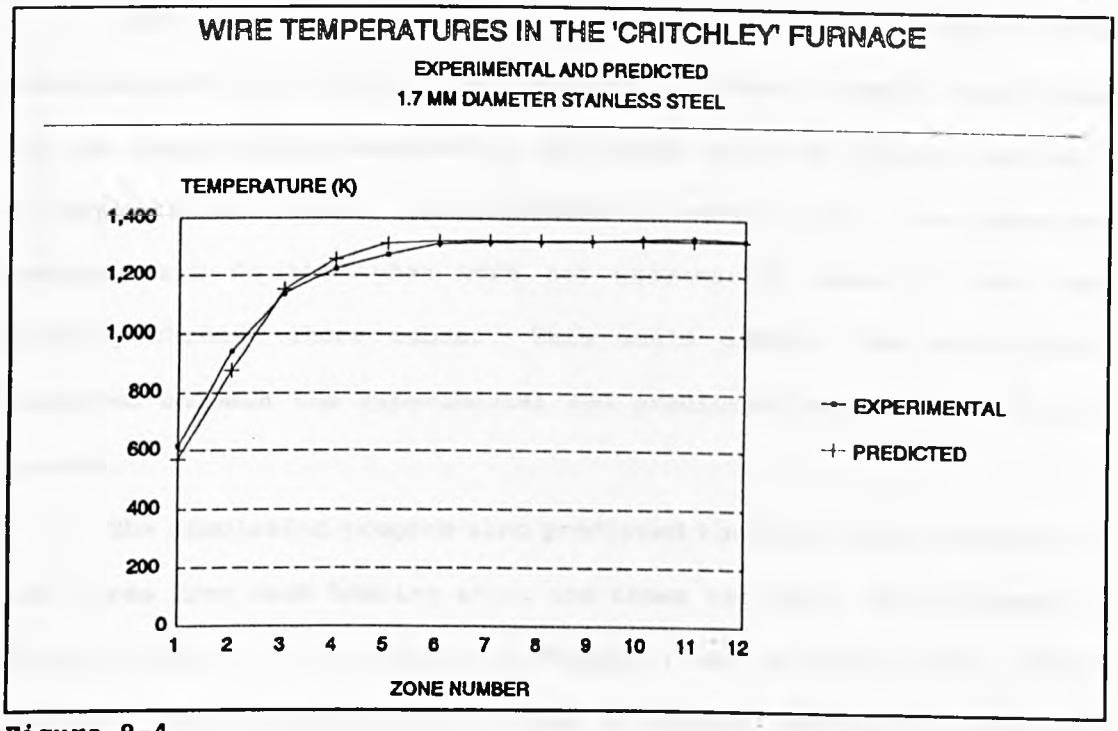

Figure 9-4.

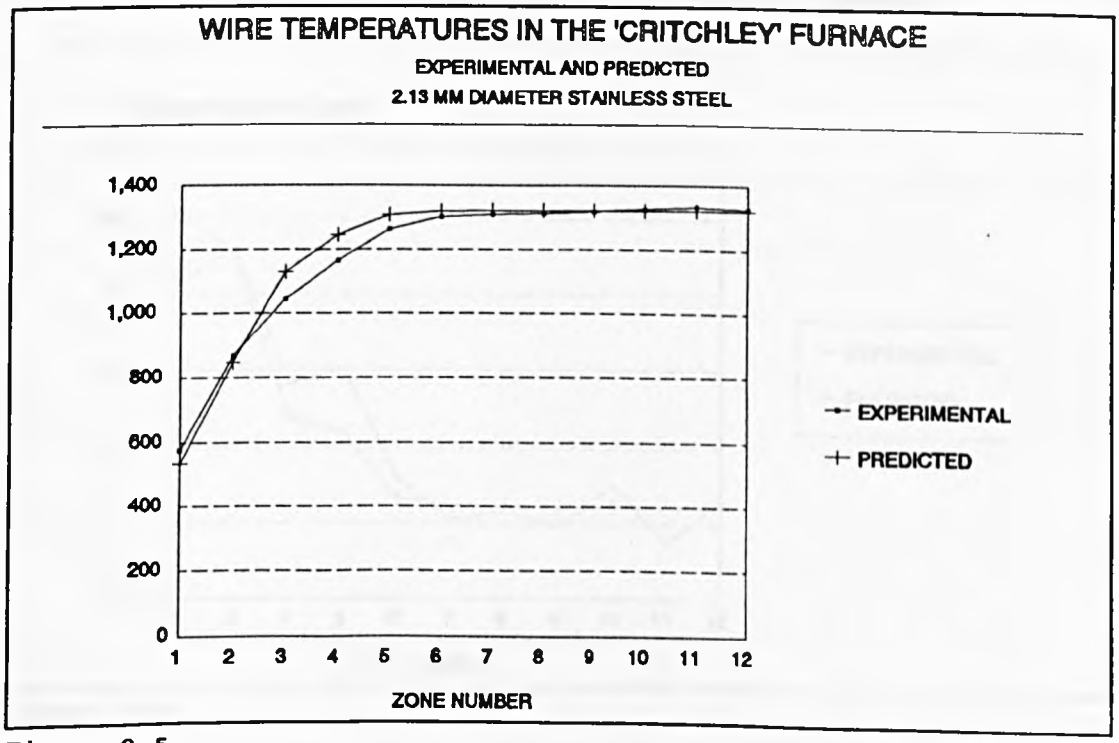

Figure 9-5.

The predicted temperature profiles of the three sizes of wire were observed from figures (9-3) to (9-5) to have a very similar shape to the temperatures measured in the tubes with the appropriate wire flowing through them. As discussed in section 4.6, the measured temperatures in the tubes were not necessarily those of the wire passing through those tubes. This would explain the differences observed between the experimental and predicted temperatures in the graphs.

The simulation program also predicted the total heat transfer to the wires from each heating zone, and these are shown in the graph in figure (9-6). Also plotted in figure (9-6) are the zonal powers measured for the running test on the 'Critchley' furnace as presented in Appendix D, table (D-8.4).

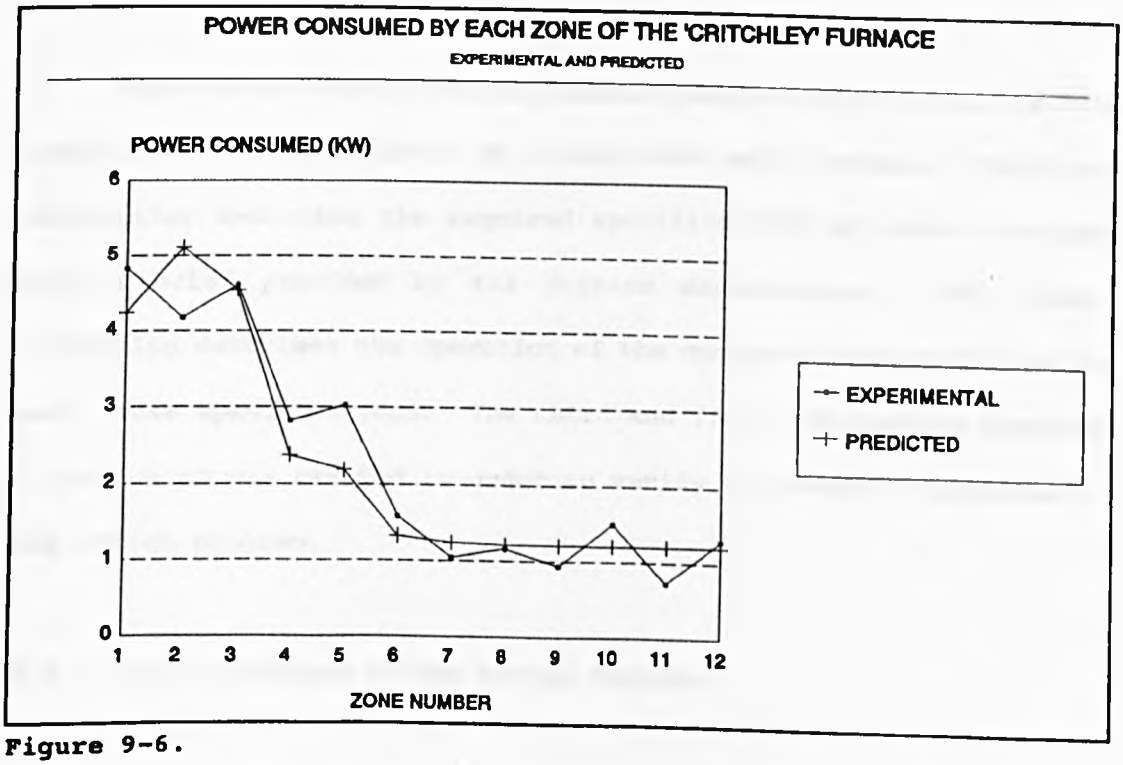

Figure 9-6.

The powers which were predicted for each zone were observed to decrease in the same manner as the measured powers as the wire temperature increased.

The powers measured to be consumed by each heating zone were observed for some zones to be different to the predicted results. This was considered to be due to the fact that there was some error involved in the reading of the Kilowatt-hour meters, as described in section 4.6.

Overall the simulation model was considered to have predicted successfully the performance of the 'Critchley' furnace when compared with the experimental results from a 'running' test on that furnace.

9.5 DISCUSSION AND TESTING OF THE DESIGN TOOL DEVELOPED.

9.5.1 Introduction.

This section describes the computer program which was written to speed up the design process of a multi-tube wire furnace. The first sub-section describes the required specifications of such a program from a brief provided by the furnace manufacturer. The second subsection describes the operation of the computer program devised to meet these specifications. The third and final sub-section contains a test which was carried in order to verify the results furnished by the design program.

9.5.2 Specifications Of The Design Program.

The specification of the design tool was basically to provide a feasible design of a multi-tube wire furnace which would fulfil all the customer's requirements.

When a wire manufacturer expresses an interest in the purchase of a wire annealing furnace, the furnace manufacturer requests from them a list of their requirements for the furnace. The requested requirements are as follows,

- **Material and size of wire to be processed.** The customer may require one or more types of wire to be processed on the furnace at any one time, therefore the diameter and material of each type of wire are requested.

- **Processing rate of each type of wire.** The amounts of each type of wire in tonnes that the customer wants to process each year are requested.

- **Process time, production time and actual utilisation of the furnace.** The process time of the furnace is the number of weeks per year that the furnace would be operational. This is dependent upon public holidays, company holidays and any other times when the factory would be closed.

The production time is the number of hours per week that the factory works, and is mainly dependent upon the number of shifts worked and the amount of overtime normally worked at the factory.

Finally, the actual utilisation of the furnace is the period of time during which wire is actually being processed in the furnace. This is determined by the maintenance requirements of the furnace and all its auxiliary machinery, and is normally given either in hours per week, or as a percentage of the production time.

This data provides the number of hours per year during which the furnace is actually able to process wire. Knowledge of this and the processing rate of the wire provides the hourly production requirements for each type of wire.

- **Maximum and minimum wire speeds.** The maximum and minimum speeds at which a type of wire can be processed are requested. These depend upon both the material and diameter of the wire, and the equipment available for winding the wire through the furnace and onto a spool.

- **Process temperature and in-furnace soak time.** The amount of annealing of a type of wire is determined by the temperature attained by the wire and the time for which it is maintained at that temperature. The annealing temperature and soak time is requested for each type of wire to be processed.

- **Process atmosphere.** The customer is asked whether a process gas is required, and if so what type of gas and its required flow rate per tube.

- **Maximum number of process tubes.** The maximum number of process tubes which the customer specifies depends upon the maximum number of 'ends' of wire which may be processed in the furnace at any one time. The number of ends is determined by the capacity of the wire winding machinery in the customer's factory.

• **Diameter and material of process tubes.** The internal diameter and material of the process tubes in the furnace are determined by the diameter and material of the types of wire to be processed. Inconel tubing is used in the majority of furnaces where stainless steel wire is being processed, however precious metals such as platinum require ceramic tubes to be used.

• **Any other features.** The customer is also asked if there are any other features required, such as wire cleaning or cooling equipment. In addition to this, there may be certain limitations on the design of the furnace, such as limited length of the furnace or limited electrical power supply.

The basic task of the computer program which comprised the design tool was to specify whether a particular design of furnace would satisfy the above requirements by simulating the furnaces performance. Having determined this, an optimum design of the furnace can be produced.

9.5.3 Description Of The Design Program.

This section describes the operation of the computer program written to provide a furnace design tool. The flow diagram in figure (9-7) illustrates the step-by-step process by which the program was used to determine an optimum design for a multi-tube furnace. The following numbered paragraphs describe in more detail the operation of the appropriate section of the design program.

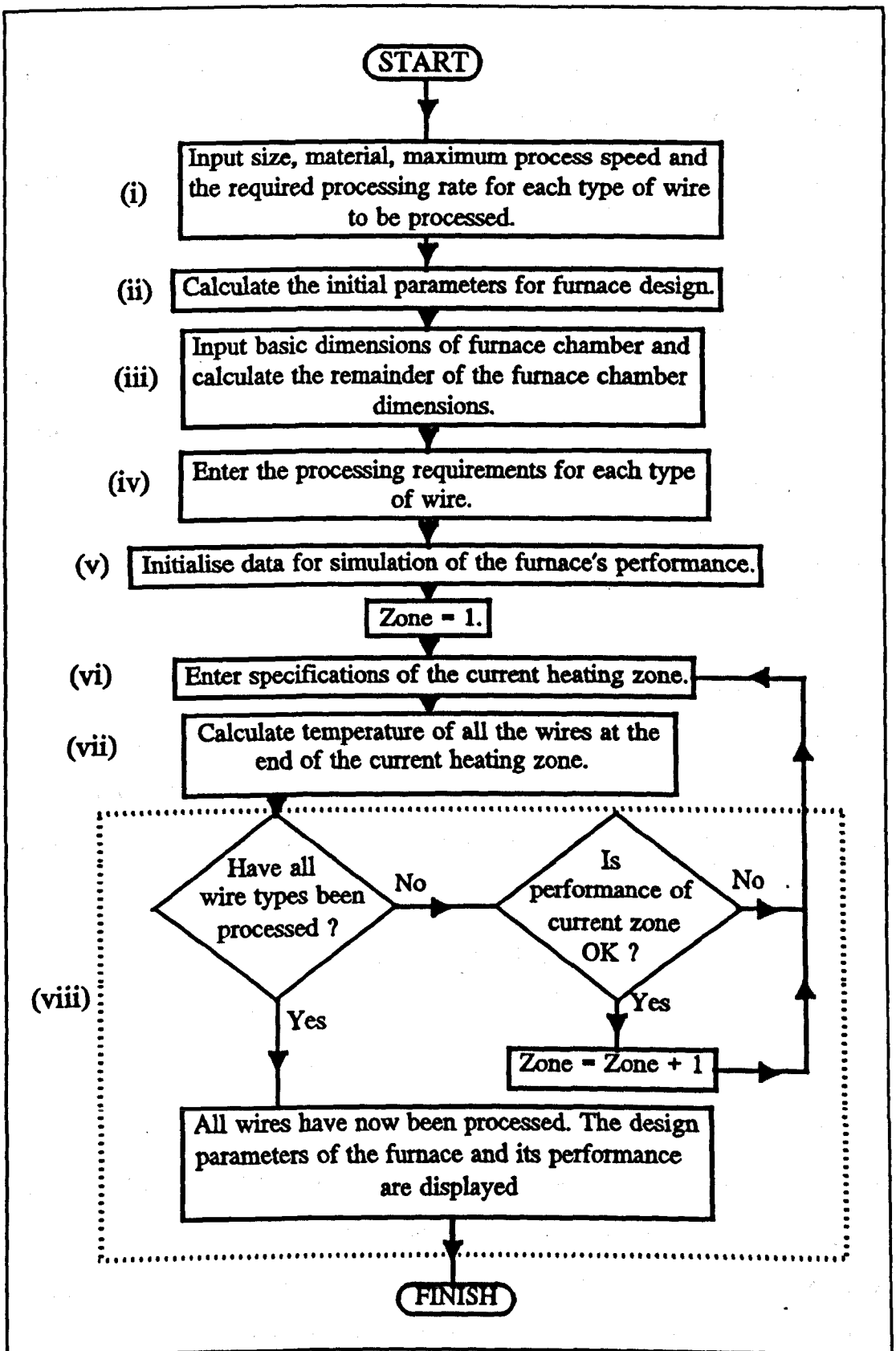

Figure 9-7. Flow diagram illustrating the operation of the design program.

(i) This section required the input of the number of types of wire (NTW) to be processed. The diameter (D_w) in meters, material number (MAT_w), processing rate (MF_w) in Kg per hour, and maximum wire speed (S_{max}) for each type of wire were then input.

(ii) The initial design parameters of the furnace were calculated in this section. The first parameter required was the minimum numbers of tubes required for the processing of each type of wire. These were found by determination of the maximum mass flow rate in Kg per hour of a given wire type through a single tube as follows,

$$MF_{max}(I) = \frac{\pi \cdot D_w(I)^2}{4} \cdot \rho_w(I) \cdot S_{max}(I) \qquad (9\text{-}8)$$

Where $\rho_w(I)$ is the density in Kg/M^3 of the material of wire type I at room temperature. The minimum number of tubes required for the desired total mass flow rate of wire type 'I' was therefore given by rounding the result of the following expression up to the nearest integer.

$$NT(I) = \frac{MF_w(I)}{MF_{max}(I)}$$

If this number exceeded the maximum number of tubes available for wire type I, then the required mass flow rate of wire type I would have to be decreased, or the capacity of the wire winding equipment increased accordingly. The total number of tubes for the furnace (NTT) could then be chosen either from the total of the minimum numbers of tubes for each wire type, or from the number of wire winding 'ends' available.

(iii) This section involved the calculation of the basic parameters for the design of the furnace chamber. The width W of the furnace chamber was determined by both the number of process tubes, and the standard widths of heater panels available. The minimum width ,W_{min} of the chamber was determined as follows,

$$W_{min} = 1.2 \cdot NTT \cdot D_t$$

Therefore the chosen width of the heater had to be greater than this value. The arrangement of the tubes in the furnace was considered to be that of equally spaced tubes, either in a single row or two staggered rows, situated centrally between the top and bottom of the furnace chamber. The two row arrangement is depicted in figure (9-1) in section 9.2. The spacing S between the axes of two adjacent tubes either on the same row for a single row arrangement, or on two rows for a two row arrangement, was determined using the following expression.

$$S = \frac{W}{NTT+1}$$

Where S, W and NTT are as described as above. The height (a_1+a_2) was then entered, along with the distance between the two rows of tubes (a_2-a_1). If a single row of tubes was being considered, then the distance between the rows (a_2-a_1) was given a value of zero. The configuration factors and the exchange areas for use in calculating radiant heat transfer from the heaters to one of the tubes were then determined using equations (9-2) to (9-5).

(iv) This section requires the entry of the process temperature and the soak time for each of the wire types being processed.

(v) The purpose of this section was to define the type, the speed and the properties of, the wire flowing in each of the process tubes. The heating zone length (LZ) was considered to be the same for all of the zones, and was input in this section, along with the maximum length of the furnace. Thus the maximum permissable number of heating zones was calculated, and the user was prompted to enter the number of zones (NZ), the value of which could not exceed this maximum. Finally the number of elemental calculations to be carried out in each zone (NI) was entered, and the elemental length (dX) was then calculated as follows,

$$dX = \frac{LZ}{NI}$$

(vi) This section required the input of the specifications of the current heating zone. These specifications comprised the set temperature of that zone, the maximum power rating of the heaters in that zone, and the estimated efficiency of that zone.

(vii) This section calculated the heat transfer to each of the wires, and the temperature profiles of each of the wires as they passed through the current heating zone. This process was carried out using the simulation program described in the previous section (9.2).

(viii) The purpose of this section of the design program was to check whether all the wires being processed had undergone their required heat treatment by the end of the current heating zone. This was determined by whether or not all the wires had been soaked at their process for the required periods of time.

If this was found to be so, then a message was displayed to that effect, and the number of heating zones and the total power required to attain full heat treatment was displayed. If heat treatment of all the wires had not been achieved, then the user is asked if the performance of the current zone in heating the wires was satisfactory. If this was not so, then the specifications of that zone were modified by returning to section (vi) of the program, and the performance of that zone was simulated again, using these new specifications. Once the performance of the current zone was considered by the user to be satisfactory, then providing that the number of heating zones analyzed thus far was less than the maximum number of zones, the next zone could be analyzed.

If the simulation had reached the end of the last permissable zone, and all the wires were not fully heat treated as specified, then it was not possible to process the given capacity of wire in a furnace of the specified design. Therefore the program returned to section (iii) so that new furnace dimensions could be entered, and the design process repeated.

The computer program which carried out the functions described in the preceding paragraphs was written on a Personal Computer using the 'Prospero FORTRAN' editor. The program was then compiled using the Prospero FORTRAN' compiler, and may be used on any IBM compatible PC running with the DOS operating system.

9.5.4 Testing Of The Design Tool.

In order to ascertain the effectiveness of the design tool, a set of customer requirements for a multi-tube wire annealing furnace were obtained from the furnace manufacturer. These requirements are listed in table (9-3) below.

Table 9-3. Customer requirements used for testing the design tool.

Wire size (mm)	1.2
Wire material	Austenitic stainless steel
Required production rate (Kg/hr)	250
Internal tube diameter (mm)	15.76
External tube diameter (mm)	21.3
Maximum wire speed (mm/s)	400
Maximum length of furnace (M)	7.5
Length of heater panels (mm)	500
Annealing temperature of wire (C)	1100
Required soak time of wire (secs)	1

The furnace manufacturer had already produced a furnace to meet this customer's requirements, and the design parameters used in this furnace were as described in table (9-4).

Table 9-4. Design parameters used by manufacturers to produce a furnace of the required specification.

Number of heating zones		15
Zone numbers	Heater Temperature (C)	Maximum power rating (KW)
1 - 3	1100	8
4 - 9	1100	5
10 - 15	1120	5
Number of tubes		20
Process speed of wire (mm/s)		391
Height of furnace chamber (mm)		160
Heater width (mm)		800
Distance (a_2-a_1) between rows of tubes (mm)		0 (single row)

The design program was run using the customer's specifications and the design parameters used to produce the furnace. The percentage of power supplied to each zone which was considered to have been used to heat the wire is given in table (9-5).

The temperature predicted to have been attained by the wires in each zone was considered to be equal for all the wires, as they were all of the same type.

Table 9-5. Efficiencies estimated for each of the 15 heating zones.

Zone number(s)	Zonal efficiency.
1	75
2	80
3	85
4	90
5-15	95

The predicted temperatures of all the wires at the beginning of each zone are plotted in figure (9-8), along with the actual power predicted to be consumed by the heaters in each zone.

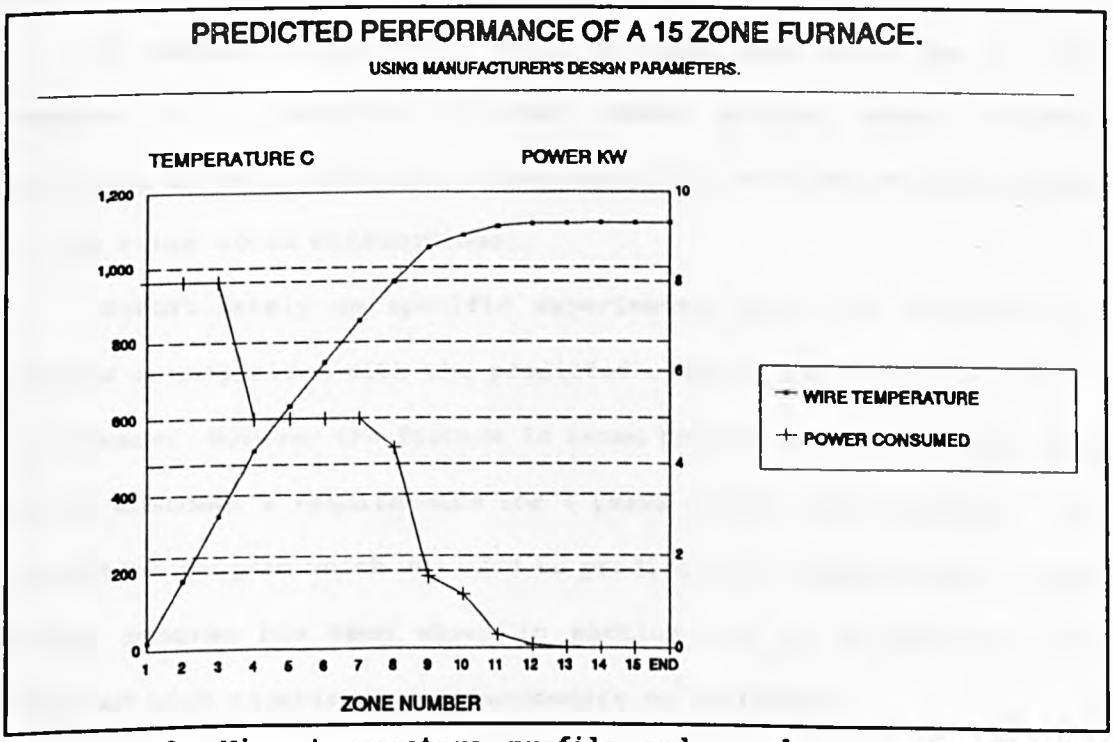

Figure 9-8. Wire temperature profile and zonal power consumption predicted using the design tool.

The wire temperature profile illustrated in figure (9-8) reaches the process temperature of 1100°C at the beginning of zone number 11. The speed of the wire was given in table (9-4) as 391 mm/s, therefore in order to undergo its required 'soak' period of 1 second, the wire would have to travel another 391 mm at this temperature. Therefore the heater in zone number 11 was required in order to maintain the wire at its process temperature for the required 'soak' period. From these results it would seem that the last 4 zones of the furnace were not required either for heating the wires or for maintaining process temperature during the 'soak' period. This was also illustrated by the fact that the predicted power consumption of the last four zones was zero, therefore they were not transferring any heat to the furnace. Hence any power supplied to the last four zones would comprise solely the losses from those zones.

A recommendation which would be made here would be for the furnace to be manufactured with twelve heating zones, thereby providing an extra zone as a safety margin in case one of the heaters in the other zones malfunctioned.

Unfortunately no specific experimental data was available to provide a comparison with the predicted results for the given design of furnace. However the furnace is known to have been processing wire to the customer's requirements for 4 years without any problems. The simulation program which was used to predict wire temperatures in this design program has been shown in section 9.4 to be accurate when compared with experimental measurements on a furnace.

10. CONCLUSIONS.

10.1 SUMMARY OF WORK CARRIED OUT.

The main object of the project reported in this thesis has been to investigate the heat transfer taking place to a wire passing through a tubular furnace. Experimental work was carried out both 'on-site', on a furnace in a wire factory, and in the laboratory, on a purpose built prototype furnace. Both sets of experimental work yielded temperature profiles of various sizes of wire passing through a furnace at different processing speeds.

The results from the tests carried out on the furnace at the wire manufacturer, Critchley, Sharp and Tetlow gave an insight into the performance of a multi-tube furnace being used to process a variety of wire sizes simultaneously. These test were carried out when the furnace was being used to heat 17 ends of wire, with diameters of 1.22, 1.7 and 2.13 mm, to a process temperature of approximately 1050°C. The heat losses from the furnace were found by measuring the power consumed by the furnace when it had reached operating temperature, but with no wire passing through it. The total measured heat losses were found to be 14.96 KW. The theoretical heat loss from the furnace was calculated as the difference between the power supplied to the furnace when the wire was being processed and the theoretical power required to heat that wire, and was determined to be 8.37 KW. The discrepancy between the theoretical and measured heat losses from the furnace was considered to be due to the fact that although the heated zones were found to have reached steady-state temperature, some parts of the furnace may not have done so at the time that the start-up test was carried out.

The data from the 'on-site' experimental work was not sufficient to build up a full picture of the heat transfer to the wires passing through the furnace.

The experimental work on the prototype furnace was designed so that the data acquired was sufficient to build a full picture of the heat transfer to wire being heated in that furnace. These results included the temperature profile of the tube, measured using a number of fixed thermocouples, and the temperature profile of the wire, measured using a thermocouple attached to the wire. In addition to this the power consumed by each of the heater zones in the furnace was recorded. These tests were carried out using 2, 3 and 4 mm diameter Austenitic Stainless Steel wire, at speeds of 15, 30, 45 and 60 mm/s, with all three heater temperatures set to 1000^{o}C. The results from ten of these tests were then chosen for further analysis.

The theoretical installation error of the wire measurement thermocouple was analyzed for each of the tests chosen, and a 'corrected' wire temperature profile produced for each test. In general the corrected wire temperatures were found to be approximately 95% of the measured value.

Several theoretical models were then devised to predict the temperature profile of a wire as it passed through a tubular furnace. The first of these calculated the temperature profile of a wire passing through a process tube, using the measured temperature profile of that tube. Initially radiation was the only heat transfer considered to be taking place from the tube to the wire. This model was used to predict the wire temperature profiles for each of the experimental test conditions presented, and these were compared with the corresponding corrected experimental wire temperature profiles.

It was found that the calculated radiant heat transfer to the wire caused the predicted wire temperature to increase at approximately 65% of the rate depicted by the experimental results.

Consequently this initial theoretical prediction model was modified so that convective heat transfer to the wire was considered in addition to the radiant heat transfer to the wire. The wire temperature profiles predicted using this model are within approximately 5% of the corresponding corrected experimental wire temperature profiles. The next theoretical prediction model to be discussed was formulated in order to predict the heat transfer from the cylindrical heaters in the prototype furnace to the process tube and thence to the wire. This model predicted both the tube and wire temperature profile for a given wire speed and diameter and a given heater temperature profile, and was used to predict the tube and wire temperature profiles for each of the experimental test conditions presented. These were then compared with the corresponding experimental temperature profiles. The average error of the wire temperature profiles predicted using this model was found to be approximately 8% when compared with the experimental results. The average error of the tube temperature profiles predicted using this model was found to be approximately 12% when compared with the experimental results. This error was mainly due to the fact that the prediction model does not include any facility for evaluating the conduction of heat along the process tube to the outside of the furnace. Therefore the model did not predict the large drop in tube temperature at the outer ends of zones 1 and 3, which is evident from all the experimental tube temperature profiles.

The effect of heat conducted along the tube would decrease with an increase in the length in the furnace. Given that the effects of conduction along the tube were not accounted for, the comparison between the experimental and predicted results was considered to be satisfactory.

This theoretical model was then modified so that it could predict the temperature profiles of a number of wires passing through a number of process tubes, the latter of which were heated by flat heater panels situated above and below the process tubes. This configuration resembles that which is inherent in the design of the majority of the high production rate wire annealing furnaces so far manufactured. This model was then used with the dimensions of the furnace at Critchley's on which the initial experimental work was carried out, in order to predict its performance. The accuracy of this model was assessed by comparing the predicted temperature profiles of the three sizes of wire which were being processed during the experimental work, with the experimental temperature profiles. The predicted values were found to be within approximately 10% of the experimental results, thus proving the validity of the theoretical prediction model which was devised.

Finally, the specifications of a multi-tube annealing furnace design tool were discussed. This tool was required to predict the ability of a given furnace design to anneal wire at the required production rate, as stipulated by the customer. The resulting design tool was based on the prediction model for a multi-tube furnace, the validity of which had been established in section 9.4. This design tool was then tested using the customer requirements for a furnace which had already been manufactured.

The design specifications of the furnace which was manufactured for that customer to meet those requirements were entered into the design program, and its performance thus investigated.

The results from the design program confirmed that the furnace built to these specifications was capable of processing wire to the customer's requirements. Therefore the design program was deemed to fulfil the objective of the project reported in this thesis, in that it was able to determine the performance of a given furnace design.

The furnace design program also provided additional information which would enable the engineer to optimise the design of a furnace, resulting in a cheaper and possibly more efficient final product. The main advantage however of such a design tool was to replace much of the 'guesswork' which was previously used when designing a very high cost piece of capital machinery.

10.2 RECOMMENDATIONS FOR FURTHER WORK.

10.2.1 Practical work.

The experimental work performed on the prototype furnace during this project provided the essential data required for the analysis of the theoretical model which was developed to predict the wire temperature profiles in that furnace. A recommendation for further practical work would be to carry out more comprehensive experimental work on a multi-tube furnace, such as that tested at 'Critchley, Sharp and Tetlow's'. Such experimental work would include the measurement of the temperature of the various wires passing through the furnace using a 'Sacrificial' thermocouple, measurement of tube temperatures, and the continuous logging of the power consumption of the heaters.

In addition to this, valuable data would be obtained from the measurement of the temperature at the surface of the heaters themselves.

Other useful practical work would be to assess the effect of varying the flow of the process gas in a tube on the temperature profile of the wire passing through that tube, and to measure the wire and tube temperature profiles in the cooling section of a furnace.

10.2.2 Theoretical Work.

When the theoretical prediction model was produced for a multi-tube furnace, a number of assumptions were made. In order to improve the accuracy of this prediction model, these assumptions would have to be re-considered, and the following theoretical aspects investigated.

- The configuration factor (F_{h-t}) for thermal radiation from the heater panels to all the tubes in the furnace was considered to be the same for each tube. In reality the tubes which were situated at the sides of the furnace would have had a lower configuration factor than those at the centre of the furnace. Further analysis of the geometry of the heater and tube arrangement would be required in order to obtain an discrete configuration factor F_{h-t} for each tube in the furnace.

- The theoretical prediction models which were developed for the single-tube prototype furnace and the multi-tube furnace only considered heat transfer from an elemental area on the heater surface to an adjacent element on a tube, and from this element to an element of the wire in that tube. More accurate results would be obtained from the calculation of the heat transfer from an elemental area on the heater surface to a number of elements on a tube, and then from each of these elements to a number of elements on the wire in that tube. In addition to this, the theoretical heat transfer occurring between the process tubes in a multi-tube furnace could be analyzed.

- The surfaces of each of the heater panels were considered to have been isothermal when considering the heat transfer from the heaters to the tubes. The heat flux from the surface of a given heater panel may in fact vary across its area, therefore causing a variation in the temperature of that heater panel across its surface. Investigation of this would require the consideration of heat transfer between various parts of the heater.

- The effects of the conduction of heat along the wires and process tubes in a furnace were not considered in the theoretical model. Investigation of these effects would provide a complete picture of the heat transfers occurring in the furnace.

Completion of this additional theoretical work would provide a more comprehensive simulation model for a multi-tube furnace, the results of which could then be verified using the results of the further practical work which was recommended in the previous section.

APPENDICES.

APPENDIX A.

THE 'ORION' DATA LOGGER

A1. INTRODUCTION.

The 'Orion' (Schlumberger Solartron 3530) Data logger is a piece of equipment designed to record and process values from a selection of sensors simultaneously. The Orion is made by Schlumberger UK by part of their instrumentation division. The Orion has a capacity to log up to two hundred independent channels, each of which may be connected to a sensor. The input to the logger, which may be analogue or digital, may be recorded at a rate of up a maximum of one thousand channels per second. This chapter describes how the Orion was connected to various sensors and how it was programmed using a BBC Microcomputer connected via an RS232 communication link. Further information on the communication to the Orion, and the method of programming it is given in the Orion Communication Manual [8]

A2. CONNECTION OF SENSORS TO THE ORION.

The Orion data logger available for use in the laboratory was only provided with facilities for inputs of analogue signals. The sensors were connected to the back of the Orion via a number of '35303A' input connectors, each of which provided connections for up to twenty sensors. The input connectors themselves were plugged onto the end of Reed Relay Selector Circuit Boards (35301A), which were situated in slots in the rear of the Orion.

The purpose of the reed relay selectors was to connect the output from the required sensors, in a given sequence, to the Orion's logging circuit for a short period of time, so that their values could be scanned.

The reed relay selectors are controlled by the Orion, which is in turn user programmable. Practically any sensor which provides an analogue output could be connected to the Orion in this manner.

A3. CONNECTION OF SENSORS TO INPUT CONNECTORS.

The input connectors provide connections for twenty channels, and each channel connection consists of three terminals, H(igh), L(ow) and G(round). The two main analogue outputs from sensors are voltage and current, the connections for which are now discussed.

A3.1 Connection for Voltage measurement.

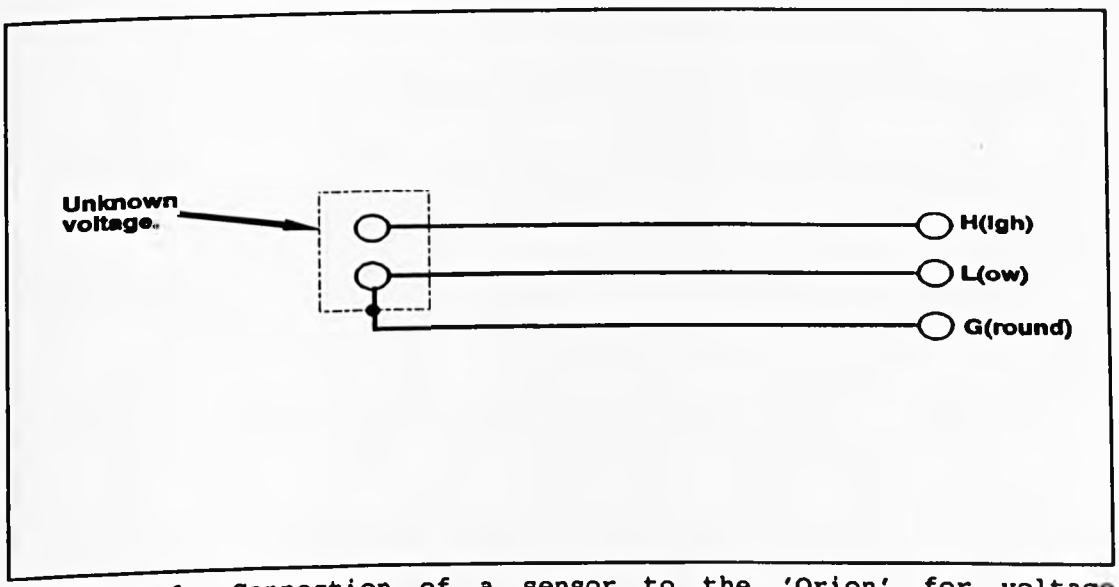

Figure A-1. Connection of a sensor to the 'Orion' for voltage measurement.

Figure (A-1) shows the practical connection diagram for voltage measurement. Any sensor producing a voltage output should be connected in this manner.

The Ground terminal of the sensor, G may be connected to either a screen, guard or source of common mode potential. Otherwise G may be connected to L either at the point where the voltage is being measured, or using the split pad in the logger. The hot junction of a thermocouple was therefore connected to the Orion in the same manner, with the cold junction (ambient) temperature being sensed in the input connector.

A3.2 Connection for Current measurement.

Figure (A-2) below shows the practical connection diagram for current measurement. Any sensor producing a current output should be connected in this manner.

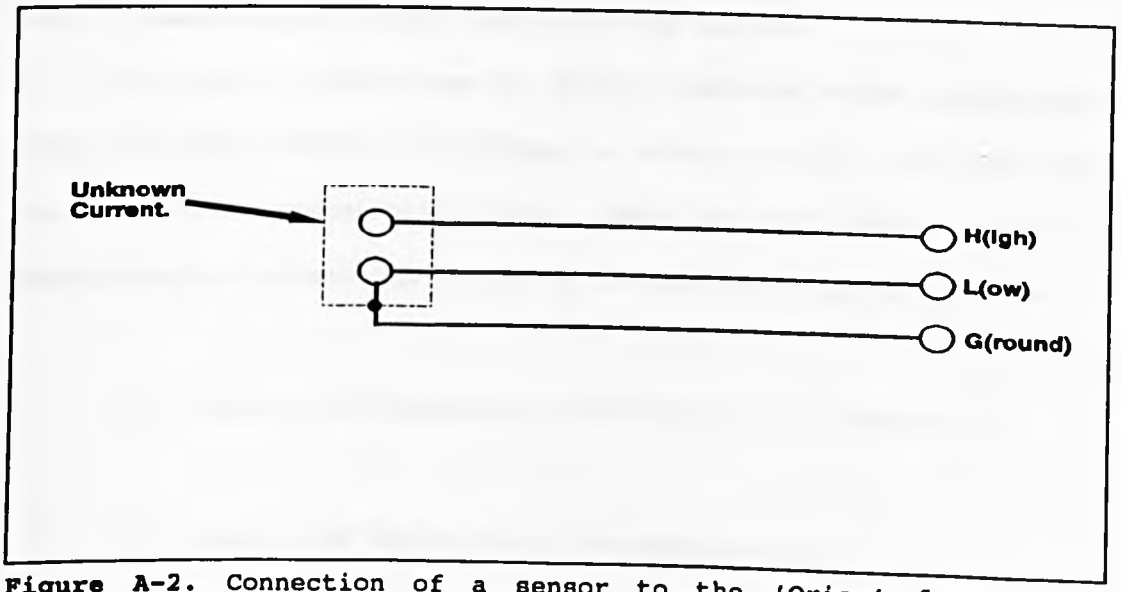

Figure A-2. Connection of a sensor to the 'Orion' for Current measurement.

The connection is obviously the same as for voltage measurement, except that a 100 ohm resistor should be fitted across each channel (between H and L).

A4. USING THE ORION WITH A BBC MICRO.

A4.1 Connection to BBC micro Via the RS232 Communications Interface.

The RS232 communications interface is a standard serial communications interface, possessed by the majority of computers, and electronic equipment which need to communicate with them.

The Orion possesses such an interface, and therefore was connected to the BBC Micro using an 'RS232' interconnecting lead, as described in [8].

A4.2 Communication between the Orion and the BBC.

This section describes the general protocol which was required when using the computer to program, or obtain results from, the Orion via the RS232 communication link. There are two distinct modes of communication between the Orion and the BBC which are as follows,

(i) Transfer of results from the Orion to the computer.

(ii) Control of the Orion by the computer to,

a) set up data-bases.

b) RUN or HALT the Orion

c) Ask the Orion for certain information.

Which of the two above modes are selected depends on the transfer of certain characters from the Orion to the BBC. The two modes of control are now described in more detail.

A4.2.1 Result Transfer Mode.

When Orion 'tasks' are run, the results are fed into a buffer and held there whilst an 'O' is sent to the computer via the RS232 communications link. If the computer then replies with a '?', the buffer is transferred to the computer. Successive interchanges of 'O' and '?' enable further results to be sent to the computer. The computer can only receive results from the Orion when it has recognised the character 'O'. Therefore the result must contain a one character buffer which can be checked from time to time to see if it contains an 'O'. This must be checked with sufficient frequency in order to ensure that the buffer (600 characters) does not become full, thereby preventing the Orion continuing its task. If the computer has been used to control Orion prior to result transfer, the communication link must be released by sending the Orion a '#'.

A4.2.2 Control Mode.

In order to gain control of the Orion, the computer must gain control of the communication link. This is done by sending a '!', which also disables the result transfer. When a '!' is sent, the Orion will respond with one of the following,

N : The computer has not identified itself to the Orion as a device which wishes to control it. This should be done by sending '%1CR'.

L : Orion recognises the computer, but is at the moment in 'Local' control. Full control may be gained here by sending the Orion '%4CR'.

C : The computer is already in full control.

P : The Orion is being controlled by a device of higher priority. Sending the Orion '%6CR' gains the computer full control.

There are two levels of control which may be attained by the computer.

(i) **Limited Control.** This occurs after a '!' is sent, whether the reply is N, C, L or P. Here the following may be actioned by the computer,

- Measure : The computer may demand single, immediate measurement of any one channel.
- Query : The computer may obtain data from a specific part of existing channel or task data bases.

For each of the above, the Orion checks the validity, and returns one of the following to the computer,

E : Means that the command is in error, and the Orion is ready to send error information.

R : Means that the Orion has actioned the command and is ready to send the results data.

On receipt of which, the computer sends a '?', and the Orion outputs the data as a string of up to 80 characters followed by a 'CR'.

(ii) Full Control. This occurs when a '!' is sent and the Orion response is 'C'. When the computer attains full control of the Orion, as well as 'Measure' and 'Query', the computer is able to,

a) Program the Orion. This involves setting up and modifying task and channel data bases in the Orion, and to run and halt various tasks.

b) Monitor. The computer can request the Orion to monitor specific channels or tasks.

c) List. To list the contents of the Orion's task and channel data bases.

d) Read cartridge. The computer can read the contents of the Orion's internal data storage device.

In the case of Monitor, List and Read Cartridge, the data is only made available once the computer has sent a '#' to the Orion, and is then transferred using the 'O' and '?' routine, as described in section A4.2.1.

In order to relinquish control of the Orion, the computer can either send it a '#' to release the control of the communications link and permit Orion to offer results, or send it '%5CR', which tells the Orion to release local lock-out (ie allow control from the Orion's front panel).

The control of the Orion can be carried out more easily by writing a control program on the BBC. One such program was written, in BASIC, and is shown at the end of this appendix.

The program 'PROGO' in section A6 carries out the initial task of communicating with the Orion, and then sends the task and channel definition data, stored in data statements in the program, to the Orion. The tasks may then be run and halted directly from the program. The results from the Orion tasks are shown on the screen in the form of time taken, channel number and result, as shown in the example below,

```
S T 1 13:31:15.1
C 001 +150.0000 DegC  C 002 +148.2300 DegC
D T 1
```

The first and third lines are the start and end of scan markers respectively, and give the time of scan, and the task number. The second line is a data line, and contains the channel numbers logged, and their respective values with the required sign and units. The data lines and marker lines each take up twenty characters of space, and the data is sent in strings of eighty characters from the Orion. The marker lines occupy the first twenty characters of this string, and the rest of the string is left empty. Each string however may contain up to four data lines, therefore the above example would require three strings sent from the Orion. Knowledge of the stream of data from the Orion to the computer enables the data to be stored in an ASCII file on the computer's floppy disc drive for future analysis.

As mentioned earlier in this section, the Orion may be programmed by sending statements from the computer in the form of data strings. A brief description of these statements is given in the next section.

A5. PROGRAMMING THE ORION.

There are two methods of programming the logger to carry out logging operations. The first method is using the keypad on the front panel of the Orion to enter instructions in response to prompts from the Orion. The second method, as previously mentioned, is to program the logger remotely from a computer. The Orion accepts instructions from a connected computer in roughly the same manner as it requests them from the front panel.

A logging program is made up of a series of one or more channel definitions, and one or more task definitions. These are described in detail below.

A5.1 Channel Definition.

A channel definition line tells the data logger what type of sensor is to be connected to each channel of the logger. The logger is then able to process the data from each of those channels when they are logged, to provide the required output value (ie temperature in the case of a thermocouple input). The channel definition also tells the logger if there is any additional processing of the signal required.

An example of a channel definition line is shown below,

DATA "CH 1-12,15-17 SE 330 PR CH WH 1.0"

When such a data statement is sent as an ASCII string to the Orion, it is interpreted as described in the following paragraphs.

CH 1-12,15-17 -This defines which channels are to be defined by the statement. In this case, channels 1 to 12 and channels 15 to 17 inclusive will be defined by the remainder of the line.

SE 330 -This defines the type of sensor which is attached to each of the above channels. The first digit (3) defines the type of sensor, which in this case is a thermocouple. The second digit (3) defines the type of thermocouple connected, which in this case is a type 'K' thermocouple. Finally the third digit (0) tells the logger to use the internal cold junction (ambient) as a reference. Therefore the voltage signals from the thermocouples are converted to temperatures (^{o}C), which are then logged as per the task.

PR CH WH 1.0 -This defines the type of processing to be applied to the values from the above channels. This statement tells the logger to only process data which has undergone a change of more than one degree centigrade from its previous value. The function of this is to reduce the amount of data which is logged, by only processing data which does not replicate the previous value.

This completes the description of a channel definition statement. The same result can be achieved by pressing the appropriate 'Soft keys' on the front panel of the Orion when it is in 'Local Control' (See section A4)

A5.2 Task definition.

The task definition tells the Orion which channel(s) to scan, and the rate at which to scan them. An example of a task definition statement is given on the following page.

```
DATA "TA1 OP ME TR TI DE 5 CO * RE IN IN 30"
DATA "TA1 CH 1-12,15-17 AT F LO PR FO CO MA VA TO SO"
```

The two data statements above contain the definition for a single task. One or more tasks may be defined for a particular program in order to log data from various channels at different rates. When the above data statements are sent to the Orion, they are interpreted as follows,

TA 1 -This tells the logger that it is task number one being defined.

OP ME -This tells the logger that the operation of task one is to measure the value of the input channels.

TR TI DE 5 -This tells the logger when to begin the task. In this case the task is triggered by the Orion's timer, after a delay of five seconds.

CO * -This tells the logger how many scans of the required channels are to be carried out by the task. The '*' indicates that unlimited logs are required, ie until the task is halted.

RE IN IN 30 -This tells the logger to scan the required channels at thirty second intervals.

CH 1-12,15-17 -This tells the logger to scan channels one to twelve and fifteen to seventeen inclusively.

AT F -This tells the logger at which preset rate to log the channels. The letter F here represents a rate of one hundred channels per second.

LO PR -This tells the logger what type of data from the channels should be logged. In this case, only processed data is to be logged, ie. results from each scan of the channels which have undergone a change of one degree centigrade or more since the last log.

FO CO -This tells the logger which format to send the logged results to the output device(s) in. The logger outputs in either full or compact format, and in this case, compact format is selected.

MA EV -This tells the logger to send a marker every time the channels are scanned. Therefore, even if none of the scanned data is to be logged, a marker showing that a scan has been carried out is still recorded.

TO SO -This tells the logger where the logged results are to be recorded to. In this case, 'SO' designates the BBC micro, via Orion's RS232 port.

The channel definition and task definition detailed here make up a complete programme on the Orion, and are sent to the Orion as described in section A4.2.

A6. 'BASIC' PROGRAM FOR ORION CONTROL.

The following BASIC program, when run on a BBC micro which is connected to an Orion via the RS232 port, sends a given task and channel specification to the logger. The program then runs the task, and sends the results to the screen and to a pre-named data file on a floppy disc.

PROGRAM - 'PROGO'

```
10  REM ****************************
20  REM * Program name  : PROGO    *
30  REM * Written       : 06-04-91*
40  REM ****************************
50  REM
60  *FX15,0
70  *FX229,1
80  *FX156,74
90  *FX7,7
100 *FX8,7
110 *FX18
120 MODE 3
121 PRINT"PUT DATA DISC IN DRIVE 1"
122 *DR.3
125 INPUT"NAME OF DISC FILE  ?";FILE$
126 FILE$="G."+FILE$:X=OPENOUT(FILE$)
130 PRINT TAB(0,23)"F0 GET LINE"
140 PRINT TAB(73,23)"F9 END"
150 PRINT TAB(0,22) STRING$(79,"_")
160 PRINT TAB(22,6)"*** SENDING ORION TASK SETUP ***"
170 VDU 28,0,20,79,0
180 Send_Task = TRUE
190 Get_line = TRUE
200 Line_Request = FALSE
210 *FX3,7
220 PRINT"£";
230 REPEAT
240 *FX2,1
250 *FX3,4
260 IF ADVAL(-2)<=0 THEN 700
270 Char=GET
280 Prompt=INSTR("OERNLCP",CHR$(Char))
290 *FX3,7
300 IF Prompt=0 THEN PROCError(1):END
310 ON Prompt GOTO 320,340,370,410,440,490,690
320 PROCGet_Data
```

```
330 GOTO 700
340 *FX3,4
350 PRINT"ORION ERROR : ";
360 GOTO 390
370 *FX3,4
380 PRINT"ORION RESPONSE : ";
390 PROCGet_data
400 GOTO 510
410 Control$="N (Device not recognised)."
420 IF Send_task THEN CMD$="%1":GOTO 470
430 GOTO 510
440 Control$="L (Orion in LOCAL control)."
450 IF Send_task THEN CMD$="%4":GOTO 470
460 GOTO 510
470 PRINTCMD$;CHR$(13);
480 GOTO 700
490 IF Send_task THEN 620
500 Control$="C (Orion in REMOTE control)."
510 *FX2,0
520 *FX3,4
530 PRINT" Orion prompt = ";Control$
540 PRINT" Press RETURN to release the line"
550 INPUT LINE "ENTER Command : "CMD$
560 IF LEN(CMD$)>80 THEN 530
570 *FX2,1
580 *FX3,7
590 IF CMD$="" THEN 650
600 PRINT CMD$;CHR$(13);
610 GOTO 700
620 READ CMD$
630 IF CMD$<> "END" THEN PRINT CMD$+CHR$(13);:GOTO 700
640 Send_task = FALSE
650 PRINT"£";
660 Line_request = FALSE
670 Get_line = FALSE
680 GOTO 700
690 PROCError(2):END
700 IF NOT Get_line OR Line_request THEN 760
710 *FX3,7
720 PRINT"!";
730 SOUND 1,-15,53,2
740 Get_line = FALSE
750 Line_request = TRUE
760 IF NOT INKEY(-33) THEN 780
770 IF Get_line OR Send_task THEN 780 ELSE Get_line = TRUE
780 IF INKEY(-120) THEN PROCError(CODE):END
790 UNTIL FALSE
800 DEF PROCGet_data
810 *FX3,7
820 PRINT"?";
830 *FX3,6
840 *FX2,1
850 INPUT LINE Data$
860 *FX3,4
```

```
870 PROCdiscfile
880 *FX3,7
890 ENDPROC
900 DEF PROCError(CODE)
910 *FX3,4
920 *FX2,0
930  IF  CODE  =  0  THEN  CLS  :  PRINT  "PROGRAM  TERMINATED"  :
PRINT£X,"Z":CLOSE£X
931 *DR.0
932 STOP
940 ON CODE GOTO 950,960
950 PRINT "INVALID PROMPT " :STOP
960 PRINT "COMMUNICATION WITH ORION PROHIBITED " : STOP
970 ENDPROC
980 DATA "HA"
990 DATA "CH 13-14 SE 330 PR CH WH 2.0"
991 DATA "CH 1-11 SE 330 PR CH WH 1.0"
992 DATA "CH 21-23 SE 114 PR ST NU 100"
1000 DATA "TA 1 OP ME TR TI DE 0 CO * RE IN IN 0.5"
1001 DATA "TA 1 CH 14 AT 5 LO PR FO CO MA VA TO SO XT 2,0,0"
1002 DATA "TA 2 OP ME TR TA DE 0 CO 3 RE IN IN 2:0.0"
1003 DATA "TA 2 CH 1-11 AT 5 LO PR FO CO MA VA TO SO XT 0,3,0"
1004 DATA "TA 3 OP ME TR TI DE 1:50.0 CO 100 RE IN IN 0.1"
1005 DATA "TA 3 CH 21-23 AT 5 LO PR FO CO MA VA TO SO XT 0,2,0"
1020 DATA "MO OF"
1030 DATA "RU"
1040 DATA "END"
1100 DEFPROCdiscfile
1106 FIL$="":P$=""
1120 T$="":CH$="":TEMP$="":D$=""
1130 DAT$=MID$(DATA$,1,20)
1135 I$=LEFT$(DAT$,1)
1140 H=INSTR("SCD",I$):IF H=0 THEN GOTO 1450
1150 ON H GOTO 1200,1250,1330
1200 T$=MID$(DAT$,7,10):FIL$=T$
1210 GOTO 1400
1250 B=1
1260 CH$=MID$(DAT$,3,3):TEMP$=MID$(DAT$,6,10)
1270 IF MID$(TEMP$,2,1) ="E" THEN GOTO 1305
1275 IF CH$=P$ THEN GOTO 1305
1280 P$=CH$
1300 FIL$=FIL$+CH$+TEMP$
1305 B=B+20:IF B=81 THEN GOTO 1400
1310 DAT$=MID$(DATA$,B,20):B$=LEFT$(DAT$,1):IF B$="C" THEN GOTO 1260
1315 GOTO 1400
1330 FIL$="D"
1400 PRINT£X,FIL$
1410 PRINT FIL$
1450 ENDPROC
```

APPENDIX B.

CALIBRATION OF THE TEMPERATURE MEASUREMENT SYSTEM.

B1. INTRODUCTION.

In order to determine the reliability of the experimental results acquired, the accuracy of the temperature measurement system used for the experiments was required. The system used to measure the wire and tube temperatures consisted of the thermocouple wire connected to the data logger via a length of compensation cable, and an input connector, as in figure (B-1) below.

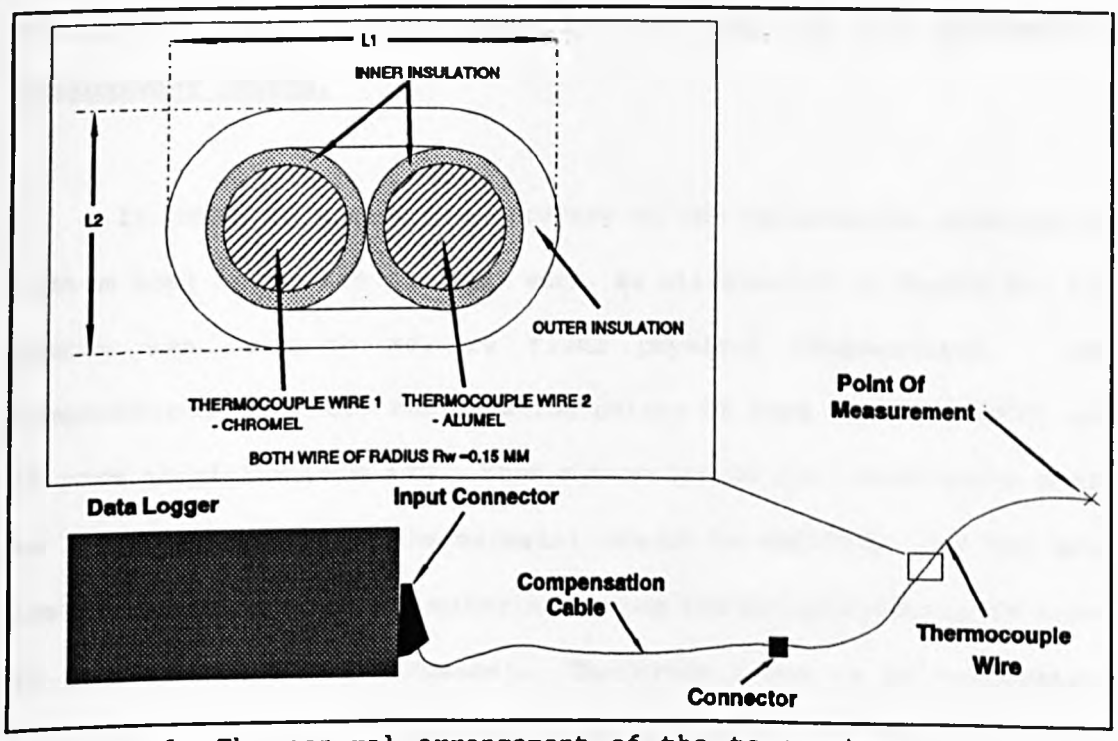

Figure B-1. The general arrangement of the temperature measurement system.

The thermocouples used in all the experiments were constructed using K-type (Chromel-Alumel) thermocouple wire, of the dimensions given in the inset of figure (B-1).

The end of the thermocouple was connected to a length of K-type compensation cable using either a block connector, or thermocouple plugs. The other end of this compensation cable was connected to the required channel of the 'Orion' using the input connector. Each of the connections in the system was considered to have been a potential source of thermocouple measurement error. This was because each connection created an additional 'junction' in the thermocouple circuit, thus causing 'stray' emf's to be present in the circuit. This appendix describes the tests carried out in order to assess the accuracy of the system, and the results of these tests.

B2. METHOD USED TO DETERMINE THE ACCURACY OF THE TEMPERATURE MEASUREMENT SYSTEM.

In order to assess the accuracy of the temperature measurement system used in the experimental work, as illustrated in figure B1, the system was used to measure fixed physical temperatures. The temperatures used were the freezing points of pure Lead (327.3^{o}C) and of pure Aluminium (660.3^{o}C). When a material in its liquid state cools to its freezing point, the material starts to solidify, and the heat lost from the mass of the material during its solidification is known as the 'Latent Heat Of Fusion'. Therefore there is no temperature drop due to the loss in internal energy of the mass of material whilst it undergoes the change of state from liquid to solid. As a result of this, that mass of material will remain at its freezing temperature until all parts of that mass have solidified.

The block of metal being used was placed in a crucible, which in turn was placed in a 'Royce' electrical furnace, which had a temperature range of 0-1000°C. The furnace was then set to a temperature of 100°C above the melting point of the metal being used, and the metal became molten after approximately half an hour. The hot junction was then inserted into the molten mass of metal as depicted in figure (B-2).

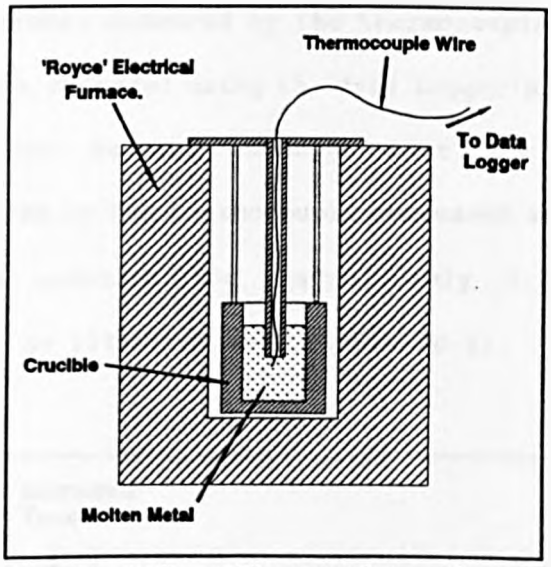

Figure B-2. Illustration of the thermocouple inserted into the molten metal in the furnace.

This thermocouple was then connected to channel 1 of the data logger in the manner illustrated in figure (B-1). This channel of the data logger was programmed to measure and record the temperature of this thermocouple at intervals of ten seconds. The crucible of metal was then removed from the furnace and placed in a supporting stand, where it was left to cool in the atmosphere. Thus the data logger was recording the temperature of the block of metal as it cooled, and underwent the transition from solid to liquid state.

This test was carried out three times, using Lead as the test metal, and a different length of thermocouple wire each time (6.5 metres, 3.5 metres and 1 metre). These three tests were then repeated using Aluminium as the test metal.

B3. RESULTS FROM THE CALIBRATION TESTS.

The temperatures measured by the thermocouple were printed out along with the time recorded using the data logger's integral printer. Examination of the results revealed that for each test, the temperature measured by the thermocouple decreased as the lead cooled, and then became constant for approximately 2.5 minutes before decreasing again, as illustrated in figure (B-3).

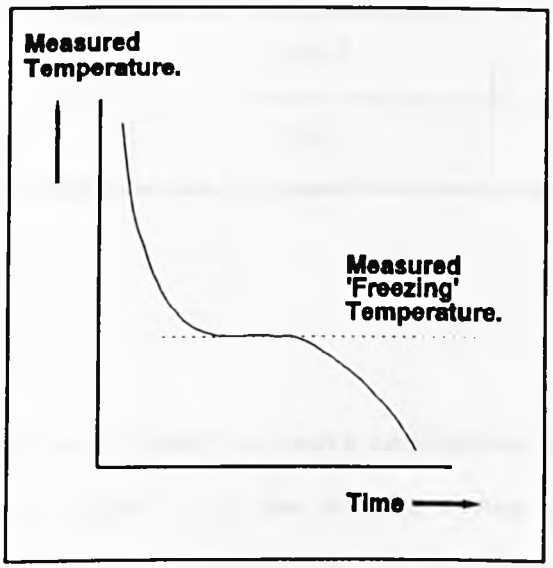

Figure B-3. General shape of the temperature measured by the thermocouple as the test metal passed its freezing point.

The 'freezing' temperature measured for each of the tests carried out on Lead and Aluminium are shown in tables (B-1) and (B-2) respectively. Also shown in tables (B-1) and (B-2) are the percentage deviation of the experimental 'freezing' temperature from the known 'freezing' temperature of the metal being used.

Table B-1. Results from the cooling test carried out on lead with a freezing point of 327.3 °C

Length of thermocouple lead (metres)	Measured 'Freezing' Temperature (C)	% Deviation from known temperature.
6.5	326.5	0.336
3.5	325.9	0.428
1.0	325.9	0.428
Average	326.1	0.397

The results from the cooling tests carried out on Lead exhibited an average error of 0.397 % of the actual freezing temperature of lead, which is 327.3 °C. There was no appreciable increase in thermocouple error when the length of the thermocouple wire was increased from 1 metre to 6.5 metres, so the voltage drop along the thermocouple wire was considered to be negligible in this case.

Table B-2. Results from the cooling tests carried out on Aluminium with a freezing point of 660.3°C.

Length of thermocouple lead (metres)	Measured 'Freezing' Temperature (C)	% Deviation from known temperature.
6.5	650.7	1.454
3.5	650.7	1.454
1.0	651.3	1.363
Average	650.9	1.424

The results from the cooling tests carried out on Aluminium are displayed in table (B-2) above. The measurement errors incurred by the system at this temperature were considered to be the percentage deviations between the measured and actual freezing points of Aluminium. The average error incurred was 1.424 % of the actual freezing temperature of Aluminium. Again the increase in thermocouple error resulting from an increase in thermocouple wire length from 1 to 6.5 metres was considered to be negligible.

The errors found from the tests on both metals arose due to the 'stray' emf's, incurred at the additional junctions caused by the connections between the thermocouple wire and the compensation cable, and the compensation cable and the input connector. Other sources of error may have been the thermal emf induced in the reed relays in the data logger, or errors may have been incurred when the data logger converted thermocouple voltage to temperature.

In order to quantify the measurement error of the system at other temperatures, the results found were used to solve the quadratic equation, Error = B x T + C x T^2, and the following relationship resulted,

$$\text{Error} = -1.453 \times 10^{-4} \times T + 3.805 \times 10^{-6} \times T^2$$

Where T was the temperature being measured in C. Therefore if the maximum temperature to be measured was 1000°C, then the maximum error would be 3.66 %. This error was not considered large enough to justify any correction of the recorded temperatures for errors caused by the measurement system used.

APPENDIX C.

DETERMINATION OF THE PROPERTIES REQUIRED FOR ANALYSIS OF HEAT TRANSFERS IN THE FURNACE.

C1. INTRODUCTION.

When considering the transfers of energy involved in the heating of wire in the tubular furnace, various temperature dependant properties were required. The properties discussed in this section are as follows,

- **Emissivities** - When calculating the radiant heat transfers in the furnace, the emissivities of the various surfaces were required. The emissivity of a particular surface depends on the condition of that surface (ie the extent of oxidation), the material of that surface and the temperature of the surface. The emissivities presented in section C2 are for Inconel and Stainless Steel with various surface conditions, over a temperature range of 0-1400 K.

- **Specific Heat Capacity** - The specific heat capacity of the wire's material was required when calculating the temperature rise of the wire resulting from a given amount of heat transferred to it. The specific heat capacities of two grades of Austenitic Stainless Steel, over a temperature range of 0-1400 K, are presented in section C3.

- **Thermal Conductivity** - When calculating the forced convective heat transfer from the tube to the wire, the thermal conductivity of the gas separating the two surfaces was required. The process gas used in all the experimental work was Hydrogen, and the thermal conductivity of this gas over a range of 0-1400 K is presented in section C4. Section C4 also contains the thermal conductivities of three selected metals over this temperature range.

Each of the properties is represented by a polynomial curve plotted over the given temperature range, and the data points which were used to obtain this curve. A statistical software package, called 'TC-PLOT' was used to carry out a polynomial regression on each of the sets of property data. The coefficients of the polynomial expression for each property are presented in tabular form. Finally the maximum error of the polynomial curve compared with the data points is given for each property.

Much of the property data found did not extend over the full temperature range of 0-1400 K. It was not considered to be sensible to extrapolate the polynomial expressions in order to obtain property values at temperatures outside the given temperature range of the data. Therefore at temperatures outside the temperature range of the data, the property of a given material or gas was considered to be that a the nearest temperature in the temperature range of the data.

C2. EMISSIVITIES.

a) Inconel. Table (C-1) shows the material, surface condition and temperature range of the data, for the sets of data points illustrated in the graph in figure (C-1). Table (C-1) also gives the source of the data for each of the properties in the form of an appropriate reference. The emissivity curves in figure (C-1) are produced by polynomial expressions of the form,

$$\varepsilon(T) = a_0 + a_1 \cdot T^{/} + a_2 \cdot T^{/2} + a_3 \cdot T^{/3} + \ldots\ldots + a_n \cdot T^{/n}$$

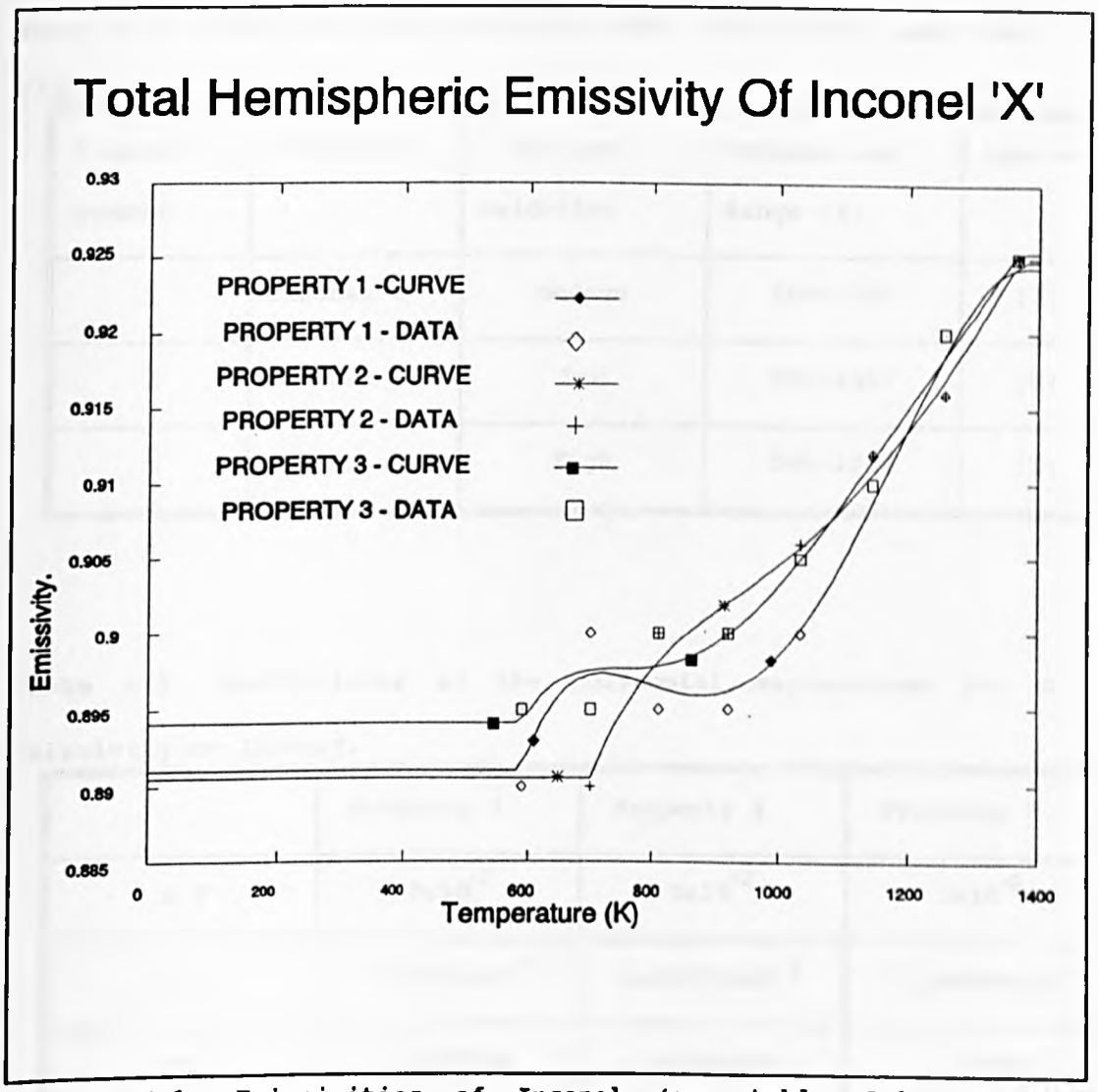

Figure C-1. Emissivities of Inconel (see table C-1 for more information).

Where SF is the relevant 'Scale Factor' such that,

$$T' = SF \cdot T$$

The coefficients of the polynomial equations for the emissivities of Inconel are given in table (C-2). As can be observed from the three curves, the emissivity of inconel increases with temperature. The emissivity can also be seen to increase with the extent of oxidation of the surface of the Inconel.

Table C-1. Description of materials whose emissivities are shown in figure C1.

Property number	Material	Surface Oxidation	Temperature Range (K)	Source
1	Inconel X	Medium	589-1367	[9]
2	Inconel X	Low	700-1367	[9]
3	Inconel X	High	589-1367	[9]

Table C-2. Coefficients of the polynomial expressions for the emissivity on Inconel.

	Property 1	Property 2	Property 3
S.F	3×10^{-2}	3×10^{-2}	1×10^{-2}
a_0	4.17035×10^{-6}	1.91817×10^{-6}	-3.104499×10^{-6}
a_1	0.139715	0.129439	0.4728
a_2	-8.19396×10^{-3}	-7.43727×10^{-3}	-9.7089×10^{-2}
a_3	2.2139×10^{-4}	2.122397×10^{-4}	9.6823×10^{-3}
a_4	-2.6552×10^{-6}	-2.9933×10^{-6}	-4.68413×10^{-4}
a_5	1.04791×10^{-8}	1.6834×10^{-8}	8.85835×10^{-6}
Max. Error	0.355%	0.2318%	0.286%

b) Stainless Steel. The emissivity of Stainless Steel was investigated for surfaces with low, medium and high oxidation. Table (C-3) lists the surface condition of the material, and the temperature range for which the data was obtained, and the source of the data for each of the sets of data points in the graph in figure (C-2).

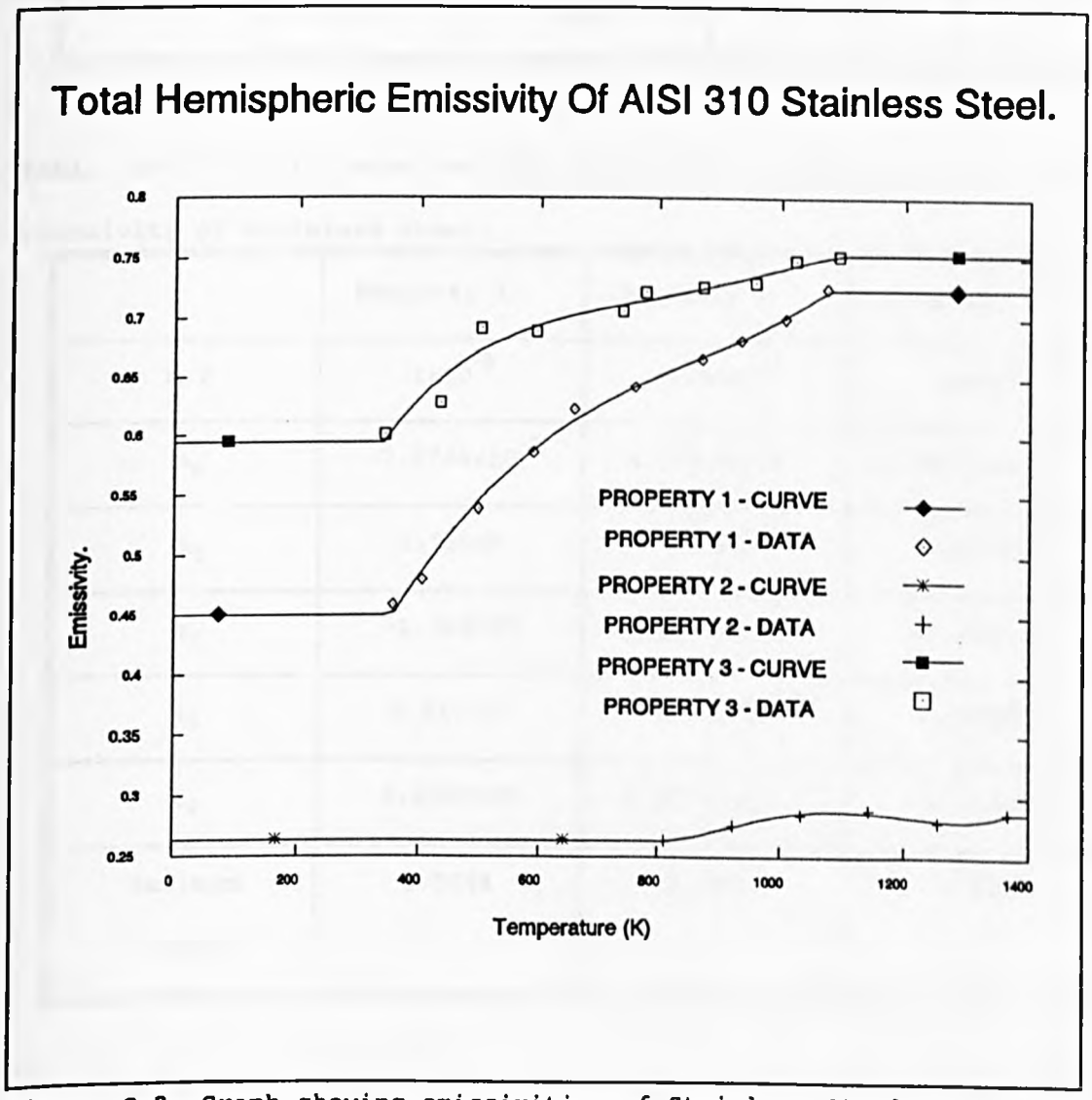

Figure C-2. Graph showing emissivities of Stainless Steel (see Table C-3 for more information).

Table C-3. Description of materials whose emissivities are shown in figure C2.

Property number	Material	Surface Oxidation	Temperature Range (K)	Source
1	AISI 310	Medium	356-1075	[9]
2	AISI 310	Low	811-1366	[9]
3	AISI 310	High	341-1093	[9]

Table C-4. Coefficients of the polynomial expressions for the emissivity of Stainless Steel.

	Property 1	Property 2	Property 3
S.F	$1x10^{-3}$	$-4.9x10^{-2}$	$1x10^{-3}$
a_0	$-7.6744x10^{-5}$	$4.94675x10^{-5}$	$-3.6617x10^{-5}$
a_1	1.76985	0.3838	3.127915
a_2	-1.554271	$1.15589x10^{-2}$	-5.324137
a_3	0.316117	$1.5147x10^{-4}$	4.097053
a_4	0.1680787	$7.30773x10^{-7}$	-1.159818
Maximum Error	1.985%	0.749%	3.23%

The property curves shown in figure (C-2) were produced by polynomial expressions as described for the Inconel curves, the coefficients of which are listed in table (C-4).

C3. SPECIFIC HEAT CAPACITY OF STAINLESS STEEL.

Figure (C-3) displays the property data for the stainless steels as listed in Table (C-5) on the following page. The polynomial curves resulting from the property data are also shown in figure (C-3), and the coefficients of the polynomial expressions are presented in table (C-6).

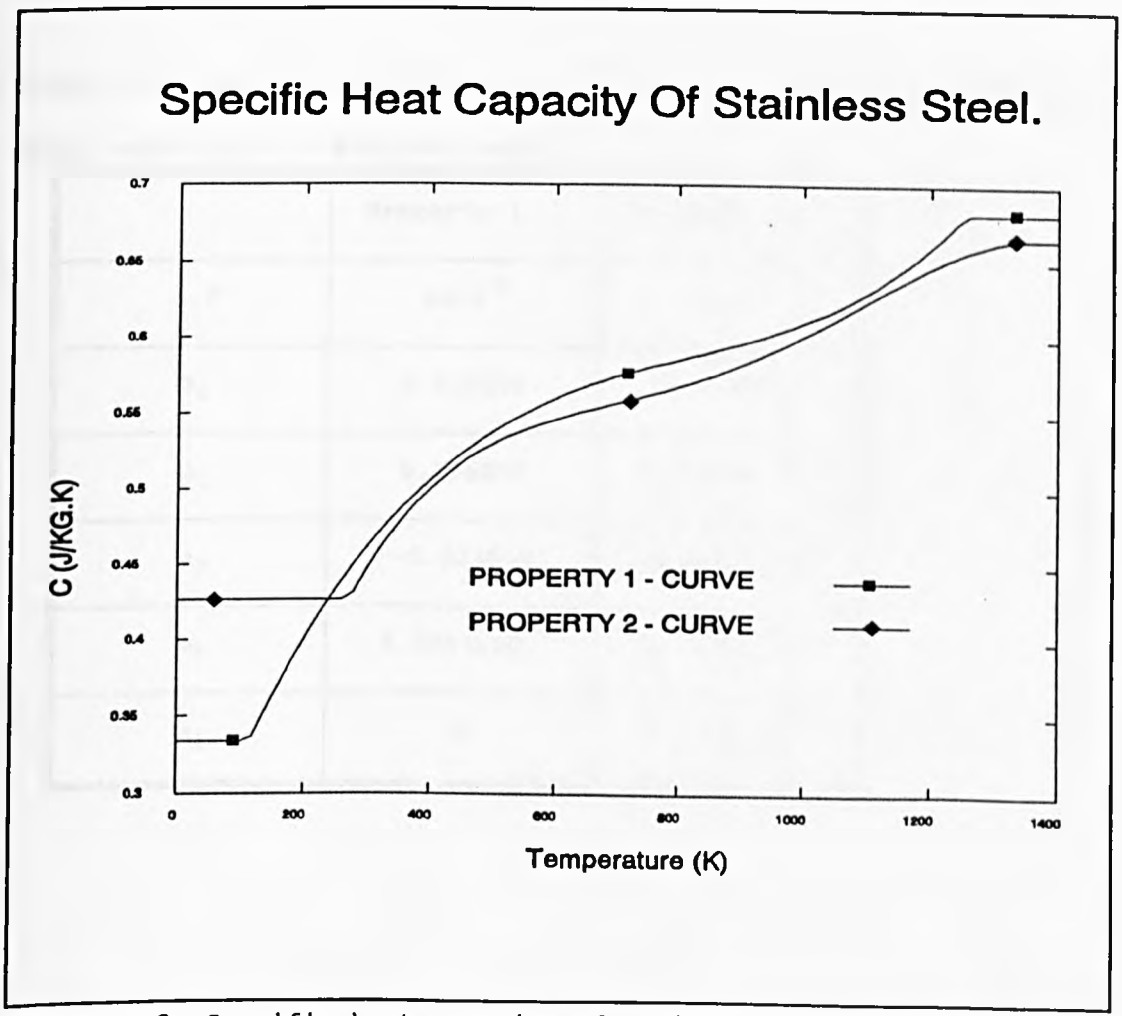

Figure C-3. Specific heat capacity of Stainless Steel (see Table C-5 for further information).

Table C-5. Description of materials whose specific heats are shown in figure C3.

Property number	Material	Temperature Range (K)	Source
1	AISI 310	116-1255	[10]
2	AISI 316	273-1366	[10]

Table C-6. Coefficients of the polynomial expressions for the specific heat capacity of stainless steels.

	Property 1	Property 2
S.F	$1x10^{-2}$	$1x10^{-1}$
a_0	0.215255	$-2.729x10^{-4}$
a_1	0.116273	$2.54653x10^{-2}$
a_2	-0.013058	$-4.50145x10^{-4}$
a_3	$5.3845x10^{-4}$	$3.55415x10^{-6}$
a_4	0	$-9.97213x10^{-9}$

C4. THERMAL CONDUCTIVITY.

a) Hydrogen. Thermal conductivity of Hydrogen was found in [11], and the data points are plotted in figure (C-4). Also shown in figure (C-4) is the polynomial curve for the thermal conductivity of Hydrogen, which is given by,

$$K(T) = -0.33882\times10^{-2} - 3.73422\times10^{-3} \times T - 1.07131\times10^{-5} \times T^2 + 1.7507\times10^{-8} \times T^3 - 1.560188\times10^{-11} \times T^4 + 7.23068\times10^{-15} \times T^5 - 1.3673\times10^{-18} \times T^6 \quad (W/M.K)$$

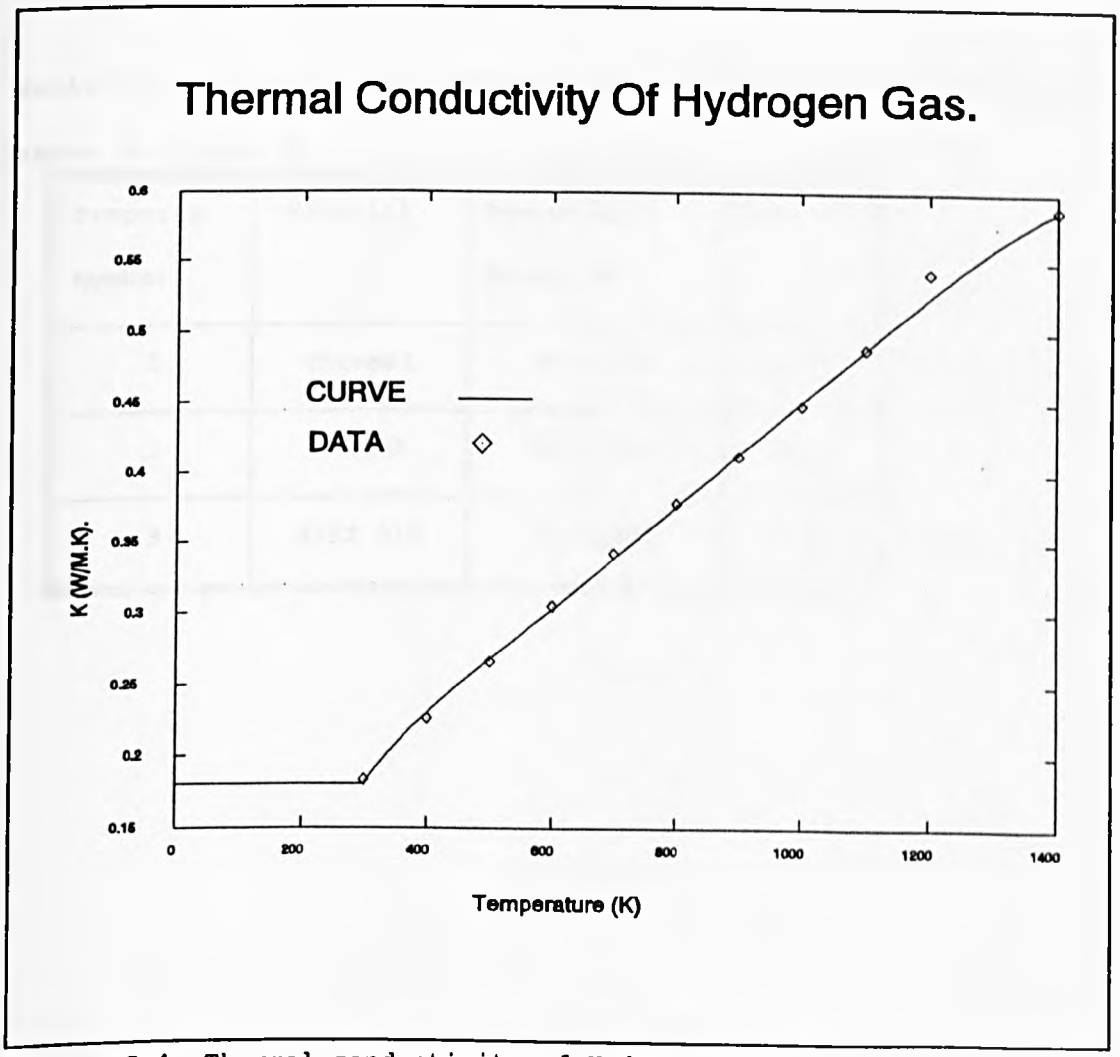

Figure C-4. Thermal conductivity of Hydrogen gas.

b) Various metals. The Thermal conductivity of assorted metals were required at various points in the analysis. The materials whose thermal conductivities are presented in this section are listed in table (C-7), along with the temperature range and the source of the data.

Figure (C-5) shows the data points and the polynomial curves for the thermal conductivities of the three metals, and the coefficients of the polynomial equations are given in table (C-8), along with the standard error of the polynomial curve.

Table C-7. Description of materials whose thermal conductivities are shown in figure C5.

Property number	Material	Temperature Range (K)	Source
1	Chromel	373-1400	[12]
2	Alumel	363-1400	[12]
3	AISI 316	343-1186	[12]

Table C-8. Coefficients of the polynomial expressions for the thermal conductivities of selected metals (see table C7).

	Property 1	Property 2	Property 3
a_0	11.85131	17.993	4.4086
a_1	1.91198×10^{-2}	2.9805×10^{-2}	1.5508×10^{-2}
Standard Error (W/M.K)	2.5617×10^{-2}	1.949×10^{-1}	1.463×10^{-1}

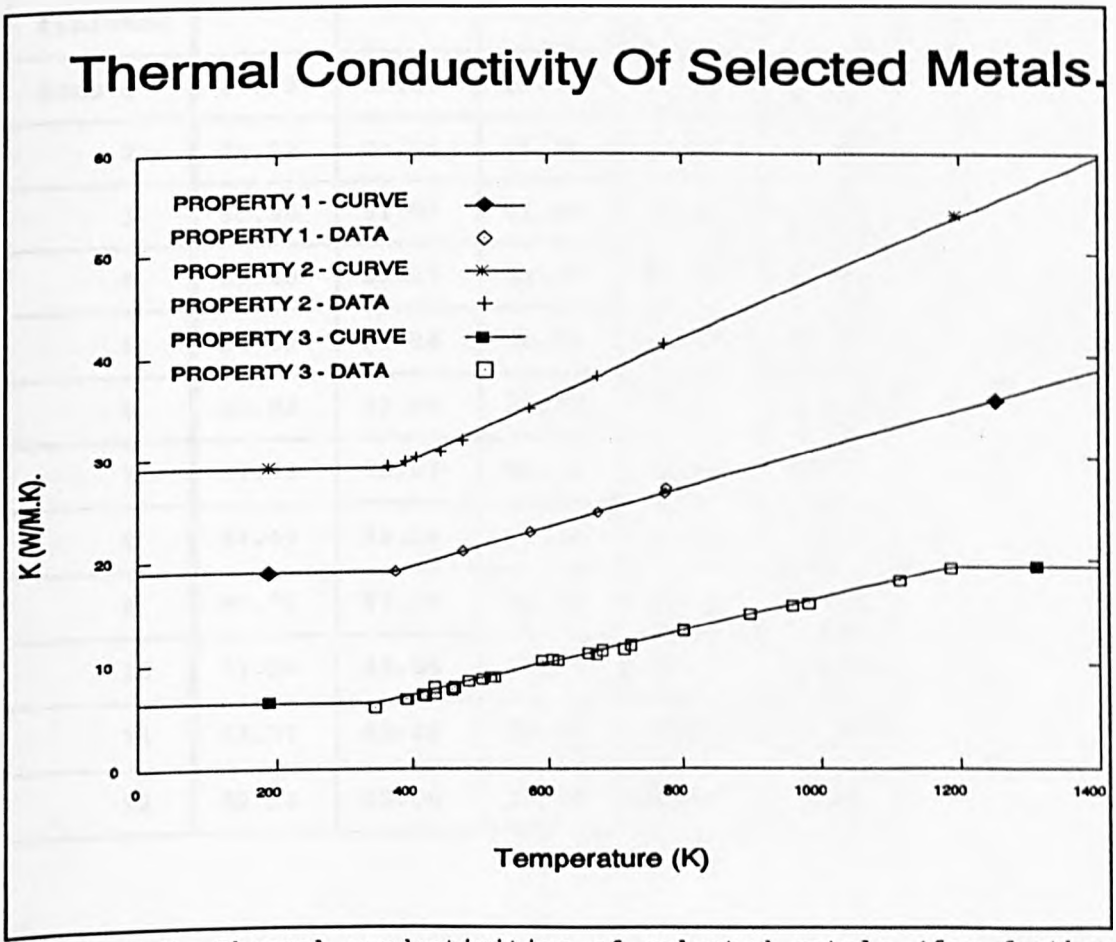

Figure C-5. Thermal conductivities of selected metals (for further information see Table C-7).

APPENDIX D.

RESULTS FROM THE EXPERIMENTAL AND THEORETICAL WORK.

The tables presented in this section contain the results from the experimental work carried out 'on-site' on the furnace at 'Critchley, Sharp and Tetlow'. The results of the analysis of this work are also presented in this section.

Table D-1.1 Readings taken from the kilowatt hour meters during the start up test, and times taken (minutes).

Time started	0:00	9:00	19:00	30:15	39:45
Time finished	2:45	11:45	21:45	33:00	42:30
zone 1	21.33	22.00	23.76	24.49	25.37
2	24.22	24.94	25.72	26.58	27.30
3	50.36	51.07	51.85	52.72	43.45
4	81.40	82.37	83.39	84.53	85.55
5	34.19	34.94	35.76	36.67	37.44
6	21.83	22.65	23.54	24.54	25.38
7	91.33	91.77	92.14	92.56	92.83
8	34.49	35.34	36.27	37.31	38.14
9	86.76	87.57	88.49	89.53	90.38
10	31.24	32.06	32.97	34.01	34.88
11	68.37	69.20	70.16	71.14	72.02
12	02.23	03.06	03.99	05.01	05.88

Table D-1.2 Readings taken from the kilowatt hour meters during the start up test, and times taken (minutes).

Time started	50:30	60:0	72:00	81:30	92:00
Time finished	53:15	62:4	74:45	84:15	94:45
Zone 1	25.370	25.86	25.89	26.00	26.04
2	28.175	28.85	29.75	29.95	30.05
3	54.285	55.01	55.92	56.63	57.22
4	86.600	87.56	88.77	89.12	89.31
5	38.315	39.08	40.05	40.81	41.67
6	26.340	27.17	28.23	29.00	29.96
7	92.890	93.19	93.39	93.79	94.23
8	39.190	40.07	41.17	42.04	42.89
9	91.370	92.27	93.30	94.01	94.14
10	35.875	36.74	37.80	38.38	38.69
11	73.005	73.87	74.96	75.67	75.83
12	06.855	07.76	08.79	09.63	10.39

Table D-1.3 Readings taken from the kilowatt hour meters during the start up test, and times taken (minutes).

Time started	102:15	112:45	123:45	135:00	145:00
Time finished	105:00	115:30	126:30	137:45	147:45
Zone 1	26.156	26.16	26.170	26.21	26.23
2	30.250	30.39	30.53	30.66	30.79
3	57.595	58.01	58.41	58.84	59.19
4	89.455	89.61	89.75	89.88	90.01
5	41.962	42.29	42.67	43.04	43.36
6	30.690	31.05	31.34	31.61	31.84
7	94.665	95.05	95.50	95.92	96.10
8	43.245	43.63	43.93	44.21	44.43
9	94.425	94.66	94.89	95.13	95.32
10	39.013	39.30	39.58	39.87	40.12
11	76.105	76.36	76.58	76.83	77.03
12	10.813	11.27	11.75	12.14	12.51

Table D-2.1 Temperatures (°C) measured in tube 10 in each zone, with times taken (minutes).

Time started	4:00	13:00	24:00	34:00	43:15
Time finished	8:40	17:40	28:40	38:40	47:55
Zone 1	43	113	405	493	637
2	45	111	384	474	658
3	49	125	419	491	681
4	48	160	445	585	750
5	41	165	389	546	680
6	37	164	355	550	661
7	30.5	147	320	415	466
8	30.5	165	400	575	690
9	29.5	178	397	610	712
10	28	189	376	608	700
11	26	192	365	620	691
12	25	204	350	617	675

Table D-2.2 Temperatures (°C) measured in tube 10 in each zone, with times taken (minutes).

Time started	54:00	63:30	75:30	85:00	96:00
Time finished	57:10	68:10	80:10	89:40	100:40
Zone 1	718	720	710	731	726
2	716	859	885	868	853
3	747	897	947	1012	996
4	835	957	1000	999	996
5	787	893	983	1046	1069
6	765	840	933	990	1067
7	490	595	690	814	920
8	807	892	987	1050	1057
9	865	935	1062	1076.5	1069.
10	867	932	1071.	1071.5	1069.
11	872	927	1069	1081	1058
12	848	879	1016	1044	1064

Table D-2.3 Temperatures (°C) measured in tube 10 in each zone, with times taken (minutes).

Time started	106:00	116:00	128:00	138:45	149:00
Time finished	110:40	120:40	132:40	143:25	153:40
Zone 1	726	713	724	710	719
2	876	855	870	854	868
3	997	992	996	988	996
4	1000	995	999	995	1000
5	1051	1053	1055	1052.5	1054.5
6	1054.	1052.5	1054	1052	1051
7	990	1027	1057	1056	1047
8	1055	1055	1056	1054	1055
9	1059	1055	1058	1055	1057
10	1069.	1067	1069.5	1069	1070
11	1062	1062	1063.5	1063	1063
12	1063	1063	1065	1064	1065

Table D-3.1 Zonal powers (Kw) calculated from the Kilowatt-hour meter readings shown in tables D-1.1 to D-1.3.

Time (minutes)	2:25	11:45	21:45	33:00	42:30
Zone 1	4.467	4.740	5.173	4.579	4.912
2	4.787	4.680	4.576	4.560	4.856
3	4.753	4.663	4.655	4.643	4.615
4	6.440	6.150	6.080	6.442	5.832
5	4.986	4.920	4.880	4.863	4.856
6	5.480	5.340	5.333	5.305	5.330
7	2.900	2.250	2.240	1.705	0.307
8	5.634	5.580	5.573	5.242	5.832
9	5.400	5.520	5.520	5.413	5.486
10	5.467	5.508	5.504	5.495	5.553
11	5.567	5.778	5.211	5.526	5.498
12	5.533	5.550	5.467	5.495	5.414

Table D-3.2 Zonal powers (Kw) calculated from the Kilowatt-hour meter readings shown in tables D-1.1 to D-1.3.

Time (minutes)	53:15	62:45	74:45	84:15	94:45
Zone 1	3.126	0.125	0.726	0.229	0.650
2	4.263	4.500	1.263	1.102	0.913
3	4.610	4.546	4.502	3.364	2.163
4	6.095	6.025	2.254	1.048	0.847
5	4.863	4.825	4.812	4.917	1.700
6	5.286	5.265	4.901	5.503	4.223
7	1.907	0.990	2.526	2.550	2.510
8	5.558	5.500	5.526	4.843	2.072
9	5.703	5.160	4.484	0.763	1.616
10	5.507	5.265	3.695	1.778	1.854
11	5.463	5.450	4.516	0.918	1.573
12	5.716	5.150	5.337	4.335	2.464

Table D-3.3 Zonal powers (Kw) calculated from the Kilowatt-hour meter readings shown in tables D-1.1 to D-1.3.

Time (minutes)	105:00	115:30	126:30	137:45	147:45
Zone 1	0.022	0.067	0.181	0.120	0.164
2	0.799	0.968	0.565	0.810	0.565
3	2.400	2.677	1.920	2.142	2.052
4	0.898	0.924	0.618	0.738	0.602
5	1.903	2.551	1.681	1.902	1.845
6	2.057	1.950	1.252	0.732	1.859
7	2.200	3.051	1.898	1.050	1.083
8	2.200	2.024	1.276	1.338	1.341
9	1.371	1.521	1.077	1.188	1.148
10	1.674	1.889	1.309	1.458	1.388
11	1.457	1.539	1.088	1.230	1.176
12	2.651	3.213	1.775	2.178	2.108

Table D-4. Steady state power consumption in each zone

Zone no.	Steady state power (Kw).
1	0.155
2	0.647
3	2.038
4	0.653
5	1.809
6	1.281
7	1.344
8	1.318
9	1.138
10	1.385
11	1.165
12	2.020
TOTAL	14.964

Table D-5.1 Temperature readings for those tubes for which measurements were possible, measured at the ends of the zones.

Tube no.	2	3	5	6	7
Temp.(°C) measured at start of zone:					
1	606	390	343	445	430
2	777	689	670	690	645
3	905	843	864	884	879
4	978	940	948	956	966.5
5	1022	999	999	996	1015
6	1042	1033	1036	1038	1045
7	1037	1038	1042	1042	1047
8	1035	1039	1044.5	1045	1049.5
9	1039	1042	1048	1049	1052.5
10	1048	1046	1056	1056	1065
11	1050	1054	1061	1062	1067
12	1048	1050	1053	1056	1060
END	1020	1031	1036	1044.5	1049

Table D-5.2 Temperature readings for those tubes for which measurements were possible, measured at the ends of the zones.

Tube no.	9	10	11	12	14
Temp.(°C) measured at start of zone :					
1	470	400	375	390	370
2	666	672	620	650	590
3	850	855	720	815	800
4	960	952	897	855	900
5	1015	999	943	986	----
6	1042	1033.5	1009	1018	----
7	1045	1042	1019	1039	----
8	1048.5	1045	1034	1045	----
9	1052.5	1052	1046	1051	----
10	1059	1060	1056	1059	----
11	1065	1066.5	----	1067.5	----
12	1060	1060	----	1060	----
END	1049	1048	----	1050	----

Table D-5.3 Temperature readings for those tubes for which measurements were possible, measured at the ends of the zones.

Tube no.	15	17	18	19	SET
Temp.(°C) measured at start of zone:					
1	305	410	581	446	
2	595	515	738	630	697
3	770	640	880	800	849
4	890	835	956	905	967
5	990	915	----	985	999
6	1030	990	----	1019	1049
7	1038	1034	----	1021.5	1049
8	1041	1038	----	1021	1050
9	1047	1043	----	1026.5	1050
10	1055	1054	----	1031.5	1050
11	1063	1056	----	1043	1050
12	1056	1052	----	1044	1050
END	1047	1038	----	1029	

Note: Those tubes for which some of the rows contain a dashed line were blocked at some point along their length, therefore the thermocouple could not measure past these points.

Table D-6. Wire data for running test carried out on 24/5/90 on the 'Critchley' furnace.

Tube number	Material (AISI)	Diameter (mm)	Speed (mm/s)
1	301	1.702	110.0
2	301	1.702	110.0
3	301	1.626	110.0
4	301	1.626	110.0
5	301	1.626	110.0
6	316	1.219	78.90
7	316	1.219	78.90
8	No wire	-------	-------
9	316	1.219	79.80
10	316	1.219	78.90
11	316	1.219	78.06
12	301	1.702	79.80
13	301	2.134	70.22
14	301	2.134	70.22
15	301	2.134	70.22
16	301	2.134	70.22
17	301	2.134	70.22
18	No wire	-------	-------
19	301	2.134	70.22

Table D-7. Kilowatt-hr meter readings and calculated average power (Kw) supplied to each zone during the running test.

Time started	0:00	145:00	215:00	Average power consumed
Time finished	2:45	147:45	217:45	
Zone 1	23.435	35.060	40.730	4.826
2	37.855	48.090	52.790	4.168
3	29.795	40.940	46.297	4.605
4	32.425	39.365	42.535	2.821
5	23.855	31.375	34.935	3.092
6	52.315	56.205	58.007	1.588
7	36.090	38.640	39.845	1.048
8	32.115	34.945	36.303	1.169
9	21.400	23.685	24.775	0.942
10	90.910	94.560	96.327	1.512
11	64.400	66.175	67.025	0.732
12	66.075	69.220	70.735	1.300
			TOTAL	27.803 Kw

Table D-8.1 Power (Kw) used in heating each wire in each zone, calculated from measured temperatures and wire data.

Tube no.	1	2	3	4	5
Zone 1	0.204	0.204	0.315	0.315	0.343
2	0.160	0.160	0.171	0.171	0.2154
3	0.095	0.095	0.113	0.113	0.0984
4	0.059	0.059	0.0715	0.0715	0.0619
5	0.028	0.028	0.042	0.042	0.046
6	-0.007	-0.007	0.0063	0.0063	0.0076
7	-0.002	-0.0028	0.0013	0.0013	0.0032
8	0.005	0.0055	0.0038	0.0038	0.0045
9	0.012	0.012	0.0051	0.0051	0.010
10	0.062	0.0628	0.010	0.010	0.0064
11	-0.002	-0.0028	-0.0051	-0.0051	-0.010
12	-0.039	-0.039	-0.0241	-0.0241	-0.022

Table D-8.2 Power (Kw) used in heating each wire in each zone, calculated from measured temperatures and wire data.

Tube no.	6	7	8	9	10
Zone 1	0.196	0.160	0.000	0.152	0.203
2	0.269	0.306	0.000	0.245	0.238
3	0.141	0.172	0.000	0.209	0.182
4	0.093	0.114	0.000	0.129	0.106
5	0.105	0.078	0.000	0.070	0.086
6	0.011	0.0054	0.000	0.0081	0.024
7	0.008	0.0068	0.000	0.0096	0.008
8	0.011	0.0082	0.000	0.011	0.019
9	0.019	0.035	0.000	0.018	0.022
10	0.017	0.0057	0.000	0.017	0.018
11	-0.017	-0.019	0.000	-0.014	-0.018
12	-0.031	-0.030	0.000	-0.031	-0.033

Table D-8.3 Power (Kw) used in heating each wire in each zone, calculated from measured temperatures and wire data.

Tube no.	11	12	13	14	15
Zone 1	0.166	0.217	0.136	0.136	0.330
2	0.100	0.0361	0.126	0.126	0.149
3	0.257	0.0361	0.126	0.126	0.149
4	0.089	0.0314	0.118	0.118	0.131
5	0.147	0.0031	0.055	0.055	0.055
6	0.025	0.021	0.011	0.011	0.011
7	0.038	0.0061	0.0042	0.0042	0.0042
8	0.031	0.0061	0.0084	0.0084	0.0084
9	0.027	0.0082	0.011	0.011	0.011
10	0.018	0.0087	0.011	0.011	0.011
11	0.009	-0.0077	-0.0099	-0.0099	-0.0099
12	-0.033	-0.010	-0.013	-0.013	-0.013

Table D-8.4 Power (Kw) used in heating each wire in each zone, calculated from measured temperatures and wire data.

Tube no.	16	17	18	19	TOTAL
Zone 1	0.330	0.120	0.000	0.213	3.740
2	0.236	0.236	0.000	0.132	3.1415
3	0.236	0.236	0.000	0.132	2.5165
4	0.101	0.101	0.000	0.105	1.5593
5	0.099	0.099	0.000	0.046	1.0841
6	0.060	0.0601	0.000	0.0027	0.2566
7	0.005	0.0056	0.000	-0.0007	0.0998
8	0.006	0.0069	0.000	0.0076	0.1560
9	0.015	0.015	0.000	0.007	0.2434
10	0.002	0.0028	0.000	0.016	0.2910
11	-0.006	-0.0056	0.000	0.0014	-0.1314
12	-0.019	-0.0196	0.000	-0.019	-0.4134

Table D-9. Percentage of the power supplied to each zone which was used to heat wire in that zone. (ie the efficiency of each zone.)

Zone no.	Efficiency %
1	77.50
2	75.37
3	54.70
4	55.30
5	35.10
6	16.16
7	9.50
8	13.34
9	25.84
10	19.25
11	-17.95
12	-31.80

Table D-10 Power used to heat wire in each tube, calculated along the whole length of the furnace

Tube no.	Power (Kw)
1	1.189
2	1.189
3	1.090
4	1.090
5	1.099
6	1.057
7	1.071
8	0.000
9	1.077
10	1.069
11	1.058
12	1.218
13	1.212
14	1.212
15	1.212
16	1.202
17	1.202
18	0.000
19	1.185
Total	19.432

Table D-11.1 Wire and tube temperatures at start of each zone, and emissivities at these temperatures

Zone no.	T_w(K)	ϵ_w (T_w)	T_{ti} (K)	ϵ_{ti}(T_{ti})
			$=T_{set}$	
1	694	0.722	970	0.615
2	919	0.818	1172	0.657
3	1086	0.844	1240	0.683
4	1193	0.857	1272	0.689
5	1265	0.863	1322	0.698
6	1300	0.866	1322	0.698
7	1310	0.867	1323	0.698
8	1313	0.867	1323	0.698
9	1318	0.867	1323	0.698
10	1326	0.868	1323	0.698
11	1332	0.868	1323	0.698
12	1327	0.868	1323	0.698

The average diameter of the wires is,

$$D_w = 1.699 \text{ mm.}$$

and the inside diameter of the tube is,

$$D_{ti} = 16.0 \text{ mm.}$$

Therefore the configuration factor is,

$$F_{ti-w} = \frac{D_w}{D_{ti}} = \frac{1.699}{16.0} = 0.1062$$

Table D-11.2 Calculated resistance factors R_{ti-w} and radiative heat transfers Q_{rad}

Zone no.	$R_{ti-w}(M^{-2})$	Q_{rad} (Kw)
1	270.95	2.323
2	243.85	3.444
3	231.32	4.054
4	226.6	2.518
5	224.9	2.115
6	224.1	0.853
7	223.9	0.511
8	223.9	0.394
9	223.9	0.198
10	223.85	-0.120
11	223.85	-0.363
12	223.85	-0.160

APPENDIX E.

INVESTIGATION OF THE CONVECTIVE HEAT TRANSFER FROM THE INNER SURFACE OF THE TUBE TO THE WIRE

E1. INTRODUCTION.

In order to obtain a full picture of the heat transfer from the tube to the wire being processed, it was necessary to assess the effect of convective heat transfer. As well as the moving wire, the furnace tube contained the process gas of Hydrogen flowing at a given rate. The first task was to investigate the flow characteristics of the process gas in the tube.

Having determined this, an empirical formula was found to suit the flow characteristics and configuration of gas flow between the wire and the tube. This formula was then used to determine the temperature of the gas for a given tube and wire temperature.

The forced convective heat transfer between the wire and the tube was then computed by considering the convection from the gas to the wire to be equal to that from the tube to the gas.

Finally a numerical calculation was carried out for a typical wire and tube temperature to illustrate the magnitude of the convective heat transfer taking place.

E2. AN INVESTIGATION OF THE FLOW CHARACTERISTICS OF THE PROCESS GAS IN THE TUBE.

The volumetric flow rate of the Hydrogen gas flowing through the process tube was one litre per minute for all the tests carried out. The dimensionless Reynolds number for gas flow through a tube was found using the following equation;

$$Re = \frac{4 \cdot \dot{m}_f}{\mu_f \cdot \pi \cdot D_{ti}} \qquad \text{(E-1)}$$

Where $\dot{m}_f$ was the mass flow rate of the gas in Kilograms per second, μ_f was the dynamic viscosity of the gas in Kilogram metres per second and D_{ti} the diameter of the tube in metres. The mass flow rate of the gas was constant at any point along the tube, and was determined using the following expression;

$$\dot{m}_f = \rho_f \cdot \dot{V}_f \quad Kg/s \qquad \text{(E-2)}$$

The volumetric flow rate $\dot{V}_f$ of the Hydrogen was measured at ambient temperature of 20°C to be 1 litre per minute. The density ρ_f was found from Rogers and Mayhew [13] to be 0.082 Kg/M^3 at 293 K, therefore the Hydrogen passed through the tube at a rate of;

$$\dot{m}_f = \frac{1 \times 10^{-3}}{60} \times 0.082 = 1.364 \times 10^{-6} \text{ Kg/s}$$

The value of μ_f was required at the mean temperature of the gas as it passed through the tube. The gas entered the tube at a temperature of 293 K and was assumed to attain the maximum tube temperature of approximately 1273 K. Therefore the average temperature of the gas was 783 K, at which temperature the dynamic viscosity of Hydrogen was found from Vargaftic [11] to be;

$$\mu_f = 2.103 \times 10^{-5} \text{ N.S/M}^2$$

The internal diameter of the process tube was;

$$D_{ti} = 17.1 \times 10^{-3} \text{ M}$$

Hence the Reynolds number was found as follows;

$$Re = \frac{4 \times 1.364 \times 10^{-6}}{2.103 \times 10^{-5} \times \pi \times 17.1 \times 10^{-3}} = 4.829$$

Internal flows with Re < 2300 are considered to be laminar, so the flow of Hydrogen through the tube was definitely laminar.

The next section discusses the formulation of the convective coefficient for laminar gas flow in a concentric annulus.

E3. DETERMINATION OF AN EMPIRICAL FORMULA FOR FORCED CONVECTION BETWEEN THE WIRE AND THE TUBE.

The convective heat transfer between the tube and the wire was analogous to that of a gas flow in a concentric annulus. Forced convection in such a configuration was discussed by Incropera and De Witt [14], and a method of formulating convective coefficients developed. This method is discussed in this section, and applied to the situation being analyzed. The annular configuration of the wire inside the tube is shown in Figure (E-1) below.

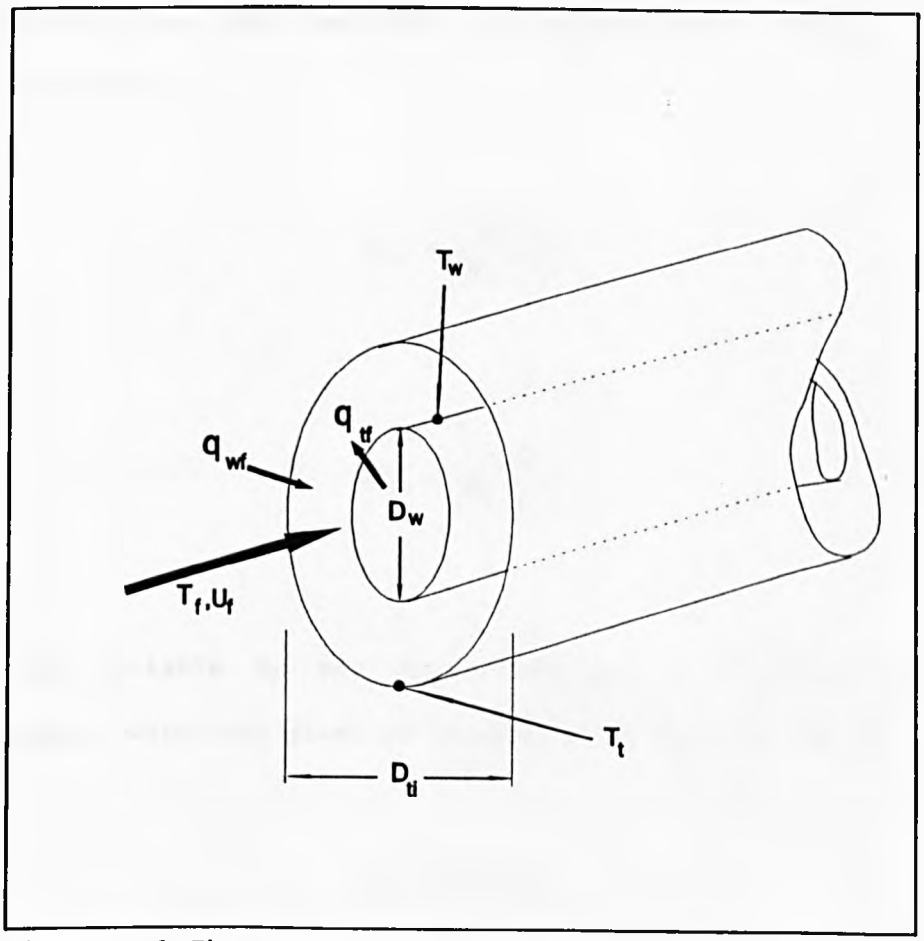

Figure E-1 The Concentric Annulus Representing The Wire Inside The Tube.

The heat flux from the wire and the tube to the gas were represented by q_{wf} and q_{tf} respectively, and were computed as follows;

$$q_{wf} = h_w \cdot (T_w - T_f) \qquad \text{(E-3)}$$

$$q_{tf} = h_t \cdot (T_t - T_f) \qquad \text{(E-4)}$$

Noting that separate convection coefficients were associated with the wire and tube surfaces. The corresponding Nusselt numbers are of the form;

$$N_{Uw} = \frac{h_w \cdot D_h}{K_f(T_F)} \qquad \text{(E-5)}$$

$$N_{Ut} = \frac{h_t \cdot D_h}{K_f(T_f)} \qquad \text{(E-6)}$$

The variable D_h was the 'Hydraulic ' diameter for the arrangement, which was given in Incropera and De Witt [14] as;

$$D_h = D_{ti} - D_w \qquad \text{(E-7)}$$

Where D_{ti} and D_w were the diameters of the inner surface of the tube and the wire respectively.

-- APPENDIX E --

For the case of fully developed laminar flow in this configuration, the Nusselt numbers were given for various diameter ratios (D_w/D_{ti}) by W.M.Kays et al [15], a selection of which are given in Table (E-1) below;

Table E-1. Nusselt number for fully developed laminar flow in a circular tube annulus.

D_w/D_t	Nu_w	Nu_{ti}
0	----	3.66
0.05	17.46	4.06
0.10	11.56	4.11
0.25	7.37	4.23
0.50	5.74	4.43
1.00	4.86	4.86

The value $K_f(T_f)$ represented the thermal conductivity of Hydrogen at the mean gas temperature T_f, an expression for the former is given in Appendix C, section C4. The calculation of the gas temperature T_f is discussed in the following section.

The convection coefficient for each surface could therefore be found from the diameter and temperature of each surface, and the gas temperature.

In order to find the Nusselt numbers for a given wire size in the tube, the following expressions were formulated relating each Nusselt number to the ratio of diameters;

$$Nu_w = 27.239 - 249.67 \times D - 1014.74 \times D^2 + 1667.46 \times D^3 + 872.99 \times D^4 \qquad (E-8)$$

$$Nu_t = 3.6826 + 7.9867 \times D - 38.574 \times D^2 + 70.617 \times D^3 - 38.852 \times D^4 \qquad (E-9)$$

Where;

$$D = D_w / D_{ti}$$

These expressions were found by carrying out a polynomial regression on the two sets of data in Table (E-1). The expressions given were accurate to within 0.2 percent of the given data points.

The Nusselt numbers presented in this chapter relate to heat transfer from a laminar flow to the surfaces of a concentric annulus, with both surfaces stationary. A more accurate formulation would consider the heat transfer from a laminar flow to a moving core, which represents the configuration of the wire moving through the process tube. Heat transfer from a laminar flow to a continuous moving surface is considered analytically by Tsou et al [16], who provide results for the boundary-layer velocity and temperature distributions, and for the surface friction and heat transfer coefficients.

Measurements of the laminar velocity field were found to be in excellent agreement with the analytical prediction. This verified that the boundary layer on a continuous moving surface may be accurately mathematically modelled.

This work is applied by Shigechi et al [17] in their analysis of the heat transfer between a fully developed laminar flow and a moving core in a concentric annular geometry. The outcome of this work was a compilation of tables which provide the Nusselt numbers for flows through annuli with varying radius ratio ($\alpha=D=D_w/D_{tf}$), and varying relative core speed ($U^*=u/U_b$). The maximum value of U^* was considered to be for the minimum bulk mean gas speed U_b, and the maximum wire speed, and was found to be approximately -1. The Nusselt numbers Nu_{tf} and Nu_w for the tube and wire surfaces respectively were then calculated form the data in [17] using this value of U^*, with α values of 0.1, 0.2 and 0.4. The Nusselt numbers were also calculated at each value of α for the case of a stationary wire ($U^*=0$), and the maximum variation was found to be approximately 2%. Therefore the fact that the wire was moving was considered to have had a negligible effect on the convective heat transfer to the wire when analyzing the total heat transfer to the wire.

-- APPENDIX E --

E4. COMPUTATION OF THE MEAN GAS TEMPERATURE FOR GIVEN WIRE AND TUBE TEMPERATURES.

In order to calculate the convective heat transfer between the tube and the wire, the mean temperature of the gas in the annulus was required. In order to simplify the analysis, it was assumed that the Hydrogen flowing between the tube and the wire had negligible thermal mass compared to the wire and the tube.

Therefore the net heat transferred per unit length by convection from the wire and the tube to the gas was assumed to be zero, as depicted below;

$$q_{net} = \pi \cdot D_t \cdot h_t \cdot (T_t - T_f) + \pi \cdot D_w \cdot h_w \cdot (T_w - T_f) = 0 \qquad \text{(E-10)}$$

Rearranging equation (E-10) provided an expression for gas temperature T_f as follows;

$$T_f = \frac{T_w \cdot D_w \cdot h_w + T_t \cdot D_{ti} \cdot h_t}{D_w \cdot h_w + D_{ti} \cdot h_t} \qquad \text{(E-11)}$$

Equations (E-5) and (E-6) were then rearranged to provide equations for h_w and h_t respectively, which were substituted into equation (E-11) to yield;

$$T_f = \frac{T_w \cdot D_w \cdot N_{Uw} + T_t \cdot D_{ti} \cdot N_{Ut}}{D_w \cdot N_{Uw} + D_{ti} \cdot N_{Ut}} \qquad \text{(E-12)}$$

It was then possible to find the gas temperature from the diameter of the wire and the tube, and the temperatures of the wire and the tube at any point along the furnace. Because of the assumption that there was no net heat transfer to the gas in the tube, the convection from the tube to the wire was assumed to be equal to that from the tube to the gas. On this basis, the heat transfer per unit length between the wire and the tube due to forced convection could be written;

$$q_{tw} = q_{tf} = h_t \cdot \pi \cdot D_{ti} \cdot (T_t - T_f) \qquad \text{(E-13)}$$

The following section contains a numerical example of finding the convection between the tube and the wire.

E5. NUMERICAL EXAMPLE.

The diameter and temperature of the wire and tube are as follows;

$D_w = 3.0 \times 10^{-3}$ M.....$T_w = 300$ K

$D_t = 17.1 \times 10^{-3}$M.....$T_t = 1100$ K

The ratio of diameters D was found to be 0.1754, which was the used in equations (E-8) and (E-9) to give the Nusselt number for the two surfaces,

$Nu_w = 7.74$

$Nu_t = 4.24$

The gas temperature T_f was then found using equation (E-12);

$$T_f = \frac{300 \times 3 \times 7.74 + 1100 \times 17.1 \times 4.24}{3 \times 7.74 + 17.1 \times 4.24} = 906 \text{ K.}$$

The thermal conductivity of Hydrogen at 906 K was found from Appendix C to be;

$$K_f = 0.4475 \text{ W/M.K}$$

The hydraulic diameter D_h was then found using equation (E-7) to be;

$$D_h = 14.1 \times 10^{-3} \text{ M}$$

The convection coefficient from the tube to the gas, h_t was then found from equation (E-6) to be;

$$h_t = 134.57 \text{ W/M}^2\text{.K}$$

Compared with the convection coefficient from the wire to the gas found from equation (E-5);

$$h_w = 245.65 \text{ W/M}^2\text{.K}$$

The convection from the tube to the gas per unit length was then found from equation (E-13) to be;

$$q_{tf} = 1403.0 \text{ W/M}$$

The corresponding convection from the wire to the gas per unit length was then found using a similar equation;

$$q_{wf} = -1403.0 \text{ W/M}$$

Therefore the net heat transferred to the gas from the wire and the tube by convection was zero.

The value calculated for the convective heat transfer from the tube to the gas was equal to the convective heat transfer from the tube to the wire. This was due to the fact that it was assumed that the amount of heat absorbed by the gas was considered to be negligible. Therefore all the heat transferred from the tube to the gas was then in turn transferred from the gas to the wire.

APPENDIX F.

ESTIMATION OF THEORETICAL THERMOCOUPLE ERROR.

F1. INTRODUCTION.

In the measurement of temperature, it is widely accepted that the output of a sensor such as a thermocouple represents an approximation to the temperature of a solid or fluid at some location. There are several factors which may cause deviations between the probe output and the actual temperature at the required location in the absence of the probe.

Firstly the presence of the probe itself may effect the thermal conditions at the point of measurement and in its surroundings, therefore altering its temperature distribution. A common example of this is the conduction of heat to or away from a thermocouple junction along its lead wires, and this is discussed in section F2.

Secondly, when a probe is being used to measure a point whose temperature is changing, the output of the probe will lag the actual temperature of that point. The amount of lag encountered depends upon the transient response time of the probe, which is discussed in section F3.

F2. ANALYSIS OF THE INSTALLATION ERROR PREDICTED FOR MEASURING THE TEMPERATURE OF A WIRE IN A PROCESS TUBE.

The object of this analysis was to provide estimates of the order of magnitude of the errors that may be expected in the measurement of wire temperature.

In order to carry out this analysis a simple model had to be devised to represent the energy transfers involved *when a thermocouple* was mounted on the surface of the wire in the tube.

The model used is shown schematically in figure (F-1) below.

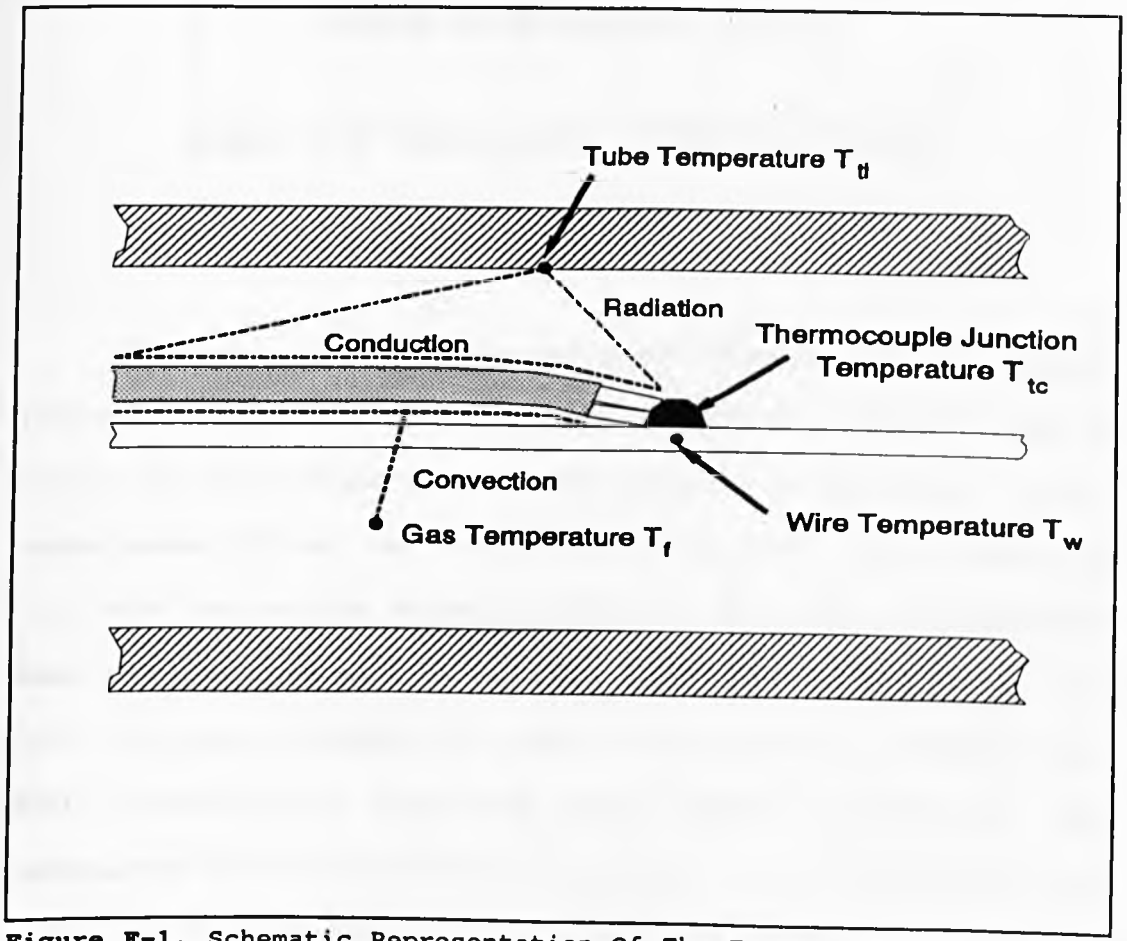

Figure F-1. Schematic Representation Of The Energy Transfers Taking Place Between The Thermocouple And Its Surroundings.

The type of thermocouple which was used in the measurement of wire temperature was constructed from Chromel-Alumel thermocouple wire of the flat paired configuration shown in figure (F-2).

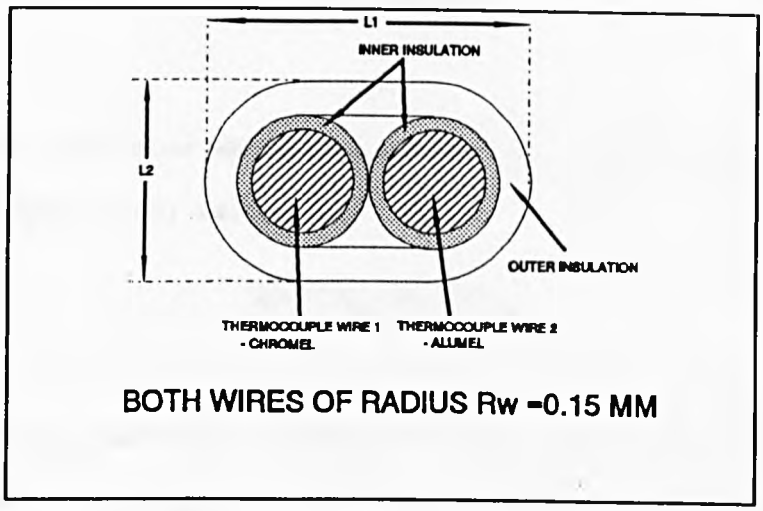

Figure F-2. Configuration Of The Thermocouple Wires.

The lead wires were considered to provide a heat conduction path between the thermocouple sensing junction attached to the wire, and an isothermal zone located at the other extremity of the leads. As the leads passed through the process gas in the tube, they transferred heat with the gas via forced convection. The leads also exchanged heat with the inner wall of the tube in the form of radiation. The paths of energy transfer are shown in figure (F-1). Due to their small diameter and relatively high thermal conductivity, the temperature of the lead wire was regarded to be a function of the axial coordinate X only. Radial conduction was then considered to occur only through the insulation of the wire.

Sparrow [18] proposed a solution whereby the heat transfer along the leads was analyzed in the same manner as that used for a fin.

The axial conduction along the wire was represented by;

$$Q_x = -\overline{KA} \cdot \frac{dT}{dX} \qquad \text{(F-1)}$$

Where the value KA was given for the thermocouple lead wire shown in figure (F-2) as;

$$\overline{KA} = (K_{W1} + K_{W2}) \cdot A_{Wtc} \qquad \text{(F-2)}$$

Where A_{wtc} was the cross sectional area of each lead wire, and K_{w1} and K_{w2} were the respective thermal conductivities of thermocouple wires 1 and 2, which may be found in Appendix C.

The radial heat transfer per unit length through the insulation of the lead wire was equal to the convective heat transfer to the surrounding gas of temperature T_f and was found to be ;

$$\frac{dQ_r}{dX} = \frac{(T - T_f)}{R_t} \qquad \text{(F-3)}$$

Where $(T-T_f)$ was the temperature difference between the thermocouple lead wires at position X and the surrounding gas, and the thermal resistance R_t was given by;

$$R_t = \frac{1}{h_{ctc} \cdot 2\pi r_2} + \frac{\ln(r_2/r_1)}{2\pi K_1} \qquad \text{(F-4)}$$

In which k_i was the thermal conductivity of the insulation of the lead wires, and r_1 and r_2 were found from the thermocouple dimensions in figure (F-2), as follows;

$$r_1=\sqrt{2}r_{wtc} \qquad \text{(F-5)}$$

and;

$$r_2=\frac{L_1+L_2}{4} \qquad \text{(F-6)}$$

The value of h_{ctc} in equation (F-4) was the forced convection heat transfer coefficient from the lead wire surface to the gas, and was found as in Appendix E. When the lead wires were attached to the wire surface via the sensing junction, heat transfer occurred either to or away from the surface of the wire, depending upon whether the gas temperature was higher or lower than the temperature of the wire. The junction was considered to be well bonded to the surface of the wire, hence the contact resistance was assumed to be negligible. The conduction of heat between the wire and the thermocouple sensing junction was found by Gröber et al [19] to be;

$$Q = 4\cdot r_1\cdot k_w(T_w)\cdot(T_{tc}-T_w) \qquad \text{(F-7)}$$

Where k_w was the thermal conductivity of the wire being measured by the thermocouple, at temperature T_w.

Under steady-state conditions the heat transferred to the thermocouple junction as described in equation (F-7) must be equal to the heat conducted along the thermocouple lead wires.

This conduction was found by Sparrow [18] and Schneider [20] from fin theory, and was shown to be;

$$Q=\sqrt{\frac{\overline{KA}}{R_t}}\cdot(T_f-T_{tc}) \qquad \text{(F-8)}$$

Where $\overline{KA}$ and R_t are given in equations (F-2) and (F-4) respectively for the thermocouple lead wire which was being used.

Eliminating Q from equations (F-7) and (F-8) and rearranging them yielded the following expression for the temperature measurement error due to installation effects;

$$E = T_{tc}-T_w = \frac{\sqrt{\frac{\overline{KA}}{R_t}}}{r_1\cdot K_w(T_w)}\cdot(T_f-T_{tc}) \qquad \text{(F-9)}$$

Therefore for a given thermocouple temperature (T_{tc}) and gas temperature (T_f) the actual temperature of the wire, T_w could be estimated using equation (F-9).

In order to find the temperature of the gas in the tube and the convective heat transfer coefficient h_{ctc} between the gas and the lead wire, the theory in Appendix E was used. However the original analysis also required the inclusion of radiant heat transfer between the lead wires and the tube to be considered.

Sparrow [18] discussed the contribution of radiation to the analysis, stating that it was especially important at elevated temperatures.

The radiative heat transfer from the tube to a point on the thermocouple lead wire surface was considered to be approximately the same as for a small body of temperature T and emissivity ϵ inside a black body enclosure of temperature T_{wall}. The radiant heat transfer from the tube to a point on the lead wire was given by;

$$q_{rad} = h_{rad} \cdot (T_{ti} - T_{surf}) \qquad \text{(F-10)}$$

Where;

$$h_{rad} = \epsilon \cdot \sigma \cdot (T^2 + T_{ti}^2) \cdot (T + T_{ti}) \qquad \text{(E-11)}$$

The temperature T used to find the radiative heat transfer coefficient in equation (F-11) was taken as the average temperature along the lead wire, which was calculated as;

$$T = \frac{T_{ti} + T_{tc}}{2} \qquad \text{(F-12)}$$

Therefore at any location X along the lead wire, the surface heat loss per unit length by combined radiation and convection was given by;

$$dQ_r = h_{ctc} \cdot 2 \cdot \pi \cdot r_2 \cdot (T_{surf} - T_f) + h_{rad} \cdot 2 \cdot \pi \cdot r_2 \cdot (T_{surf} - T_{ti}) \qquad \text{(F-13)}$$

Where T_{surf} was the surface temperature of the lead wire insulation.

Equation (F-13) was then rephrased in terms of an effective heat transfer coefficient $\bar{h}$ and an effective environment temperature $\bar{T}$ as follows;

$$dQ_r = \bar{h} \cdot 2 \cdot \pi \cdot r_2 \cdot (T_{surf} - \bar{T}) \qquad \text{(F-14)}$$

Where;

$$\bar{h} = h_{ctc} + h_{rad} \qquad \text{(F-15)}$$

And;

$$\bar{T} = \frac{(h \cdot T_f + h_{rad} \cdot T_{ti})}{\bar{h}} \qquad \text{(F-16)}$$

The combined heat transfer equation (F-13) was then used to find the thermocouple error in the same manner as for convection only. This was carried out by including the effective heat transfer coefficient and environment temperature in equations (F-4) and (F-9) respectively to yield,

$$E = T_{tc} - T_w = \frac{\sqrt{\frac{\overline{KA}}{R_t}}}{4 \cdot r_1 \cdot K_w(T_w)} \cdot (\bar{T} - T_{tc}) \qquad \text{(F-17)}$$

Where R_t is now given by the equation,

$$R = \frac{1}{\bar{h} \cdot 2\pi r_2} + \frac{\ln(r_2/r_1)}{2\pi K_i} \qquad \text{(F-18)}$$

F2.1 Numerical Example Of thermocouple Installation Error Calculation.

Two example calculations were carried out to assess the magnitude of the thermocouple installation error discussed in the above theory. The first case was that of the thermocouple measuring a wire temperature of 400 K with the wire in a tube of wall temperature 1000 K. The estimated actual temperature of the wire was then calculated as follows;

Thermocouple dimensions

$r_{wtc} = 1.5 \times 10^{-4}$ M

$L_1 = 18 \times 10^{-4}$ M

$L_2 = 11 \times 10^{-4}$ M

$r_1 = 2.121 \times 10^{-4}$ M

$r_2 = 7.25 \times 10^{-4}$ M

The gas temperature was estimated for the purposes of this basic calculation to be;

$T_f = 800$ K

And the average temperature of the lead wire surface along its length was calculated using equation (F-12);

$T = 700$ K

Using the theory in appendix E, the convective heat transfer coefficient h_{ctc} from the thermocouple lead wire and the surrounding gas was formulated at the gas temperature, T_f to be

$$h_{ctc} = 71.33 \text{ W/M}^2\text{K}$$

In order to find the radiative heat transfer coefficient h_{rad}, the emissivity of the fibre-glass insulation at T=700 K was found from [21] to be 0.5, therefore;

$$h_{rad} = 71.81 \text{ W/M}^2\text{K}$$

The effective heat transfer coefficient $\bar{h}$ and the effective heat environment temperature $\bar{T}$ were then found using equations (F-15) and (F-16) respectively;

$$\bar{h} = 143.14 \text{ W/M}^2\text{K}$$

$$\bar{T} = 900 \text{ K}$$

The thermal conductivity of the fibre glass insulation at T=700 K was then found from [21] to be;

$$k_f = 0.04 \text{ W/MK}$$

The thermal resistance R_t was then found using equation (F-18) to be;

$$R_T = 6.4255 \text{ MK/W}$$

-- APPENDIX F --

The thermal conductivity of the stainless steel wire ($k_w(T_w)$) was found at the thermocouple temperature of 400 K to be 18.3 W/MK using the data in appendix C. The difference between the temperature indicated by the thermocouple and the actual wire temperature was then found using equation (F-17) to be;

$$T_{tc}-T_w = 33.5 \text{ K}$$

Therefore the actual temperature of the wire was then estimated as follows;

$$T_w = T_{tc} - 33.5 = 366.5 \text{ K}$$

The error incurred by the surface mounted thermocouple in the above example was found to be;

E = 8.375 % of indicated value.

Another set of calculations were then carried out using the same conditions as above, except that the tube temperature and indicated thermocouple temperature were increased to 1250 K and 1100 K respectively. The resulting difference in indicated thermocouple and actual wire temperatures was found to be;

$$T_{tc} - T_w = 14.5 \text{ K}$$

Therefore the estimated actual temperature of the wire in this example was;

$$T_w = 1100 - 14.5 = 1085 \text{ K}$$

Giving an error of 1.3% of the indicated value.

From these calculations it has been shown that the magnitude of the installation error for the thermocouple increases with the difference between the tube and wire temperatures.

The graph in figure (F-3) illustrates how the installation error varies as the measured temperature of the wire increases from 300 K to 1300 K with a constant tube temperature of 1300 K.

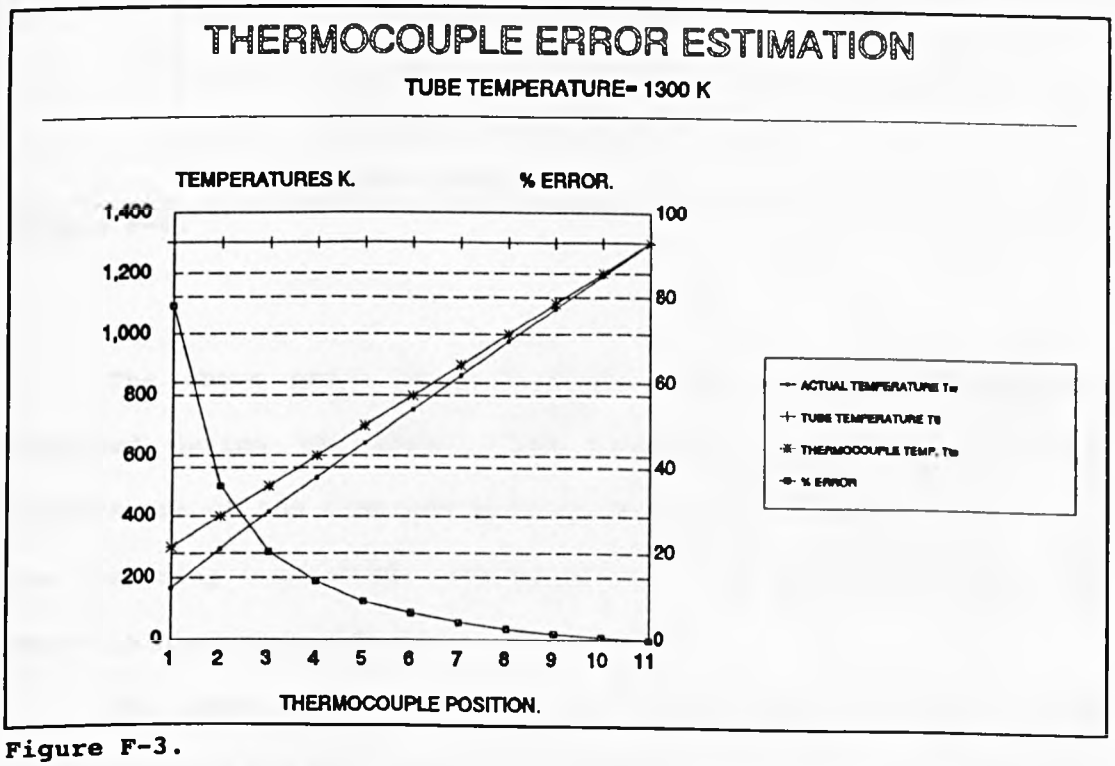

Figure F-3.

The percentage error was at its highest (78 %) for a temperature difference of 1000 K, and decreased to 0.66 % for a temperature difference of 100 K.

Following this, the temperatures of the wire and tube measured along the furnace in test 4.3 (presented in chapter 7) were analyzed in the same manner to provide the graph in figure (F-4).

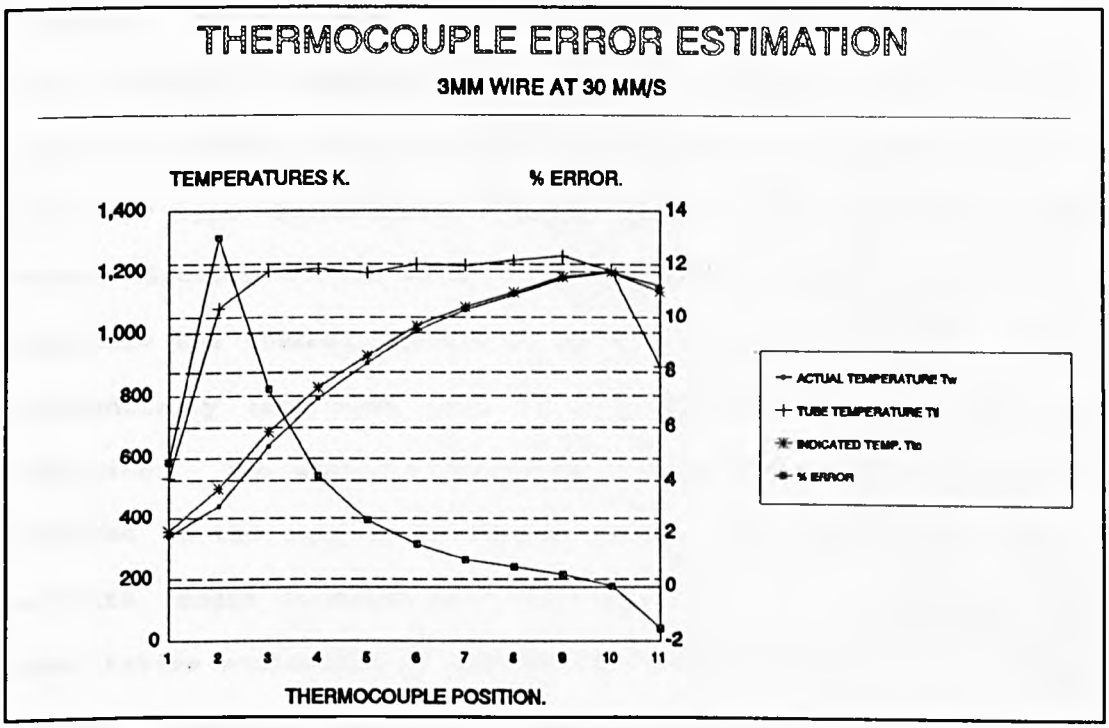

Figure F-4.

The above graph shows that the tube and wire temperatures recorded during the test. The error was calculated from the temperature of the tube and wire at each thermocouple position, and the resulting 'corrected' wire temperatures and percentage error are shown plotted alongside them.

The installation error for the thermocouple was found to be greatest where the wire entered the furnace, and was found to decrease as the wire was heated by the furnace.

F3. TRANSIENT RESPONSE OF THE THERMOCOUPLE JUNCTION ATTACHED TO THE WIRE.

The transient response of the thermocouple discussed here is the time taken for the sensing junction to respond to a given change in the temperature of its environment. The transient response of an intrinsic thermocouple is investigated both analytically and experimentally by Henning and Parker [22]. Unlike the welded-bead type thermocouple which was used to measure the wire temperature, the intrinsic type thermocouple consists of the two thermocouple wires welded directly to the metal whose temperature is being measured. Therefore the thermal inertia of an intrinsic type thermocouple is substantially less than that of a welded-bead type of the same dimensions. The analysis discussed considers the thermocouple wire attached to the surface to behave in the same manner as a pin of infinite length attached to a semi-infinite body. This led to a quantitative evaluation of the effect of thermocouple wire size and thermal properties upon the thermocouple response time. Both the analytical results and the experimental data conclude that thermocouple wire of small diameter and low thermal conductivity respond most rapidly. Due to practical difficulties, an intrinsic type thermocouple could not be used to measure the wire temperature as it passed through the furnace. Therefore it is necessary to consider the thermal inertia of the welded bead which comprised the thermocouple junction. In addition to this, the effect of the temperature of the environment surrounding the thermocouple junction also requires consideration in the analysis.

For this analysis the thermocouple junction was considered to be a hemisphere as depicted in figure (F-5) below. The configuration shown in figure (F-5) shows the energy transfers taking place between the junction and its environment and the junction and the wire.

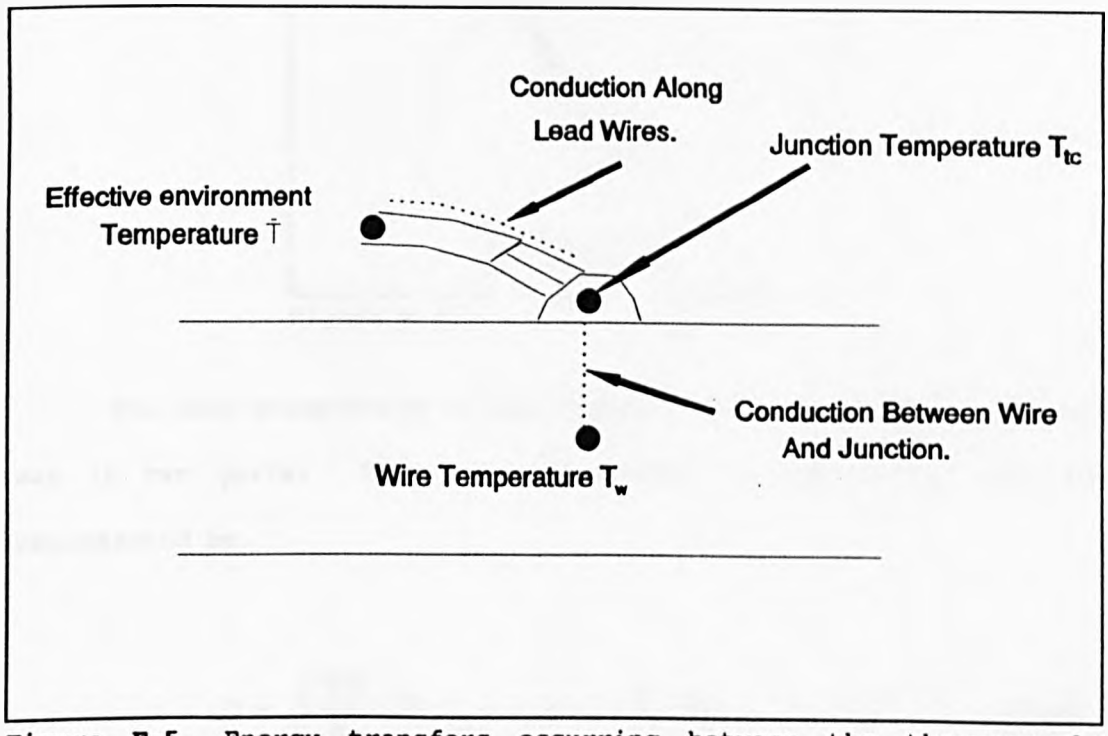

Figure F-5. Energy transfers occurring between the thermocouple junction and its environment, and the junction and the wire.

The direct radiative and convective heat transfers to and from the junction itself were considered to be negligible in this analysis due to the small size of the junction compared with its leads.

In order to analyze the transient response of the thermocouple junction in figure (F-5), the total energy transfer to junction was analyzed as shown in figure (F-6). The heat transferred to the junction in the arrangement shown in figure (F-6) was represented by;

$$Q = h_{tc} \cdot A_1 \cdot (T_\infty - T_{tc}) \qquad \textbf{(F-19)}$$

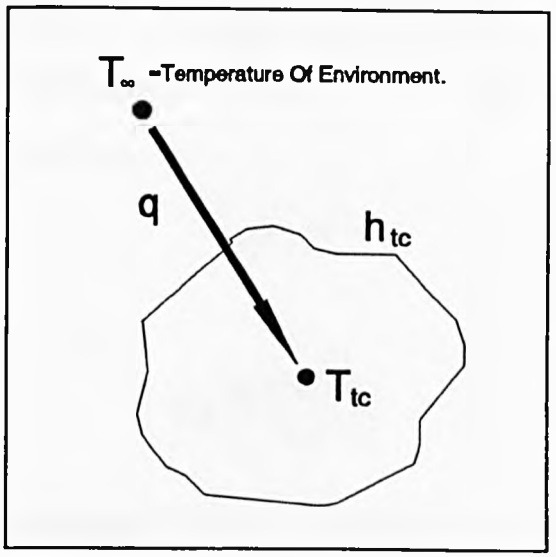

Figure F-6.

The heat transferred to the junction, as shown in figure (F-5), was in two parts. These were discussed in section F2, and are represented by,

$$Q = \sqrt{\frac{\overline{KA}}{R_t}} \cdot (\overline{T} - T_{tc}) + 4 \cdot r_1 \cdot (k_w(T_w)) \cdot (T_w - T_{tc}) \qquad \textbf{(F-20)}$$

Which was simplified to;

$$Q = h_1 \cdot A_1 \cdot (\overline{T} - T_{tc}) + h_2 \cdot A_1 \cdot (T_w - T_{tc}) \qquad \textbf{(F-21)}$$

Where;

$$h_1 = \frac{1}{A_1} \cdot \sqrt{\frac{\overline{KA}}{R_t}} \qquad \textbf{(F-22)}$$

And;

$$h_2 = \frac{4 \cdot r_1 \cdot k_w(T_w)}{A_1} \qquad \textbf{(F-23)}$$

The expression for heat transfer in equation (F-21) was then equated to that in equation (F-19) to provide the following expressions for h_{tc} and T_∞ ;

$$h_{tc}=h_1+h_2 \qquad \textbf{(F-24)}$$

And;

$$T_\infty=\frac{h_1\cdot\overline{T}+h_2\cdot T_w}{h_{tc}} \qquad \textbf{(F-25)}$$

As the wire passed down the furnace tube, the environmental temperature T_∞ underwent what could be described as a 'ramp' change over a small change in time, as illustrated in figure (F-7).

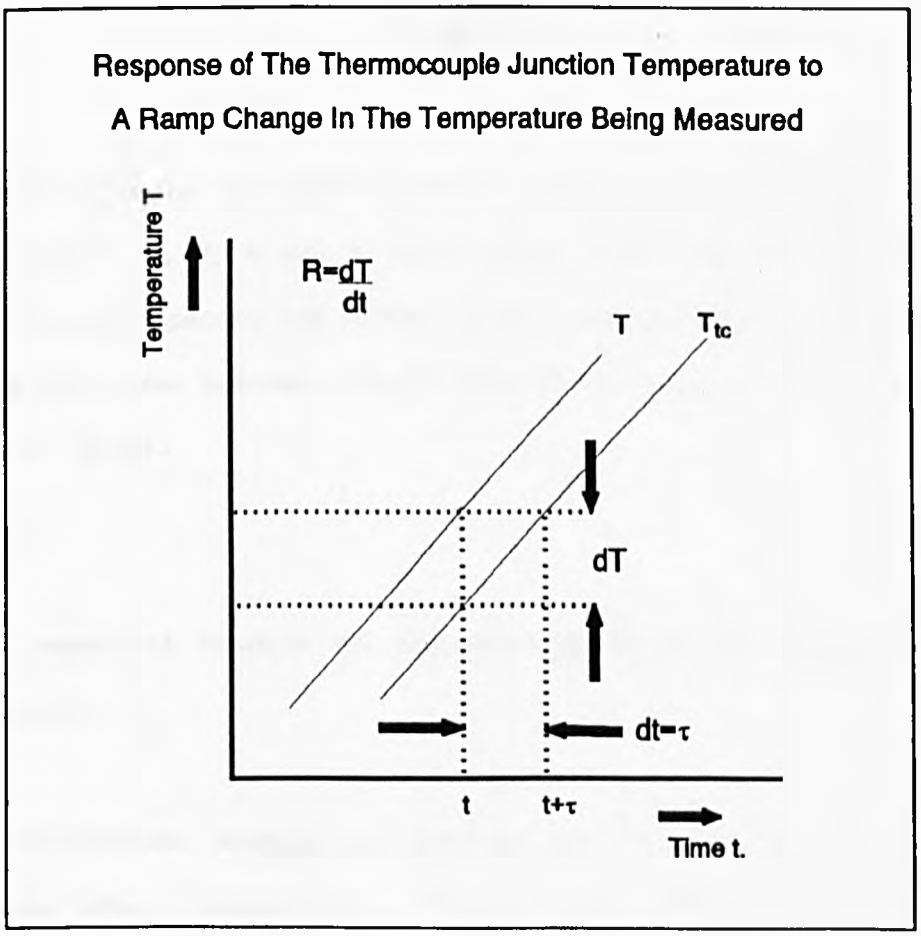

Figure F-7.

The temperature of the thermocouple T_{tc} is shown in figure (F-7) to 'lag' the environment temperature T_∞ by an amount given by the expression;

$$T_\infty - T_{tc} = R \cdot \tau \qquad \text{(F-26)}$$

Where R is the rate of change of the environmental temperature (dT_∞/dt) in Kelvin per second, and τ the response time of the thermocouple junction in seconds.

The time constant τ in equation (F-26) was discussed by Benedict [23] using lumped-capacitance theory, and was found to be equal to;

$$\tau = \frac{\rho \cdot V \cdot C}{h_{tc} \cdot A_1} \qquad \text{(F-27)}$$

In terms of the thermocouple junction shown in figure (F-6). The variables ρ, V, C and A_1 were respectively the density, volume, specific heat capacity and surface area of the junction. The value of the combined heat transfer coefficient of the junction was found from equation (F-24).

F3.1 Numerical Example Of thermocouple Transient response Error Calculation.

A numerical example was carried out in order to quantify the transient error produced for a typical wire temperature measurement situation.

The temperatures from the first example in section F2.1 were used as follows,

T_{ti} = 1000 K

T_f = 800 K

T_{tc}= 400 K

The resulting wire temperature was,

T_w = 366.5 K

The following values, calculated in section F2.1 were also used,

h = 143.14 W/M^2K

$\bar{T}$ = 900 K

R_t = 6.4255 MK/W

$\overline{KA}$ =6.9696 W/MK

The exchange area of the thermocouple junction A_1 was then calculated as follows,

$$A_1 = \pi \times r_1^2 = 1.4133 \times 10^{-7}\ M^2$$

And from equation (F-22),

h_1 = 23303 W/M^2K

From equation (F-23),

$$h_2 = 109869 \text{ W/M}^2\text{K}$$

Then from equation (F-24);

$$h_{tc} = 23303 + 109869 = 133172 \text{ W/M}^2\text{K}$$

Hence the environment temperature T_∞ was determined from equation (F-25) to be,

$$T_\infty = 460 \text{ K}$$

In order to find the rate of change in the environment temperature T_∞, the changes in the effective environment temperature $\bar{T}$ and the wire temperature T_w were considered over a one second interval to be;

$$d\bar{T} = 5 \text{ K}$$

$$dT_w = 15 \text{ K}$$

Putting the new values of these temperatures into equation (F-25) yielded a rise in the environment temperature T_∞ as follows;

$$dT_\infty = 13.3 \text{ K}$$

Therefore the rate of change in the environmental temperature R was found to be;

$$R = 13.3 \text{ K/Second.}$$

The following properties for a Chromel-Alumel thermocouple junction were found from Benedict [23];

$$\rho = 8000 \text{ Kg/M}^3, \quad C = 600 \text{ J/Kg.K}$$

The junction's time constant τ was then found using equation (F-27) to be,

$$\tau = 5.097 \times 10^{-3} \text{ Seconds.}$$

Therefore the temperature measurement error of the thermocouple due to the time lag could be found from equation (F-26);

$$E = (T - T_{tc}) = 13.3 \times 5.097 \times 10^{-3}$$
$$= 0.067 \text{ K}$$

The temperature measurement error due to time lag for this example was observed in this example to be very small. The rate of temperature rise R used in this example was the maximum temperature rise encountered in measurements on the furnace. Therefore the error calculated above was probably the maximum error to be encountered due to the transient response of the thermocouple.

This was considered to be sufficiently small compared with the thermocouple installation error discussed in section F2 to be ignored in any analyses of the results.

LIST OF REFERENCES.

[1] **Holman, J.P.,** *'Heat Transfer.'*, Sixth Edition, Chapter 1, McGraw-Hill Inc. (1986).

[2] **Holman, J.P.,** *'Heat Transfer.'*, Sixth Edition, Chapter 8, McGraw-Hill Inc. (1986).

[3] **Leuenberger, H. and R.A.Person,** *'Compilation of Radiation Shape Factors for Cylindrical Assemblies'*, ASME Paper 56-A-144, ASME Annual Meeting, New York (1956).

[4] **Wiebelt, J.A. and S.Y.Rou,** *'Radiant Interchange Factors for Finite Right Circular Cylinder to Rectangular Planes'*, International Journal of Heat and Mass Transfer, Vol 6, 1963, pp 143-146.

[5] **Feingold, A. and K.G.Gupta,** *'New Analytical Approach to the Evaluation of Configuration Factors in Radiation From Spheres and Infinitely Long Cylinders'*, Journal of Heat Transfer, Trans ASME, Series C, Vol 92, 1970, pp 69-76.

[6] **Solartron Group,** *'3530 Orion Data Logging System - Operating Manual.'*, Published by Solartron Instruments, a Division of Schlumberger UK Ltd. (1982).

[7] **Siegel, R., and J.R. Howell,** *'Thermal Radiation Heat Transfer.'*, Appendix D, *'Radiative Properties.'*, Second Edition, McGraw-Hill Inc. (1981).

[8] **Solartron Group,** *'3530 Orion Data Logging System - Communicating With The Orion.'*, Published by Solartron Instruments, a Division of Schlumberger UK Ltd. (1982).

[9] Touloukian, Y.S. and C.Y.Ho, Eds., *'Thermophysical Properties of Matter'*; Vol 7, *'Thermal Radiative Properties of Metallic Elements and Alloys'*, pp 1212-1345, Plenum Press, New York (1972).

[10] Touloukian, Y.S. and C.Y.Ho, Eds., *'Thermophysical Properties of Matter'*; Vol 4, *'Specific Heat of Metallic Elements and Alloys'*, pp 324-328, Plenum Press, New York (1972).

[11] Vargaftik, N.B., *'Tables on the Thermophysical Properties of Liquids and Gases.'*, Second Edition, Chapter One, John Wiley and Sons, Inc. (1975).

[12] Touloukian, Y.S. and C.Y.Ho, Eds., *'Thermophysical Properties of Matter'*; Vol 4, *'Thermal Conductivities of Metallic Elements and Alloys'*, page 698 and 1169, Plenum Press, New York (1972).

[13] Rogers, G.F.C., and Y.R. Mayhew, *'Thermodynamic and Transport Properties of Fluids.'*, Third Edition, page 15, Basil Blackwell (1980).

[14] Incropera, F.P., and De Witt, D.P., *'Fundamentals of Heat and Mass Transfer.'*, Chapter 8, Second Edition, John Wiley and Sons (1977).

[15] Kays, W.M., and H.C. Perkins, in *'Handbook of Heat Transfer.'*, Chapter 7, W.M.Rohsenow and J.P.Hartnett, Eds., McGraw-Hill (1972).

[16] Tsou, F.K., Sparrow, E.M. and R.J.Goldstein, *'Flow and Heat Transfer in the Boundary Layer on a Continuous Moving Surface'*, International Journal of Heat and Mass Transfer, Vol. 10, 1967, pp 219-235.

[17] Shigechi,T. and Y.Lee, *'An Analysis on Fully Developed Laminar Fluid Flow and Heat Transfer in Concentric Annuli With Moving Cores'*, International Journal of Heat and Mass Transfer, Vol. 34, 1991, pp 2593-2601.

[18] Sparrow, E.M., in *'Measurement Techniques in Heat Transfer.'*, Chapter 1, Ekert E.R.G. and R.J.Goldstein, Eds., The Advisory Group for Aerospace Research and Development of NATO (1970).

[19] Gröber, H., Erk, S., and Grigull, U., *'Fundamentals of Heat Transfer.'*, McGraw-Hill, New York (1961).

[20] Schneider, P.J., *'Conduction Heat Transfer.'*, Addison Wesley, Reading, Massachusetts (1955).

[21] Incropera, F.P., and De Witt, D.P., *'Fundamentals of Heat and Mass Transfer.'*, Appendix A, Second Edition, John Wiley and Sons (1977).

[22] Henning, C.D. and R.Parker, *'Transient Response of an Intrinsic Thermocouple'*, Journal of Heat Transfer, Trans ASME, Series C, Vol 89, 1967, pp 146-154.

[23] Benedict, R.P., *'Fundamentals of Temperature, Pressure and Flow Measurements.'*, Chapter 13, Second Edition, John Wiley and Sons (1977).